1989

Studies in iron ore reduction with particular reference to Indonesian iron ores

Pramusanto
University of Wollongong

STUDIES IN IRON ORE REDUCTION WITH PARTICULAR REFERENCE TO INDONESIAN IRON ORES

A thesis submitted in partial fulfilment of the requirements for the award of the degree

DOCTOR OF PHILOSOPHY

from

THE UNIVERSITY OF WOLLONGONG

by

PRAMUSANTO, Ir.(*I.T. BANDUNG*, INDONESIA)

DEPARTMENT OF MATERIALS ENGINEERING
(1989)

ACKNOWLEDGEMENTS

The author is indebted to Assoc.Professor N. Standish for his supervision, advice and encouragement during the course of this work.

The author also wishes to express his appreciation of the financial support through overseas scholarship scheme which was provided by the Australian International Development Assistance Bureau.

Grateful acknowledgements are given to the staff and post-graduate students of Department Materials Engineering of the University of Wollongong for their cooperation, in particular Mr. G.K. Hamilton for his invaluable assistance with the experimental set-up and computing program.

The cooperation of BHP-Central Research Laboratories and Electrolytic Refining & Smelting Co. Aust. Ltd. in respectively offering their facilities for chemical and microscopic analysis is also gratefully appreciated.

Many thanks is given for English preparation of this Thesis to Mrs. J. Eshman.

Finally, the author wish to express his sincere appreciation for help and encouragement given to him by his wife, Inne.

TABLE OF CONTENTS

Appendices

ABSTRACT

The reduction characteristics of Lampung (Sumatra) lump ore uses carbon monoxide have been studied by thermogravimetry. The course of reaction has been expressed in term of degree of reduction defined as weight loss measured at a given time with respect to the maximum possible weight loss. The results of the reduction characteristics of the ore have shown that the presence of goethite, identified by X-ray diffraction, in an essential magneto-hematite ore complicates the reduction. Some fixed time reduction experiments have been carried out on ore samples where the reduced sample was examined under optical and SEM and also some physical properties were measured. The resulting reduction and porosity curves shows considerable variation behaviour and reflect the physical variation in the individual ore.

The reduction results with different parameters indicate that mixed control was operative during the course of reduction.

Possible improvement techniques considered involved in microwave pre-treatment prior to reduction. Physical properties changes, i.e. cracks after treatment deduced from the microscopic examinations were found to depend mainly on the time spend during pretreatment. X-ray diffraction analysis indicates that microwave treatment also resulted in some subtle structural changes of the sample.

The results of this investigation indicate that the treatment of the ore enhances reduction but benefit optimum exist.

NOMENCLATURE

C	concentration of gaseous reactant A
D	effective diffusivity of gas through product layer
d_0	density of particle
K	constant
K_c	first order rate constant for shrinking of the unreacted core
m,n	stoichiometric coefficients
R	radius of spherical pellet
r_0	radius
T	temperature
t	time
X	conversion of the whole pellet

Greek symbols

ρ_s	molar density of solid reactant S_1
τ	time needed for complete conversion of pellet

INTRODUCTION

In an attempt to reduce the tonnage of pig iron imported for foundry use throughout Indonesia, a demonstration iron smelting plant was started in 1985 at Lampung on the southern tip of Sumatra (LLoyd, 1988). Based on laboratory studies carried out at the National Institute of Metallurgy of the Indonesian Institute of Science (LMN-LIPI) in Bandung, an indigenous iron ore deposit is being mined and smelted in a small size, low shaft blast furnace using wood charcoal as the fuel and reductant. An expected daily production rate of 25 t of pig iron and a charcoal consumption rate of 1 t/t of iron was never reached. One reason is that the two important parameters of the operation viz. the reactivity of the charcoal and the reducibility of the ore had not been studied until the former had been reported by Tanjung (1987). The latter investigation, described in this work, was concerned with the characteristics and reduction behaviour of iron ore supplied by NIM. This study will provide some fundamental aspects (Standish, 1988) of ironmaking in the charcoal blast furnace to improve its productivity.

Many studies of reaction mechanism and rate on both macroscopic and microstructural aspects of iron oxide reduction have been conducted to clarify issues relevant to plant design and operation. Some of these studies concentrated on specific ores (Koo and Evans, 1979), whereas others focused on a particular stage of the overall reaction - notably, the reduction of hematite to magnetite (Hayes and Grieveson, 1981a,b), reduction of magnetite to iron (Al-Kahtany and Rao, 1980) and the reduction of wustite to iron (St. John *et al*, 1985). The influence of impurities (Dou *et al*, 1988) and additives (Wright, 1981) on the reduction of iron oxide and iron ores has also been the subject of previous studies. The rate of reaction depends on

the nature of the ore, the process temperature, pressure and gas composition. For a given type of ore and reaction conditions, the overall rate of reaction is generally low for carbon monoxide, high for hydrogen and intermediate for CO/H_2 mixtures. The advantage of reduction in carbon monoxide is the low cost of reducing gas and in hydrogen it is the high rate of reduction. The present investigation was undertaken with the intention of determining the reduction behaviour of lump ore using carbon monoxide as gas reductant used in the blast furnace.

Microwave energy may be useful in several ways in enhancing the reduction of iron ore. A higher degree of reduction is commonly obtained by using traditional methods such as sintering and pelletizing but these would be highly uneconomical for small operations. In order to avoid preagglomeration steps as much as possible, microwave pretreatment of iron ore is being introduced.

It has been known for many years that microwaves are absorbed more readily by some minerals than others (Jacobs *et al*, 1982; Chen *et al*, 1984; McGill and Walkiewicz, 1987; Woodcock *et al*, 1989; Lanigan, 1989), leading to preferential heating of such minerals. This type of heating may give different effect to those obtained by application of conventional thermal energy (Worner *et al*, 1989). Few results have been published on the microwave heating characteristics of iron ore and those results which have been reported were concerned with pretreatment stages to some extractive metallurgical processes. More recently Barnsley *et al* (1989) have demonstrated some experimental alternatives in iron and steelmaking with microwaves. The purpose of the second part of this work is to illustrate some of the possible applications of microwave pretreatment of iron ore. This includes the effect of microwave treatment on the reducibility and the strength of iron ore and microscopical observation of the structural changes after microwave treatment.

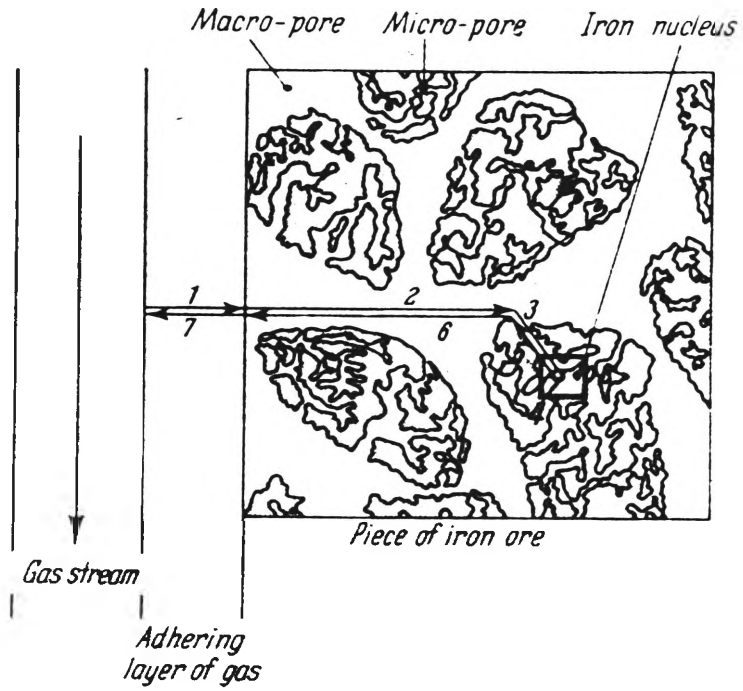

Figure 2.1. Outline of the reduction mechanism for porous iron ores

1. Diffusion of CO (H_2) across the boundary layer
2. Diffusion of CO (H_2) through the macropores in the ore
3. Diffusion of CO (H_2) through the micropores to the reaction position
4. Phase boundary reaction
5. Diffusion of CO_2 (H_2O) through the micropores
6. Diffusion of CO_2 (H_2O) through the macropores
7. Diffusion of CO_2 (H_2O) across the boundary layer. Migration of Fe^{2+} and 2 e to the iron nucleus.

(after Bogdandy *et al*, 1963)

2. THEORY

2.1. REDUCTION OF IRON ORES

The reduction of iron oxides has been the subject of numerous investigations. A collection and assessment of the work prior to 1967 has been given by Bogdandy and Engell (1971). More extensive studies have been reviewed (Evans and Koo, 1979) in detailed account of research carried out on a macroscopic scale; that is, on pellets, sinter or lump ore such as fed to the iron blast furnace or a direct reduction unit. The structure of the solid product during iron oxide reduction has an important role in all heterogeneous reactions.

2.1.1. MECHANISM OF REDUCTION

The transformation of iron oxide according to reaction

$$Fe_nO_m + m\,CO\,(H_2) \rightarrow n\,Fe + m\,CO_2\,(H_2O) \qquad [2.1]$$

and n = 1, 2 or 3 when m = 1, 3 or 4

in a number of subsidiary processes is shown diagrammatically in Figure 2.1 (Bogdandy *et al*, 1963).

For a goethite containing ore, initially, the goethite converts to hematite (Brown, 1980) on heating at moderate temperature by the following equation (Uwadiale and Whewell, 1988)

$$2\,FeO(OH) \rightarrow Fe_2O_3 + H_2O \qquad [2.2]$$

Then, hematite (Fe_2O_3) reacts with the gas reactant through reaction [2.1] to form magnetite (Fe_3O_4), wustite (FeO) and metallic iron.

2.1.2. KINETICS OF REACTION

Before the 1970's iron oxide reduction kinetics were generally interpreted by using the so-called 'shrinking core' or topochemical models, which postulated that the reacted, partially reacted, and unreacted regions in an iron oxide particle were separated by sharp interfaces. Good examples of descriptions of these shrinking core models are the papers by McKewan (1960),Spitzer *et al* (1968) and Hara *et al* (1976); these later workers developed models of considerable sophistication, postulating the existence of sharp interfaces between the progressively receding hematite - magnetite - wustite and iron layers in the course of reaction.

In general, these models were found to agree with overall rate measurements but, as was shown by Szekely *et al* (1976), the overall rate at which spherical pellets reacted with a reducing gas mixture was not very sensitive to the particular mechanism assumed, provided the interpretation was developed within the framework of a shrinking core model. It follows that the agreement between measurements and predictions could not really be used for the explanation of these models.

The 1970's brought a new approach to the study of gas-solid reactions. It was realized that when porous pellets were made to react with a reducing gas, the shrinking core representation was valid only as a limiting case, when the overall rate of reaction was limited by pore diffusion control. It follows that models postulating shrinking core behaviour for the reaction of porous pellets in the chemical or mixed control regimes would, in essence, constitute a contradiction in terms.

An important step in the understanding of hematite reduction kinetics with pure hydrogen was provided by Turkdogan and Vinters (1971, 1972) and Turkdogan *et al* (1971) who in a series of papers, reported on careful kinetics and structural measurements. They examined the reduction kinetics of a high-grade hematite ore with particle sizes ranging from about 0.4 to 15 mm diameter. There are three basic limiting rate processes in the gaseous reduction of sintered dense hematite pellets and natural hematite ore: (1) uniform internal reduction, (2) limiting mixed control and (3) gas diffusion in reduced iron layer, depending on particle size, temperature and gas composition. The key to a better understanding of rate phenomena involved in the reduction is the concept of partial internal reduction ahead of the nominal iron/wustite interface. Through a mathematical analysis, a rate equation was derived (Tien and Turkdogan, 1972) in a general form of partial internal reduction involving slow gas-wustite reaction and incomplete gas diffusion in the pores.

There is little agreement in the technical literature on the interpretation of experimental coverage of all the pertinent variables which have decisive influence on the rate of reduction. Also, because of the porous nature of iron oxides and the reaction products, the reactions investigated are inherently complex. The stagewise reduction from Fe_2O_3 -> Fe_3O_4 -> FeO -> Fe and the complexity of the individual steps makes the interpretation of the microstructural changes attributable to each of these transformations very difficult.

The complexity of the reduction process combined with the fact that under different experimental conditions the controlling stage of the reduction process may not be necessarily the same, has led workers in this field to a wide diversity of opinions regarding the reduction mechanism. Some authors studied gas diffusion controlled reaction (Warner, 1964), solid state diffusion controlled reaction (Edstrom and Bitsianes, 1955) and chemically controlled reactions (Watts *et al*, 1988) and also in mixed control kinetics (Yagi and Ono, 1975). Many others derived

mathematical models describing the reduction process as reviewed by Ramachandran and Doraiswamy (1982), but most of them are limited for certain conditions. Reduction with hydrogen (Turkdogan and Vinters, 1971), carbon monoxide (Fakhoury and Rosenqvist, 1978), mixture of hydrogen and carbon monoxide gasses (El-Geassy and Rajakumar, 1985; Meraikib and Friedrichs, 1987), natural gas (Wright, 1977) and gas methane (Ghosh *et al*, 1984) were also studied.

Macroscopic studies of iron oxide reduction at temperatures encountered in industrial processes have frequently led to the conclusion that the pore diffusion of gases is rate controlling, except for small particles (Turkdogan and Vinters, 1972). The pore diffusion of gases referred to here is the diffusion of gaseous reactants and products through porous reactant or product. The pore structure (porosity, pore size distribution) is therefore of significance in determining the reaction under conditions of pore diffusion or mixed control. Turkdogan *et al* (1971) showed that the structure of porous iron formed on reduction was very dependent on reduction temperature, being coarsest at higher reduction temperature. Structural changes were observed by Bradshaw and Matyas (1976) in the reduction of hematite. The reduction rate decreased with an increase in temperature and no microporosity was present in magnetite form at 1000° C and above. Koo and Evans (1979) showed that the structure of porous iron ores could be markedly altered by holding the sample at temperature prior to reduction. An important microstructural aspect of iron oxide reduction is therefore the development of porosity in solid reaction products.

Edstrom (1953) and Edstrom and Bitsianes (1955) used optical microscopy to study the relation between microstructure and reduction rate. They observed that the reduction of hematite occurred more rapidly when there was early and extensive formation of pores in the solid reaction products. Brill-Edwards *et al* (1965) studied the reduction of polycrystalline hematite and observed randomly distributed spherical pores for reduction temperatures between 400° and 700° C with elongated pores between 700° and 900° C. Edstrom (1953) also showed that iron

oxides reduced in hydrogen produced reduced oxides with finer pores than oxides reduced in carbon monoxide. Turkdogan and Vinters (1971) and Wright and Tyler (1979) confirmed this difference in pore structure caused by changing the reducing gas from hydrogen to carbon monoxide, and Turkdogan and Vinters (1972) also showed that the specific surface area decreased with increase in the temperature at which the oxide was reduced in carbon monoxide.

2.2. MODELS FOR GAS-SOLID REACTION

The shrinking core model was introduced by Yagi and Kunii (1955) as a first sample representation of the progressive conversion of solid particles by reaction with a gas. This model visualized a shrinking unreacted core surrounded by a growing layer of solid product with the controlling step being either reaction at the core boundary (reaction control) or diffusion through the product layer (ash diffusion control). For the stoichiometry

$$A_{(g)} + S_{1\,(s)} \rightarrow R_{(g)} + S_{2\,(s)} \qquad [2.3]$$

they obtained (Yagi and Kunii, 1955; Levenspiel, 1972) from this model the following simple solid conversion-time expression for spherical reacting particle; For reaction control

$$\frac{t}{\tau} = 1 - (1 - X)^{1/3} \quad ; \quad t = \frac{r_s R}{K_c C} \qquad [2.4]$$

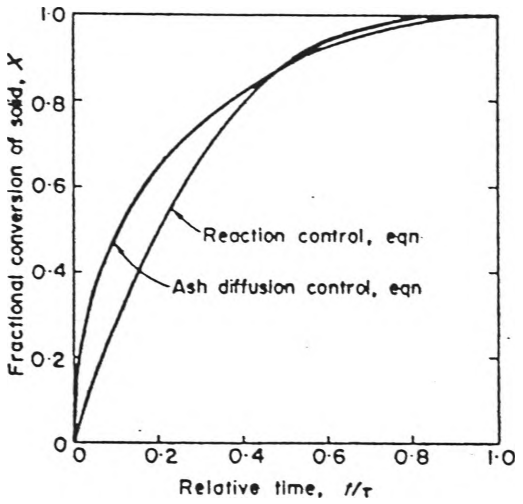

Figure 2.2. Conversion of solid vs time of reaction for the shrinking core model.

(after Park and Levenspiel, 1975)

For ash diffusion control

$$\frac{t}{\tau} = 1 - 3(1 - X)^{2/3} + 2(1 - X) \quad ; \quad t = \frac{r_s R^2}{6DC} \qquad [2.5]$$

where τ is the time required for complete conversion.

Figure 2.2 shows how the conversion of solids changes with time for this model and a plot of the above expressions provides a simple test for the predictions of the model. Because of its simplicity and reasonably good fit for a variety of reacting solids, Levenspiel (1972) recommended that this model be tried first.

Numerous extensions to this model have been proposed. Most of these fall into two general classes, typical of which are the porous pellet model of Ishida and Wen (1968), and the grainy porous pellet model of Sohn and Szekely (1972).

Ishida and Wen (1968) visualized gas penetrating the porous pellet, reacting progressively with it, eventually leaving behind a growing layer of completely converted solid.

Somewhat different to this, Sohn and Szekely (1972) viewed the pellet as a porous solid consisting of grains. Reactant gas diffused through interstices between grains into the pellet attacking each of the grains according to the shrinking core model.

Both these models and their variations viewed the pellet as originally porous, both included diffusional gradients, both had at least two parameter models and the latter required a computer generated numerical solution for the conversion-time expression (Levenspiel, 1972).

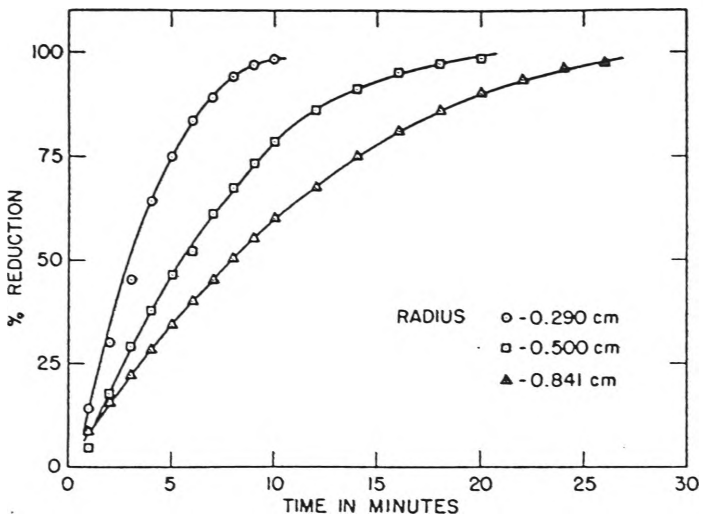

Figure 2.3. Reduction of sintered spheres of Venezuelan ore at 811° C in hydrogen.

(after McKewan, 1960)

Park and Levenspiel (1975) proposed a one parameter model to represent the reaction of an initially non-porous solid with gas. At one extreme this model reduced to the simple shrinking core model, at the other extreme it predicted uniform conversion of solid throughout the pellet following an instantaneous conversion to intermediate. Simple conversion-time expressions were obtained, methods of comparison with data were suggested, and a good fit was shown for reported iron ore reduction data.

McKewan (1960) reported that in the reduction of iron oxide using hydrogen, the rate of hydrogen consumption varied greatly depending on the temperature, gas concentration and the size of the particle. Also a considerable excess over actual reaction requirements was necessary to maintain proper reduction equilibrium. Typical normal reduction curves shown in Figure 2.3, as reported by McKewan (1960) shows continually decreasing weight losses per unit time as the reduction proceeds. However, if the gas supply was inadequate, the weight loss per unit time remains constant for some period. McKewan also suggested that it is possible to recognize and avoid the effect of gas starvation by using equation :

$$r_0 d_0 [\, 1 - (1 - X)^{1/3} \,] = K t \qquad [2.6]$$

This mathematical model was developed in support of the mechanism based on the assumption that the reaction rate is proportional to the surface area of the reacting interface. The fractional reduction X is, defined as the weight of oxygen removed, divided by the total weight of oxygen originally present as iron oxide. From the experimental data of the type shown in Figure 2.3, values of $r_0 d_0 [\, 1 - (1 - X)^{1/3} \,]$ can be determined and plotted against time, t. A straight line plot indicates that the reduction process obeys the model upon which the formula is based. In addition the

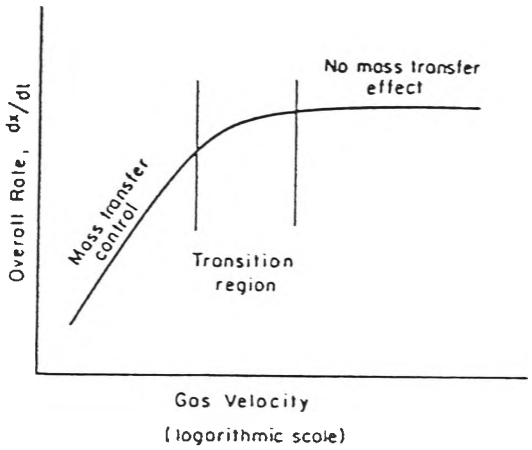

Figure 2.4. The minimization of external mass transfer effects by operation at high gas velocities.

(after Szekely *et al*, 1976)

slope of this plot gives the value of reaction rate constant, *K*. Many experimental results have shown a linear relation between the growth of the porous layer and time, at least during the early stages of reduction and sometimes up to 60 to 80% reduction. Beyond this, the plot deviates from a straight line showing that some other mechanism is controlling the rate of reduction. Because the thickness of the reduced iron layer is increasing with time, it is reasonable to assume the gaseous diffusion is controlling.

2.3. DETERMINATION OF THE RATE CONTROLLING FACTOR

The kinetics and rate-controlling factors of gas-solid reaction are deduced by noting how the progressive conversion of particles is influenced by particle size and operating temperature (Levenspiel, 1972). This information can be obtained in various way, depending on the facilities available and materials at hand. The following observations are a guide to experimentation and to the interpretation of experimental data.

2.3.1. EFFECT OF FLOWRATE

Szekely *et al* (1976) suggested that the first step in experimental studies of gas-solid reaction was to establish whether gas phase mass transfer (gas film boundary layer) was rate controlling, or at least played an important role. This could be done by reacting specimens of regular geometry (preferably spheres) with a moving gas stream at various gas velocities. Furthermore mass transfer effects could be minimized by operating the gas-solid reaction system at sufficiently high velocities, so that any further increase in the gas velocity did not produce an increase in the overall reaction rate, as shown in Figure 2.4. Under these conditions some factor other than mass transfer would become rate controlling. While this

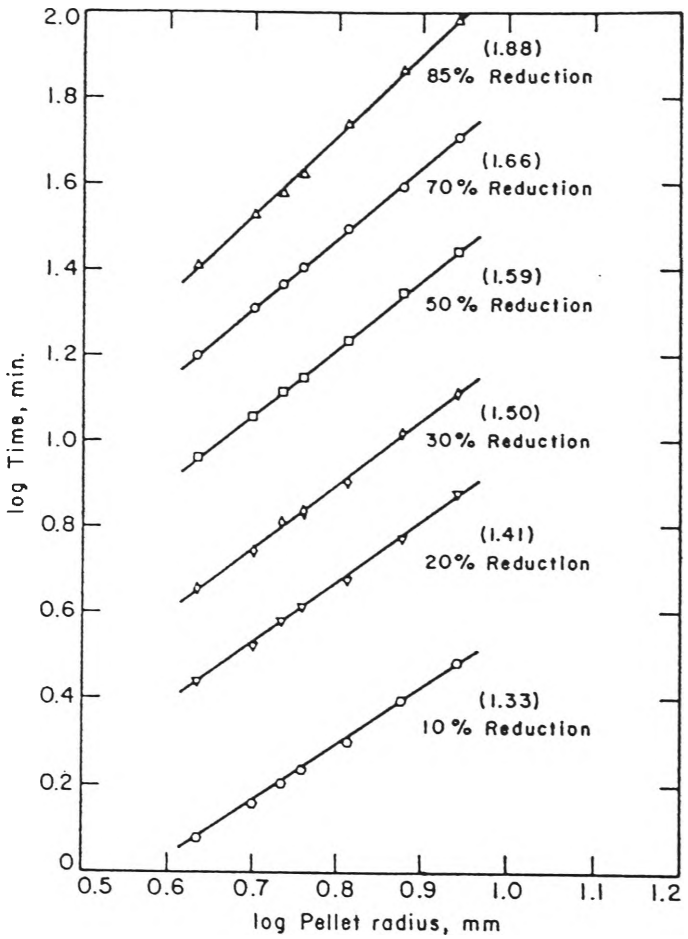

Figure 2.5. Plot of log time versus log pellet radius.

(after Seth and Ross, 1965)

procedure appears attractive in principle, it may not be feasible in practice, particularly as the mass transfer coefficient is proportional to the square root of gas velocity and high gas velocities would interfere with the operation of conventional recording balance. Although the boundary layer effect cannot be completely eliminated, it can be decreased to negligible proportion in comparison to other effects, so that it will not be the rate determining step (Ross, 1980).

2.3.2. EFFECT OF PARTICLE SIZE

Mixed control has been proposed by several experimenters to reconcile the complexities and conflicting results obtained with the simpler mechanism. In mixed control, the gas-boundary layer, the phase-boundary and gaseous diffusion act together under pseudo-steady state conditions to determine the overall reaction rate.

Because the time for reduction is proportional to the particle size for reaction control (Equation 2.4) and to the square of particle size for gaseous diffusion control (Equation 2.5), a logarithmic plot of time, t, versus particle size with degree of reduction as a parameter should yield slopes of unity and two for reaction and diffusion control respectively. For mixed control the slope of such a plot should be between 1 and 2 and should be expected to increase in value as the reduction becomes more complete. Figure 2.5 shows plot of log time versus log pellet radius from various stages of reduction for hematite pellets varying in size from 8.6 to 17.5 mm in diameter reduced at 750° C. These plots show that initially (10% reduction) the slope is 1.33 but as reduction proceeds the slope gradually increases to a value of 1.88 for 85% reduction. These results indicate that reduction process is controlled by a combination of reaction and gaseous diffusion. Initially, when the slope is close to unity, the rate of reduction depends predominantly on the reaction, but as reaction

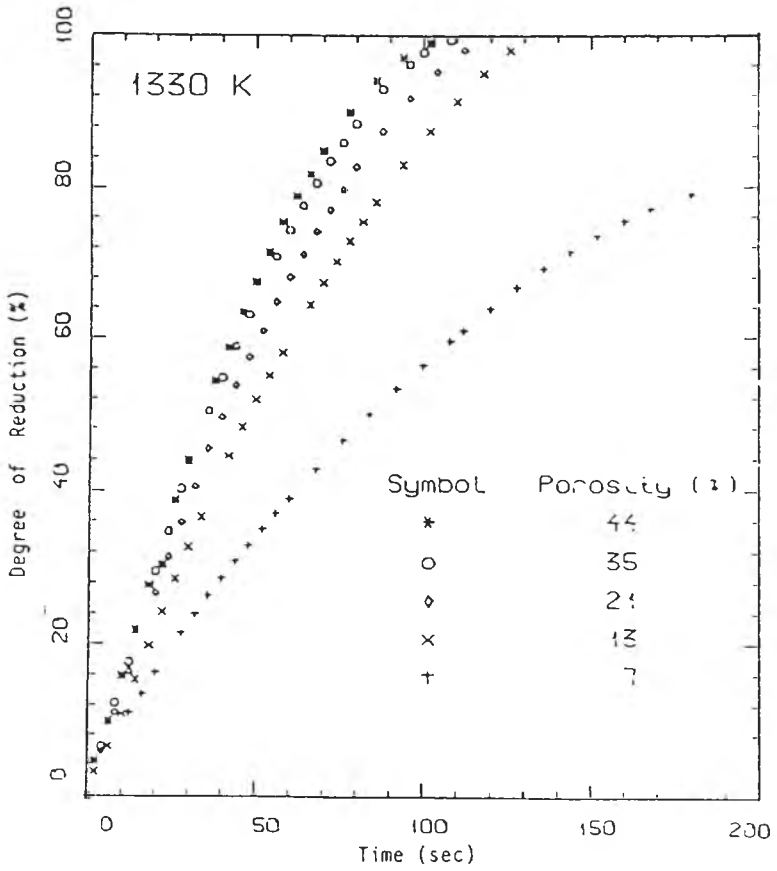

Figure 2.6. Effect of sample porosity on the kinetics of reduction of hematite by hydrogen.

(after Du *et al*, 1988)

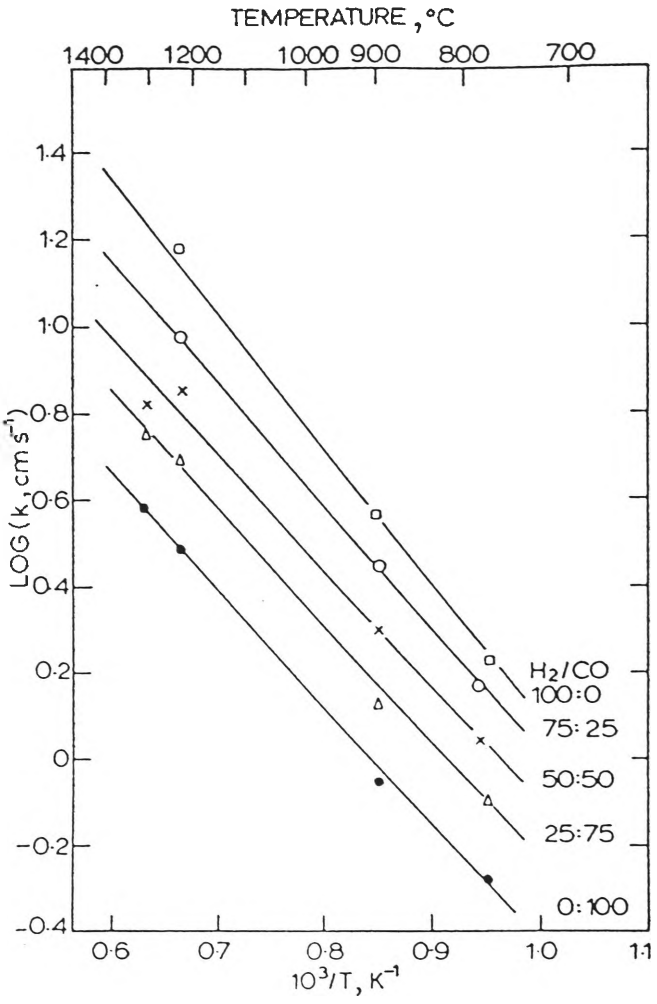

Figure 2.7. Arrhenius plot corresponding to initial reduction rate.

(after Towhidi and Szekely, 1981)

proceeds, the uniform and gradual increase in the slope shows that gaseous diffusion is becoming more and more important.

Levenspiel (1972) also showed that the time needed to achieve the same fractional conversion for particles of different but unchanging sizes is given by

$t \propto R^{1.5 \text{ to } 2.0}$ for gas film diffusion controlling

$t \propto R^2$ for ash diffusion controlling

$t \propto R$ for chemical reaction controlling

Because of the complexity of these reduction processes, no single mechanism can properly describe the reduction path over the ranges of temperature, gas composition, particle size and chemical composition of practical and experimental importance. It is reasonable to conclude, however, that gaseous diffusion is the most important factor in the kinetics of iron oxide reduction, as was revealed by recent work of Du *et al* (1988) in Figure 2.6 on the effect of the initial porosity of the ore particle on reduction kinetics.

2.3.3. EFFECT OF TEMPERATURE

It is well known that the rate of chemical reaction increases as the temperature increases; hence, experiments at different temperatures should easily distinguish between ash or gas-film diffusion on the one hand and chemical reaction on the other hand as the controlling step. Apparent activation energy obtained from the slopes of the Arrhenius type plot corresponding to the reduction rate indicate that reactions with high activation energies are very temperature-sensitive and reactions with low activation energies are relatively temperature-insensitive (Levenspiel, 1972).

Figure 2.7 (after Towhidi and Szekely, 1981) show the apparent rate constant increased with increasing hydrogen content of the reducing gas. The apparent activation energies appear to range from 12.5 kcal/gmol for CO reduction to 14.5 kcal/gmol for the reduction with hydrogen.

2.4. MICROWAVE HEATING

The effect of microwave energy on selected minerals and their general behaviour has been reported by Chen *et al* (1984) and more recently the effect of microwave heating in mineral processing was studied by McGill *et al* (1988), which showed that many minerals absorb microwaves and are rapidly heated.

Further research by Walkiewicz *et al* (1988) showed that microwave energy induced thermal stress cracking which decreased the grinding energy and by considering other factors in the extractive process, the use of microwave energy could be economical. This was because thermal expansion of the selectively heated materials and not of the adjacent gangue matrix also offered the potential to more cleanly liberate ore minerals at larger ground-particle sizes. This would reduce the grinding energy requirements as well as improve the concentrate grade and metal recovery after beneficiation. More selective leaching, more efficient flotation or better magnetic separation could be accomplished on the microwaved ores. Metal extraction from laterite ores using microwave energy has also been reported (Kruesi and Kruesi, 1984), in the extraction of gold (Woodcock *et al*, 1989) and in the processing of manganese ore (Lanigan, 1989). More recently microwave treatment of composite ores (Worner *et al*, 1989) produced metal alloys and it has been reported (Barnsley, 1989) that iron and steel could be produced by microwave energy in combination with other forms of energy.

2.4.1. THERMAL CONVERSION MECHANISM WITH MICROWAVES

Microwaves are forms of energy that are manifested as heat through their interaction with materials as stated by Schiffmann (1987). If dipolar rotation is the major microwave heating mechanism, then the power absorbed in a unit volume of dielectric material and dissipated as heat, depends on the dielectric properties of the material and the electromagnetic field parameters, i.e. the frequency of the electromagnetic waves (f, Hz) and the field intensity within the material E (V/m). The power is given by (Strumillo and Kudra, 1986; Schiffmann, 1987)

$$P = k E^2 f \varepsilon' \tan \delta \qquad [2.7]$$

or

$$P = k E^2 f \varepsilon'' \qquad [2.8]$$

where k = constant dependent upon the unit of measurement used
$= 2\pi\varepsilon_o$

ε_o = the permittivity of free space (8.854×10^{-12} F/m)

E = electric field strength, in volt per unit distance

f = frequency

ε' = relative dielectric constant

$\tan \delta$ = loss tangent or dissipation factor

ε'' = loss factor
$= \varepsilon' \tan \delta$

The above expressions show that the power absorbed is proportional to the square of the electric field in the material. Furthermore, the heating rate of a sample being irradiated should increase with an increase in power as predicted by McGill *et al* (1988). However, a further examination of this equation (Schiffmann, 1987) reveals that E and f are function of the equipment, whereas ε', ε'', and $\tan \delta$ are factors related to the material being heated. It is possible that those factors related to the

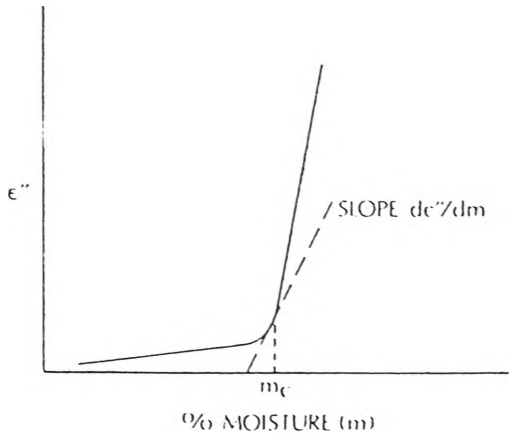

Figure 2.8. The critical moisture content m_c.

ε" is the dielectric loss factor. The region below m_c is indicative of bound water, whereas above free water is more easily removed.

(after Metaxas, 1974)

materials could eliminate the effect of the the power input. This may prevent increase of temperature under otherwise similar conditions of microwave irradiation.

2.4.2. MICROWAVE DRYING

If microwave drying is concerned with removal of water as stated by Schiffmann (1976), Figure 2.8 shows a general graph of the variation in loss factor with moisture content (after Metaxas, 1974). The different regions of the graph, as indicated by the change of slope (d£"/dm), show that at low moisture content, the region below the critical moisture content is associated with bound water; above the critical moisture content primarily free water is involved. Furthermore Schiffmann stated that the change in the slope may be quite gradual for some materials, making positive identification fairly difficult and estimated that for non-hygroscopic material the critical moisture content was in the region of about 1%.

Water, as already noted (Emsley, 1988), is a strong absorber of microwave energy and heats up when irradiated. Hence wet, or damp, minerals or ore also heat up and tend to dry out when treated with microwaves. This heating could provide a 'triggering' effect for further heating or other reactions. Water-containing minerals (*i.e.* containing water of crystallization or even water in the lattice) would be expected to absorb microwave energy and heat up. They could lose the water and this would cause changes in their crystal structure.

The US Bureau of Mines has studied the effect of microwave input power on the heating rates of selected chemicals and minerals. It was found that some materials showed negligible changes with increased power, including extremely high loss (PbS, Fe_3O_4) and low loss (SiO_2, $CaCO_3$) materials. It was also reported that many of the minerals reached a critical temperature at which an uncontrolled rise in temperature occurred, known as the 'run-away' effect. The temperature rise

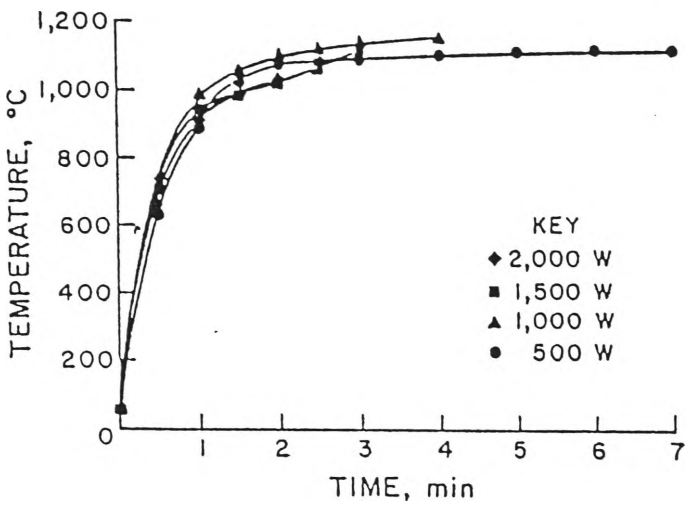

Figure 2.9. Effect of microwave incident power on the heating rate of Fe_3O_4.

(after McGill *et al.* 1988)

Table 2.1. Effect of microwave heating on the temperature of natural minerals.[a,b]

(after McGill *et al*, 1988)

Mineral	Chemical composition	Temp, °C	Time, min
Albite	$NaAlSi_3O_8$	82	7.
Arizonite	$Fe_2O_3 \cdot 3TiO_2$	290	10.
Chalcocite	Cu_2S	746	7.
Chalcopyrite	$CuFeS_2$	920	1.
Chromite	$FeCr_2O_4$	155	7.
Cinnabar	HgS	144	8.
Galena	PbS	956	7.
Hematite	Fe_2O_3	182	7.
Magnetite	Fe_3O_4	1,258	2.75
Marble	$CaCO_3$	74	4.25
Molybdenite	MoS_2	192	7.
Orpiment	As_2S_3	92	4.5
Orthoclase	$KAlSi_3O_8$	67	7.
Pyrite	FeS_2	1,019	6.75
Pyrrhotite	$Fe_{1-x}S$	886	1.75
Quartz	SiO_2	79	7.
Sphalerite	ZnS	87	7.
Tetrahedrite	$Cu_{12}Sb_4S_{13}$	151	7.
Zircon	$ZrSiO_4$	52	7.

[a]Maximum temperature obtained in the indicated time interval.
[b]High purity as identified by X-ray diffraction.

caused the loss factor of the material to increase, which, in turn, resulted in a further temperature increase. It was reported that Fe_3O_4 reached a temperature of 1000° C in less than 1 minute as shown in Figure 2.9 (after McGill *et al*, 1988) and the data showed that an increase in power would not improve the heating rate of Fe_3O_4 but that 500 W was as effective as 1000 and 2000 W. Further results as tabulated in Table 2.1, showed that Fe_2O_3 only slightly increased in temperature after 7 minutes treatment as compared with the Fe_3O_4 after less than 3 minutes. It was suggested that the selection process for good ore candidates for continued fracturing studies as reported by McGill *et al* (1988) would be improved by using these power and heating rate data. The power level necessary for the heating effect also could be predicted using these empirical data.

Baghurst and Mingos (1988) reported that at power levels of 50 - 500 W some oxides, including Fe_2O_3, did not greatly absorb microwave energy.

Walkiewicz *et al* (1988), also reported that the addition of a good microwave absorber, such as magnetite, to a feed that was transparent to microwaves was useful to broaden the range of potential applications for microwave heating of ores and concentrates. They found that although little or no microwave heating was obtained with Hg, HgS or the concentrate, adding 20 % magnetite to the mercury concentrate raised the temperature above 600° C which was hot enough to vaporize mercury and sulfur from the sample.

Woodcock *et al* (1989) reported that iron oxide, especially magnetite, readily absorbed microwave energy and became hot. While hematite remained unchanged chemically by such treatment, magnetite could be converted to hematite due to exothermic oxidation encouraged at high temperature (Lanigan, 1989). However it was also reported that more work was required with goethite and limonite on the effect of microwave treatment.

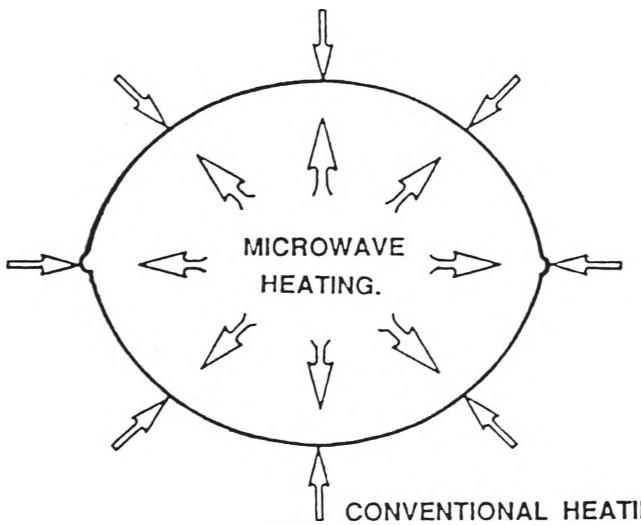

Figure 2.10. Two ways of heating a pillow shape briquette.

(after Worner *et al*, 1989)

The distinction of microwave heating from the conventional techniques or radiation heating is shown diagrammatically in Figure 2.10 (after Worner *et al.* 1989). It appears that microwaves heat from the inside and conventional heating heats from the surface of the ores.

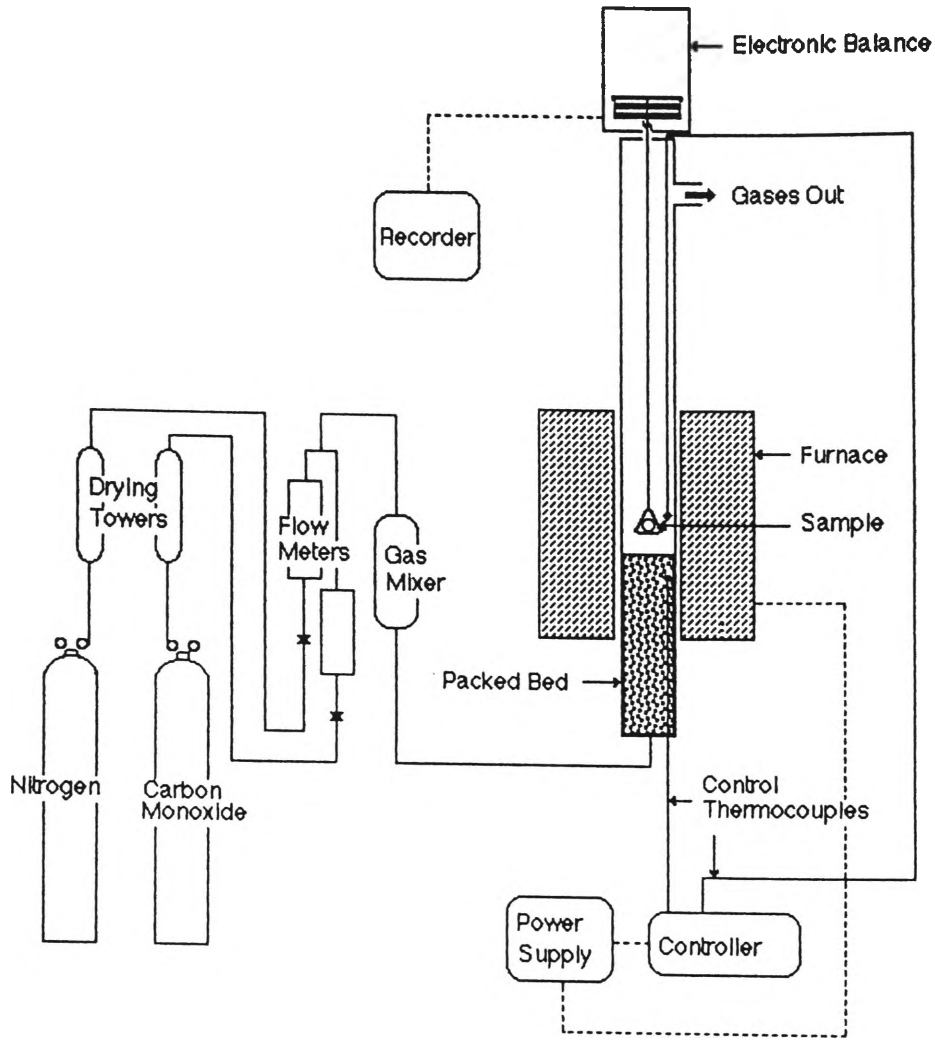

Figure 3.1. Schematic diagram of thermogravimetric apparatus.

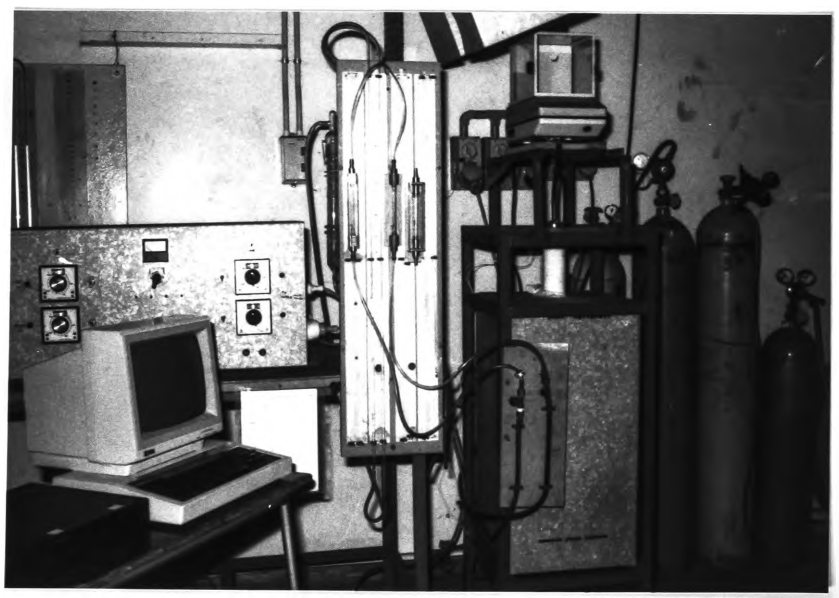

Figure 3.2. Photograph of the experimental set-up.

3. EXPERIMENTAL

3.1. PREPARATION OF MATERIALS

Magneto-hematite lumps of ore were supplied as blast furnace feed from Lampung iron mines. To obtain approximately the same size of surface on every sample, the ore was crushed in a mortar and pestle and wet ground into spherical shape by using Boehler SURFMET II belt grinder Grit P120 in the size range from 7 to 16 mm of diameter, and was dried for 24 hours at 120° C before being tested.

These samples were divided into 3 groups of sizes, small (7 to 9 mm), medium (10 to 12 mm) and large (13 to 15 mm) diameter. Prior to the reduction studies the ore samples were examined by optical and scanning electron microscopy, x-ray diffraction, and density and porosity measurements by oil impregnation were also carried out. Some of these techniques were also used to characterize the ore following microwave pretreatment and to investigate the samples after reduction.

3.2. REDUCTION TEST

3.2.1. APPARATUS

Figure 3.1 is a schematic diagram of the apparatus used in the experiment as a typical system for studying gas - solid reactions using a recording balance and the experimental set up used is shown in Figure 3.2.

As illustrated in the thermogravimetric apparatus (Figure 3.1), a sample particle that was to be reacted was suspended by a wire rod from a sensitive electronic balance. The sample was positioned in a vertical tube furnace, the reaction gas was passed up the tube through a packed bed of alumina rings from an inlet in the base of the tube to provide a plug gas flow and preheat. To begin the experiment, the sample was attached to the sample holder, an inert gas (in this experiment, nitrogen) was passed through the tube, and the furnace is brought to the reaction temperature. The reaction is started by replacing nitrogen with carbon - monoxide.

3.2.2. ELECTRONIC BALANCE

The electronic balance was the CHYO model JP-300W, with a sensitivity of 0.001 g and 0.01 g for up to 30 g and 300 g of sample weight, respectively. The single-pan digital balance was able to weigh samples from both the top and the bottom of the weighing pan. During the experiment, a continuous weight loss measurement of the sample was able to be recorded on the attached computer and also displayed on the video display unit.

3.2.3. COMPUTER

A BBC Micro computer model B with a memory of 32K bytes was linked to the balance via interface RS 232 and RS 423 in the balance and the computer respectively. A data logger program was used to continuously record the signal indicating the sample weight changes during the experimental run. The program is attached in Appendix A-1; the results were also used to plot conversion-time data and possible correlations with various reduction models.

3.2.4. TUBE FURNACE

The furnace consisted of an alumina vertical tube, two heating element units, two Pt - Pt + 13% Rh thermocouples, sample holder and alumina rings.

The tube was 1000 mm in height and 70 mm ID. Alumina rings were packed 250 mm in height at the lower part of the tube to preheat the reactant gas as the gas entered through an inlet in the base of the tube and was passed upward. To prevent excessive concentration of carbon monoxide in the laboratory, adequate ventilation was provided by means of a hood equipped with an exhaust fan at the outlet on the top of the furnace and a carbon monoxide alarm was also in continuous use.

Heating was provided by eight Crusilite elements which were divided into two units. Each unit was symmetrically placed around the tube at the upper and the lower part of the tube.

The furnace temperature was controlled by two Pt - Pt + 13% Rh thermocouples attached to a control box. Each of the thermocouple tips was placed close to the hottest part of the upper and the lower part of the furnace. The furnace temperature profiles for different temperature are indicated in Appendix A-2.

The sample holder used was made from 0.75 mm Ni-Cr wire and was suspended from the balance by Ni-Cr wire hooks. The length of the wire was adjusted to place the sample holder in the hot zone of the upper furnace and at about 5 mm from the tip of the thermocouple.

3.2.5. HEATING AND CONTROL CIRCUITRY

The control thermocouples were attached to two West MC 30 MK II adjustable temperature controllers up to 1600 °C, TRIAC-25 amperes solid state contactor and a 15 amperes transformer.

A constant voltage transformer made it possible to maintain a centre - zone temperature in the furnace constant to ± 5 °C. A manual switch was used to adjust the output of the transformer at any desired value i.e. either high or low temperature.

3.2.6. REACTANT GAS

Carbon monoxide and nitrogen, obtained from the Commonwealth Industrial Gases Pty Ltd (CIG), were used as reactant gases in most experiments. CO gas was a C.P. Grade with the purity of 99.5% min. and N_2 gas was of High-Purity ('oxygen free') grade with above 99.99%. CO and N_2 gas cylinders contained 4.9 m^3 and 6.4 m^3 of the gas respectively.

3.2.7. GAS FLOWMETER

A rotameter, GA Platon Flow Control type C6 having a range of 200-4000 cc/min was used to measure the flowrate of both CO and N_2 gas from pressurized cylinders. A general calibration curve for the gas is given in Appendix A-3.

3.2.8. SINGLE PARTICLE EXPERIMENT

Before each experimental run, the weight, diameter and the type of the sample were noted and stored as a computer file.

The sample particle was then placed in the sample holder suspended from the base of the balance with an adjusted wire. The furnace was flushed with nitrogen and the nitrogen flow was continued as the sample and the tube furnace were slowly heated to the desired temperature. After reaching the desired temperature and a constant weight of the sample being observed, the nitrogen gas

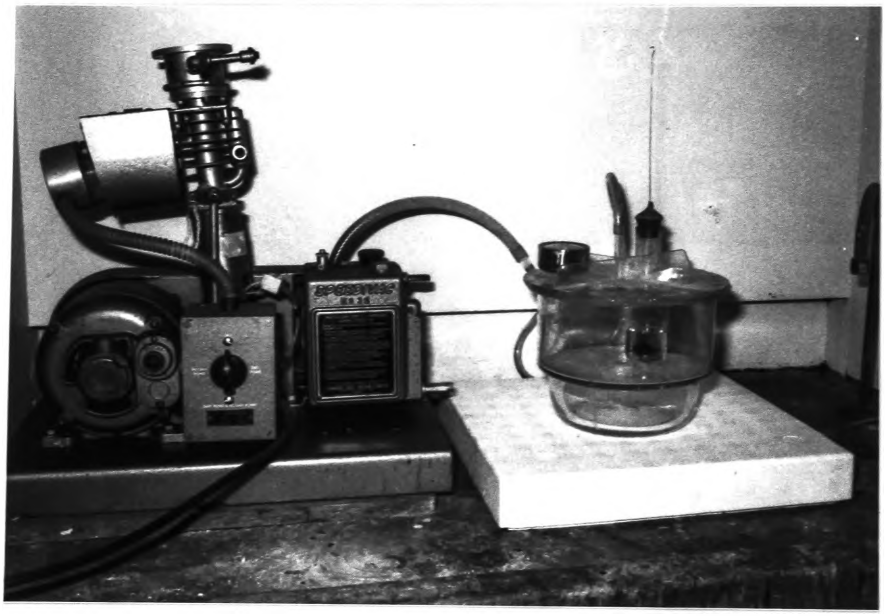

Figure 3.3. Photograph of the impregnation unit.

was then replaced by carbon monoxide and the weight of the sample, temperature and gas flowrate were monitored from that moment until the end of the reaction or the pre-determined degree of reaction. The computer was also activated to monitor the sample weight - loss and recorded the data every 60 seconds.

At the end of each run the furnace was switched off and a stream of nitrogen flush was introduced so that the sample was cooled to room temperature in about 1 hour. The sample weight was recorded immediately after each run and the sample was then subjected to programmed tests.

3.3. MICROSCOPIC ANALYSIS

3.3.1. PREPARATION OF SAMPLES

Sample specimens i.e. raw ore particles and reduced materials were cast in a LECO reusable plastic mold. The resin used was Araldite M with an Araldite HY 957 as a hardener in ratio of 10 to 1 by volume. This epoxy resin was normally left to harden overnight at room temperature but the hardening time could be reduced to approximately 3 hours by heating in the oven at around 60 °C.

A simple impregnation unit (Kopp and Muller, 1985) with a low evacuation volume and a pressure gauge were used to provide a good penetration especially for porous samples as shown in Figure 3.3. The evacuation chamber was connected to the vacuum pump whereby the impregnated resin could be sucked into the evacuated chamber containing the specimen by a further plastic tube that could be closed. The pumping time varied from between 5 and 30 minutes depending on the porosity. The required amount of resin was then thoroughly mixed with the hardener for approximately 2 minutes

Figure 3.4. Photograph of the metallographic microscope.

Before introducing the resin the pressure at the manometer was monitored and adjusted by careful venting to between 80 to 130 mbar. At low pressure the inflowing resin began to boil as its highly volatile components escaped. The resin was then slowly fed in by opening the tube clamp until the mold was filled. The increasing pressure forced the resin into the hollow spaces.

The next step was a two-stage grinding procedure. The sample mount was removed from the mold and ground on a pregrinder fitted with a 240 grit silicon carbide paper disc using water as lubricant. After flattening the surface, grinding was continued until the sample was sufficiently exposed on the surface of the specimen. The specimen was then washed and transferred to a pregrinder fitted with 600 grit paper. Grinding was carried out manually without undue pressure and normally took from 3 to 5 minutes per specimen. After drying, the specimen was ready for polishing.

Polishing was carried out on another manual cloth coated disc using diamond paste. For most materials (Van de Pijpekamp, 1971) three stages of polishing were used, employing 6, 3 and 1 µm diamond pastes. An ultrasonic cleaner was required for cleaning the samples after each stage. On average total polishing times were from 1 to 2 hours, depending on the nature of the specimen being polished.

3.3.2. OPTICAL MICROSCOPY

3.3.2.1. APPARATUS

The microscope was of the inverted type, LEITZ Micro - Metallograph Model MM6, where specimen and stage surfaces were in one identical plane as shown in Figure 3.4. This unit consisted of visual microscopy, viewing screen, large-format camera and 35 mm camera Orthomat. The latter was used in reproducing the image

of the polished samples throughout the experiment. The magnification range from 5 to 200 times could be obtained in the negative point.

3.3.2.2. PROCEDURE

The filament lamp controlled by a separate transformer was switched on and the ammeter was set to approximately 4 amperes. The appropriate objective was selected by lowering the objective carrier thus giving free access to the nosepiece for selection of desired objective. It was ensured that the nosepiece click stop was properly engaged. When positioning the polished sample specimen, the centre position of the stage was adjusted so that its index lined up with scale values 10 and 30. The objective selection lever was then swung frontwards into working position. The analyzer control lever was turned to the 45 degree position and polarized or reflected light was selected. The brightfield/darkfield lever was turned fully to the right, into the brightfield position. The stage was brought down to its end stop by turning the coarse focusing knob. After checking that the two levers were in "V" position, the field diaphragm was closed by turning its lever, and the aperture diaphragm was opened by turning the lever downwards. The fine focusing control was turned until the sharp image of the field diaphragm came into view and then the field diaphragm was opened until its image was just below the periphery of the visible field. The eyelenses were adjusted on both eyepieces so that the eyepiece diaphragm was sharp in focus. The specimen image was refocused with fine focusing control if needed.

A photograph of the specimen image was taken by pressing the camera exposure button from the control panel which was built into the microscope base and for photographic purposes a Xenon arc lamp was used.

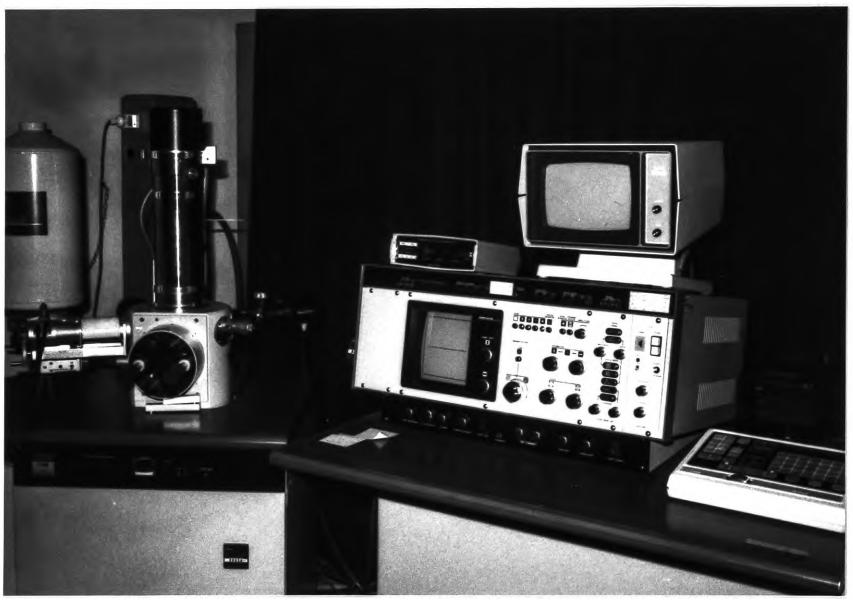

Figure 3.5. Photograph of the scanning electron microscopy apparatus.

3.3.3. SCANNING ELECTRON MICROSCOPY

3.3.3.1. APPARATUS

Scanning electron microscope used was HITACHI model S-450 with magnification ability in the range of 20 to 20,000 times. This equipment consisted of the main console, a displaying unit and a photographical unit as shown in photograph in Figure 3.5.

3.3.3.2. PROCEDURE

A similar sample for optical microscopy observation was used particularly when the magnification required during observation was beyond the capability of the optical microscopy. For this purpose the mounted sample had to be put on the specimen stub being inserted into the specimen stage of the unit.

The operation was begun by turning on the main power distribution panel and tap water was run to cool the vacuum pump. Making sure the liquid nitrogen tank was full, the rotary pump was switched on to start the evacuation pump. The automatic evacuation was started by depressing the evacuation push button switch and finished in about 20 minutes with the high vacuum indicator on.

Specimen exchange could be done by depressing the "off" push button switch on the display unit and the control specimen stage knobs were set to the exchange position. Then the air switch button was pushed on to evacuate the chamber so the specimen stage could be pulled out. The specimen stub for the previous observation was removed from the specimen holder and the new specimen was re-installed in the specimen chamber after being fixed securely on the specimen holder. The chamber was again evacuated.

Back Scattered Electrons (BSE) were used to provide better atomic number contrast image than the Secondary Electron (SE) on an atomic number contrast specimen. A preliminary step operating the display unit was to ensure that the Robinson Detector Electron Microscopy (RDEM) unit was fully engaged. The appropriate accelerating voltage was selected to 25 kV and the power for RDEM was turned on, the brightness control was adjusted until the scan-line was readily visible.

A good image of the sample on the screen could be made by adjusting the contrast and brightness buttons. By adjusting the scan-line to the middle of the screen and the intensity width to about 10 mm. a good image could be produced. A sharp image then could be obtained after operating the viewing mode. focus and astigmatism controls.

Photo recording was taken for the selected image of the sample by depressing the photo exposure button after making sure that the previous exposure was advanced and the shield was removed.

A different electron microscope in BHP Central Research Laboratory. model PHILIPS-505 provided with an Energy Dispersive X-ray analyzer. EDAX model PV 9100/65, was used to obtain the compositions of the various phases.

3.4. DENSITY AND POROSITY MEASUREMENTS

The density and porosity of the sample before and after the reduction test were determined (ANSI/ASTM B 328-73, 1979) by measuring the weight of the sample in air and in water. The weight of an oil-impregnated sample was obtained after the sample was immersed in oil held at room temperature to about 15 in.Hg pressure for 30 minutes, or until no visible air bubbles came out of the sample, in an evacuating chamber as used in the impregnation of resin mold as shown in Figure

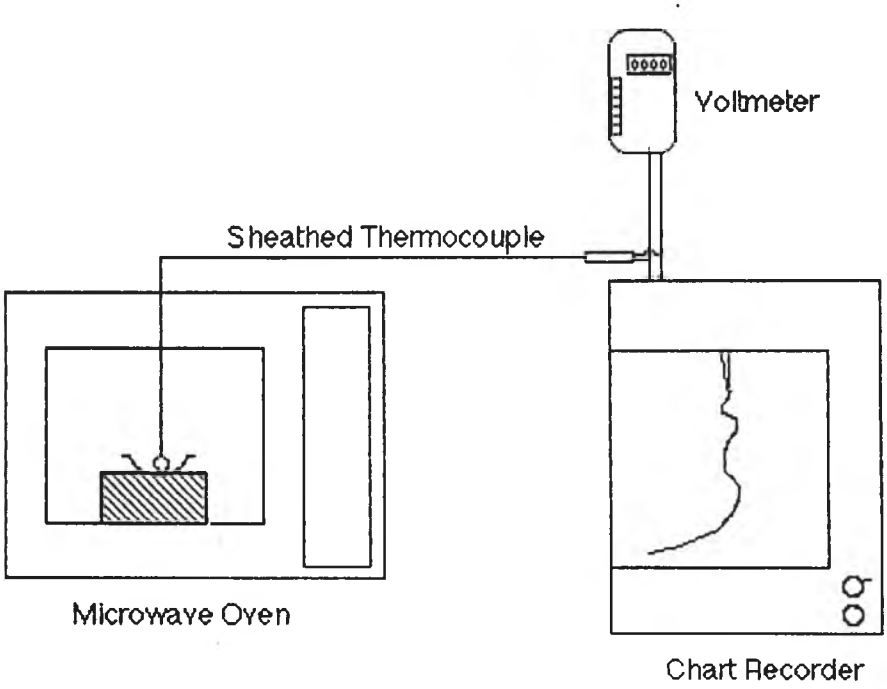

Figure 3.6. Schematic diagram of microwave treatment apparatus.

3.3. After which the pressure was permitted to increase to atmospheric pressure and the sample remained in oil for another 15 mins.

A single-pan electronic balance (CHYO model JP-300W) was used to measure the weight of the dry and oil-impregnated sample. A fine wire, 0.20 mm in diameter, suspended from the bottom hook of the balance, supported the sample in a beaker of distilled water. The wire was twisted around the sample and suspended from the hook so that the sample was completely immersed in the water. Care was taken to ensure that the sample was covered by about 10 mm of water, the wire twist was completely submerged and that no air bubbles adhered to the sample on the wire. After the weight of sample and wire in water were measured, the sample was removed and the wire was reweighed in water, immersed to the same point as before.

3.5. MICROWAVE TREATMENT

3.5.1. APPARATUS

Microwave treatment was carried out in commercial domestic ovens, Sharp model R-2370 and R-9360 ovens, with a peak output power rating of 1300 and 700 W, respectively, at a frequency of 2450 MHz. The power setting was 100%, and the samples were irradiated continuously inside the oven.

Each sample was placed in a ceramic crucible and supported on an insulation brick in the centre of the oven. The apparatus arrangement is shown in Figure 3.6. The effect of microwave treatment was studied by exposing the sample to microwave irradiation for a definite time. At the end of the microwave treatment, the samples were air cooled and then weighed.

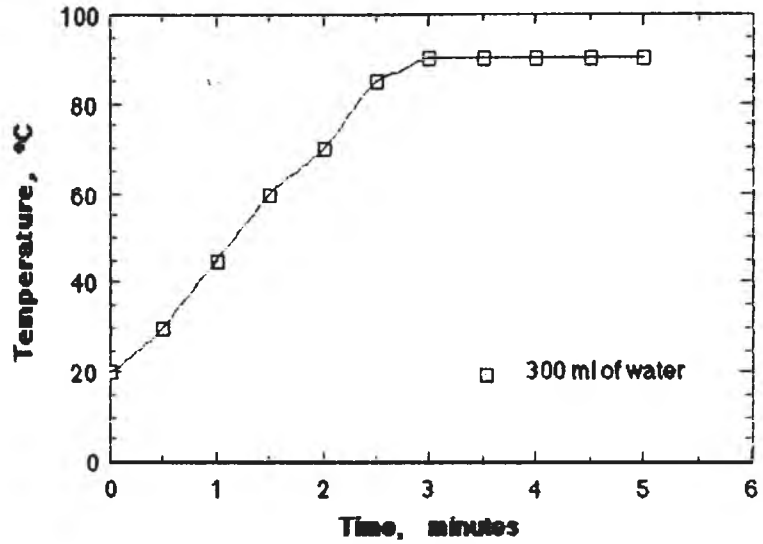

Figure 3.7. The effect of 700 W microwave treatment on heating rate of 300 ml of water.

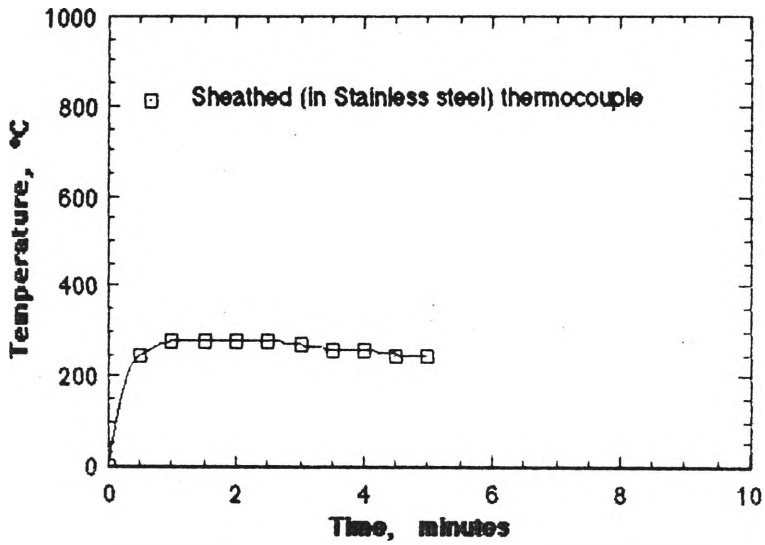

Figure 3.8. The effect of 700W microwave treatment on thermocouple indicator.

3.5.2. TEMPERATURE MEASUREMENT

A sheathed thermocouple (Walkiewicz *et al*, 1988) was inserted through the roof of the cavity into a hole drilled in the sample to continuously monitor temperature. The thermocouple was Chromel-Alumel in a Stainless-steel sheath with an ungrounded tip. However, in order to prevent fluctuations of the results the sheath was properly grounded either to the oven or the chart recorder. A millivolt meter was also used to calibrate the output display of the measured temperature.

First attempts to monitor the temperature changes of the sample during microwave treatment were made by inserting the tip of thermocouple into the sample's drill hole and cementing with alumina powder and water-glass mixture. However, after it was discovered that the the mixture in both dried and wet conditions produced a high temperature under microwave treatment, the subsequent temperature measurements were made without using cement. This method was sufficient because the sheathed thermocouple was rigid enough to remain in its position provided that there was no movement of the sample when the temperature measurements were made. The accuracy of thermocouple data was within ± 5 %. However at lower temperature, an error greater than 5 % would be expected as shown in Figure 3.7 for boiling water measurement. The temperature measurement for a thermocouple without load in the 700W microwave oven is shown in Figure 3.8.

3.5.3. STRENGTH TEST

The general operating procedures and apparatus for reduction tests in Section 3.2 were applied for this test. The samples used were in a larger amount of about 100 gram and placed in a Ni-Cr basket. The basket was suspended from a

The samples were selected by crushing the ore to the size -12.5 +10 mm and the tests were made under following conditions:

a. Heating in air

Apparatus	: reduction test apparatus
Weight of sample	: 100 g
Heating temperature	: 700° C
Heating time	: 1 hr

b. Microwave heating

Apparatus	: 700 and 1300W microwave ovens
Weight of sample	: 100 g
Treatment time	: 6 and 10 mins.

c. Reduction test

Apparatus	: reduction test apparatus
Weight of sample	: 100 g
Reducing gas	: 100 % CO
Gas flowrate	: 4 l/min
Reducing temperature	: 1000° C

For all procedures the specimens after testing were air cooled and placed in a plastic bag and were dropped once from a height of 2 m onto an iron plate, after which the material was sieved in 6.3, 3.35 and 0.5 mm sieves. It should be noted that three different procedures applied prior to the reduction test *i.e* the untreated ore, the air heated and the microwave treated ore, and then followed by the reduction test.

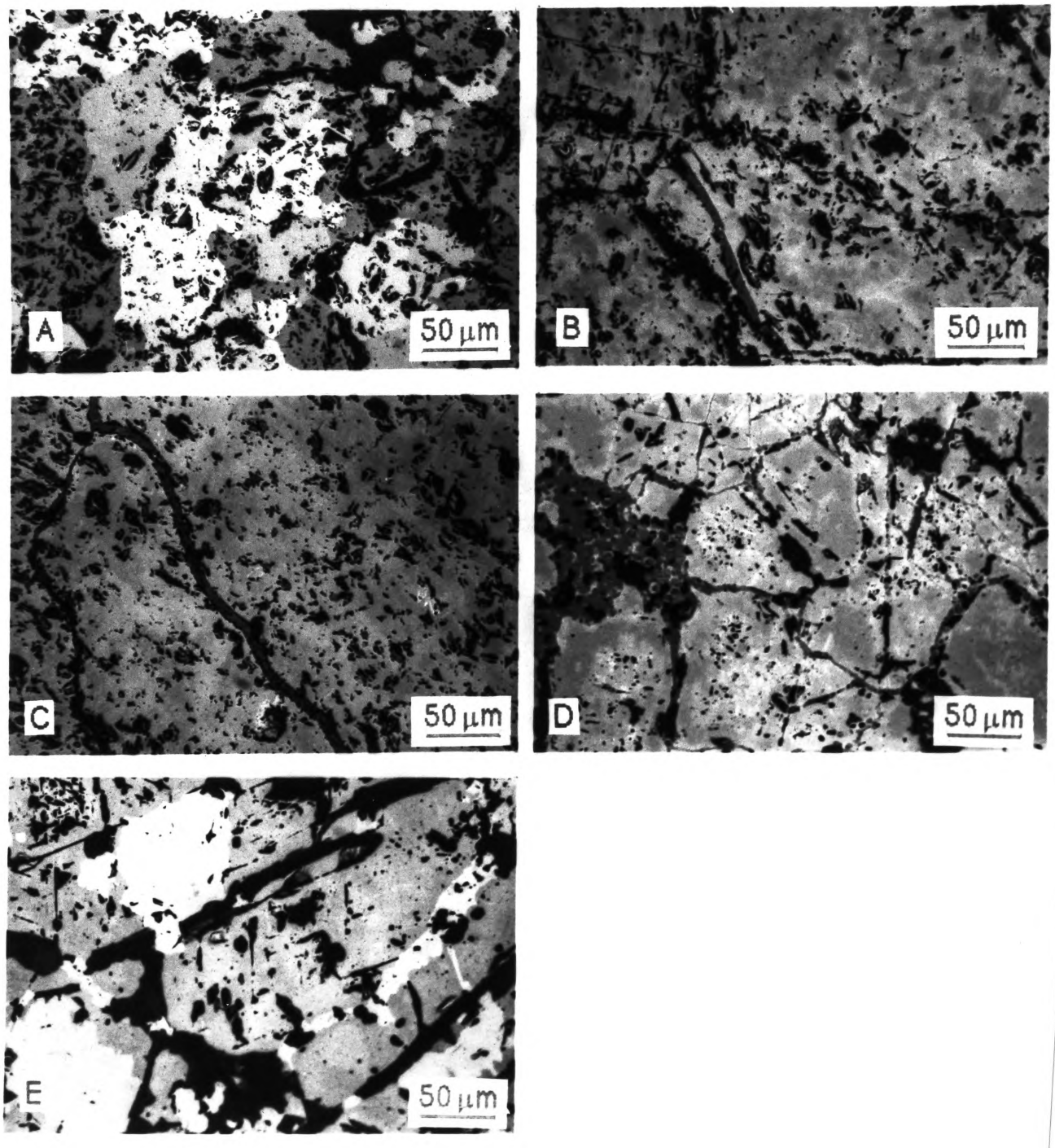

Figure 4.1. Photomicrograph of polished samples
(A) Sample No.1
(B) Sample No.2
(C) Sample No.3
(D) Sample No.4
(E) Sample No.5

4. RESULTS AND DISCUSSIONS

4.1. RAW MATERIALS

4.1.1. ANALYSIS OF THE COMPOSITION

Several different lumps of ore were tested, the compositions most generally encountered are presented in Table 4.1. The Fe^{2+} content was not as high as in magnetite ore used by Edstrom (1953), Roth and Rao (1986), but was close to hematite ore used by Slack and Li (1982). Slack and Li used natural hematite ore from Rio Doce mine in Brazil which had the composition 69.7 % Fe (9.3 % as Fe^{2+} and 60.4 % as Fe^{3+}) with initial porosity of lump ore equal to 0.21. On the other hand, ores used by both Edstrom (1953) and Roth and Rao (1986) contained more than 22 % Fe^{2+} indicating that the ores were of a high magnetite content.

Table 4.1. Chemical Composition of Ore, %

Ore Sample No.	Fe_{total}	Fe^{2+}	SiO_2	Al_2O_3	CaO	TiO_2	Mn_{total}	P_2O_5
1	66.9	9.34	1.23	1.43	<0.01	0.01	0.61	0.04
2	66.9	7.23	0.32	0.34	<0.01	0.07	0.76	<0.02
3	63.8	6.02	2.8	3.0	<0.01	<0.02	1.00	<0.05
4	67.0	9.06	<0.1	0.5	<0.01	<0.01	0.70	0.09
5	66.8	5.80	0.3	0.6	<0.01	<0.02	0.66	0.06

The typical appearance of the raw ore samples on the photomicrograph under optical microscopy is shown in Figure 4.1 (A-E), respectively for samples No.1

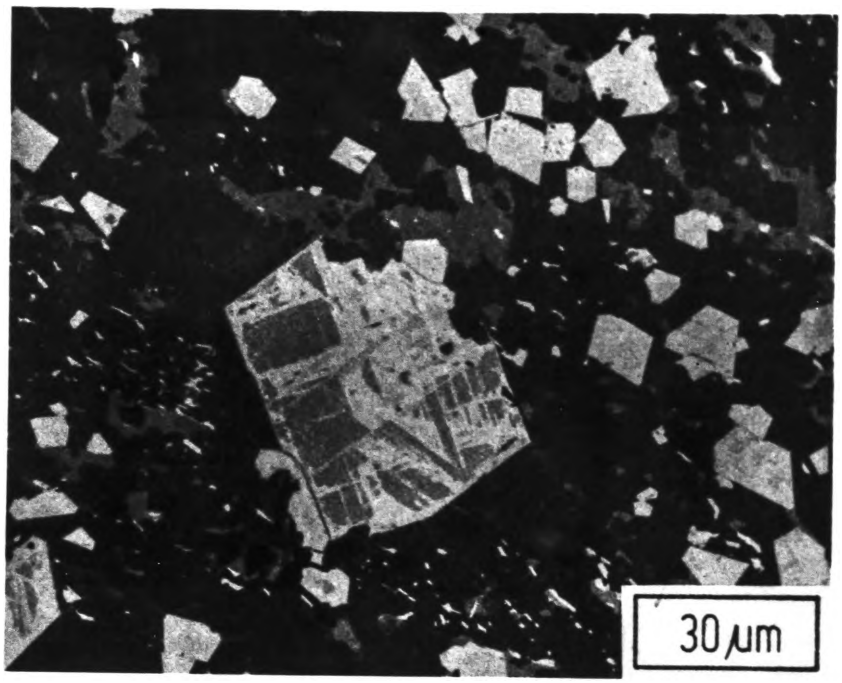

Figure 4.2. Banded iron formation containing martite crystal composed of hematite (white) containing angular relict area of magnetite (grey). Reflected light.

(after Ostwald, 1981)

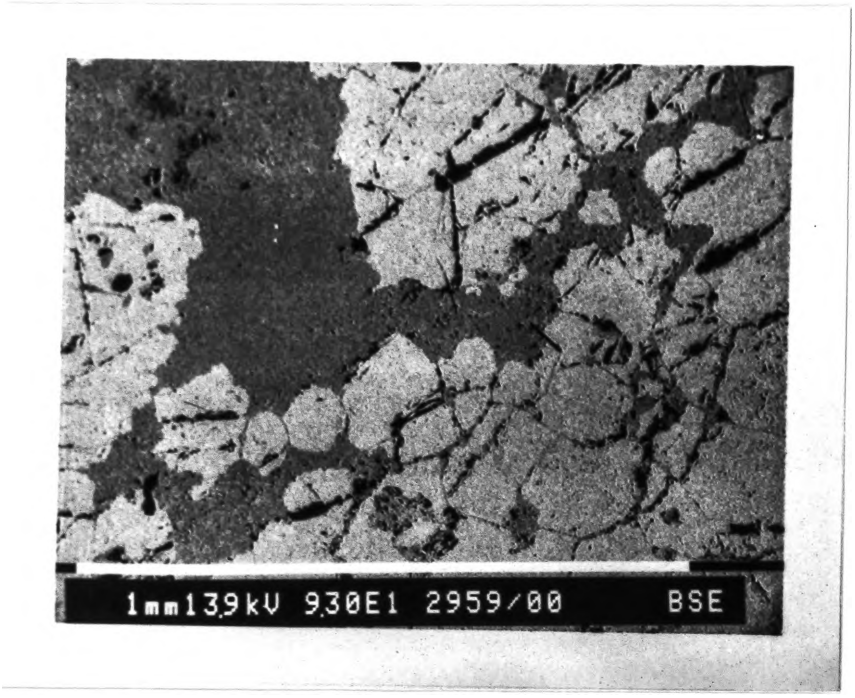

Figure 4.3. SEM photomicrograph analysis of ore, sample No.4.

to No.5. Hematite (greyish white) and magnetite (grey) were visible in most of the samples, while goethite (dark grey) is seen retained between the grain boundaries in Figure 4.1 (B-D). A wide variation in geometry and size of the grains was apparent, and this result therefore agrees with that reported recently by Rustiadi (1985). Rustiadi in his microstructural study of Lampung iron ore found that the iron oxide consisted of hematite, magnetite, goethite and maghemite (γFe_2O_3) but found no evidence of the presence of titaniferrous minerals. By contrast, in this investigation small amounts of titanium oxide were found from chemical analysis (Table 4.1). However, it is not expected that the presence of these small amount of TiO_2 would significantly alter the principal reaction process.

Microscopic examination of iron ore was extensively studied by Ostwald (1981) and showed that at low temperature oxidation effects, often related to leaching and water table movement, commonly convert the magnetite crystal structure to hematite grains with the octahedral form of magnetite as seen in Figure 4.2.

The anisotropic nature of hematite (magnetite is isotropic), colour and reflectance as studied by The 54th (Ironmaking) Committee (1967) and England and Turner (1983) are the optically distinguishing properties for identification in plane polarized light.

The presence of goethite was confirmed during the microstructural study of the original sample (no.4) by using a scanning electron microscope. Figure 4.3 shows a backscattered electron (BSE) image obtained in the study. The light grey and dark grey phases in the photograph correspond to magnetite and goethite, respectively. The high brightness of high density minerals and materials in BSE imaging has been a major feature in the use of scanning electron microscopy. England and Turner (1984) reported that the BSE image is able to show an excellent atomic number contrast of goethite. However it is not possible to

(a)

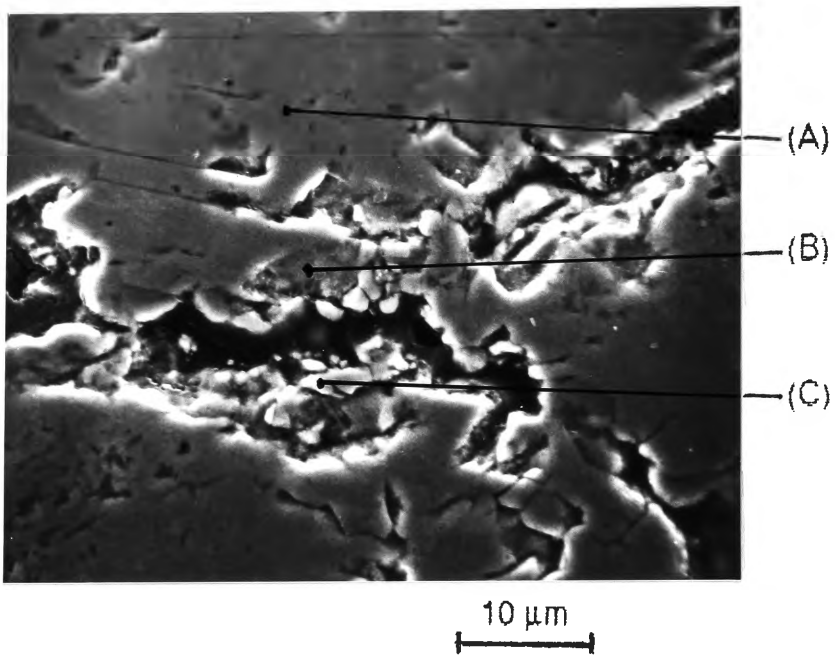

Figure 4.4. (a) SEM photomicrograph analysis of sample No.1, showing cavities in the grains boundary, together with the corresponding EDX microanalysis from (b) Area A (c) Area B and (d) Area C.

(continued on next page)

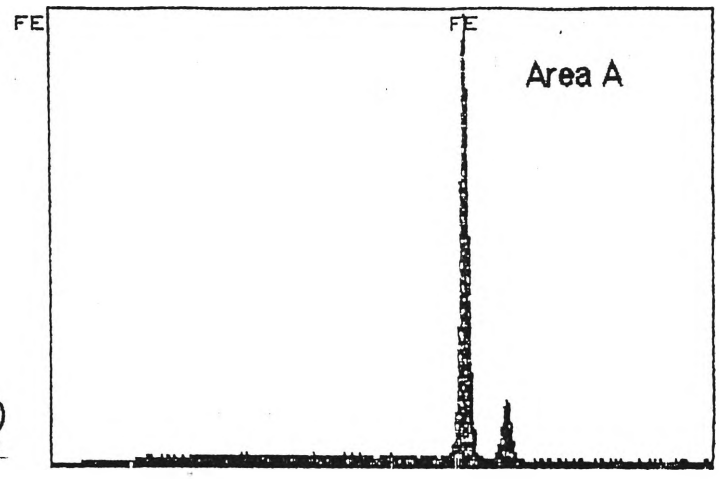

(b)

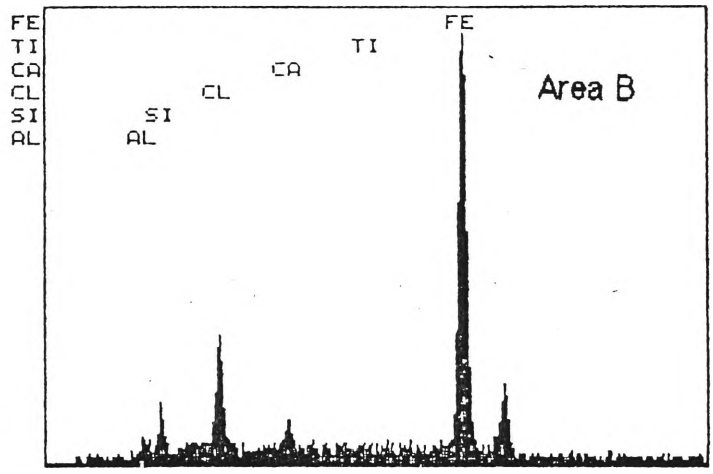

(c)

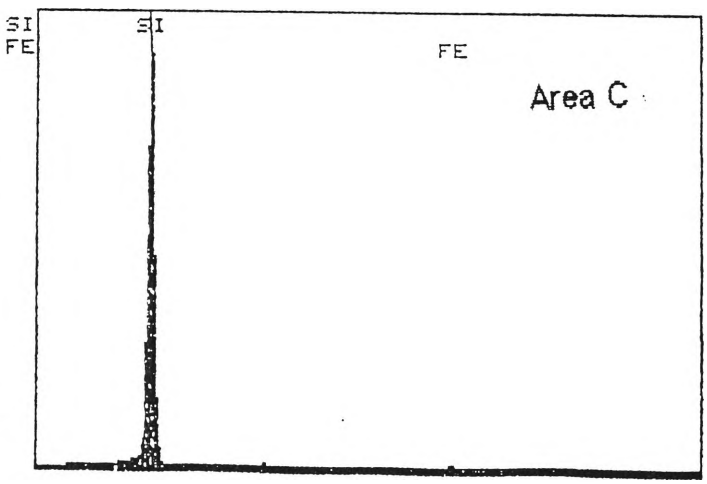

(d)

Figure 4.4. (Continued)

small fraction of gangue minerals can be clearly seen. Area A in the centre of the grain was found to contain a significant level of Fe with almost no other elements present, suggesting a high concentration of iron oxide. Area B was found to contain a high proportion of Fe, with lower levels of Al, Si, Ca and a trace of Ti element. A small particle in area C was found to be rich in Si with a small amount of Fe suggesting the presence of SiO_2. Chlorine was also detected during analysis, but was assumed as being characteristic of the resin chemistry.

Appendix A-4 shows cavities in the grain boundary of sample No.2, together with the EDX microanalysis from the area indicated. It can be seen that the area A contains a high level of Fe, with lower levels of Mn and Mg suggesting manganese and magnesium oxides were associated with iron oxide. A small particle in area B contains a high proportion of Fe, with lower levels of Al, Si, S, K and traces of Ti and Mn elements. Area C at the edge of the grain contains a high level of Fe and lower levels of Mg, Al and Si. Si-rich crystalline area was not detected within this cavities, suggesting that the presence of SiO_2 was associated with the other oxide minerals.

Hematite ore from Whyalla is shown in Appendix A-5 and a typical microanalysis showed that this area contains a high level of Fe with a lower level of Mn and a trace of P element suggesting the presence of manganese oxide associated with the iron oxide. Previous study on iron ores from the Whyalla area by England and Turner (1983) has shown that manganiferous ore from Iron Monarch was containing up to 20% of Mn.

4.1.2. DENSITY AND POROSITY

Porous natural-ore bodies normally do not possess a uniform pore texture and distribution as previously reported by Basu and Ghosh (1970). The relationship between measured particle density and porosity (Appendix A-6) of ore samples is

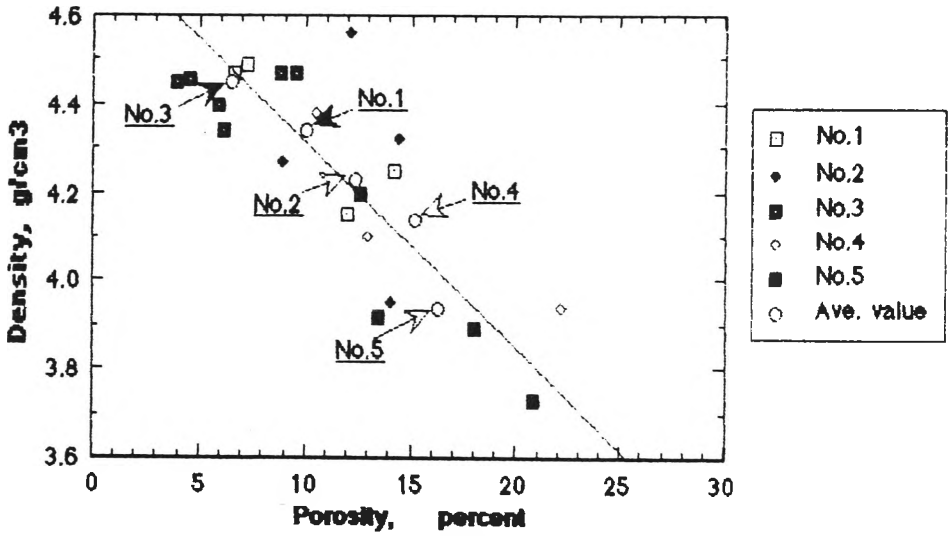

Figure 4.5. Relation between density of raw ores and porosity

shown in Figure 4.5. The average values of the measurements are tabulated in Table 4.3. and are also plotted in Figure 4.5. In the raw samples, particle density was inversely proportional to particle porosity. The variations are linear with some scatter. The scatter is not unexpected in view of the irregularities in the pore structure as seen in the photomicrograph. In the photomicrograph in Figure 4.1 C, sample No.3 was less porous compared with sample No.5 (Figure 4.1 E) since the grain boundaries in sample No.3 (Figure 4.1 C) were filled with goethite which was not the case in sample No.5. The values of density and porosity measured for other samples lay between these two extremes. However, if the fine pores in the grain of particles as seen in Figure 4.1 were 'blind pores', the average of the individual values would depend upon the extensive amount of the fine pores in the grain. El-Geassy *et al* (1976) divided samples into porous, having 35% porosity and dense for 7%. Ghosh *et al* (1986), used pellets, with porosity from 24 to 32% being designated as porous and those with porosity 5 to 7% as dense pellets. In the present study the average porosity ranged from 5.5 to 16% and this was considered as dense to medium density.

Table 4.3. Physical properties of raw ore sample

Ore Sample No.	Av. Density g/cm^3	Av. Porosity %
1	4.34	10.0
2	4.23	12.4
3	4.45	6.4
4	4.14	15.2
5	3.94	16.2

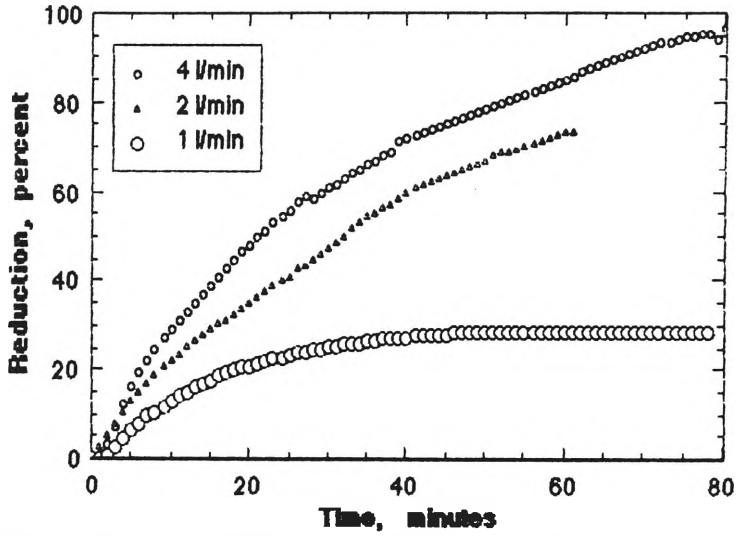

Figure 4.6. Reduction curves for sample No.2 (ø = 14 mm) at flowrate 4, 2, and 1 l/min

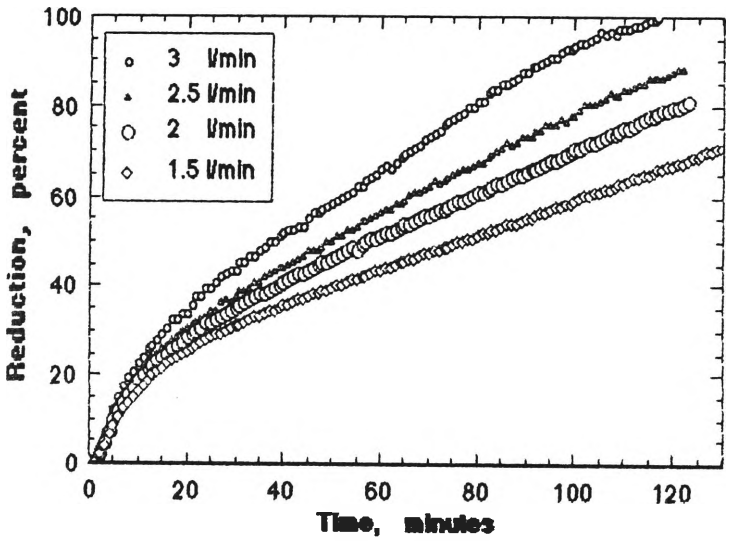

Figure 4.7. Reduction curves for sample No.1 (ø = 15 mm) at flowrate 3, 2.5, 2, and 1.5 l/min

4.2. REDUCTION TESTS

All samples were reduced at constant temperature within the range from 900 to 1200 °C, and the extent of reduction was calculated (Turkdogan *et al*, 1971; Du *et al*, 1988) from

$$\text{Reduction } X,\% = \frac{\text{weight of oxygen removed}}{\text{weight of calculated removable oxygen in unreduced sample}} \times 100\%$$

From the recorded weight loss, the reduction percent was calculated (Appendix A-9) and plotted against the reduction time as exemplified in Figure 4.6.

4.2.1. EFFECT OF FLOWRATE

The initial reduction tests were carried out to determine the flowrate required to ensure an adequate supply of gas. For this purpose test runs at flow rates from 1 to 4 l/min of pure CO gas at 1000 °C were conducted.

The effect of gas flowrate on reduction kinetics was investigated on large particle sizes, *viz* 14 and 15 mm diam. of samples No.2 and No.1, respectively. The results for reduction on sample No.2 are summarized in Figure 4.6. It is clear from Figure4.6 that with higher flowrate (2 and 4 l/min) there was significant improvement in reduction rate compared with that at low flowrate (1 l/min) especially for reduction beyond about 20%. The second tests were conducted on sample No.1 having 15 mm diam. particles at flowrates of 1.5, 2, 2.5 and 3 l/min. and the results are shown in Figure 4.7. It is apparent that with increased CO gas flow through the reactor, there was less accumulation of CO_2-product in the reducing gas with the result that there was less rate-inhibition.

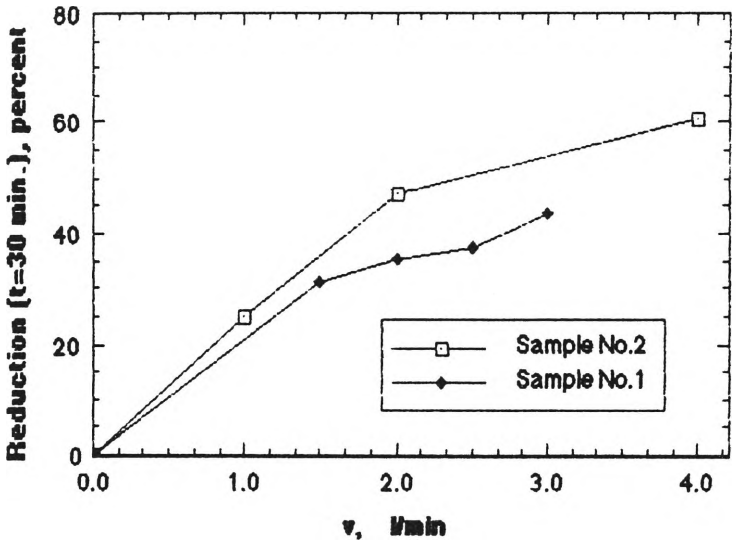

Figure 4.8. Effect of flowrates on the reduction.

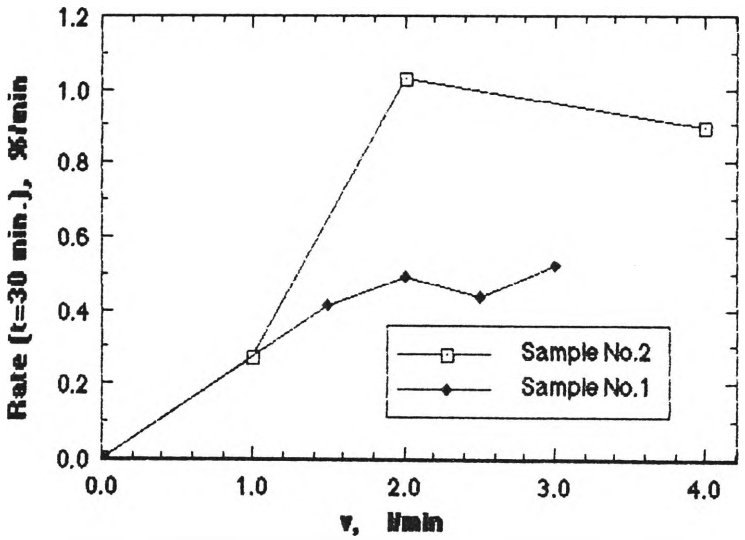

Figure 4.9. Effect of flowrates on the rate of reduction.

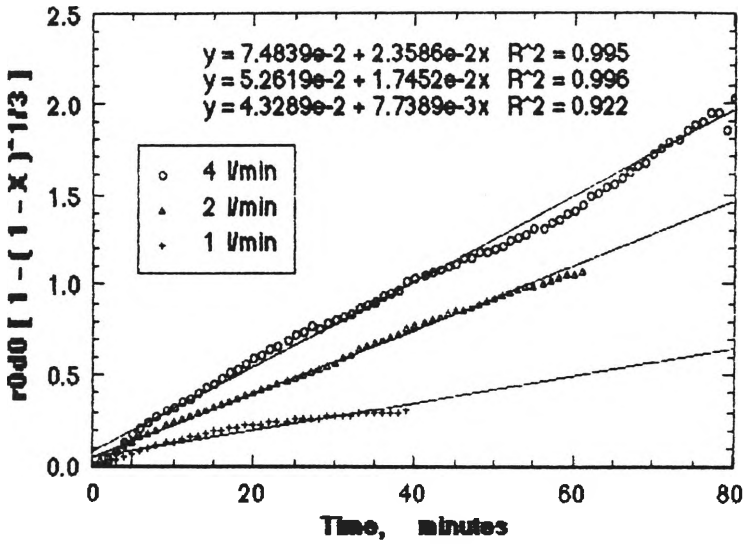

Figure 4.10. Linear plot of data from Fig. 4.6.

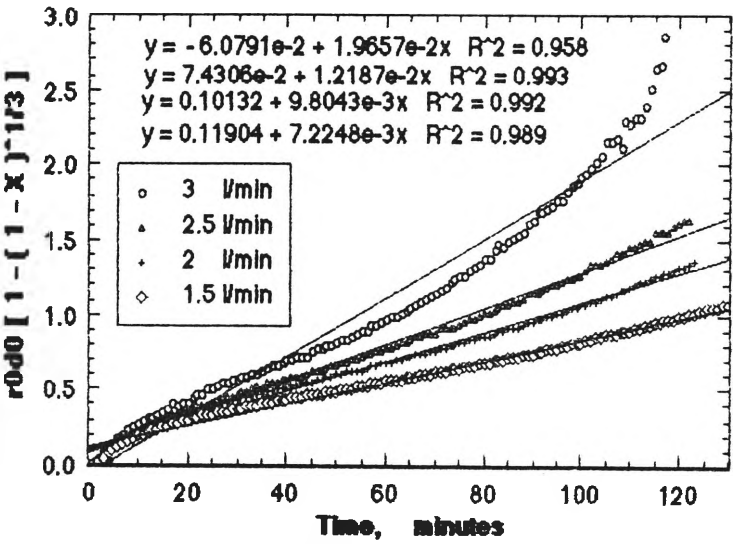

Figure 4.11. Linear plot of data from Fig. 4.7.

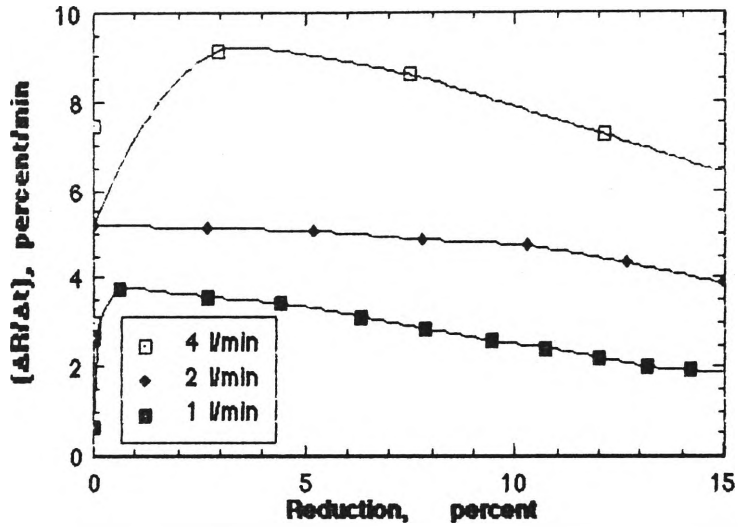

Figure 4.12. Initial rate of reduction for sample No.2 (ø = 14mm) at flowrate 4, 2, and 1 l/min

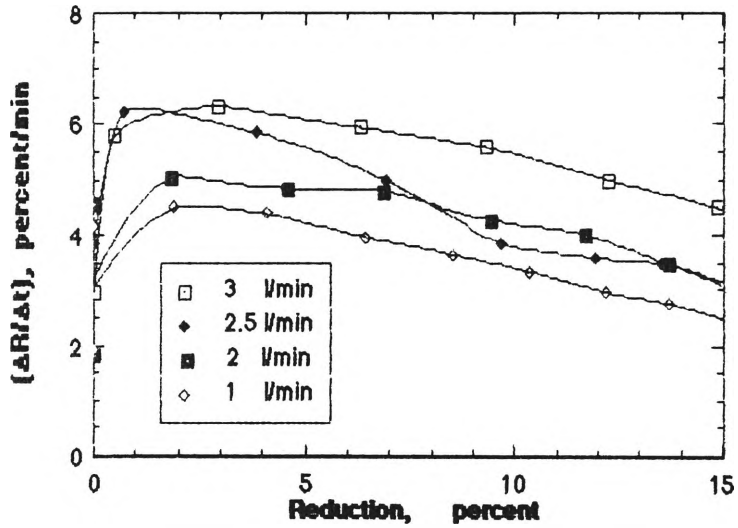

Figure 4.13. Initial rate of reduction for sample No.1 (ø = 15mm) at flowrate 3, 2.5, 2, and 1.5 l/min

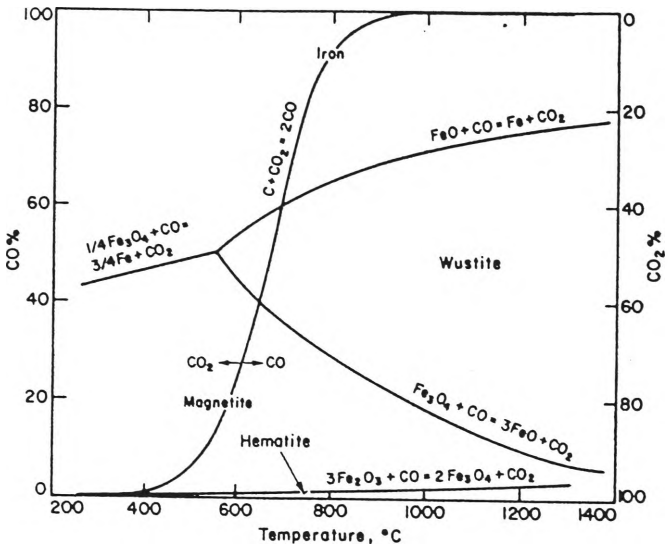

Figure 4.14. Equilibrium gas composition *vs* temperature diagram for the iron-carbon-oxygen system.

(after Ross, 1980)

Figures 4.8 and 4.9 show the effect of flowrate on the degree of reduction and on the rate of reduction at t = 30 minutes obtained from data in Figures. 4.6 and 4.7. For sample No.2, the reduction increased from 25.15 % to 47.47 % and 60.81% at 1, 2 and 4 l/min of flowrate, respectively. For sample No.1, the reduction increased from 31.16 % to 35.10 %, 37.47 % and 43.60 % at 1.5, 2, 2.5 and 3 l/min of flowrate, respectively. It is clear the reduction for sample No.2 was significantly increased up to 22.33 % by multiplying the flowrate from 1 to 2 l/min. compared with the value of 13.34 % at the flowrate from 2 to 4 l/min. A further result for sample No.1 in a closer range of flowrates from 1.5 to 3 l/min. had a small influence on the degree of reduction i.e. 12.44 %

The results obtained on the rate of reduction as shown in Figure 4.9 show that beyond 2 l/min the increase is less significant for both samples No.1 and No.2.

From data in Figure 4.6 and Figure 4.7 using Equation [2.6] the effect of flowrate on large particle were observed. The results were plotted in Figure 4.10 and Figure 4.11 and the rate constant, K, values were obtained. For sample no.2 the K values were 0.0236, 0.0175 and 0.0077 g/cm^2 at flowrate 4, 2 and 1 l/min, respectively, and for sample no.1, the K values were 0.0197, 0.0122, 0.0098 and 0.072 g/cm^2 corresponding to gas flowrate of 3, 2.5, 2 and 1.5 l/min respectively. The K values indicated that for sample no.2 at K = 0.0077 g/cm^2 the effect of gas starvation was present, which differed from sample no.1 at K = 0.0072 g/cm^2 where normal reduction proceeded.

Calculated data in Table 4.4, obtained from the initial rate of reduction using data in Figure 4.12 and Figure 4.13 indicate that the gas concentration during initial reduction where the highest rate of reduction prevailed, was reasonably high above the equilibrium of iron oxide system as seen in Figure 4.14 (after Ross, 1980).

Table 4.4. Calculated Gas Composition at Different Flowrates at 1000 °C

Gas Flowrate	Rate	Gas CO		pCO
	$(\Delta R/\Delta t)_{R=0.05}$	inlet	outlet	
(l/min)	(%/min)	(moles/min)		(%)
	Sample no.2 (ø = 14 mm)			
4	9.	0.178571	0.170134	95.3
2	5.	0.089285	0.084598	94.7
1	3.3	0.044643	0.041549	93.0
	Sample no.1 (ø = 15 mm)			
3	6.1	0.133928	0.1263035	94.3
2.5	5.5	0.111607	0.104732	93.8
2	4.75	0.089285	0.083348	93.3
1.5	4.2	0.006696	0.061714	92.1

On the above evidence it was considered that the subsequent reduction experiments should be conducted at 2 l/min, which is equivalent to the empty tube velocity at STP 1.2 cm/sec of CO flowrate to ensure excess CO conditions and the economy of CO useage.

4.2.2. EFFECT OF PARTICLE SIZE AND TYPE OF ORE

Kinetic data with different sizes of particles may be used to distinguish between reactions in which the chemical and physical steps control (Section 2.2).

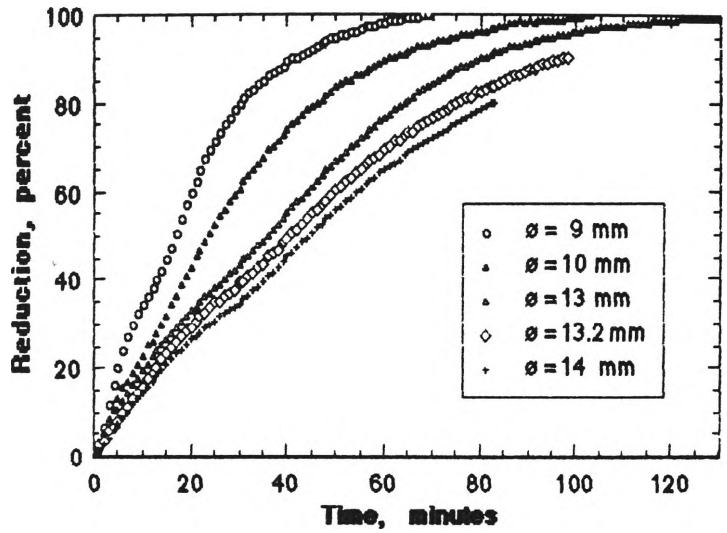

Figure 4.15. Effect of particle size on reduction of sample No.1

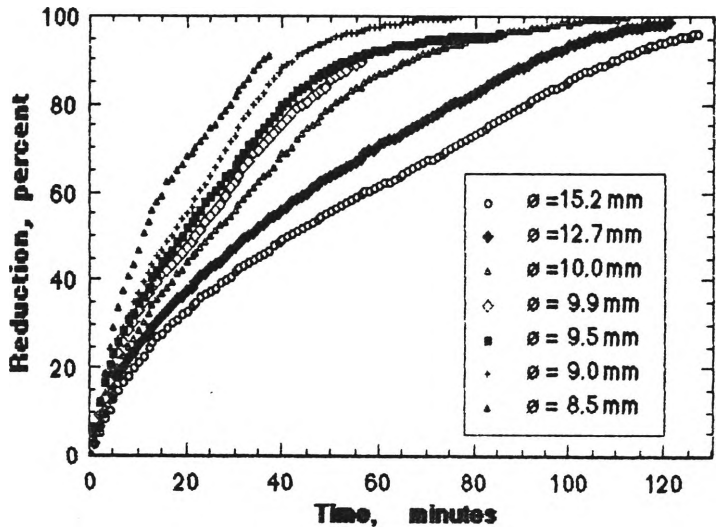

Figure 4.16. Effect of particle size on reduction of sample No.2

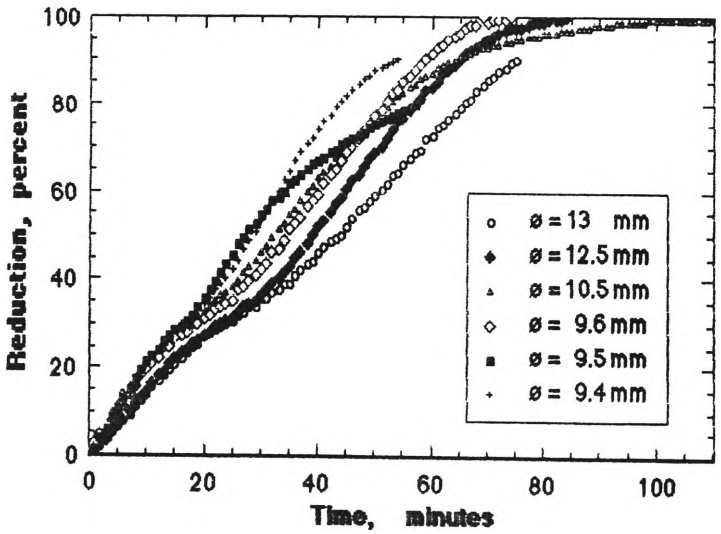

Figure 4.17. Effect of particle size on reduction of sample No.3

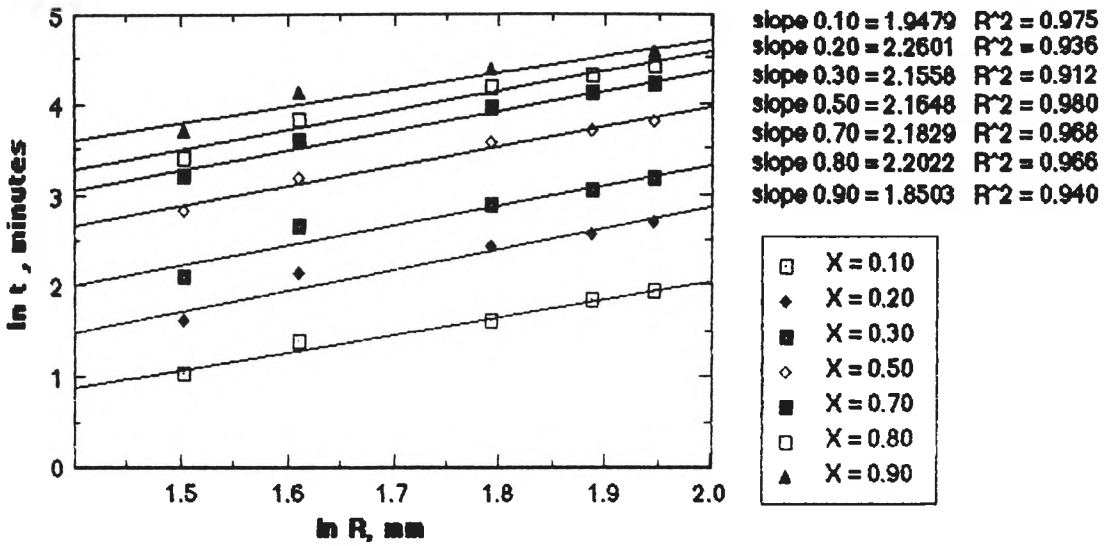

Figure 4.18. Effect of particle size of sample no.1

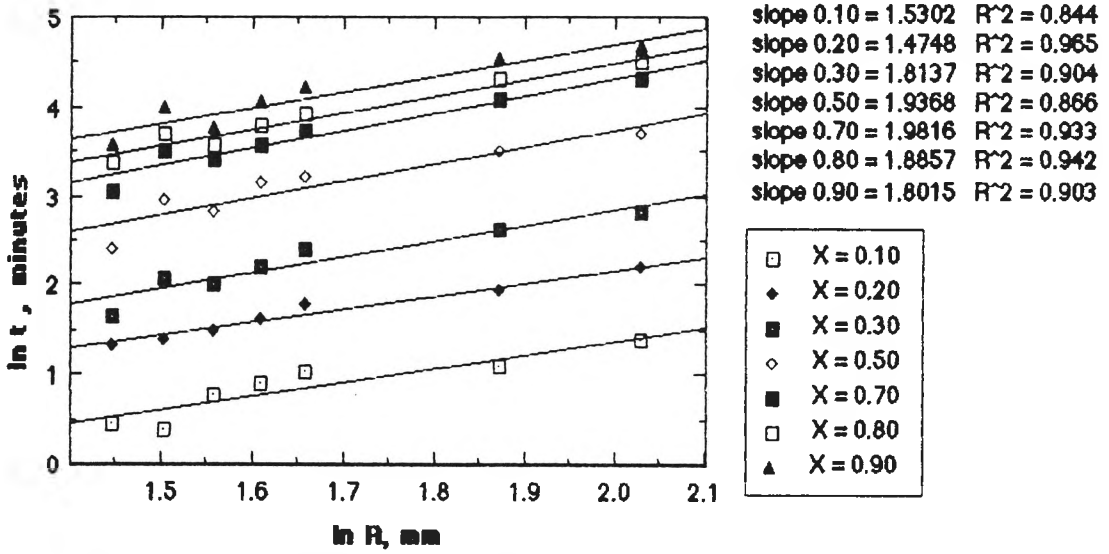

Figure 4.19. Effect of particle size of sample no.2

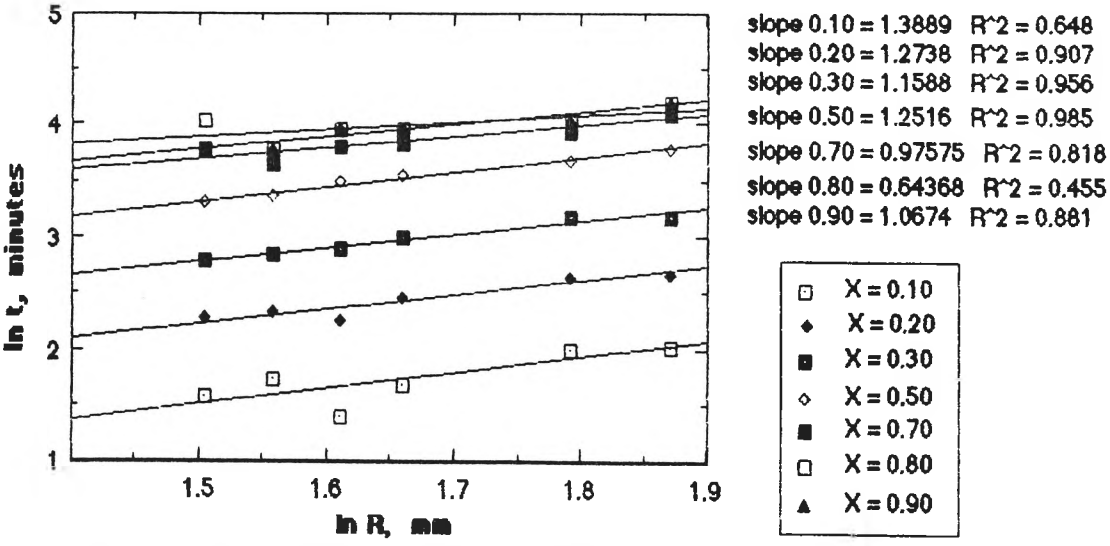

Figure 4.20. Effect of particle size of sample no.3

Sets of experiments using 3 different samples with sizes ranging from small to large were conducted at 1000 °C and constant gas flowrate 2 l/min. The reduction curves are plotted in Figures 4.15, 4.16 and 4.17 for samples no.1, no.2 and no.3, respectively. From these reduction curves, the influence of particle size at stages of reduction (X = 10 to 90 %) are presented in Figures 4.18, 4.19 and 4.20 as natural logarithm plot of time against particle size. The plot yielded values of slopes; for sample no.1 initial slope was 1.85 (X = 10 %) then the slope increased to a value of 2.20 (X = 20 %) and remained at a relatively constant value of 2.20 up to 90 % of reduction. For sample no.2, at X = 10 % the slope was 1.80, then it gradually increased to a value of 1.98 (X = 30 %) before decreasing to a value of 1.53 (X = 90 %). For sample no.3, the slope at X = 10 % had a value of 1.06 which then decreased to a value of 0.64 (X = 20 %) and then it gradually increased to a value of 1.38 (X = 90 %).

Levenspiel (1972) and Ross (1980) have shown that the time for reduction is proportional to the particle size for phase boundary reaction control and to the square of the particle size for gaseous diffusion control. Therefore a plot of logarithm of time, t versus particle size with degree of reduction as a parameter should yield slopes of unity and two for phase boundary reaction and gaseous diffusion control, respectively. Ross (1980) also pointed out that for mixed control the slope of such a plot should be between 1 and 2 and should be expected to increase in value as the reduction becomes more complete. Levenspiel (1979), on the other hand, expressed the view that for film diffusion control the slope is between 1.5 to 2.0 and the value drops as the particle size increases.

The results indicate that for sample no.1 mixed control would be considered to be rate controlling and likewise in sample no.2 as its initial reduction (X = 10%) yielded a slope of >1. For sample no.3 for which even the highest value of the slope was 1.38, a mixed control is indicated. It should be noted that for each particle size the data were first calculated by computer and subsequently simple plotter analysis

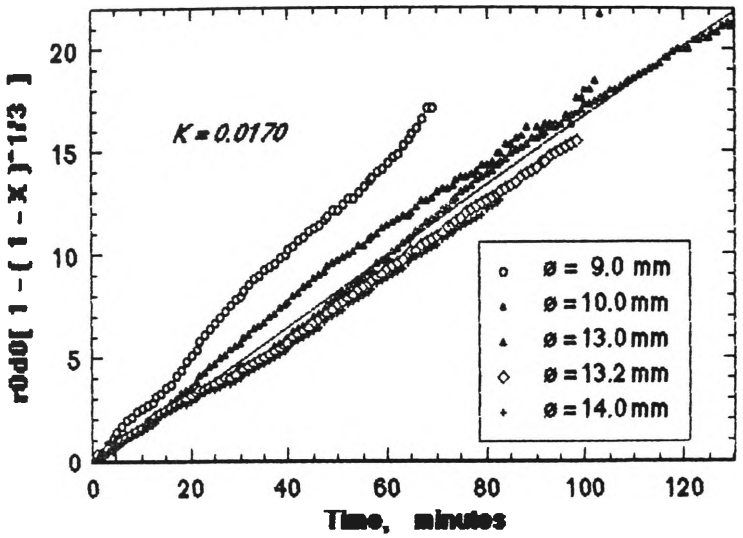

Figure 4.21. Linear plot for sample No.1

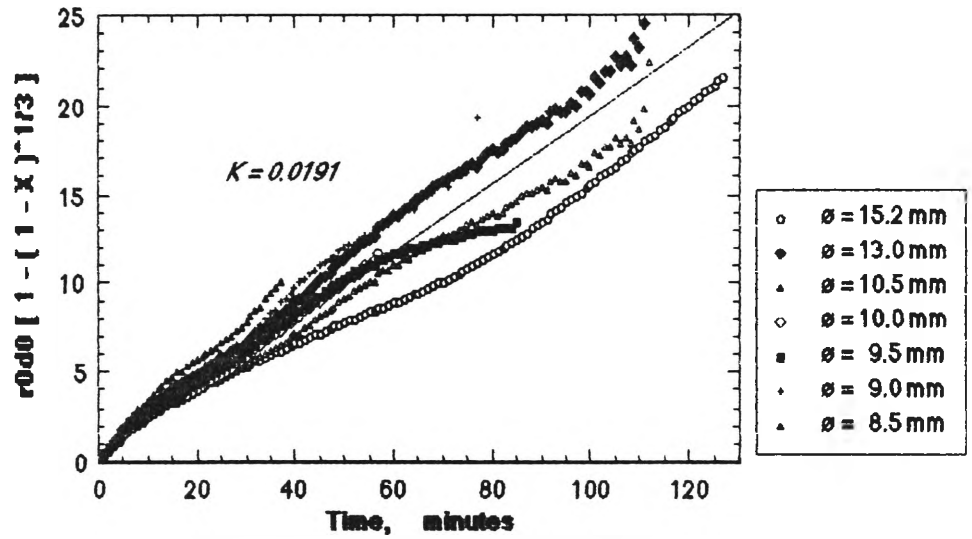

Figure 4.22. Linear plot sample No.2

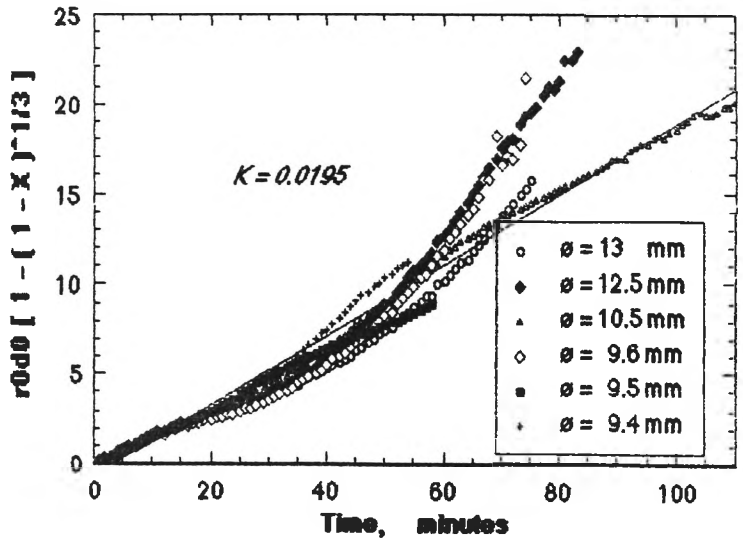

Figure 4.23. Linear plot for sample No.3

was carried out to determine the straight line of best fit. By inspection of each sample data, especially for sample No.3, the values of the slopes were inconsistent with gas film diffusion control proposed by Levenspiel.

Equation [2.6] has been developed by McKewan (1960) based on the assumption that reaction rate is proportional to the surface area of reacting interface. From experimental data in Figures 4.15, 4.16 and 4.17, values of $r_0 d_0[1-(1-X)^{1/3}]$ were determined and plotted against time, t , as shown in Figures 4.21, 4.22 and 4.23, respectively. A straight line indicates that the reduction process obeyed the model upon which the formula was based. It is seen in Figure 4.21 for sample No.1 reasonably straight lines were obtained initially up to 30% of reduction with a rate constant K = 0.0195 g/cm^2. Ross (1980) also reported that many experimental results have shown a linear relation during the early stages of reduction and sometimes also up to 60 to 80 % of reduction. Beyond this, the plot deviated from a straight line indicating that some other mechanism may control the rate of reduction.

Using Equation [2.6], initially up to about 30 % of reduction, sample No.1 had a slightly lower value of rate constant compared to the rate constant of both samples No.2 and No.3. However, beyond this degree of reduction, except for small particle sizes, the constant rate deviated to a lower value before gradually increasing to some higher value. The subsequent departure from linearity is consistent with a slowing down of reaction as another resistance became important. This slowing down would appear to be associated with conditions where all the higher oxides (depending on the hematite/magnetite mix in the ore) as reported by Koo and Evans (1979) were reduced to wustite before any wustite reduction took place. Inspection of the data in Figure 4.21 for sample No.1 shows that after initial common linearity of reduction, the results branch out as a family of essentially straight lines of different slopes, particularly for samples No.2 and No.3 (Figures. 4.22 and 4.23, respectively). These results indicate that in sample no.1 reaction control had shifted from one level to another which is unexplainable by the model

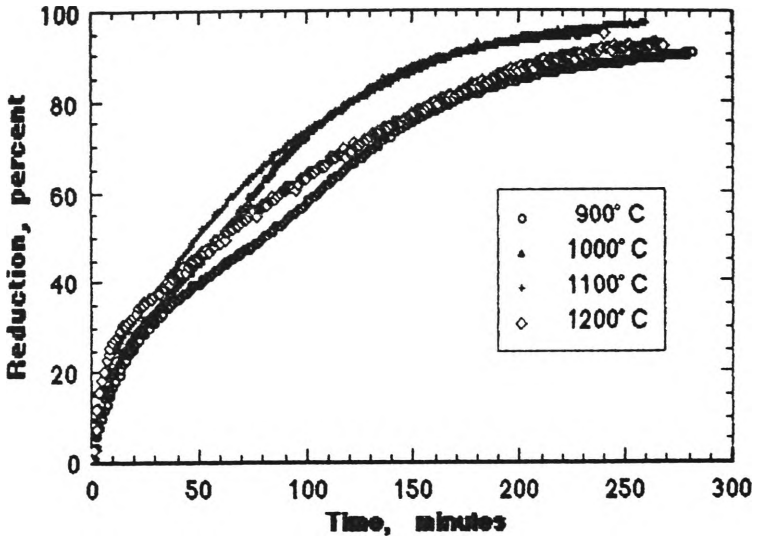

Figure 4.24. Effect of temperature on reduction of sample no.2

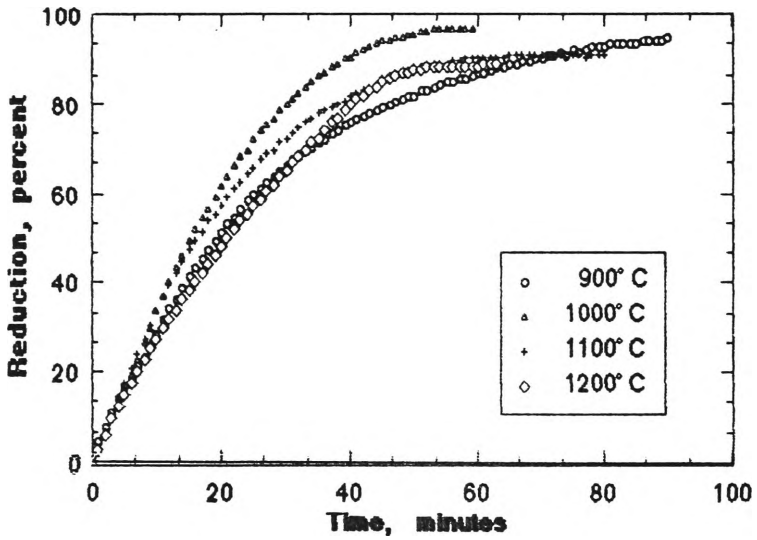

Figure 4.25. Effect of temperature on reduction of sample no. 5

applied. Therefore, to evaluate these results a more appropriate model of reduction is required.

4.2.3. EFFECT OF TEMPERATURE

The effect of temperature on the extent of reduction of two different samples of magneto-hematite is shown in Figure 4.24 for sample No.2 and in Figure 4.25 for sample No.5, for various temperatures within the range 900° to 1200° C.

Up to 1000° C, the extent of reduction for both samples No.2 and No.5 at any given time increased with increasing temperature. However, at higher temperature i.e. 1100° and 1200° C, the extent of reduction was slower than at 1000° C. At 1100° C, the reduction rate, for sample No.2 above 80 % reduction level and for sample No.5 above 40 % reduction level, was slower than at 1000° C. At 1200° C and at the reduction level above 50 % and 10 % for both these samples, the reduction rate was also slower than at 1000° C. These results indicate a change in the rate controlling process at high temperature.

The effect of an increased reduction temperature on the nature of the growth behaviour of magnetite may be related to a reduced rate of nucleus formation as reported by Bradshaw and Matyas (1976). These authors studied kinetics and structural changes for reduction of Carol Lake hematite pellets to magnetite in CO - CO_2 atmospheres at 600° to 1000° C. It was found that the highest reaction rate was at 800° to 850° C. Above this temperature a particularly dense magnetite was formed which more than offset the advantage of higher temperature.

The difference in chemical composition of samples no.2 and no.5 which contained 7.23 % Fe^{2+} (approx. 30 % magnetite) and 5.80 % Fe^{2+} (approx. 24 % magnetite) respectively and the difference in the average porosity of these samples, 12.4 % for sample no.2 and 16.0 % for sample no.5, may be expected to have an

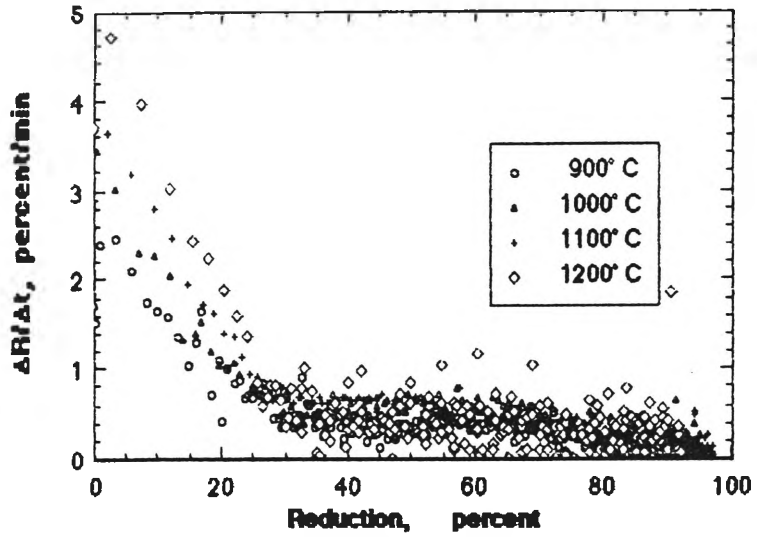

Figure 4.26. Rate vs Reduction curves for sample no. 2 at range temperature 900° - 1200° C

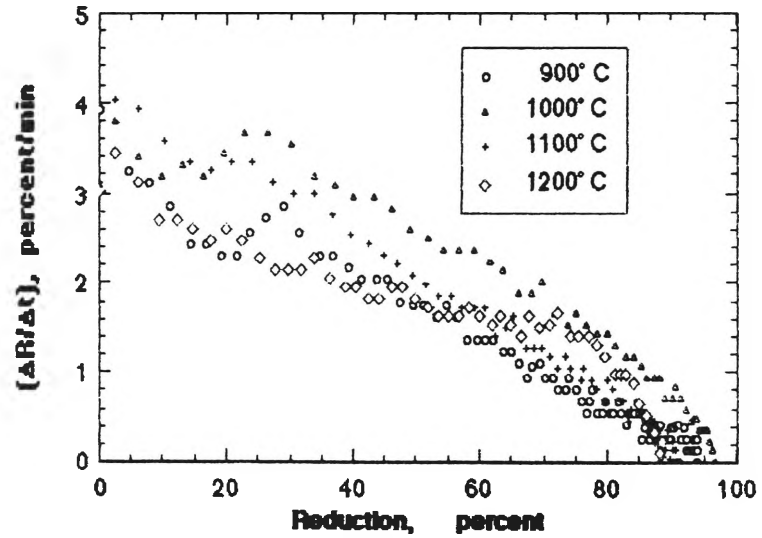

Figure 4.27. Rate vs Reduction curves for sample No.5 at range temperature 900 - 1200° C

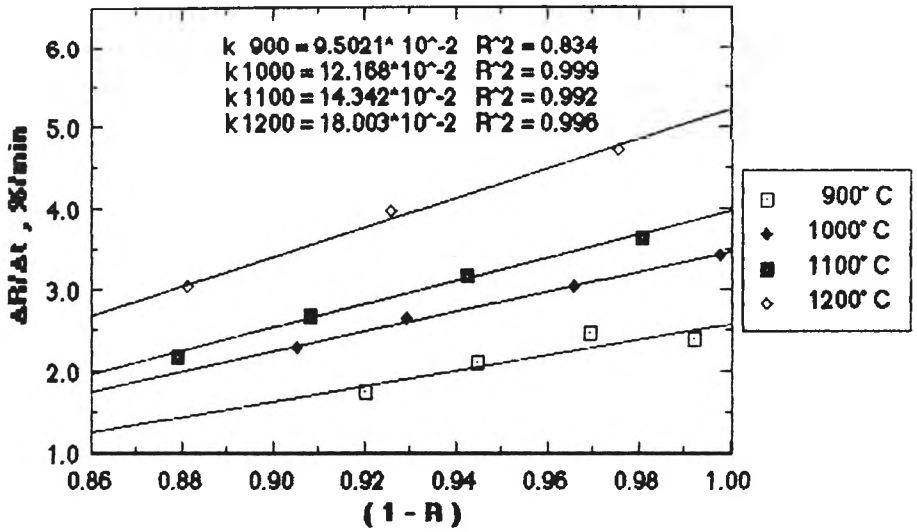

Figure 4.28. Rate constant, k for sample No.2 at initial stage of reduction

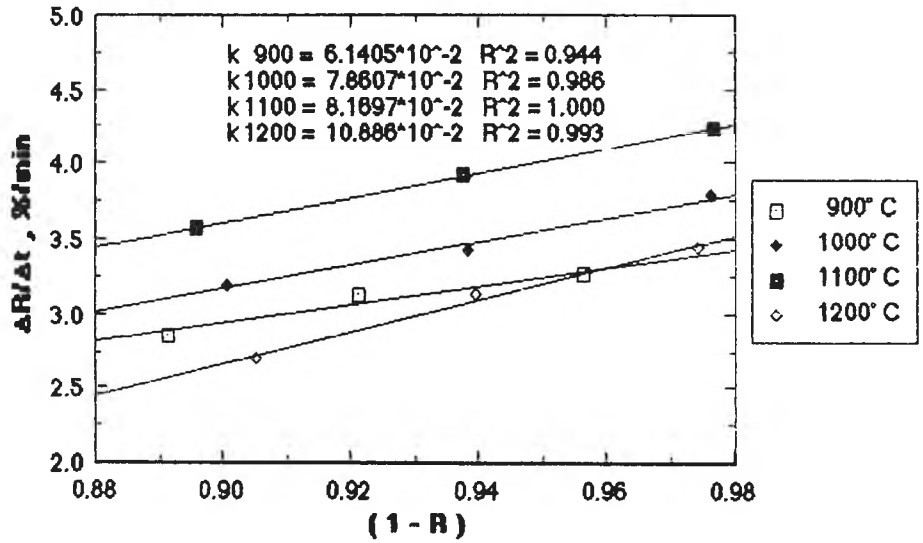

Figure 4.29 Rate constant, k for sample No.5 at initial stage of reduction

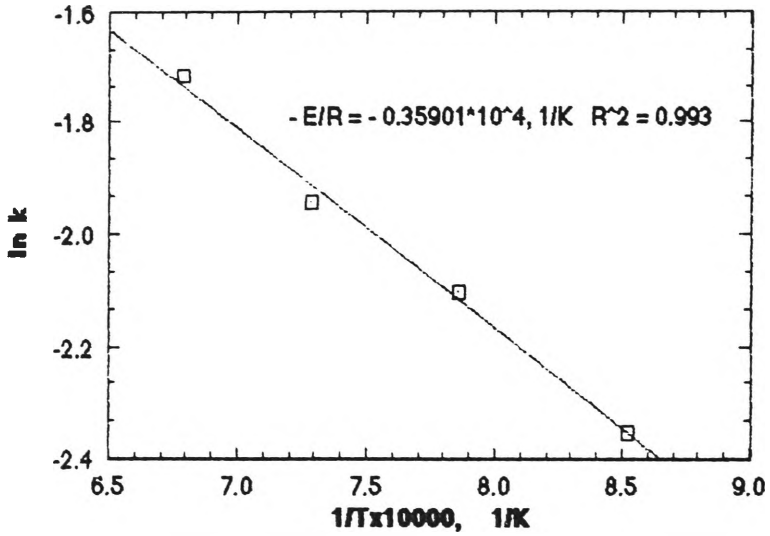

Figure 4.30. Arrhenius plot for sample No.2 at initial stage of reduction

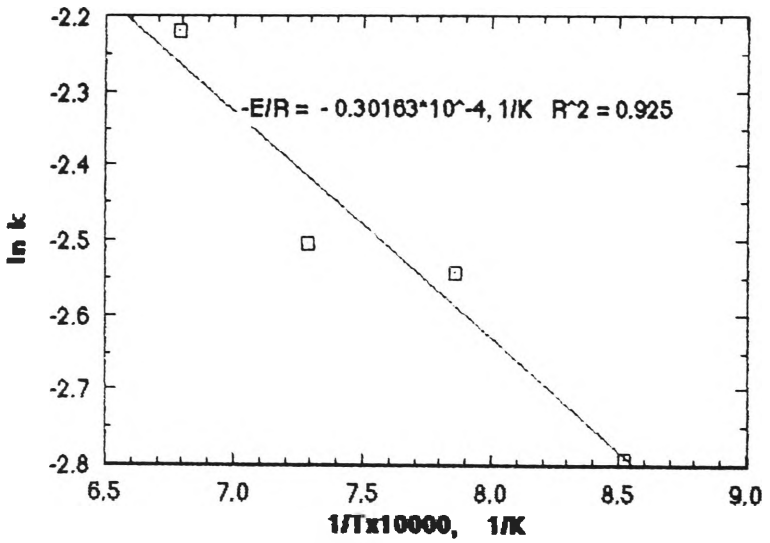

Figure 4.31. Arrhenius plot for sample No.5 at initial stage of reduction

influence on the extent of reduction. Slack and Li (1982) indicated that in addition to solid composition another important parameter affecting a gas-solid reaction was the network of pores through which the gaseous reducing agent and product must diffuse. This network includes intergranular and intragranular pores, one or the other of which often playing a dominant role in the reaction kinetics. However the dominant type can change during the course of reduction. A structural observation may reveal the reason for the gradual decrease in the rate of reduction at higher temperature. This is discussed in Section 4.2.4.

4.2.3.1. ACTIVATION ENERGY

The effect of temperature on reaction rates is expected to follow the Arrhenius equation. For the reduction of the iron ore used, in order to obtain the activation energy, which is determined from the slope of a plot ln k - 1/T, rate constants (k) were evaluated.

The experimental rate constants were calculated from the initial rate of the reduction data in Figures 4.24 and 4.25 respectively for sample No.2 and No.5. The instantaneous rate ($\frac{\Delta R}{\Delta t}$) used in the calculation is the percentage of reduction change in each minute from the recorded data. From the instantaneous rate plots during reduction in Figures 4.26 and 4.27, it is seen that for both samples No.2 and No.5 the highest rates are obtained during initial reduction, as expected, and then they gradually decreased as the reduction increased. By using the initial rate data (at 0 - 10% reduction) and plotting these against (1 - X) as shown in Figures 4.28 and 4.29, the rate constant values obtained are given in Table 4.5. The ln k - 1/T plot is given in Figures 4.30 and 4.31 for samples No.2 and No.5, respectively.

Table 4.5. Calculated Rate Constant at Different Temperates

No.	Temperature (°C)	Rate Constant, k (%/min.)	
		Sample No.2	Sample No.5
1	900	9.502×10^{-2}	6.140×10^{-2}
2	1000	12.168×10^{-2}	7.861×10^{-2}
3	1100	14.342×10^{-2}	8.170×10^{-2}
4	1200	18.003×10^{-2}	10.886×10^{-2}

It is seen from Figures 4.30 and 4.31 that the initial reduction rate for both samples No.2 and No.5 showed apparent Arrhenius behaviour throughout the temperature range 900° - 1200° C. The reduction of samples No.2 and No.5 was associated with activation energies of 29.8 and 25.1 kJ/mol, respectively. The activation energies obtained in this investigation compared with the activation energies reported by Koo and Evans (1979) (in Table 4.6) are seen to be low.

However, the present values are comparable to those obtained by El Geassy *et al* (1977) for dense iron oxide briquettes (Table 4.7). More recently, Du *et al* (1988) reported that on reduction of pellets containing pure Fe_2O_3, Fe_2O_3 - 3% CaO and Fe_2O_3 - 6%CaO in temperature range 1191 - 1372 K, the activation energy values were 40, 26 and 34.5 kJ/mol, respectively.

Table 4.6. Activation Energy for Iron Ore Reduction

(after Koo and Evans, 1979)

	Activation Energy	
	kcal/g.mol	kJ/g.mol
1st sample (Cerro Bolivar)	10.87	45.52
2nd sample (HIB feed)	12.47	52.22
3rd sample (Altamira)	14.83	62.10
Other investigations		
Hematite (McKewan, 1958)	14.78	61.89
Hematite (McKewan, 1962)	14.70	61.55
Hematite (McKewan, 1962)	13.88	58.12
Hematite (McKewan, 1962)	9.66	40.45
Hematite (Hocking, 1960)	11.79	49.37
Hematite (Hocking, 1960)	11.71	49.03

For sample no.2 the initial portions of the reduction curves which were mostly linear, were small (up to 20 - 30% reduction depending on temperature). However, for sample no.5 larger initial portions of the curves were linear (up to 30 - 50 % reduction depending on temperature) indicating a larger constant rate of reduction. From Figure 4.26 for sample No.2, a sharp decrease in reduction rate is observed at 20 - 30% reduction. On the other hand, the rate data for sample No.5 in Figure 4.27 shows the reduction rate gradually decreasing up to the final stage of reduction.

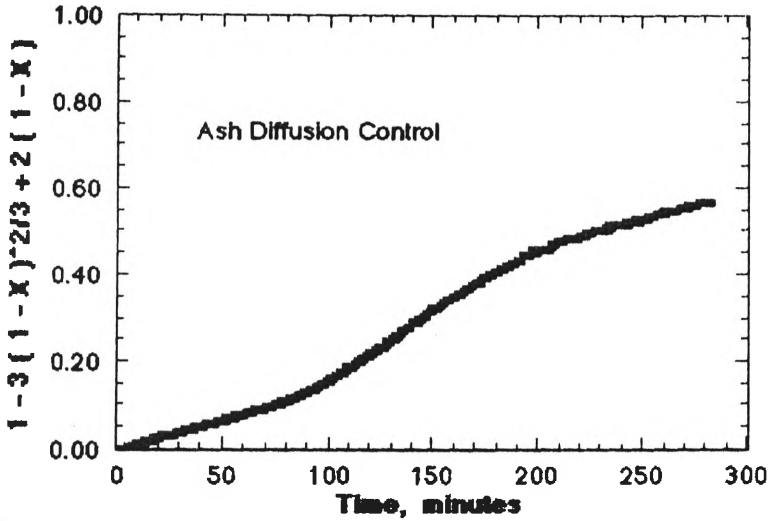

Figure 4.32. Ash Diffusion Control plot for sample No.2 at temperature 900° C

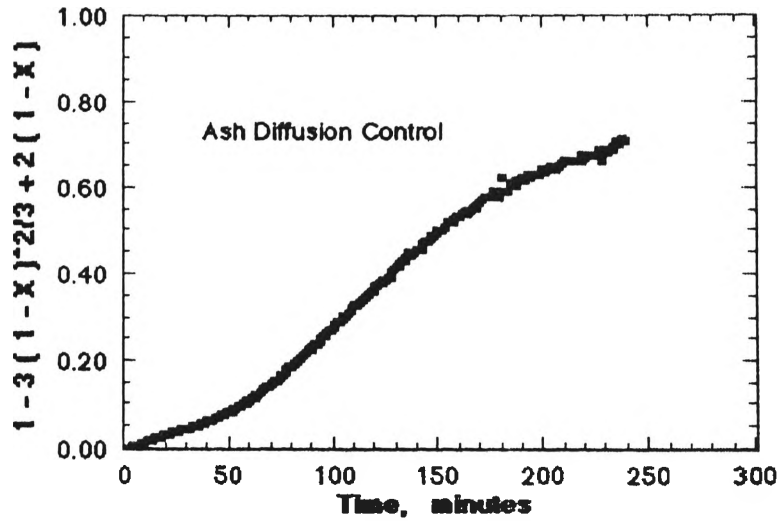

Figure 4.33. Ash Diffusion Control plot for sample No.2 at temperature 1000° C

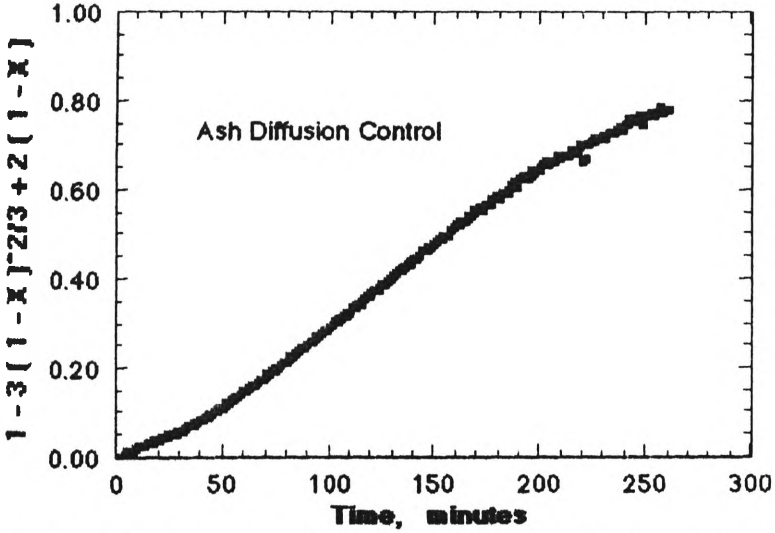

Figure 4.34. Ash Diffusion Control plot for sample No.2 at temperature 1100° C

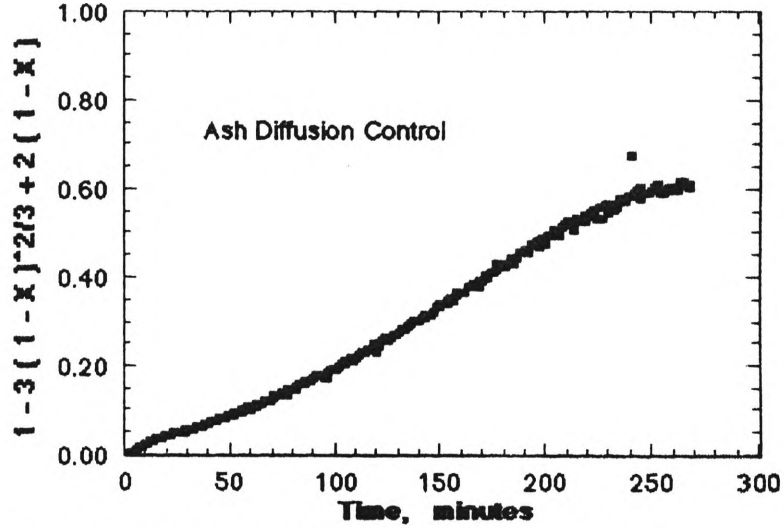

Figure 4.35. Ash Diffusion Control plot for sample No.2 at temperature 1200° C

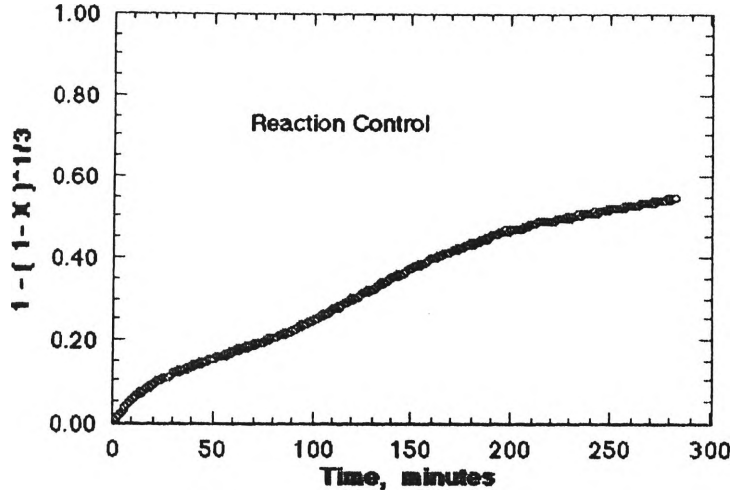

Figure 4.36. Chemical Reaction Control plot for sample No.2 at temperature 900° C

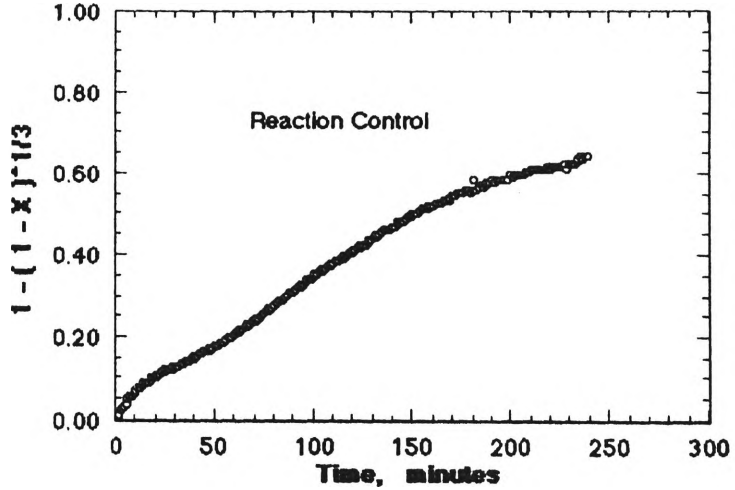

Figure 4.37. Chemical Reaction Control plot for sample No.2 at temperature 1000° C

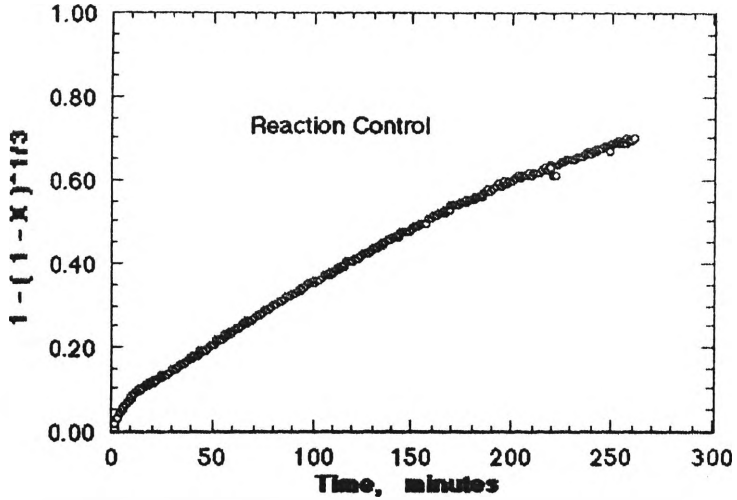

Figure 4.38. Chemical Reaction Control plot for sample No.2 at temperature 1100° C

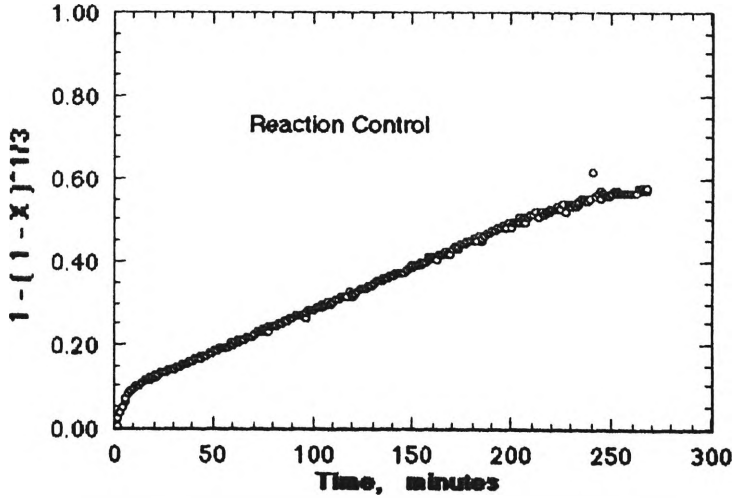

Figure 4.39. Chemical Reaction Control plot for sample No.2 at temperature 1200° C

Table 4.7. Activation Energies for Reduction of Dense Briquettes (after El-Geassy *et al*, 1977)

Reducing Gas	E , kcal/mol	kJ/mol
100% CO	7.55	31.59
75% CO + 25% H_2	8.94	37.40
50% CO + 50% H_2	9.59	40.12
25% CO + 75% H_2	10.83	45.31
100% H_2	12.80	53.56

The activation energy obtained for this case, indicates a diffusion controlling step for both sample no.2 and no.5 at the initial stage of reduction . However, during the progress of the reduction a transition in the mechanism of reduction was obvious between sample No.2 and No.5.

4.2.4. RATE CONTROLLING STEP

A more definitive way of delineating the region of either diffusion control or reaction control, for spherical particles, is to plot the function $f(x) = 1 - 3(1-X)^{2/3} + 2(1-X)$ or $f(x) = 1 - (1-X)^{1/3}$ against time which is expected to be a linear function of time, based on the shrinking core model (Section 2.2). For sample no.2, Figures 4.32 to 4.35 show plots of $f(x) = 1 - 3(1-X)^{2/3} + 2(1-X)$ for 900°, 1000°, 1100° and 1200° C, respectively and Figures 4.36 to 4.39 are plots of $f(x) = 1 - (1-X)^{1/3}$ for 900°, 1000°, 1100° and 1200° C, respectively. It is seen that all these plots have a linear portion and the higher the temperature the greater the linear parts are, indicating mixed control in the lower temperature region and either chemical or diffusion controlling step at the higher temperature.

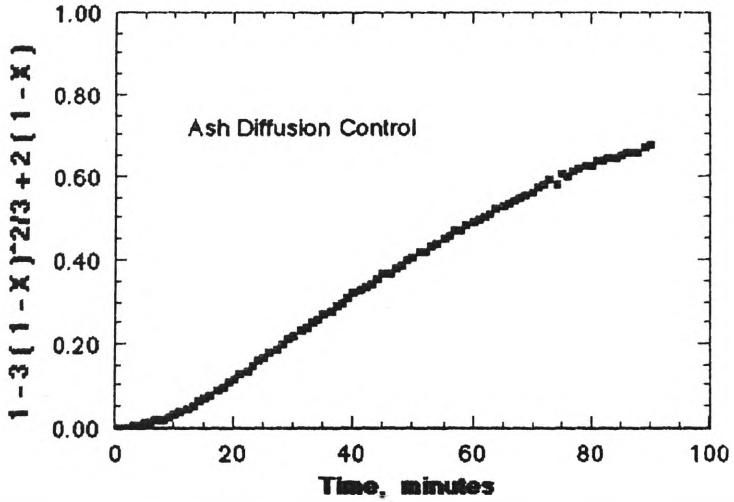

Figure 4.40. Ash Diffusion Control plot for sample No.5 at temperature 900° C

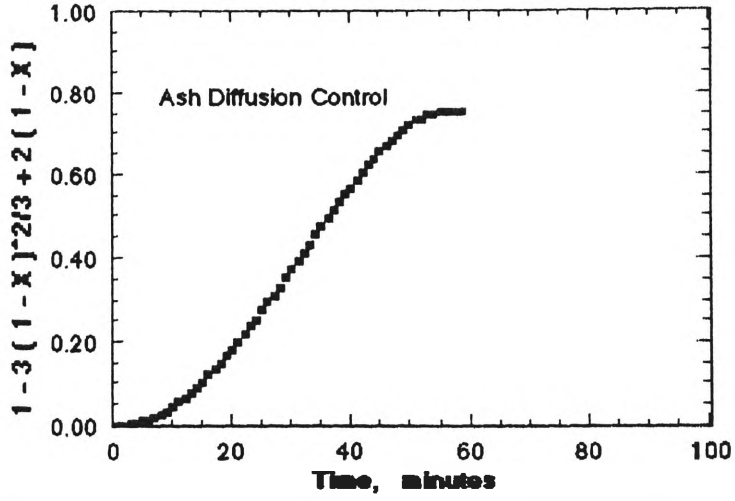

Figure 4.41. Ash Diffusion Control plot for sample No.5 at temperature 1000° C

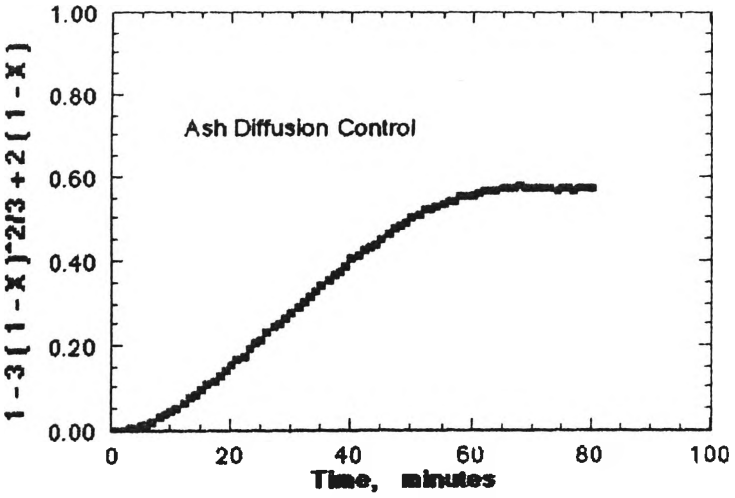

Figure 4.42. Ash Diffusion Control plot for sample No.5 at temperature 1100° C

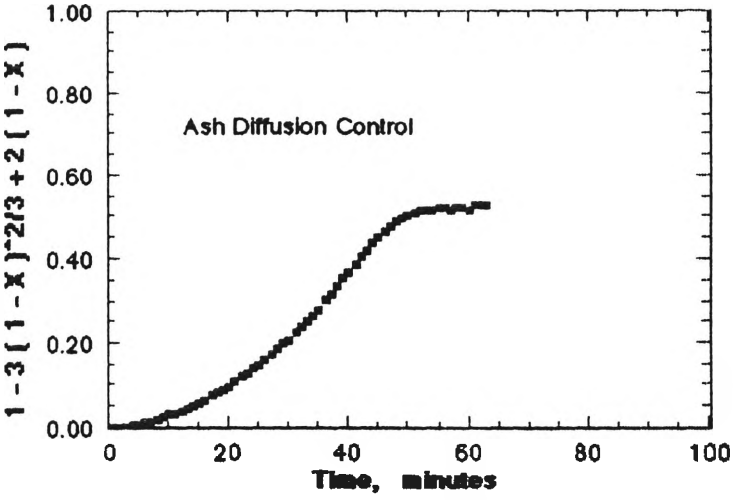

Figure 4.43. Ash Diffusion Control plot for sample No.5 at temperature 1200° C

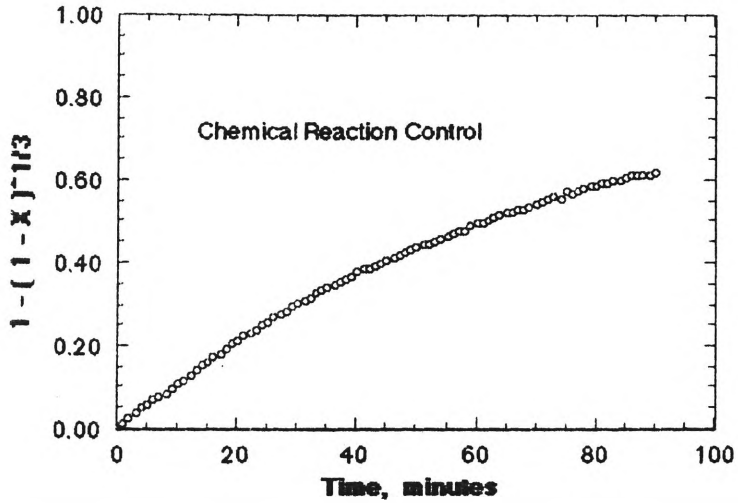

Figure 4.44. Chemical Reaction Control plot for sample No.5 at temperature 900° C

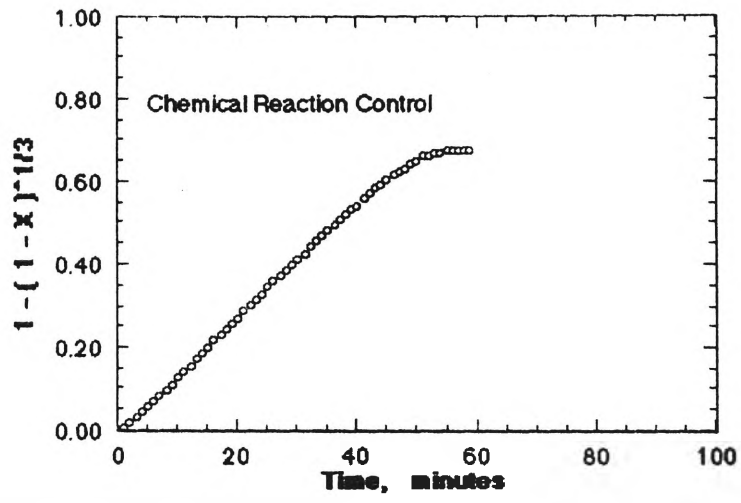

Figure 4.45. Chemical Reaction Control plot for sample No.5 at temperature 1000° C

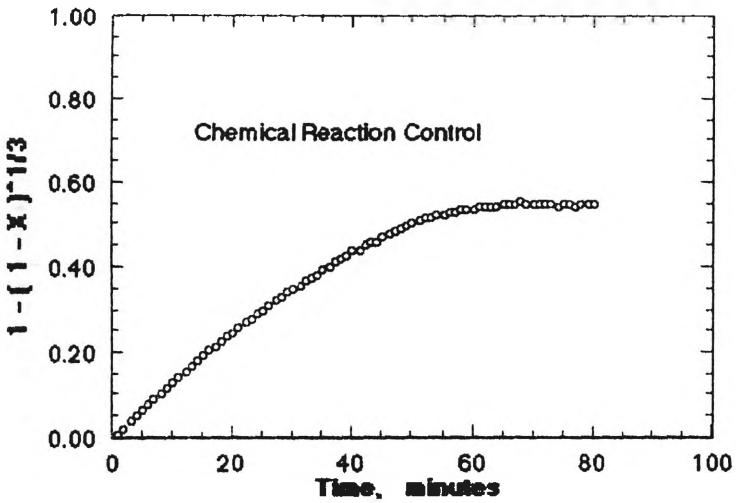

Figure 4.46. Chemical Reaction Control plot for sample No.5 at temperature 1100° C

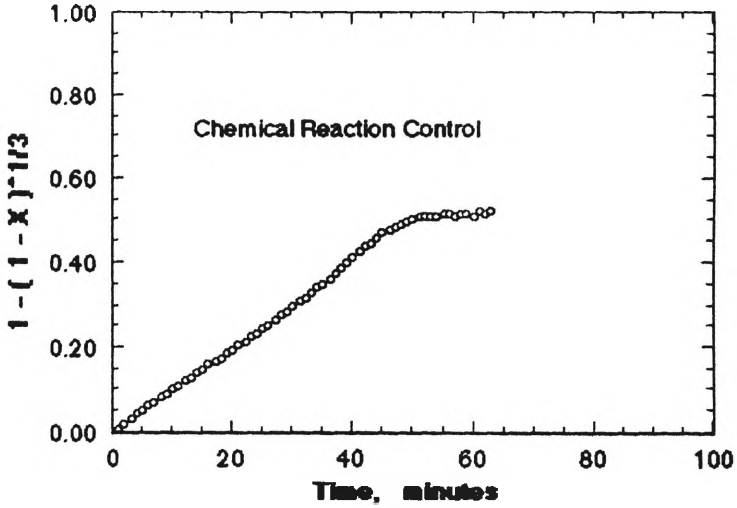

Figure 4.47. Chemical Reaction Control plot for sample No.5 at temperature 1200° C

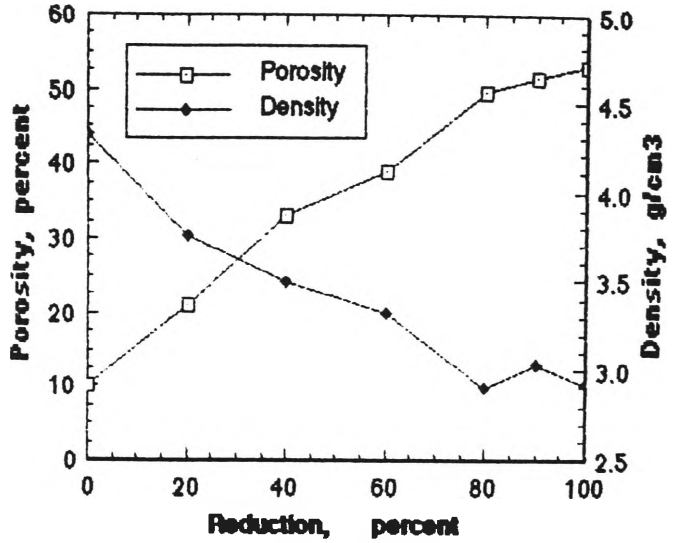

Figure 4.48. Porosity and density changes of sample No.1 during reduction.

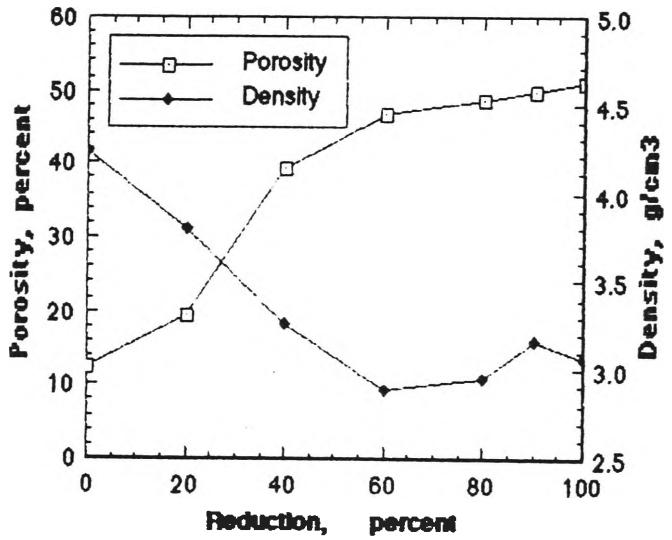

Figure 4.49. Porosity and density changes of sample No.2 during reduction.

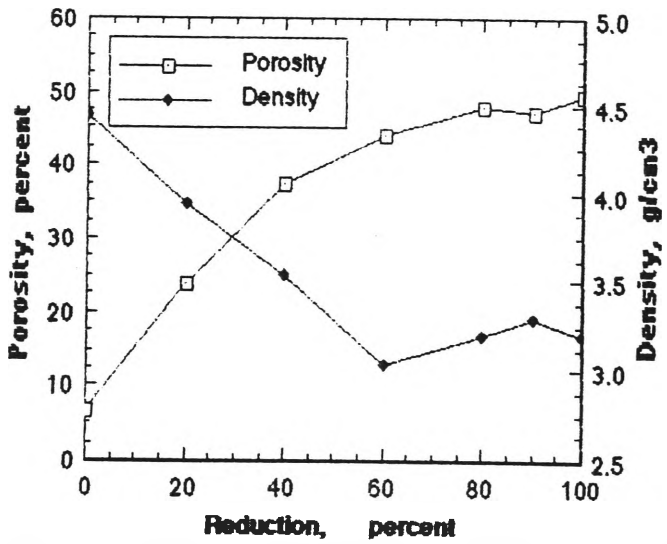

Figure 4.50. Porosity and density changes of sample No.3 during reduction.

Similar plots made for sample no.5 are shown in Figures 4.40 - 43 for diffusion control at temperatures 900° to 1200° C and Figures 4.44 - 47 for chemical reaction control. The results show that neither step alone controlled the reduction and that both steps seemed to be operative during the course of reduction even in the lower range of temperature. In other words, sample no.5 appeared to be a mixed control case throughout.

4.2.5. STRUCTURAL CHANGES

The results of porosity (i.e. accessible pore volume) measurements on ore reduced at a temperature of 1000° C are shown in Figures 4.48, 4.49 and 4.50 respectively for samples No.1, No.2 and No.3 associated with the initial porosities of 10.00, 12.39 and 6.44 percent (Table 4.3). It is seen that in each case the porosity of the samples increases and the density decreases with the extent of the reduction, as expected from theory (Sect 2.1.2). This increase is within the range 19.4 to 53.1 percent which corresponds to density within 3.9 to 2.9 g cm^{-3} (Appendix A-7), respectively. It is also seen that porosities of the final iron product are 53.10, 51.05 and 49.57 % respectively for samples No.1 to No.3 which may be compared to the value of 68 % for product iron in the temperature range of 200° to 1200° C as reported by Turkdogan *et al*(1971). These authors used ore with an average 31 % porosity in their study of reduction of hematite ore by hydrogen.

Recently, Du *et al*(1988) have reported the effect of initial sample porosity on the kinetics of reduction of pure hematite pellets as shown in Figure 2.6 (Section 2.1.2). Their results showed that at relatively low porosity in the sample, the reduction rate increased sharply with increasing porosity. However, the increase in reduction rate decreased rapidly as porosity increased beyond about 35 %. Furthermore, the initial reduction rate data (Table 4.8 after Du *et al*, 1988) indicated a higher rate of increase at high porosities. Similar effects were found in the present

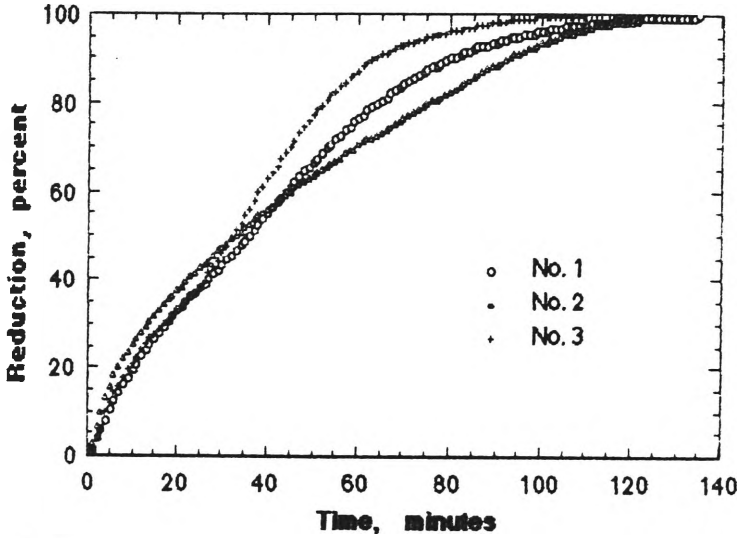

Figure 4.51. Effect of different particles on reduction

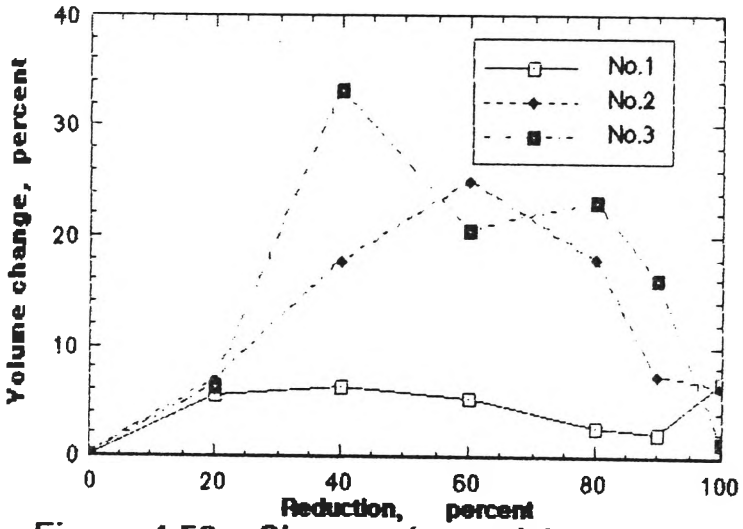

Figure 4.52. Changes in particle volume with the extent of reduction for samples reduced at 1000° C

Table 4.9. Reduction of hematite to magnetite.

(after Brill-Edwards *et al.* 1965)

Reduction temperature, °C	Apparent volume change, %	Remarks
525	+25·6	Grain boundary and transcrystalline failure of magnetite and random spherical porosity
625	+23·6	Grain boundary and transcrystalline failure of magnetite and random spherical porosity
740	+17·3	Grain boundary failure of haematite and elongated directional porosity
825	+16·2	Grain boundary failure of haematite and elongated directional porosity
903	+19·8	Grain boundary and transgranular failure of haematite, porosity decreasing as temperature increases
955	+21·0	Grain boundary and transgranular failure of haematite, porosity decreasing as temperature increases
1025	+23·1	Grain boundary and transgranular failure of haematite, but no evidence of granular porosity
1075	+25·4	Grain boundary and transgranular failure of haematite, but no evidence of granular porosity

Table 4.10. Reduction of hematite to wustite.

(after Brill-Edwards *et al.* 1965)

Reduction temperature, °C	Apparent volume change, %	Remarks
825	+18·0	Transgranular failure (during haematite to magnetite reduction) and large directional pores
875	+18·8	Transgranular failure (during haematite to magnetite reduction) and large directional pores
925	+23·2	Transgranular failure (during haematite to magnetite reduction) and large directional pores
975	+23·9	Transgranular failure (during haematite to magnetite reduction) and large directional pores
1025	+24·9	Transgranular failure (during haematite to magnetite reduction) and elongated pores at the grain surface
1075	+27·1	Transgranular failure as above but no evidence of granular porosity

study for samples No.1 to 3 during the first stage of reduction up to about 40 % of reduction as shown in Figure 4.51; however, beyond that point the figure shows an interesting pattern. The reduction rate for sample No.3 significantly improved as compared with No.1 and No.2 rates which continuously decrease. A further decrease in reduction rate for sample No.2 was observed at 60% reduction. It is apparent from Figure 4.51 that the initial rate of reduction depends on the initial porosity. However, it is also apparent that during the progress of reduction another structural change occurred causing deviation in the rates. From the porosity data shown in Figures. 4.48 to 4.50, it is clear that the porosity changes are a function of reduction stages and are independent of the type of ore.

A comparison of changes in volume with reduction stages for samples No.1 to 3 at 1000° C is shown in Figure 4.52 (from data in Appendix A-7). Inspection of this figure reveals for sample No.3 a marked volume change (33.33 %) at 40 % of reduction compared with changes in samples No.1 (6.20 %) and No.2 (17.57 %). It is also seen that the changes in volume decreased after the maximum value had been reached, *viz* at 40 % reduction for samples No.1 and No.3, and at 60 % of reduction for sample No.2. These changes may explain why the reduction of sample No.3 was higher than that of the other two samples.

It is generally accepted that during the stepwise reduction of hematite through magnetite and wustite to metallic iron, changes in crystal structure take place (Edstrom, 1953; Brill-Edwards *et al*, 1965; Wright, 1977). The swelling of ore or pellets occurring during transformation of the hexagonal hematite into cubic magnetite results in considerable increase in the apparent volume. The increase in volume is about 25 % (Edstrom, 1953) as also can be seen in Table 4.9 (after Brill-Edwards *et al*, 1965). Further increase of 7 to 13 % in the transformation to wustite (Edstrom, 1953) is also seen in Table 4.10 (after Brill-Edwards *et al*, 1965). According to Wright (1977) the swelling of fired pellets occurrs in two stages. 'Normal' swelling, up to 20 %, occurring during transformation of hematite to

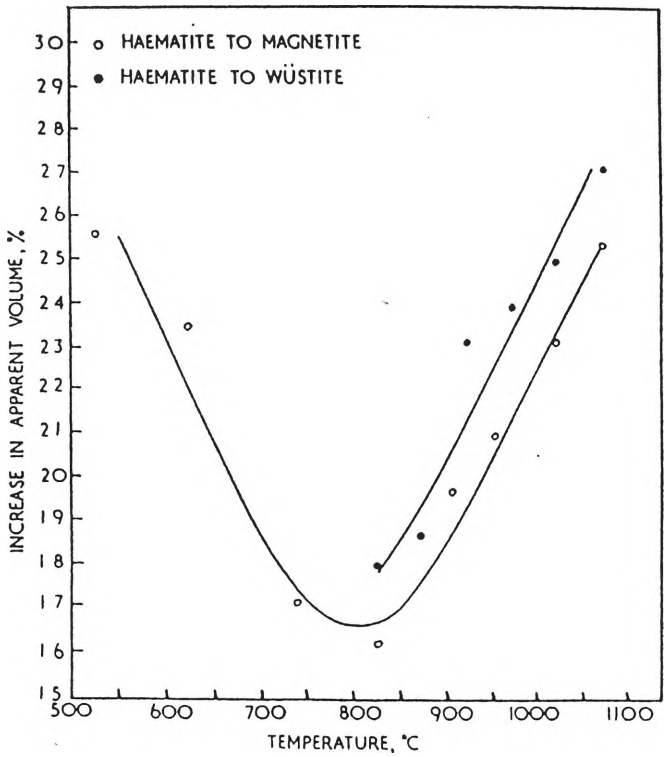

Figure 4.53. Effect of reduction temperature on apparent volume increase of hematite.

(after Brill-Edwards *et al.* 1965)

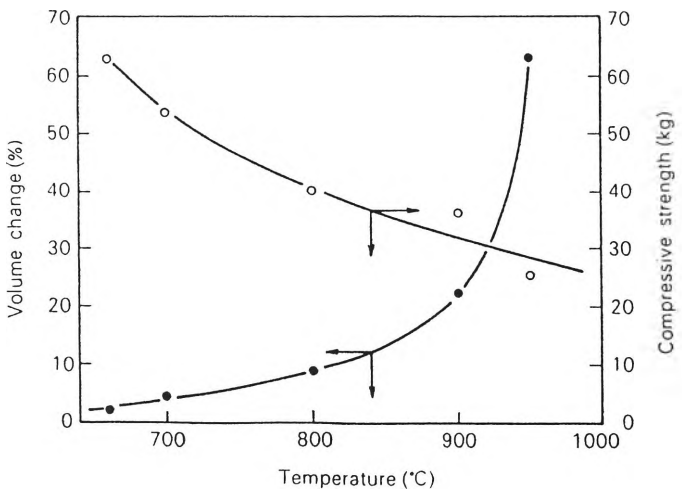

Figure 4.54. Effect of reduction temperature on volume change and strength of metallized pellets.

(after Wright, 1977)

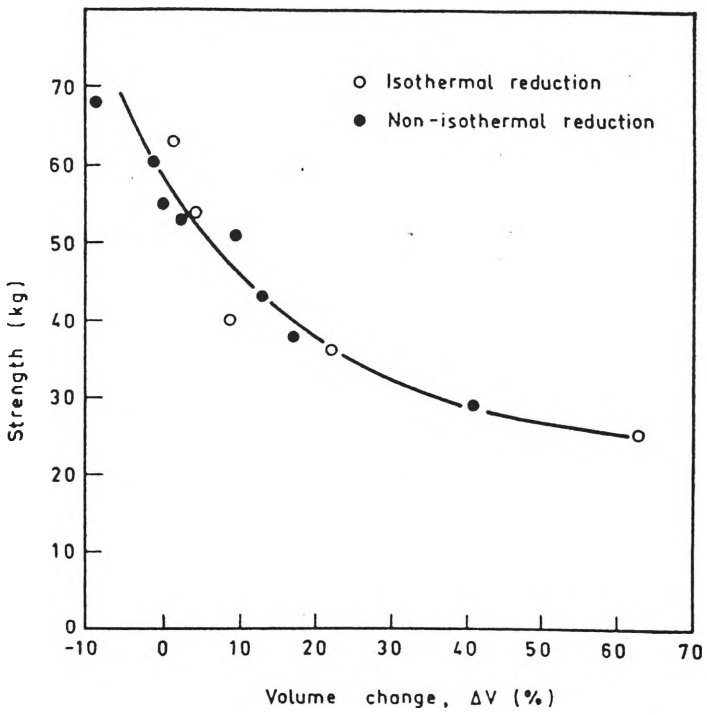

Figure 4.55. Strength of metallized plotted against volume change after reduction.

(after Wright, 1977)

magnetite and 'abnormal' swelling occuring during transformation of wustite to iron which could result in a further volume increase well in excess of 20 %. It should also be noted that transformation of magnetite to wustite results in only a small increase in volume (Edstrom, 1953). The changes in volume from these three different samples (as seen in Appendix A-7) were different (Figure 4.52) but still in the 'normal' range of swelling. These results suggest that the differences in iron oxide composition (hematite and magnetite content) in the ore had influenced the changes of volume which resulted in the observed differences of reducibility.

The volume change is also temperature dependent as reported by Brill-Edwards *et al* (1965) and Wright (1977) shown here in Figures 4.53 and 4.54 respectively. It is seen in Figure 4.53 that the apparent volume changes that occur during the reduction to wustite are approximately of the same order as those observed during the corresponding reduction to magnetite. Further study by Wright (1977) showed that the strength of metallized pellets was a function of volume change only and was independent of the reduction procedure, either isothermal or non-isothermal (as shown in Figure 4.55). These studies are not of direct relevance to the present work, because the present results were obtained at one temperature (i.e. 1000° C). However, the above findings on the relation of volume change and the strength of metallized pellets could provide additional information to predict the physical properties behaviour of the material during reduction. It is apparent from the above that the present volume changes should not result in a condition of poor compressive strength. Hence, a possible size degradation as a consequence of catastrophic swelling, which could have an adverse impact on the permeability of the furnace and therefore, on its productivity, may be avoided.

Turkdogan *et al* (1971) and Wright (1977) have also shown that the average pore size and total pore volume increase with increasing reduction temperature and Wright (1979) has also found that at high temperature (>900° C) the pore size is similar to that observed in the reduced pellet. Furthermore, it was also found that the

average pore size of the individual metallized ore and pellets depended strongly on the chemical nature of the ores and the treatment received before reduction. Koo and Evans (1979) showed that the structure of porous iron can be markedly altered by holding at high temperatures prior to reduction. Similarly, Wright (1979) showed that the pore volume of the sintered compacts can decrease with increasing temperature and time, owing to the progressive elimination of the smallest pores present in the compacts.

From their finding, it is clear that the porosity of metallized ore, in regard to the pore volume distribution, during reduction at high temperature depended on the initial porosity. If the initial porosity is adjusted by treatment before reduction. then the result would provide a better access to the reducing gas to reach the ore surface and, on the other hand, the excessive swelling during reduction could be prevented.

If the differences in the ore chemistry do not seem to be enough to account for the large differences in reduction, another possible explanation could be the reduction reaction being affected by the presence of micropores. Perhaps as the micropores are not readily accessible to the reducing gas, under condition where the macropores are accessible, then their contribution to the reaction may be negligible. However, because there is no supporting data (such as porosimetry measurements) available in this work, future study on the pore size distribution to confirm this argument is indicated.

4.2.6. MICROSCOPIC OBSERVATION

Polished specimens of the raw ore and the partially reduced sample were observed under optical microscopy. The structure of both unreduced and partially reduced samples no. 1, 2 and 3 after stages of reduction at 1000° C in pure CO at a

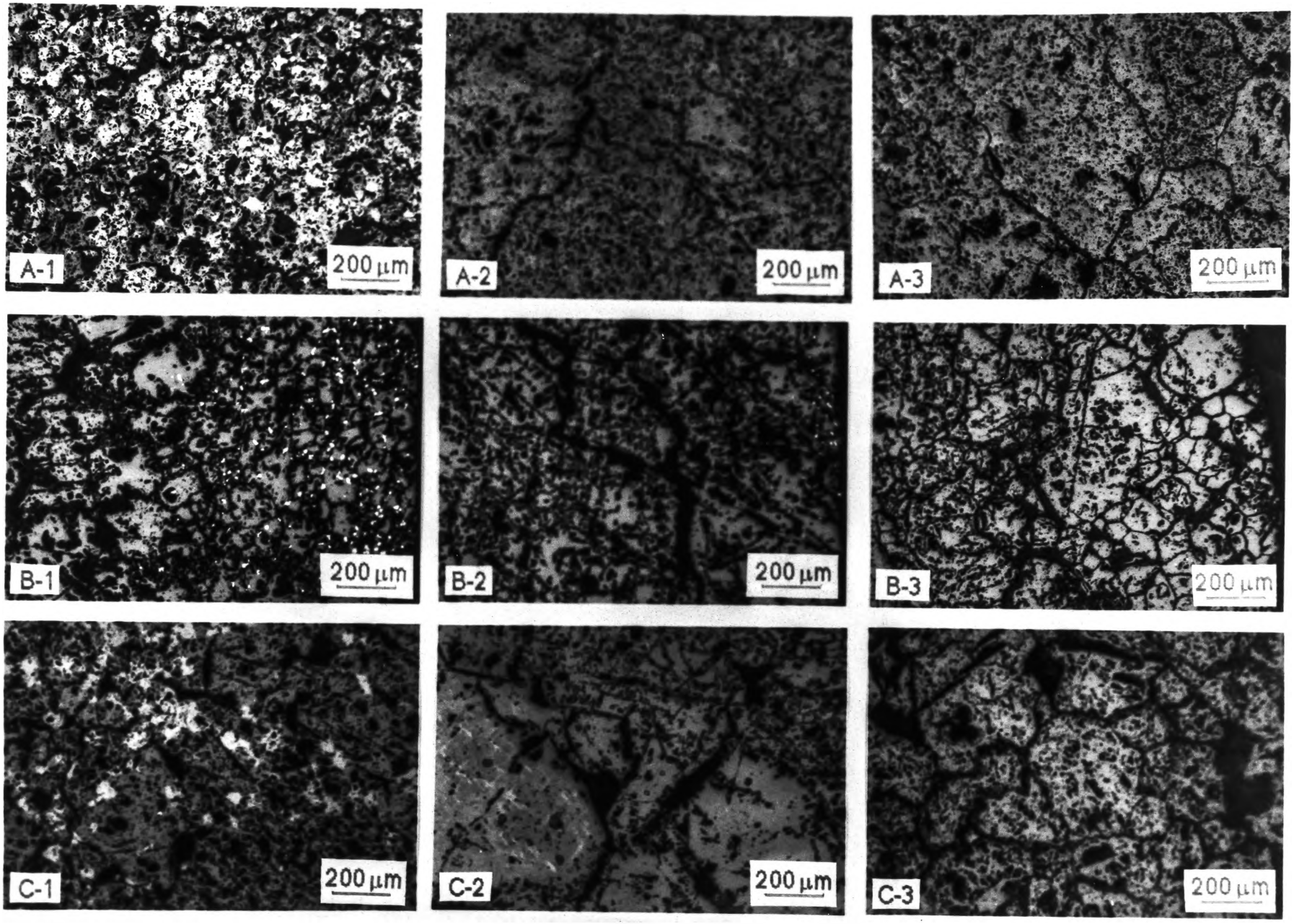

Figure 4.56. Microstructure of raw ores and reduced ores at 1000° C.

(continued on next page)

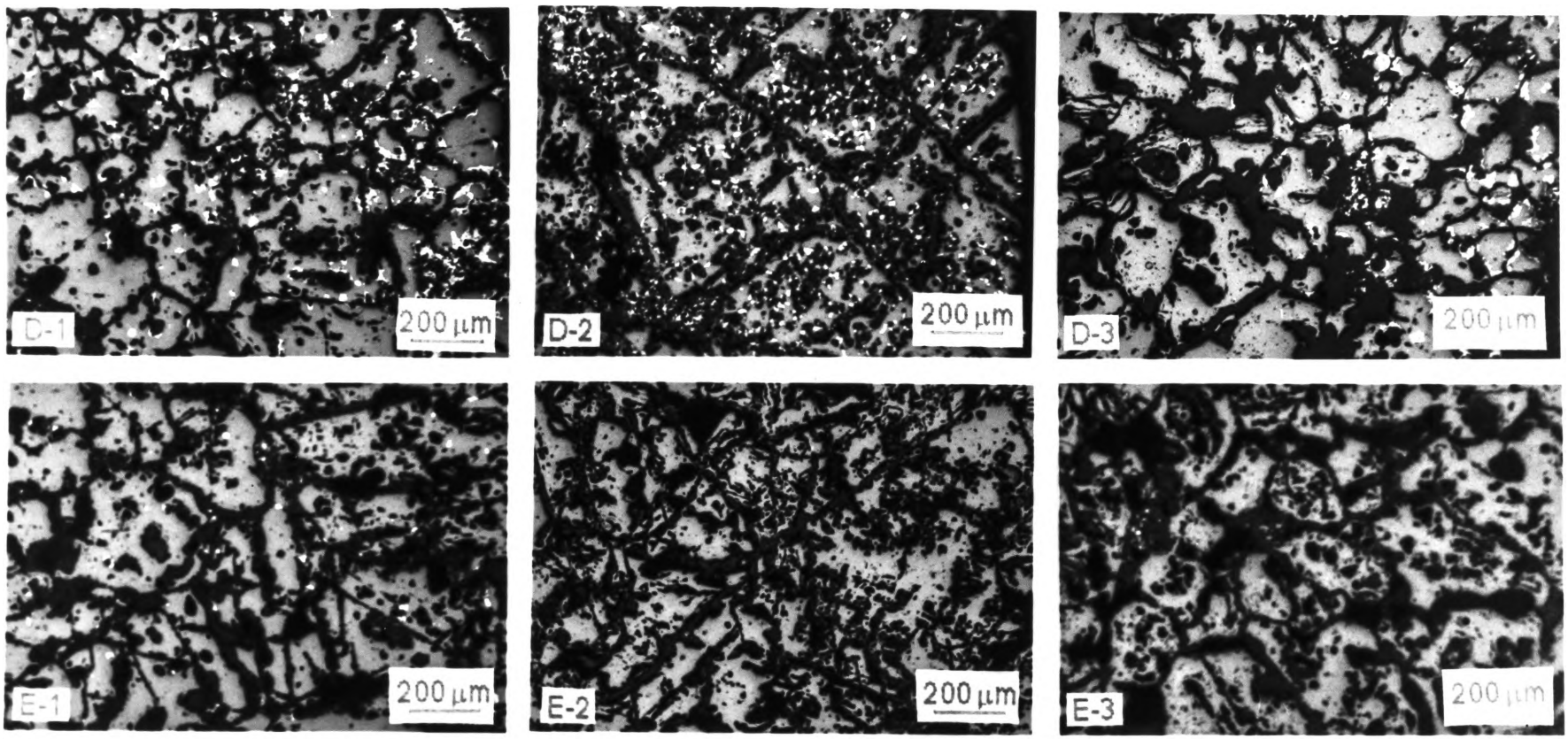

Figure 4.56. (Continued)
Raw ores of Samples (A-1) No.1, (A-2) No.2 and (A-3) No.3.
At X = 20%, edge of Samples (B-1) No.1, (B-2) No.2 and (B-3) No.3, cracks (dark) development and specks of metallic iron (white). Centre of Samples (C-1) No.1, (C-2) No.2 and (C-3) No.3, fine cracks and patches of hematite (light grey).
At X = 40%, edge of Samples (D-1) No.1, (D-2) No.2 and (D-3) No.3, dense wustite (grey) and growth of metallic iron. Centre of Samples (E-1) No.1, (E-2) No.2 and (E-3) No.3, dense wustite (grey) and specks of metallic iron (white).

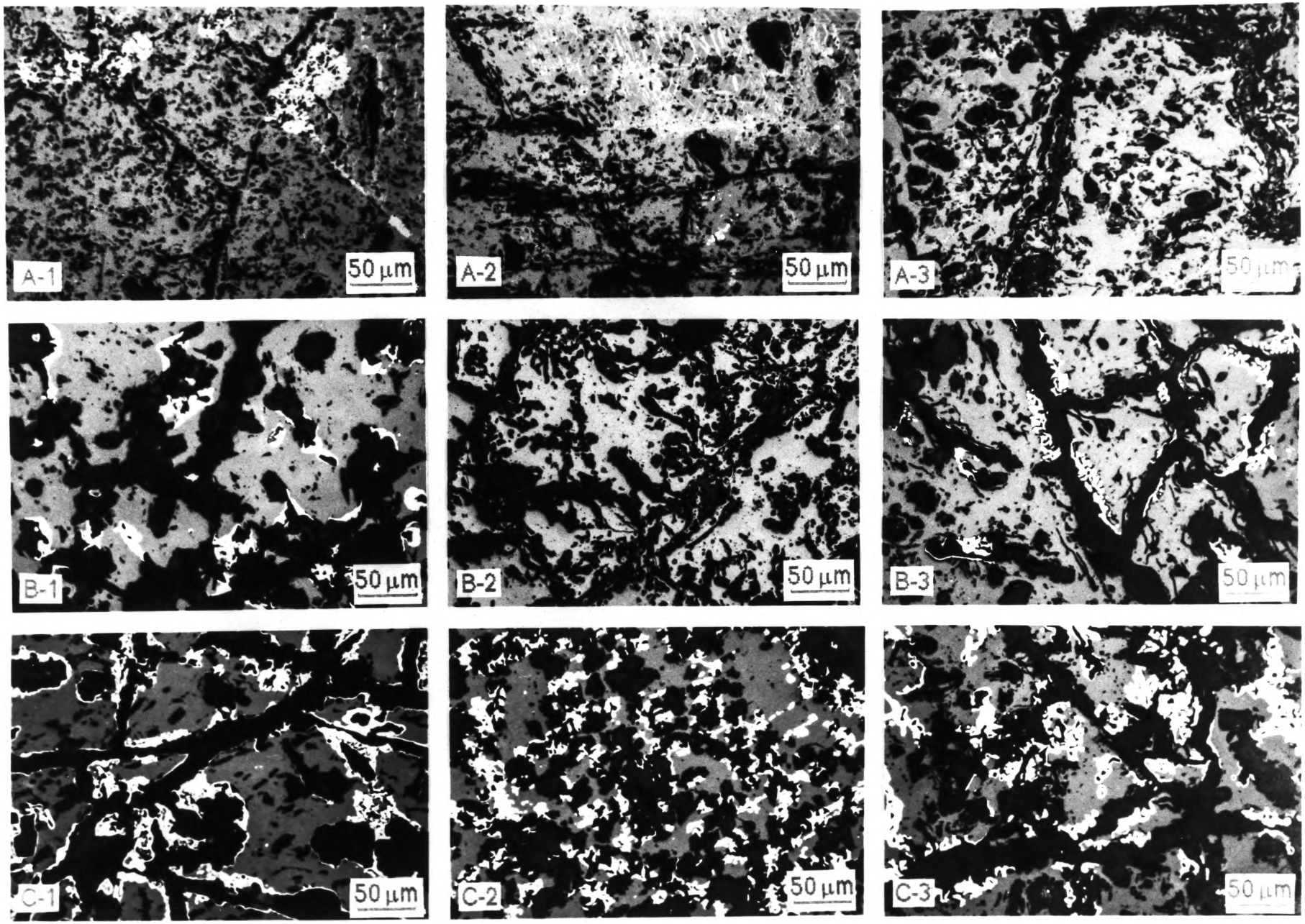

Figure 4.57. Microstructure of reduced ore after reduction at 1000° C

(continued on next page)

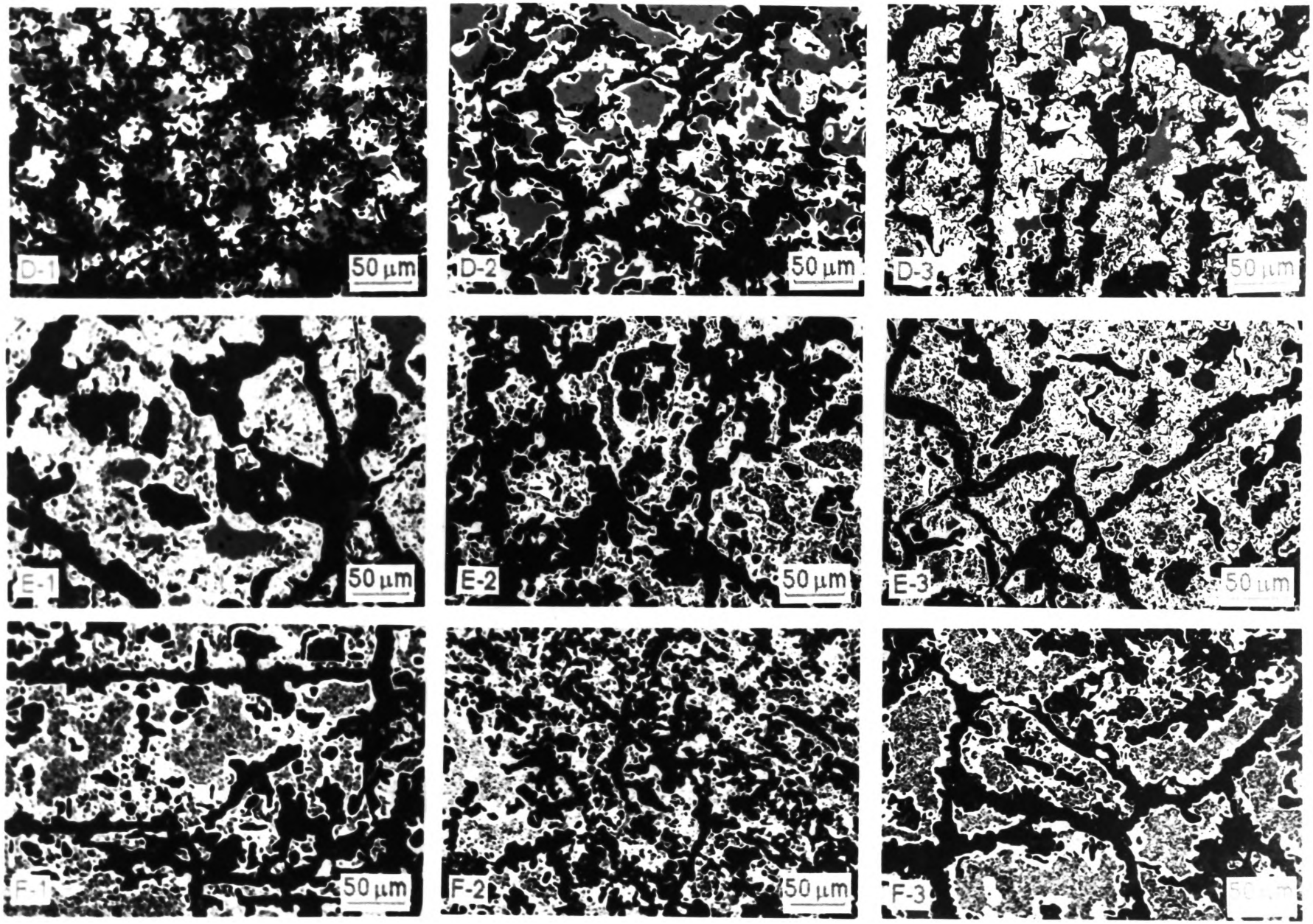

Figure 4.57. (Continued)

(continued on next page)

Figure 4.57. (Continued)
Micrographs labelled -1, -2 and -3 correspond with Samples No.1, No.2 and No.3.
(A-1), (A-2) and (A-3) at X = 20%. Cracks at the boundary, patches of hematite (light grey).
(B-1), (B-2) and (B-3) at X = 40%. Formation of void (dark), growth of metallic iron (white).
(C-1), (C-2) and (C-3) at X = 60%. Continuous formation of metallic iron.
(D-1), (D-2) and (D-3) at X = 80%. Porous metallis iron and dense wustite (grey).
(E-1), (E-2) and (E-3) at X = 90%. Dense wustite surrounded by metallic iron.
(F-1), (F-2) and (F-3) at X = 100%. Metallic iron.

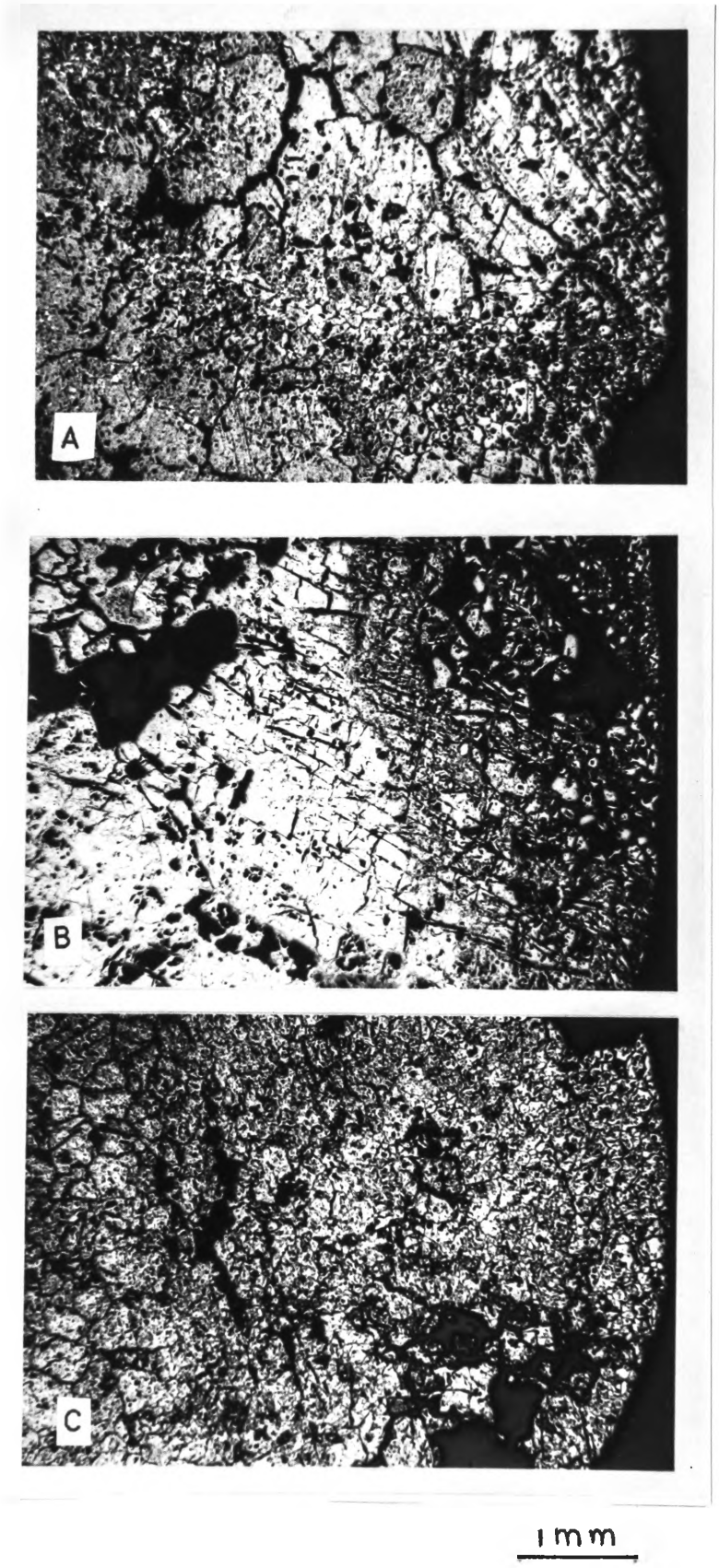

Figure 4.58. Under low magnification showing polished samples from the edge to the centre for (A) Sample No.1, (B) Sample No.2 and (C) Sample No.3.

rate of 2 l/min are shown in Figures 4.56 (A-E) and 4.57 (A-F) at a lower (75x) and higher (300x) magnification, respectively.

In each reduced sample some particles were at a more advanced stage of reduction than others, especially in the early stages of reduction. All samples were expected to have experienced the same reduction conditions. However, the rates of reduction at the early stage of reduction were faster than the reduction rates at the later stage of reduction so difficulties were experienced in controlling the final stage of reduction. At the early stages of reduction (i.e. up to 40%) even after the reactant gas was changed to the inert gas, it was generally observed that the reduction was still progressing to some extent. Therefore, the percentage of reduction of each sample shown in Figures 4.56 (B-C) and 4.57 (A-F) is not exactly the same as the percentage indicated. However, stages occurring in the progressive reduction of the sample are clearly shown in these series.

Figure 4.56 (A-1 to A-3) show the pore structure of raw ore no.1, 2 and 3. As expected from porosity data in Appendix A-6, sample no.1 and 2 showed some larger pores and cracks between grain boundary filled by resin. Less resin penetrated deeply into the sample no.3 and it can also be seen that the grain boundaries are filled with goethite.

Partially reduced samples revealed the lack of sharp boundaries between phases which mask the true topochemical appearance of reduction. Figure 4.56 (B) shows the structure near the edge of the samples after 20% reduction. All the samples show similarity in development of fine cracks towards the centre, widening gaps between grain boundary and specks of metallic iron (white in colour) formed near the surface. At this stage of reduction no evidence of a sharp-interface between product and reactant can be observed.

From Figure 4.58 (A to C) at X = 20% at low (15x) magnification, it can be seen that the small porous and the large porous grains are entirely reacted, but the

small dense and the large dense grains are likely being reduced in a shrinking-core manner leaving a number of groups of partly reacted grains in the sample. Larger cracks and pores are evident in sample no.2 at the early stage of reduction suggesting that the rate of reduction was relatively higher compared with the other samples. This was confirmed by the reduction curves of these samples presented in Figure 4.51 which shows that the reduction of sample no.2 begins at a very rapid rate which then decreases after about 20% of reduction has been reached.

Figure 4.56 (C) depicting the structure at the centre of the samples shows the partially reduced hematite (light grey) in the larger grain, separated by some larger pores for sample no.1 and 2 and only finer cracks, distributed more or less uniformly throughout the cross-section, in sample no.3. These results therefore suggest that the reducing potential for the next stage of reduction may be relatively higher for sample no.3 compared with the other two samples.

No hematite is visible in Figure 4.56 (D-E) after 40% of reduction and in all cases larger cracks and pores are present throughout the samples, suggesting that a similar reduction behaviour was operative. This was confirmed by the relatively parallel curves of reduction from the three samples up to 40% of reduction in Figure 4.58.

El-Geassy and Rajakumar (1985) reported that on reduction of wustite with pure CO, at 25% of reduction, growth of iron was observed. Dou *et al* (1988) found no evidence of iron nuclei at 17% of reduction, whereas, at 39% the number of iron nuclei was uniformly observed throughout the particle. So it could be expected that metallic iron would appear at about 20 % reduction.

Figure 4.57 (A) at higher magnification, again shows the extent of reduction at 20% and that more larger cracks and finer cracks have developed in sample no.2 compared with the other two samples, therefore a higher reduction rate would be expected during this stage of reduction.

Figure 4.57 (B) shows, at 40% reduction, the growth of iron nucleation on the wustite particle. It is also obvious that more porous iron had developed in sample no.3 compared to sample no.1 and that there has been but little growth of iron in sample no.2 as already shown in Figure 4.56 (B).

The above finding is therefore in line with that reported by previous investigators that the growth of iron nuclei takes place during reduction.

Figure 4.57 (C) shows the ore structure at an advanced stage of reduction (60%) from which it is evident that iron had formed continuous layers in the macropore walls with a sharp boundary being apparent between iron layers and wustite. It is also evident from Figure 4.57 (C) that in sample no.2 more dense iron nucleation developed compared with sample no.1 and 3, suggesting that beyond this reduction degree a slower rate of reduction could be expected. This conclusion is confirmed by the results in Figure 4.58 which show that at this stage of reduction the rates of reduction of sample no.1 and 3 were higher compared with that of sample no.2. The above indicates that the number of cracks and pores developed in the early stage of reduction had little influence on the later stage of reduction; on the other hand the finer distributed pores in the early stage of reduction had great influence. This is in agreement with the generally accepted view that uniformly distributed pore materials, such as pellets and some ores have a better reducibility as also reported by Wright (1979).

Figure 4.57 (D) shows the stage of reduction at 80%. The degree of reduction of pore walls appears to be independent of position within the particle in that similar features are evident throughout the particle, suggesting that gaseous diffusion within the macropore was rapid relative to the rate of reaction.

From Figs. 4.57 (C-D) it is also evident that some sections of the pore walls were completely reduced although no pore structure is visible in the reduced

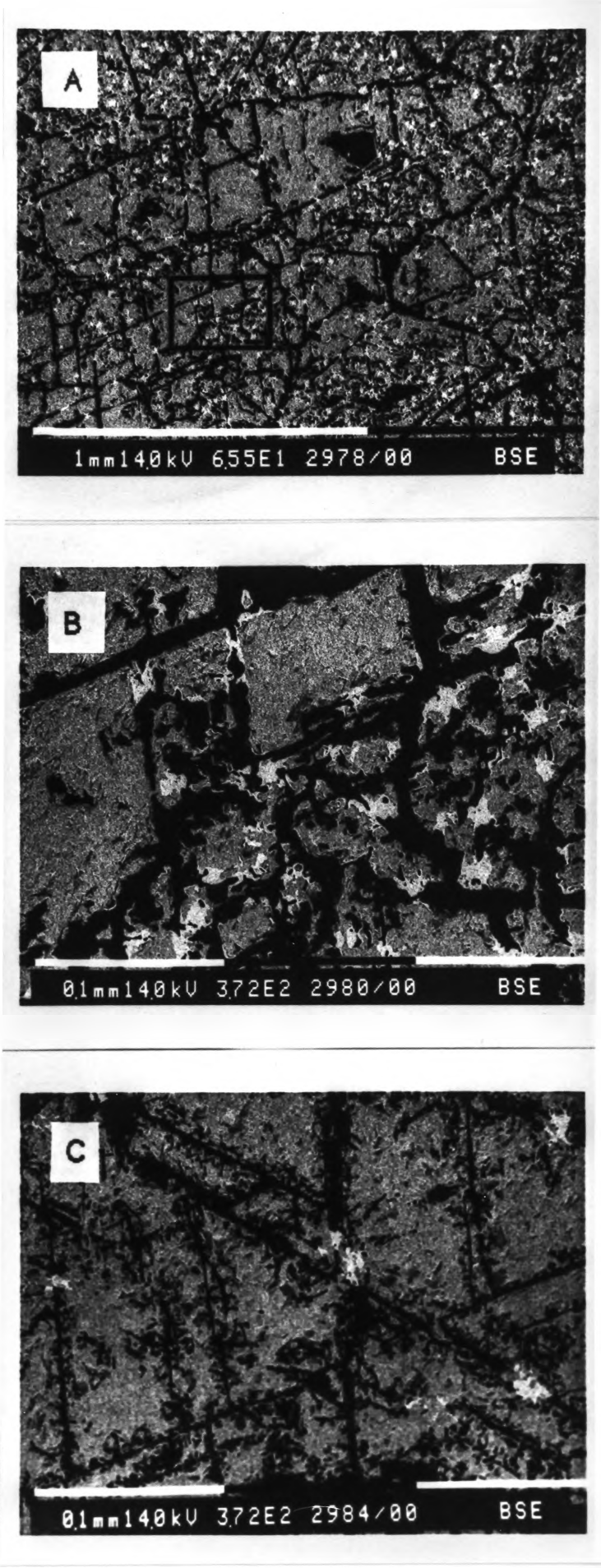

Figure 4.59. SEM micrograph for Sample No.2 at X = 50% showing (A) edge of sample, (B) increased magnification of the boxed area, showing wustite replacing magnetite with small areas of metallic iron and (C) near centre of sample showing wustite and patches of metallic iron.

sections. This suggests that the reactant gas could easily penetrate the microstructure of the particle in either wustite or in the layer of product iron.

Figure 4.57 (D-E) shows that, after high extent of reduction (80 to 90%), on the dense wustite, a topochemical reduction commenced and the phase boundary between iron and wustite decreased slowly. Dense wustite is surrounded by large masses of porous iron as shown in Fig 4.57 (D) for sample no.1 and for samples no.2 and 3 partially reduced wustite is surrounded by a thin, dense iron layer. These layers would almost certainly cause a decrease in the rate of reduction throughout the final reduction stages as observed from the time-reduction curves (Figure 4.51).

Finally, in all cases, the fine porous iron product was always surrounded by relatively dense iron as shown in Figure 4.57 (D).

The scanning electron micrograph at 50 % reduction in Figure 4.59 shows that at this stage all the iron oxide was reduced to wustite and also confirms that metallic iron was present throughout the particle and the growth is less extensive near the centre compared with the edge of the sample. It is seen that larger pore size formed as more metallic iron present at the edge compared with the near centre of the sample.

Edstrom (1955) used optical microscopy to study the relationship between microstructure and reaction rate and observed that reduction of hematite occurred more rapidly when there was early and extensive formation of pores in the solid reaction product. It was also reported that iron produced from magnetite was finely porous, while iron produced from hematite had large, elongated pores - a structure seen also in the wustite stage.

Turkdogan and Vinters (1971) have shown on partially reduced hematite ore that there was a diffuse iron and wustite interface and their observation indicated

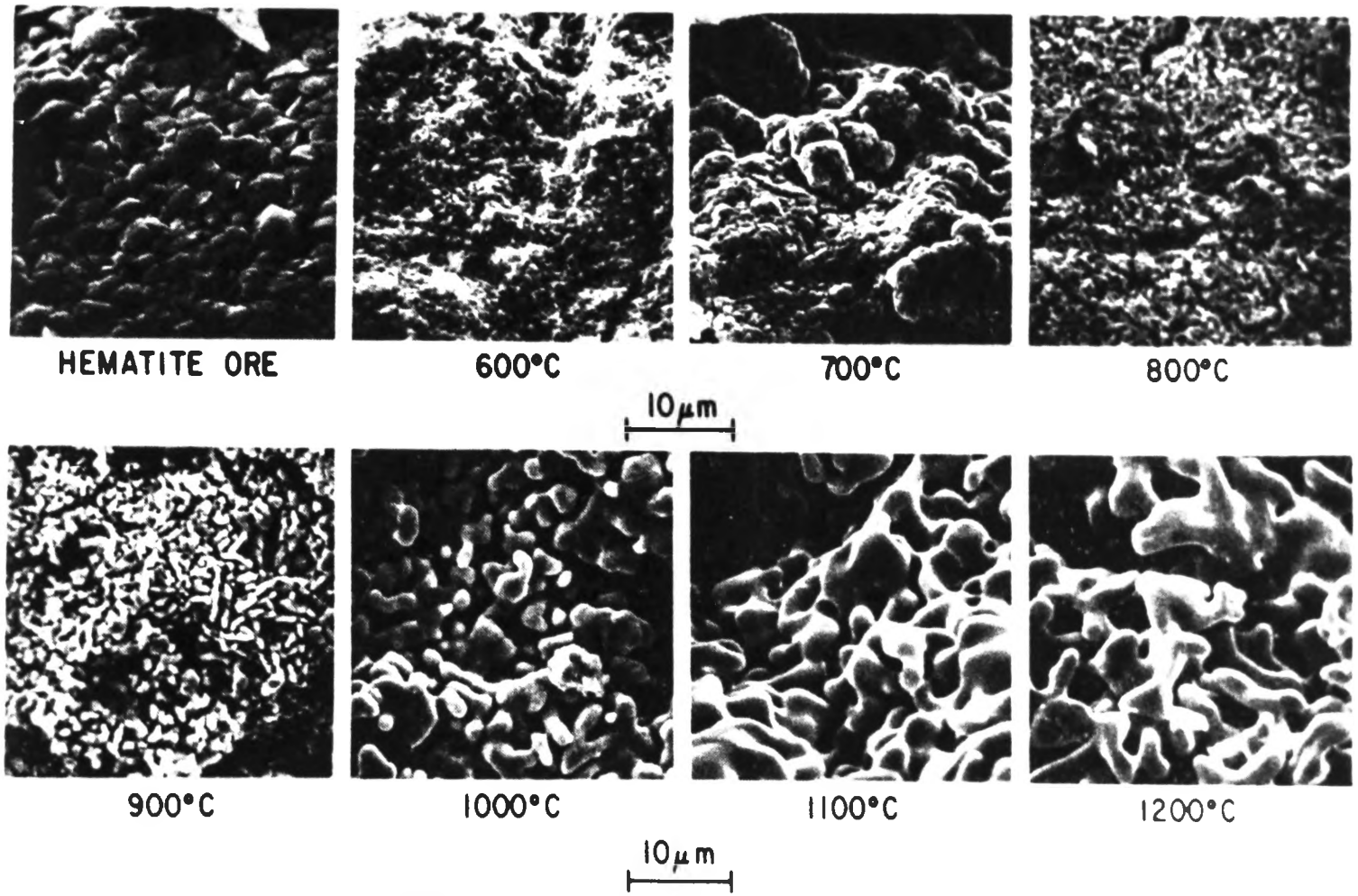

Figure 4.60. Fracture surfaces of hematite ore and porous iron reduced in hydrogen at 600° to 11200° C as viewed in the SEM.

(after Turkdogan and Vinters, 1971)

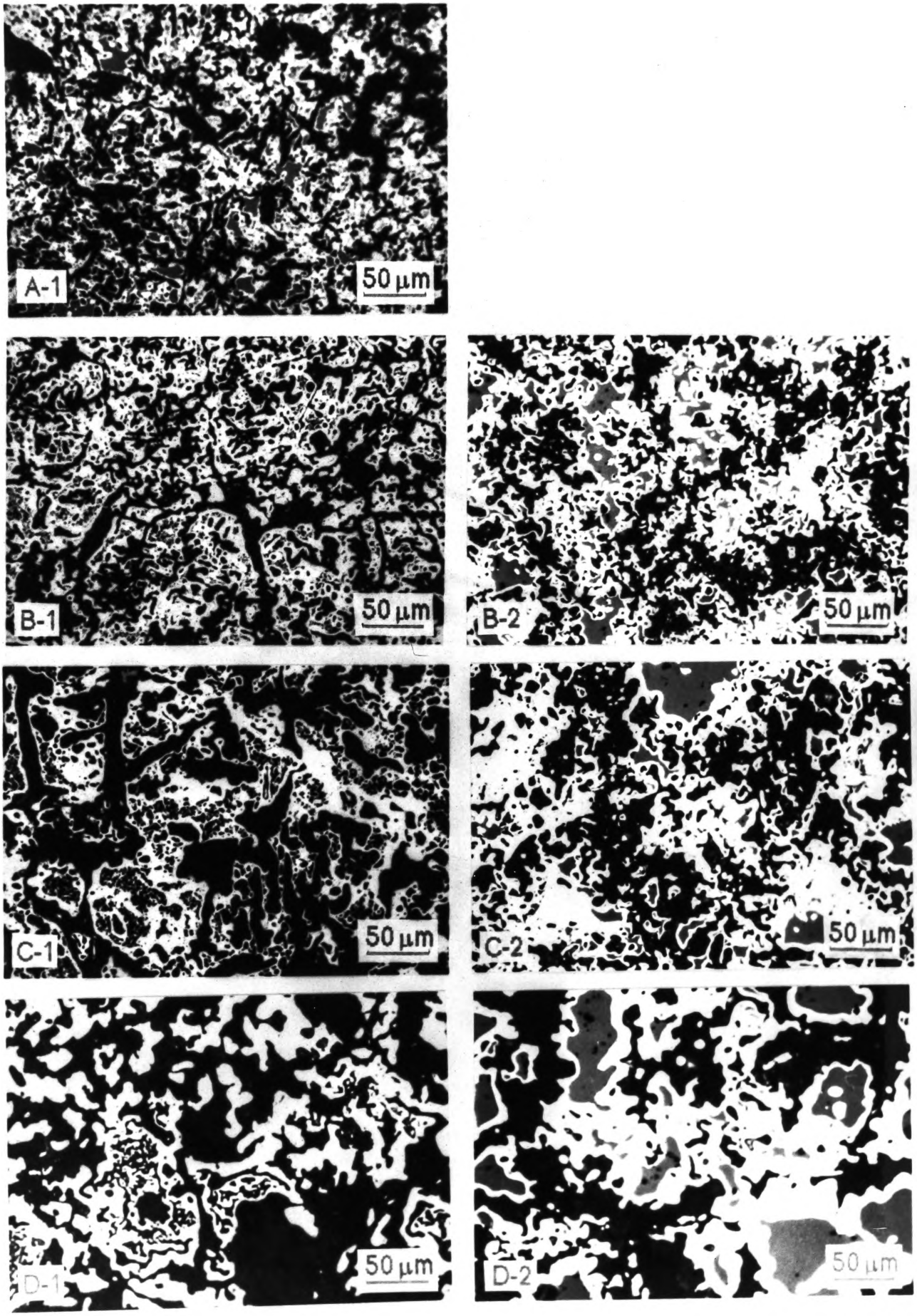

Figure 4.61. Microstructure of ore samples after reduction at (A) 900°, (B) 1000°, (C) 1100° and (D) 1200° C. -1 and -2 correspond to Samples No.5 and No.2.

that there was sufficient gas diffusion resulting in some internal reduction occurring ahead of the advancing iron/wustite interface.

The present investigation involved samples containing both hematite and magnetite, so it would be expected that the iron product after reduction would be characterized by the combination of both phases. At the early stage of reduction, hematite appears to be reduced more rapidly than magnetite, as expected. However, after about 40% of reduction the following stage of reduction was characterized by the reduction of wustite to iron and a topochemical reduction was observed suggesting a change of the rate controlling step.

Turkdogan and Vinters (1971) also have shown from the scanning electron micrograph (Figure 4.60) that the pore structure of reduced iron became progressively coarser with increasing reduction temperature. Their result is comparable to the optical microscopic observation obtained in Figure 4.61 (A-D) showing iron produced in the present case after reduction at 900°, 1000°, 1100° and 1200° C respectively. Evidence of residual wustite trapped in the coarser layer is clearly apparent at increasing temperature. At high temperature, it would appear that the decreasing rate of reduction could be attributed to diffusion control.

4.2.7. SUMMARY

The conclusion at this stage from the reduction curves obtained is, that the initial porosity indeed determines the initial rates of reduction as shown in Figure 4.51, however as the reduction proceeds there are some other influencing factors.

The results of the 'reaction' or the 'difussion' plots, the linearity of which would signify the controlling mechanism, are in fact not linear over the major part of the reduction run.

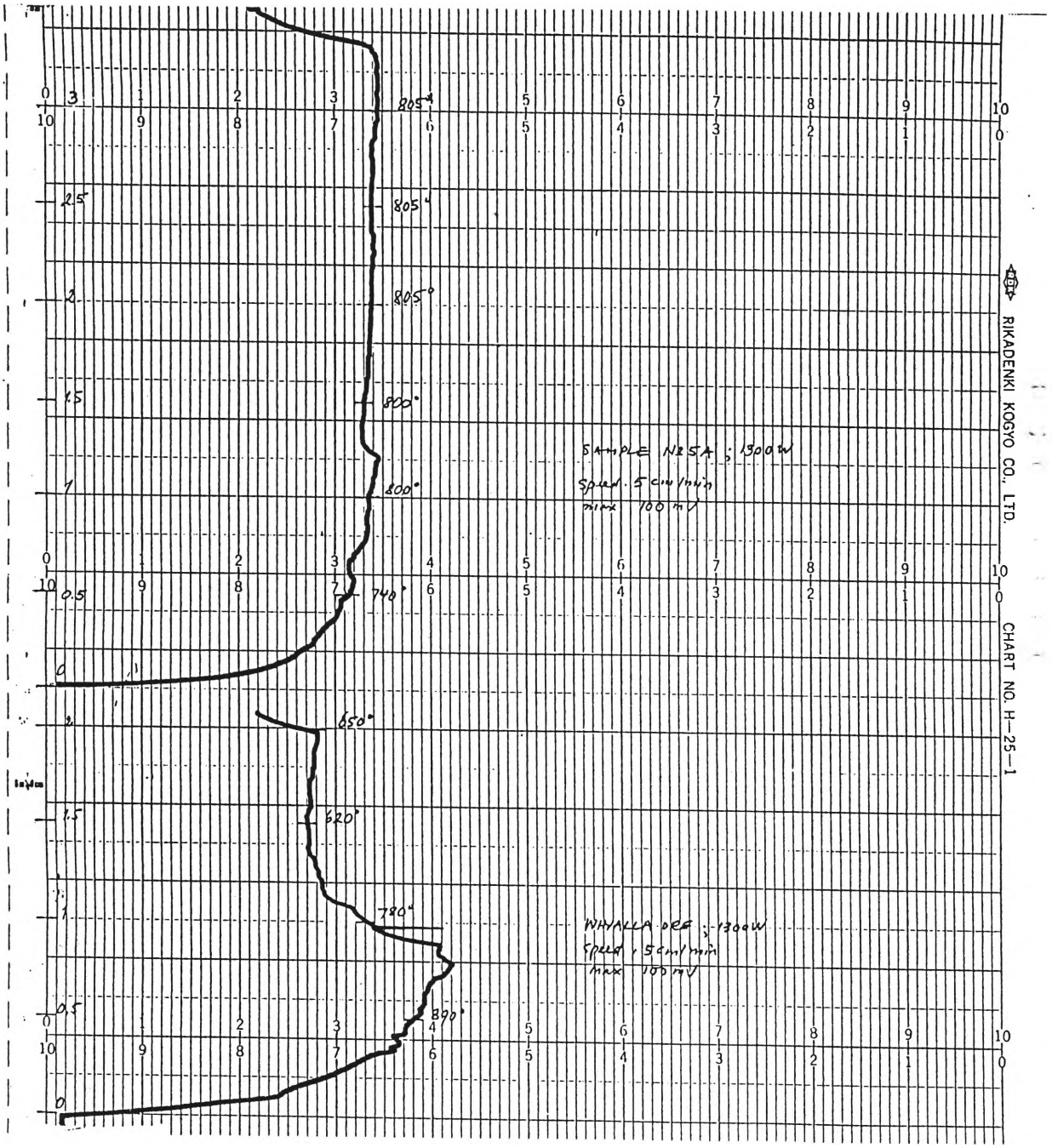

Figure 4.62. Typical Chart Recording of the microwave temperature measurements.

The preliminary morphological studies conducted in this work under optical microscopy, indicate that the iron phase already appeared before the whole sample had been reduced to wustite. This finding is more likely attributed to the less porous and larger size of the individual magneto-hematite grains.

4.3. MICROWAVE TREATMENT

4.3.1. GENERAL

In the reduction of iron ore, improved reducibility is obtained by using conventional methods such as sintering and pelletizing. These methods have already demonstrated (Tyler and Wright, 1979; Sakamoto *et al*, 1984; Kokubu *et al*, 1986) that the products (sinter and pellets) are highly porous and homogeneous which is required in the gas reduction process. Recently it was shown that microwave energy reduced energy consumption for grinding of minerals (including iron ores) because thermal stress fracturing occurred (McGill *et al*, 1988). However further potential effect on the reduction of the microwaved ore has not been investigated. The following part of the present study is therefore an original investigation of the effect of microwave energy on the reduction of magneto-hematite ore as a possible alternative to the conventional methods.

4.3.2. TEMPERATURE MEASUREMENT

The results of temperature measurements for sample No.5 and Whyalla ore during microwave treatment are shown in Figure 4.62. It is seen that reasonably smooth graphs were produced indicating that the changes of temperature during the treatment were able to be properly monitored. As noted in Section 3.5.2, if the

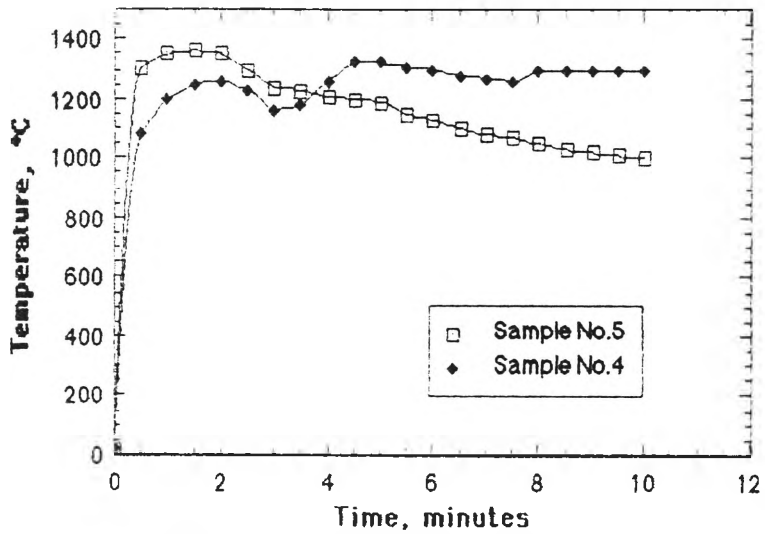

Figure 4.63. Temperature measurements of cemented thermocouples at 700 W.

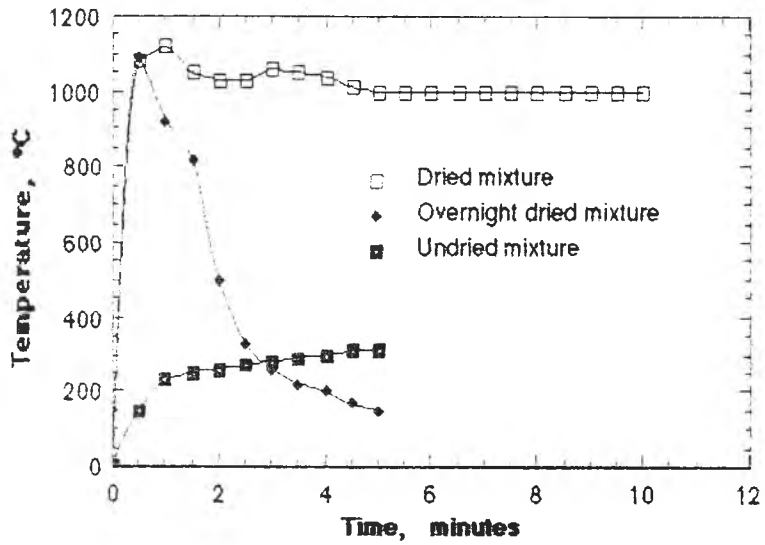

Figure 4.64. The effect of 700 W microwave treatment on heating rate of alumina+waterglass.

sheath was not properly grounded the outcome of the temperature measurement would be a rapid fluctuation of temperatures.

Figure 4.63 was obtained by replotting the initial temperature data as exemplified in Figure 4.62 into time-temperature curves for samples No.4 and 5. As stated before in Section 3.5.2, because the results of the initial temperature measurement were suspiciously too high compared with the previous finding (Chen *et al*, 1984; Walkiewicz *et al*, 1988) - for both samples the highest temperature reached about 1300° C as shown in Figure 4.63, the suspected variables that could have contributed to the high temperature rise during microwave treatment were measured separately. The results are shown in Figures 4.64 and 3.8 (in Section 3.5.2) for microwave heating of alumina powder and water-glass mixture and of the thermocouple only, respectively. For the alumina and water-glass mixture, the results were surprisingly high, especially for the dried mixture, the temperature of which reached more than 1000° C. This result contrasts with that previously reported (Chen *et al*, 1984; Walkiewicz, 1988) that both alumina and silicate were poor microwave absorbers. For thermocouple measurement under microwave treatment without load, the result was apparently stable at about 250° C (Figure 3.8 in Section 3.5.2), as expected, due to the interaction of the thermocouple with the microwave field (Fanslow *et al*, 1988). In view of these findings subsequent temperature measurements were made using an uncemented thermocouple.

The microwave heating characteristics of magneto-hematite ore (sample No.5), tested at two levels of microwave power, i.e. 700 and 1300 W, are shown in Figure 4.65. All samples were of similar size to the sample size used in the reduction tests and with a 5 mm drill hole to insert the thermocouple tip.

For the investigation with high power heating, the tests were terminated when the temperature became stabilized or when arcing occurred at the tip of the thermocouple and destroyed it.

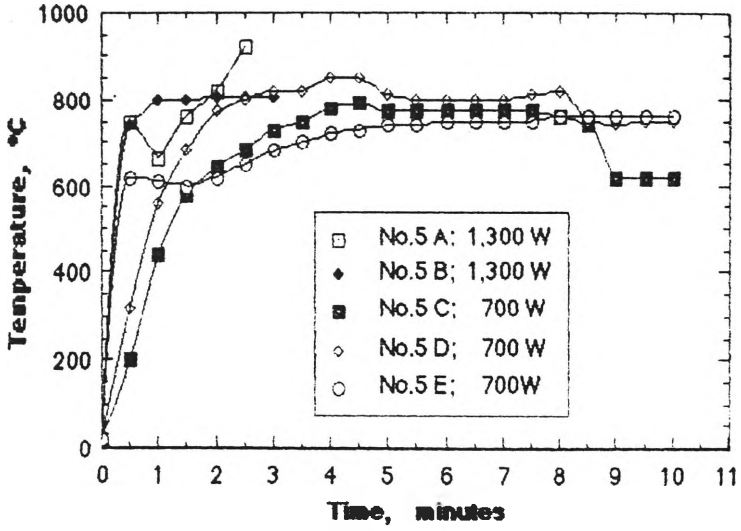

Figure 4.65. The effect of microwave treatment on heating rate of Sample No.5.

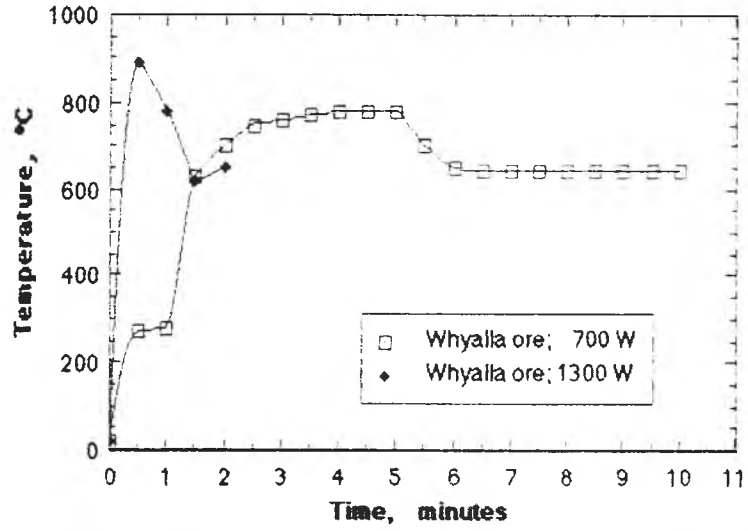

Figure 4.66. The effect of microwave treatment on heating rate of Whyalla ores.

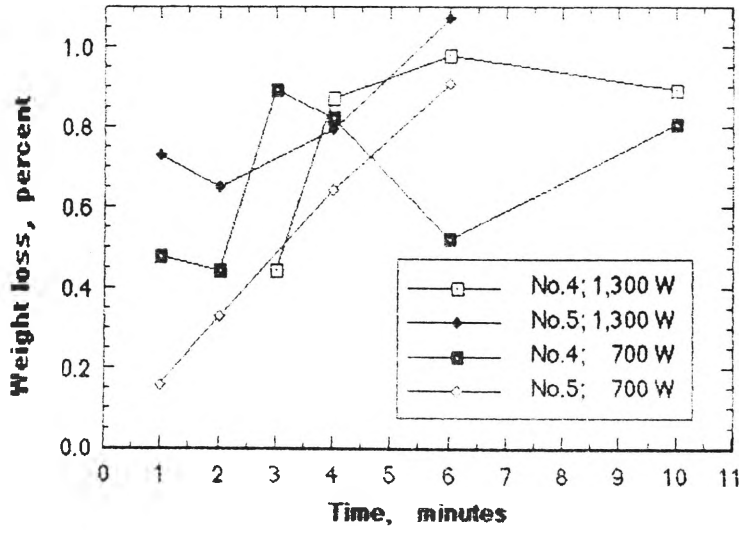

Figure 4.67. Percent weight loss after microwave treatment.

The initial heating rates at 1300 W were remarkably faster than at 700 W, as expected from Section 2.4, before the temperature stabilized at about 800° C. This result is in line with the previous finding by McGill *et al* (1988) in microwave heating of selected minerals that in general, heating rates increased as input power increased. Their results of the effect of microwave heating on the temperature of natural minerals are given in Table 2.1 and those of the effect of microwave power on the heating rate of magnetite are shown in Figure 2.9 (Section 2.4.2).

For comparison, hematite ore from Whyalla, South Australia was tested and the results, shown in Figure 4.66, were unexpectedly high for such hematite ore. However, previous structural study of this ore by Ostwald (1981) and England and Turner (1983) found that the ore consisted of hematite with minor amount of magnetite and also manganese oxide. The presence of manganese was confirmed from qualitative EDX analysis as shown in Appendix A-5. Both of these oxides, magnetite and manganese oxide are known to be excellent microwave energy receptor and also had reached the highest temperature (above 1200° C) during microwave heating as reported by McGill *et al* (1988). This may explain the higher temperature reached for Whyalla hematite compared with pure hematite used by Chen *et al* (1984) and McGill *et al* (1988). More recently Lanigan (1989) reported that the effect of microwave heating of iron ore from Whyalla ranged from intermediate to strong compared to H_2O.

4.3.3. WEIGHT LOSS

The effect of microwave treatment on the weight loss of sample No.4 and No.5 is shown in Figure 4.67. The weight (%) losses indicated were obtained after treatment for periods of 1 to 10 minutes.

At 700 W power, sample No.4 reached a maximum weight loss of 0.89 % in 3 minutes which then decreased to 0.52 % in 6 minutes before again increasing to 0.81 % in 10 minutes. With an increase in power to 1300 W, this sample reached a maximum weight loss of 0.98 % in 6 minutes before decreasing to 0.89 % in 10 minutes.

Sample No.5, at 700 W, after 6 minutes heating reached 0.91 % weight loss. At 1300 W, after 1 minute heating weight loss reached 0.79 % and only slightly increased to 0.79 % after 4 minutes before reaching 1.07 % after 6 minutes.

As samples for both the reduction experiments (Section 3.1) and microwave treatment were dried in the conventional oven for 24 hours, it is expected that the free water no longer remained in the sample. Furthermore, the magneto-hematite ore is classified as a non hygroscopic material, so the amount of water removed during microwave treatment would be the bound water as is clear from Metaxas (1976) data. Table 4.11, giving the result before reduction tests, indicates that the total weight loss is identical to that estimated by Schiffmann (Section 3.4).

The magneto-hematite ore, as compared with adding 20 % magnetite ore to the mercury concentrate (Section 2.3), contained from 24 to 40 % of magnetite as calculated in Appendix A-8. Therefore, the temperatures reached were expected to be not only considerably high to remove the moisture content but also to create stress fracturing in the sample.

Additional data were obtained from as received samples (about 5 cm in diameter) treated for 5 minutes in microwave ovens at 700 and 1300 W respectively and are given in Table 4.12. Observation during microwave treatment showed that the whole sample started to glow unevenly after 1.5 to 2 minutes treatment and became brighter as the time proceeded, indicating that the temperature also increased. The conclusion from Table 4.12 is that the higher energy produced

higher temperature and the weight loss varied, with the maximum value reaching about 1%.

Table 4.11. Percentage Weight Loss of Iron Ore Before Reduction

Microwave Time,	Weight Loss, percent		
minutes	after microwave	in N_2 heating	Total Loss
0	-	0.74 ~ 1.40	0.74 ~ 1.40
1 ; 700 W	0.48	0.69	1.17
2 ; 700 W	0.44	0.59	1.03
3 ; 1300 W	0.44	0.67	1.11
4 ; 700 W	0.82	0.17	0.99
6 ; 1300 W	0.98	0.15	1.13
10;1300 W	1.07	-	1.07

After the required heating time, the sample was quickly withdrawn and the temperature was measured directly at the brightest part of the glowing sample. All temperature readings were about 700° C or more, as expected from the previous temperature data. However, as it had already been observed that the glow was not uniformly generated throughout the sample, this may explain the variation of the weight loss resulting from this test. To prevent the effect of 'hot spots' inside the cavity and to produce in average a homogeneous distribution of the microwave field, mostly rotating antennas or rotating metal vanes are used, which changes the distribution slowly (Groll, 1987). Another important point is that as the nature of the material is relatively inhomogeneous it is possible that some parts of the particle will absorb microwave energy strongly compared with the others.

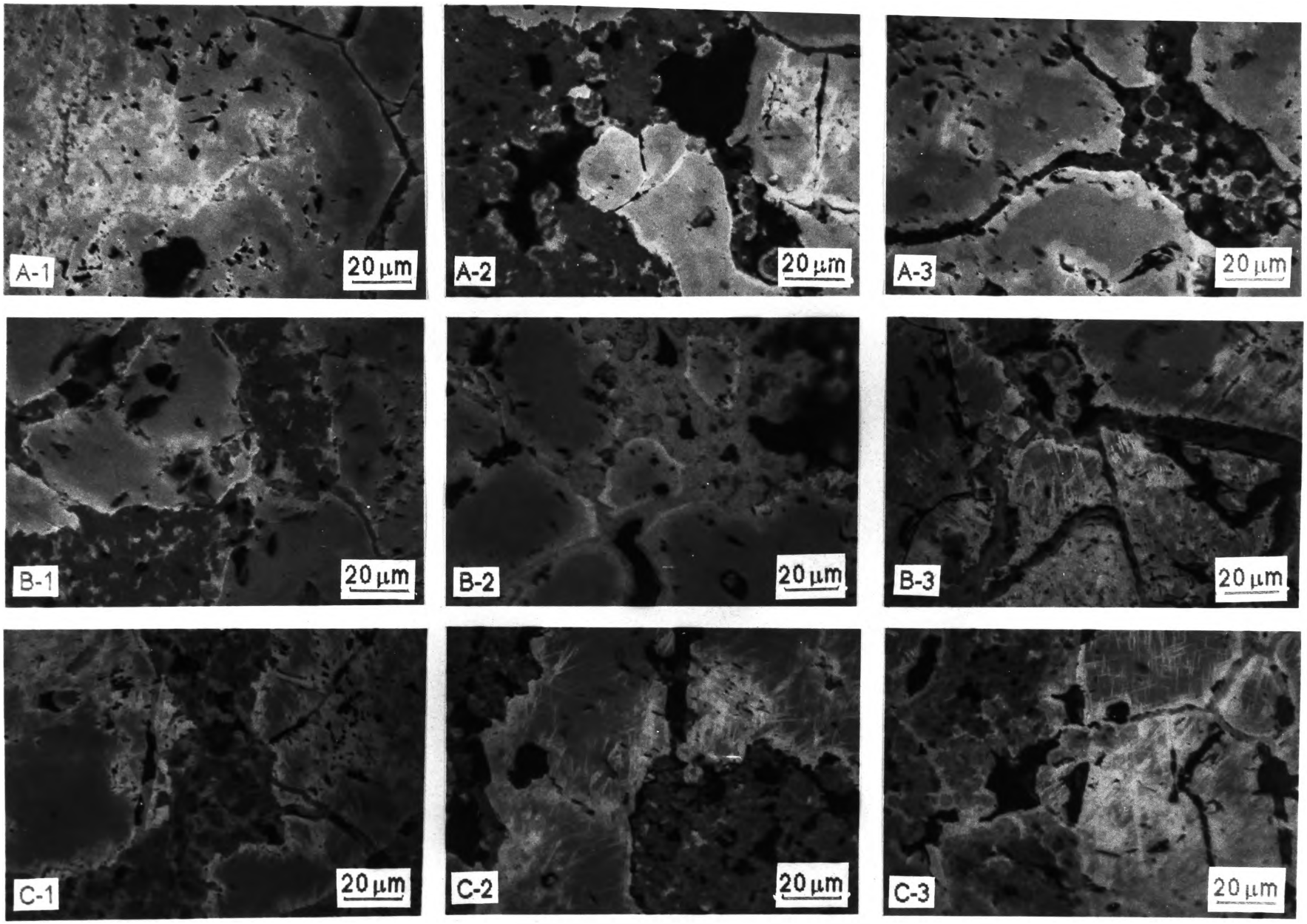

Figure 4.68. Optical micrograph of (A) raw ore, (B) 700 W - microwave pretreatment and (C) 1300 W - microwave pretreatment.

Table 4.12. Weight Loss of As Received Ore After 5 Minutes Microwave Heating

	700 W		1,300 W	
	1 (gram)	2 (gram)	1 (gram)	2 (gram)
Before Heating				
Crucible	124.35	128.21	124.32	128.16
Ore	130.51	151.01	109.30	97.79
After Heating				
Crucible	124.33	128.19	124.30	128.14
Ore	129.64	149.54	108.88	97.04
Loss of Weight				
Ore (gram)	0.87	1.47	0.42	0.75
(%)	0.67	0.97	0.38	0.77
End Temp.				
° C	720	680	916	756

4.3.4. MICROSCOPIC OBSERVATION

Recent data reported by Walkiewicz *et al* (1988) demonstrated that the stress forces generated by heating depended on the heating rate as well as the temperature attained, so it may not be necessary to heat an ore to a high temperature. Rapid and selective heating of ores to relatively low temperatures may result in differential stressing that is economically advantageous.

Figure 4.68 is a sequence of optical micrographs under polarized light showing the results of microwave heating of sample No.4 at 700 and 1300 W

respectively. In general, the matrix material in the grains shows two constituents, one light grey and the other grey, corresponding to hematite and magnetite phases, respectively. Cavities in the iron ores are often filled with finely layered goethite as reported by Ostwald (1980). This is seen in Figure 4.68 (A-1 to A-3) showing the intergranular gaps between grains partly filled with goethite matrix (dark grey) in the raw ore. It is often found that the hematite structure envelops goethite in nodular-like structure.

Brighter goethite appeared after 1 minute microwave heating at 700 W (Figure 4.68 (B-1)) and even more brighter after 2 minutes (Figure 4.68 (B-2)) suggesting that formation of fine hematite resulted from dehydration of the goethite matrix. At 4 minutes, in Figure 4.68 (B-3), the former thin layer of hematite around the grains has grown extensively toward the centre of the grain. This suggests that the oxidation of magnetite occurred in the grain at elevated temperature. At this stage of treatment, it is also seen that, as expected, some cracks formed along the grain boundaries.

At 1300 W after 3 minutes treatment, as seen in Figure 4.68 (C-1), the growth of hematite in the grain was strong. It is also seen that thermal cracks developed between the grains and goethite layer as well as through the goethite matrix. On further treatment after 6 and 10 minutes in Figure 4.68 (C-2) and (C-3), respectively, the above results are even more obvious. It is also apparent that continuous structure of hematite is replacing the goethite matrix.

The effect of heating in air was also observed and compared with the microwave heating as shown in Figure 4.69. After heating in air for 1 hour at 400°, 800° and 1000° C (in Figure 4.69 (A-1) to (A-3)), it is seen under polarized light that goethite was transformed into a hematite-like pattern and magnetite grains were oxidized to hematite. The grains were apparently attacked from the edge at 400° C and the attack became uniformly extended throughout the grain after 1000° C.

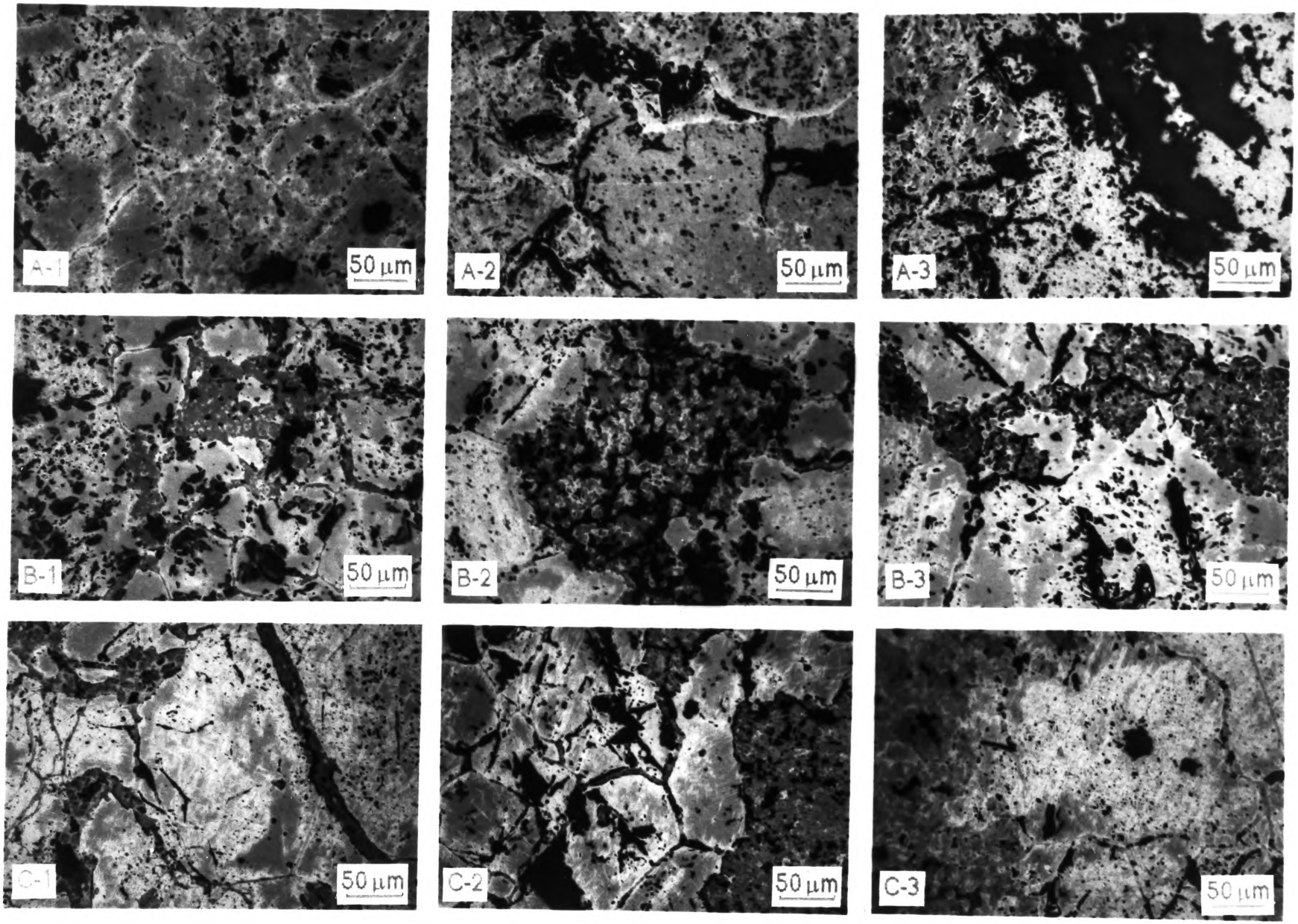

Figure 4.69. Optical micrograph of (A) air heated ore, (B) 700 W - microwave pretreatment and (C) 1300 W - microwave pretreatment.

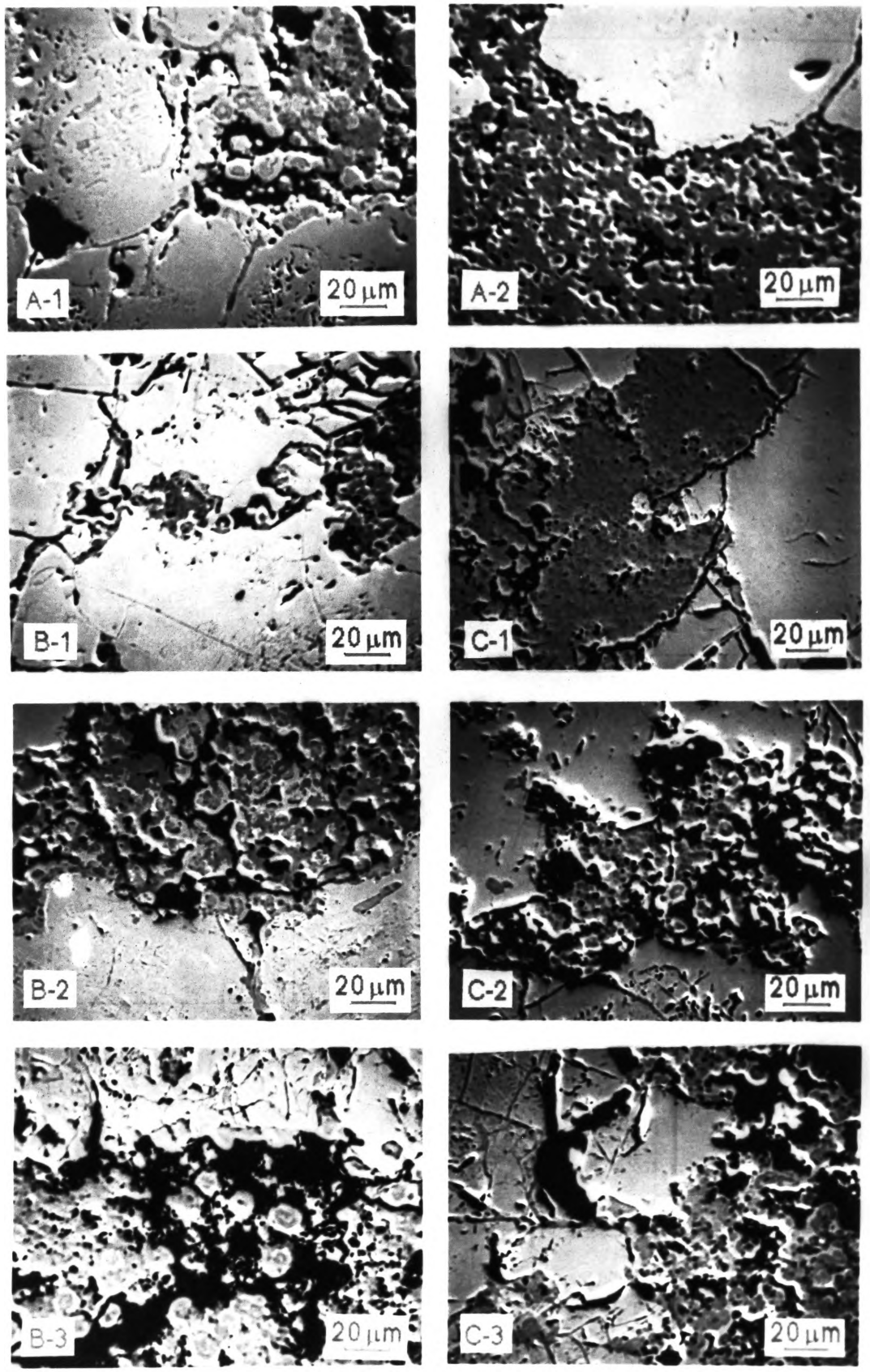

Figure 4.70. SEM micrograph of (A) raw ore, (B) 700 W, microwave pretreatment and (C) 1300 W, microwave pretreatment.

Cracks also appeared after 800° and 1000° C heating. To compare the above result with the effect of microwave heating at 700 and 1300 W, Figure 4.69 (B-C) was obtained with similar sequence of microwave heating as shown in Figure 4.68 (B-C). It appears that the magnetite grain was oxidized before goethite. Cracks were observed after 2 and 4 mins. microwave heating at 700 W and more obviously after 3, 6 and 10 mins. at 1300 W of microwave heating. In Figure 4.69 (C-3), after 10 mins. at 1300 W microwave heating, it is seen that similar goethite structure to that observed after heating in air appeared. This result can be explained by the fact that magnetite is a good microwave absorber and heated rapidly, whereas goethite is a poor microwave absorber which was mostly found between the magnetite grains heated gradually after the surrounding grains were at high temperature.

To confirm the structural conversion of goethite to hematite, SEM observation was conducted. Figures 4.70 (A-C) show SEM photomicrograph of the polished sample of the raw ore and after microwave treatment of 3, 6 and 10 minutes respectively. The specimen shown in Figure 4.70 (A-2) displays a large goethite phase between the magneto-hematite grains. After 3 minutes treatment at 1300 W, stress cracking can be readily seen along the grain boundaries of the magneto-hematite phase as well as through some of the dark goethite matrix (Figure 4.70 (C-1)). Similar stress cracking can be seen in Figure 4.70 (C-2)) after microwave exposure for 6 minutes. The dark phase of goethite is lighter in some parts, suggesting that the goethite phase was transformed to hematite as some of the bound water was removed. Figure 4.70 (C-3) shows that gaps along the grain boundaries widened and fine cracks developed in the magneto-hematite grain after 10 minutes of microwave exposure. However, cracks in the goethite phase decreased and were replaced by pores. Solid hematite in the boundaries also developed. This may be explained by possible sintering of the surface at high temperature.

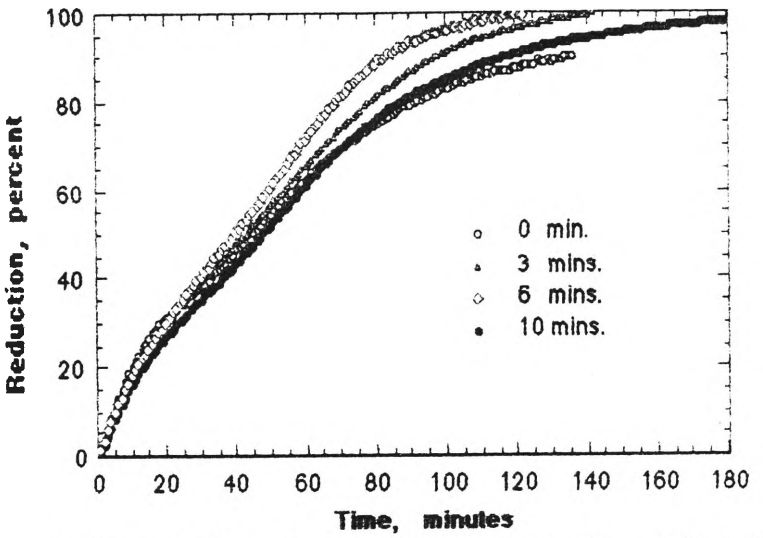

Figure 4.71. Reduction curves after 1300 W microwave pretreatment.

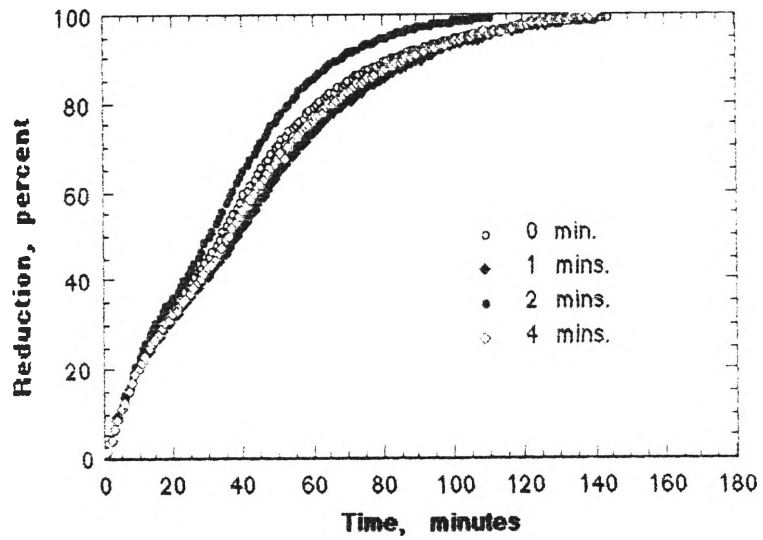

Figure 4.72. Reduction curves after 700 W microwave pretreatment.

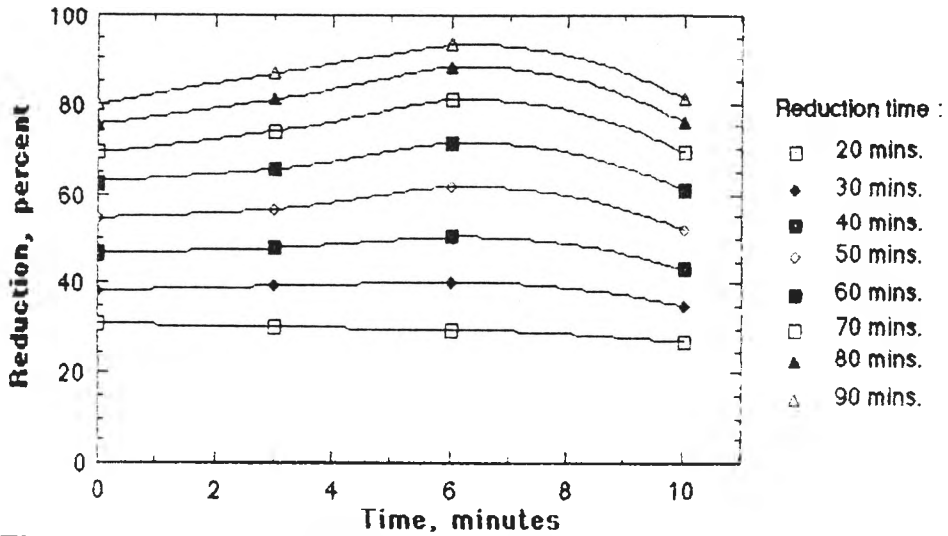

Figure 4.73. Percentage of reduction after 1300 W microwave pretreatment for different times.

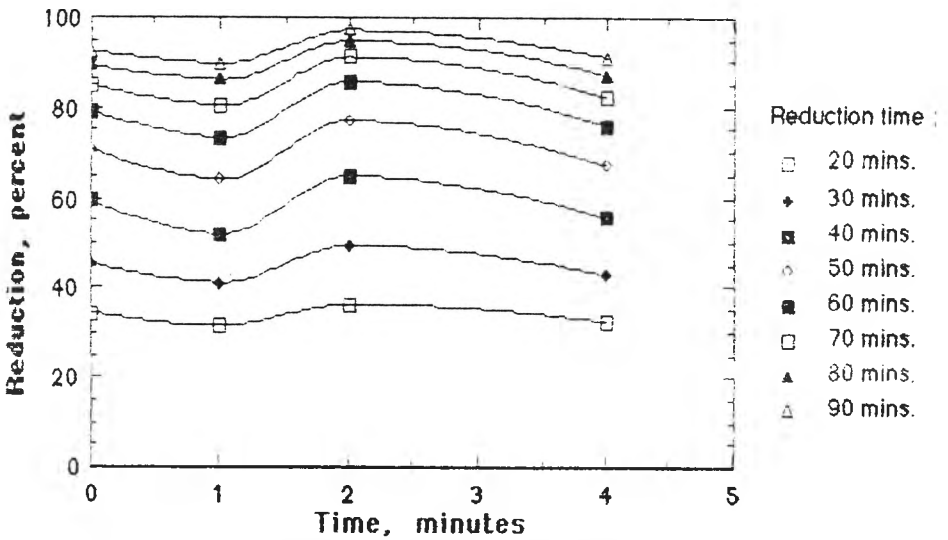

Figure 4.74. Percentage of reduction after 700 W microwave pretreatment for different times.

The above finding is therefore in line with that reported by Walkiewicz *et al* (1988); that microwave energy does induce thermal stress cracking and the result may be cost effective when other factors in the extractive process are considered.

4.3.5. REDUCTION TESTS

Reduction tests were carried out to determine the effectiveness of microwave treatment in the reduction process. The time-reduction curves for sample No.4 after microwave treatment using 1500 and 700 W respectively are shown in Figures 4.71 and 4.72.

It is obvious from Figure 4.71 that the reduction after 6 minutes microwave treatment and from Figure 4.72, the reduction after 2 minutes, are higher than the non microwave treatment.

To better illustrate the degree of improvement the results are replotted on constant reduction basis in Figures 4.73 and 4.74. It can be seen from both figures that reduction has been markedly improved in the later stage of reduction rather than in the early stage of reduction. From Figure 4.73 it is seen that after 20 minutes of reduction the degree of reduction is almost equal to the untreated sample. Gradually after 50 minutes it became 6 % higher and finally at 90 minutes the reduction was improved by about 10 %. It is also shown in Figure 4.74 that after 20 minutes of reduction time (after 4 minutes treatment) there was only about 2 % improvement which gradually increased to about 5 % after 90 minutes of reduction. Both figures also show that the other results were lower than those already described and in some cases they were even lower than the untreated samples.

From the foregoing results it may be concluded that the microwave energy had an effect on the reduction results with a maximum effect at a certain level of microwave exposure, particularly on the final degree of reduction. Below that level

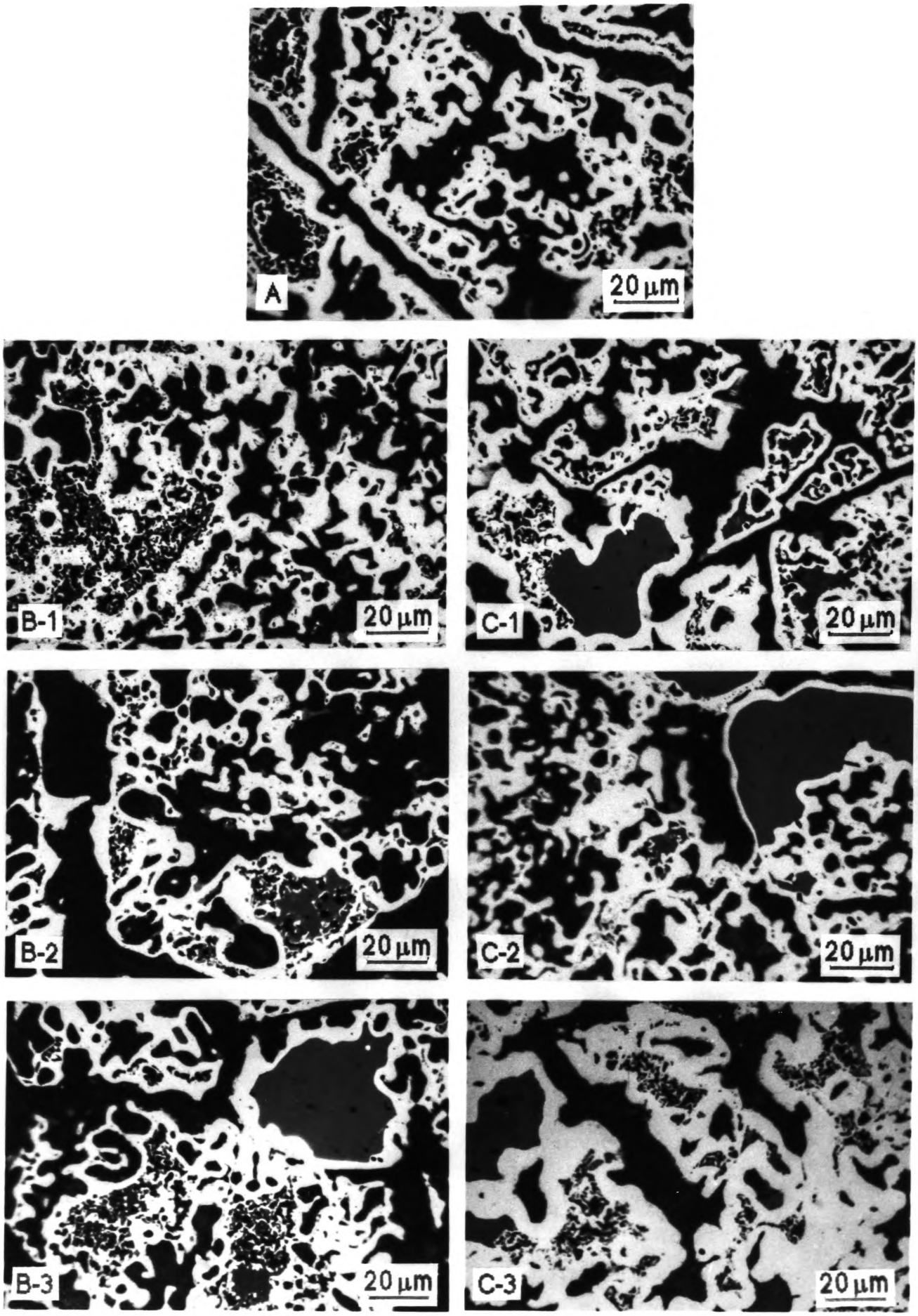

Figure 4.75. Optical micrograph of reduced samples for (A) non-microwave, (B) 700 W, microwave pretreatment and (C) 1300 W, microwave pretreatment.

the effects were not significant. In some cases they were less than the reduction effect on untreated sample. Furthermore beyond that level the reduction degree decreased also. These maxima effects were also observed (Worner and Standish, 1989) for microwave irradiation of Fe_2O_3 - $CaCO_3$ composites and several other systems but the reason for these effects is unknown. However, it was confirmed that the extent of this effect appeared to be related to the permittivity of the material in the microwaved sample.

The increase in the percentage of reduction in the final stages of the reduction process suggests that the diffusion of reactant gas was no longer the controlling factor after sufficient cracks had developed toward the centre of the particle during microwave treatment. If excessive treatment is conducted, the temperature generated might be sufficiently high to produce sintering on the surface of the phase leading to a decrease in the rate of reduction.

Optical micrographs after reduction (Figure 4.75) show a series of the structure of porous metallic iron for microwave treated ore compared with the untreated ore. In general, both in the microwaved samples as well as the raw ore, finer porous metallic iron surrounded by dense metallic structure and often dense wustite particles were entrapped inside the iron-shell. The latter may explain why the rate of the reduction became much slower after 90% of reduction.

However, for 10 minutes of 1300 W microwave treatment the difference became obvious, as shown in Figure 4.75 (C-3) in that less finely porous metallic iron appeared and a thicker iron shell around the wustite grains isolated them from direct contact with the reducing gas and hence hindered the reduction rate. This may explain why the overall reduction of this sample was lower than both the other treated samples and the raw ore.

4.3.6. X-RAY DIFFRACTION ANALYSIS

Some selected X-ray diffraction studies were also conducted to determine and confirm that the phases examined were the principal oxides believed to be present. The results are tabulated in Table 4.13.

Table 4.13. X-Ray Diffraction Analysis for Raw Ore and Microwaved Samples

Microwave time, minutes	Sample	Phases presents
-	No.4	hematite, magnetite, goethite, maghemite
1; 700 W	No.4	hematite, magnetite, goethite
2; 700 W	No.4	hematite, magnetite
4; 700 W	No.4	hematite, magnetite
6; 1300 W	No.4	hematite, magnetite
10; 1300 W	No.4	hematite, magnetite
-	No.5	hematite, magnetite, maghemite
1; 700 W	No.5	hematite, magnetite
2; 700 W	No.5	hematite, magnetite
3; 700 W	No.5	hematite, magnetite

The No.4 raw ore gave the strongest lines for hematite, magnetite was present in smaller proportion and there was goethite and possibly maghemite. This agrees with the ore's calculated constituent hematite 56.93 %, magnetite 37.56 % (Appendix A-8).

X-ray analysis of No.4 microwaved samples revealed the presence of hematite and magnetite and also the disappearance of goethite.

The No.5 raw ore contained hematite, magnetite and possibly maghemite. Goethite was undetected in this ore. Calculation of constituents, carried out in a similar manner to those for sample No.4, gave the values of 70.63 % hematite and 24.05 % magnetite.

The No.5 microwaved sample again revealed stronger intensity lines of hematite compared to the raw ore and weakening lines of magnetite.

The ultimate product of heating iron oxides (in air) is hematite as summarized by Brown (1980) and presented in Table 4.14. The material produced from goethite immediate product after dehydration (about 300° C) gives a hematite-like pattern and on further heating the reflection gradually becomes sharper until at 900° the typical pattern of well-crystallized hematite develops. The heating curves of magneto-hematite sample under microwave power as shown in Figure 4.65 clearly show that the dehydration temperature is reached immediately in the beginning of microwave exposure. It is apparent that the bound water is released from the oxides before the onset of further stages of microwave heating. However for some oxides the contact time with air may not be sufficient to completely transform the phases to hematite.

4.3.7. STRENGTH TEST

Since the standard strength test (Watanabe and Yoshinaga, 1968; Wright and Morrison,1985) requires a large amount of ore (about 500 gram for each test), the sample in this investigation was prepared by combining the individual ore as magneto-hematite ore A. Furthermore, due to the limited avaibility of the samples, it was decided that each of test run was conducted using 100 gram of sample.

The results of a modified drop test (Section 3.5.3) are presented in Table 4.15 and include the results obtained before reduction and after reduction. For

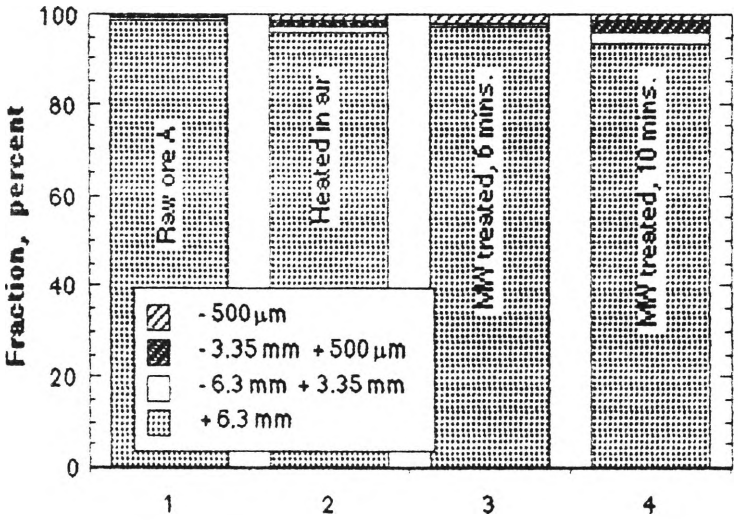

Figure 4.76. Size distribution diagram for ore A before reduction.

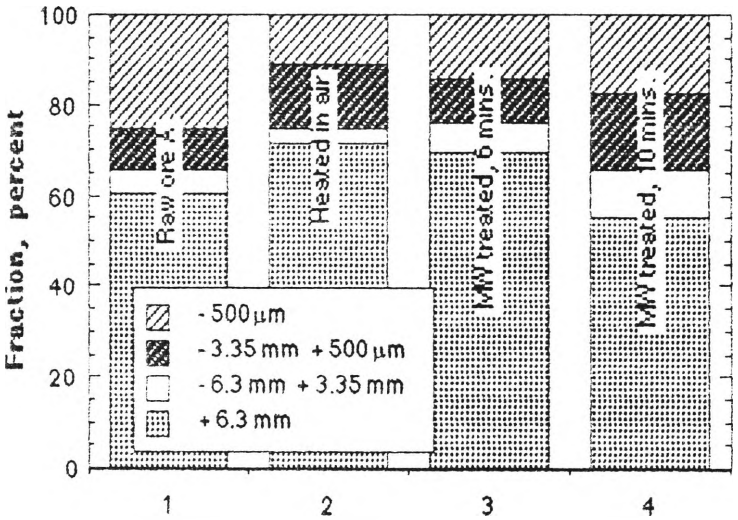

Figure 4.77. Size distribution diagram for ore A after reduction.

conveniece there are also shown diagramaticaly in Figures 4.76 and 4.77, respectively.

Table 4.15. Results of modified drop test on magneto-hematite ore

	Weight, percent			
	+ 6.3 mm	- 6.3 mm + 3.35 mm	- 3.35 mm + 500 µm	- 500 µm
Ore A	98.8	0.8	0.3	0.1
Ore A heating in air (700°C, 1hr)	96.0	1.1	1.8	1.1
Ore A MW treatment (1300W, 6 mins)	97.3	0.9	-	1.8
Ore A MW treatment (1300W, 10 mins)	93.2	3.2	2.5	1.1
Ore A reduced*	60.6	4.7	9.2	25.5
Ore A reduced (heating in air, 700°C)	71.2	3.7	14.1	11.0
Ore A reduced (6 mins MW treatment)	69.4	6.4	9.6	14.6
Ore A reduced (10 mins MW treatment)	55.3	10.0	17.2	17.5

*Reducing atmosphere 100% CO, 1000°C
Reduction degree : constant (20%)

By taking 90% of the + 6.3 mm fraction after dropping as a standard level of the strength of the ore, all the unreduced samples are seen to be above the standard level (Figure 4.76). After 20% reduction, the strength of the ore was decreased significantly below the standard level. It can also be seen that the strength of the ore after heating at 700° C and the one after 10 mins. microwave treatment are at a comparable level (71.2 and 69.4%). However, the strength after 10 mins. microwave treatment was considerably lower. This is may be explained by the excessive reoxidazion which occured in the magnetite grains as seen in Figure 4.69 (C-3) (Section 4.3.4).

If the heating tests for both in the furnace and in the microwave oven are viewed as a decrepitation test method, then the decrepitation index would be measured by the proportion of -500 µm fines generated after 20% reduction and the subsequent drop test. From Table 4.15 and in Figure 4.77, it may be of interest to

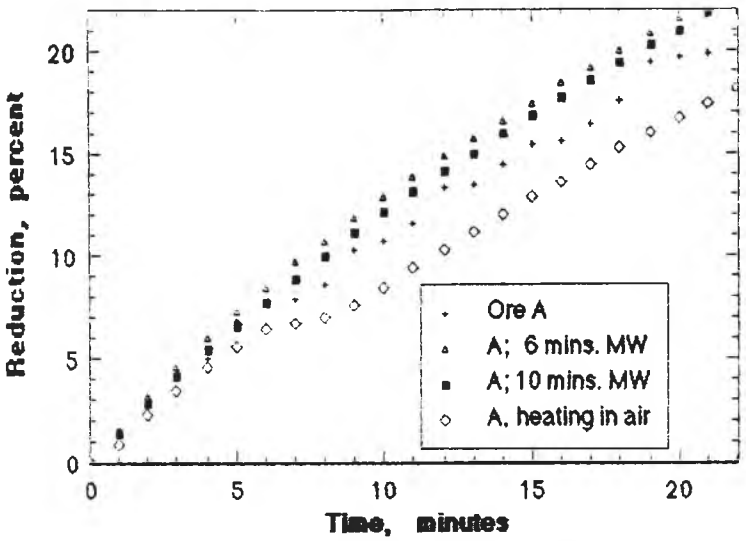

Figure 4.78. Reduction curves of ore A.

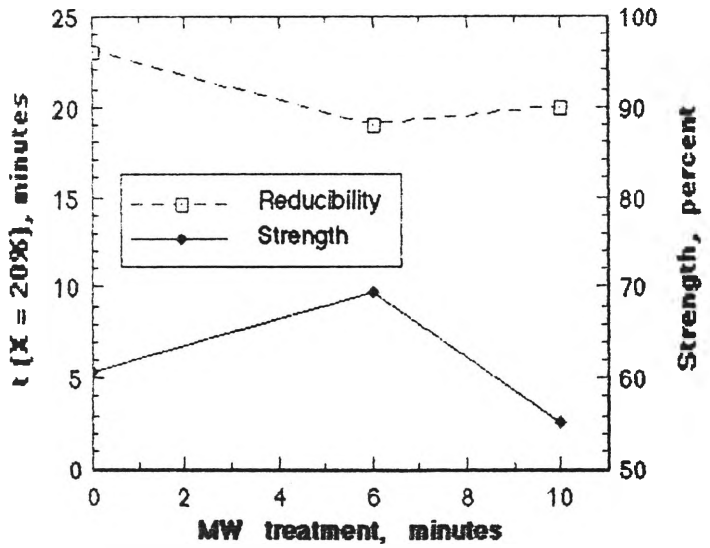

Figure 4.79. Effect of MW treatment on reduction time and strength of ore A.

remark that the decrepitation indices were decreased from 25.5% to 11.0% after heating in air and to 14.6 and 17.5% after 6 and 10 mins. microwave treatment, respectively.

From reduction curves in Figure 4.78, it is also clear that the reduction was faster for microwave treated ore compared with the non-microwaved one, indicating that the reducibility of the ore had improved after microwave treatment.

Figure 4.79 shows reduction time at X = 20 % and strength plotted against time of microwave treatment. It is seen from this result that ore A after 6 mins. microwave treatment gave a better reducibility, moderate strength and decrepitation index compared with the other results. This therefore confirms again the enhancement of the reducibility of the present ores after microwave treatment (Section 4.3.5)

Because of the possibility that in future this ore may have to be supplemented by adjoining ore some practical information on the microwave behaviour of this ore, here termed ore B, were obtained. Ore A is the currently mined ore in Lampung. This ore deposit also contains an area of ore with a higher content of goethite (Rustiadi, 1985).

Similar microwave tests were carried out on ore B as on ore A and the results are presented in Appendix A-10. It is shown there that the decrepitation index decreased from 8.1 to 2.2 % after heating in air; however, the index increased to 15.6% after 6 mins. microwave treatment and then it decreased to 4.9% after 10 mins. treatment. From Appendix A-10, ore B, after 10 mins. microwave treatment, gave a better reducibility compared with the other microwave irradiation times. However the decrepitation index was slightly higher than that after heating in air.

The effect of combined water on decrepitation in several kinds of ores was reported by Watanabe and Yoshinaga (1968). They found that as goethite

dehydrated at about 350° C, in the case where it was intimately associated with the hematite aggregates, the expulsion of water vapour was so difficult that the ore was forced to decrepitate due to an increase in vapour pressure. Furthermore, when an iron ore was composed of large amounts of goethite, the water vapour could be rather easily expelled without decrepitation. These findings may also provide the answer for the different performance between ores A and B.

From the reduction curves for ore B in Appendix A-10, it is also clear that the reduction was faster for microwave treated sample compared with the untreated one, again indicating that the reducibility of the ore improved after microwave treatment.

4.3.8. SUMMARY

The conclusion from this work (Figures 4.79 and Appendix A-10) is that microwave treatment had improved the reducibility as well as strength and decrepitation index of magneto-hematite ore. The difference in the characteristics of the Lampung ores can therefore be overcome by varying the treatment time in the microwave irradiation.

CONCLUSIONS

The results of this study have shown the following

1. The reduction of the iron ore employed depends to a great extent on the nature of the ore.

2. Initial porosity of the ore influences the initial stage of reduction. but the later stages of reduction depend more on the chemical composition.

3. Mixed control was operative during the course of reduction.

4. The effect of temperature on the reduction followed the Arrhenius equation. The activation energy of the samples were 25.1 and 29.8 kJ/mol.

5. Volume changes during reduction were in the normal range. hence possible size degradation in subsequent operations may be avoided.

6. Microwave treatment enhances reduction but benefit optima exist. In the present ore such an optimum value was obtained at 6 minutes, with 1300 W power.

7. The present temperature techniques was able to measure the changes of particle temperature satisfactorily during microwave treatment at 700 and 1300 W.

8. The presence of magnetite in the ore has considerable effect on the microwave treatment and the oxidation of the goethite is obtained after the magneto-hematite grains are almost entirely oxidized to hematite.

This investigation has highlighted the new area of microwave application in the treatment of iron ores. The results obtained here are considered promising and similar investigation with other ores, including non ferrous ores, are indicated.

REFERENCES

AL-KAHTANY, M.M. and RAO, Y.K., 1980. Reduction of magnetite with hydrogen: Part 1 intrinsic kinetics, *Ironmaking and Steelmaking*, 2: 49-58.

ANSI / ASTM B 328-73, 1979. Standard test method for density and interconnected porosity of sintered powder, metal structural parts and oil-impregnated bearing, in *"1979 Annual Book of ASTM Standards"*, Part 9, American Society for Testing and Materials, Philadelphia.

BAGHURST, D.R. and MINGOS, D.M.P., 1988. Application of microwave heating techniques for the synthesis of solid state inorganic compounds, *J. Chem. Soc., Chem. Commun.*: 829-830.

BAGHURST, D.R., CHIPPINDALE, A.M. and MINGOS, D.M.P., 1988. Microwave syntheses for superconducting ceramics, *Nature*, Mar., 332, 24: 311.

BARNSLEY, B.P., REILLY, L., JONES, J. and ESHMAN, J., 1989. Iron and steelmaking with microwaves, *Symp. Proc. The First Australia Symposium on Microwave Power Application*, Wollongong, NSW, 15-17 Feb. : 189-201.

BASU, S.N. and GHOSH, A., 1970. Influence of porosity on the kinetics of reduction of hematite by hydrogen, *J. the Iron and Steel Institute*, Aug.: 765-768.

BLOMGREN, S., 1987. A method for direct reduction of iron ore to malleable iron and steel in industrial use one hundred years ago, *Scandinavian Journal of Metalurrgy*, 16: 220-228.

BOGDANDY, L.v. and ENGELL, H.J., 1971. *"The Reduction of Iron Ores"*, Berlin, Springer-Verlag.

BOGDANDY, L.v., SCHULZ, H.P., WURZNER, B. and STRAWSKI, I.N., 1963. Der mechanismus der reduktion von porigen eisenerzen durch wasserstoff, *Archiv Eisenhuttenwes*, 34, 6 : 1146-1153.

BRILL-EDWARDS, H. and SAMUEL, R.L., 1965. Structural changes accompanying the reduction of polycrystalline hematite, *J. the Iron and Steel Institute*, Apr.: 361-368.

BROWN, G., 1980. *Crystal structures of clay minerals and their x-ray identification* (eds. G.M. Brindley and G. Brown), Mineralogical Society Monograph No.5, Chapter Six, Mineralogical Society, London.

BUTTS, J.R., LEWIS, J.E. and STEWARD, F.R., 1983. Microwave heating of New Brunswick oil-shale, *J. Microwave Power*, 18, 1: 37-43.

CHEN, T.T., DUTRIZAC, J.E., HAQUE, K.E., WYSLOUZIL, W. and KASHYAP, S., 1984. The relative transparency of minerals to microwave radiation, *Canadian Metallurgical Quarterly*, 23, 3: 349-351.

CORES, A., LARREA, M.T., GUTIERREZ, A. and FORMOSO, A., 1988. Preliminary study of iron ore reduction. *Ironmaking and Steelmaking*, 15, 2: 65-73.

DAM GONZALES, O.G. and JEFFES, J.H.E., 1987. Model for detailed assessment of chemical composition of reduced iron ores from single measurements, *Ironmaking and Steelmaking*, 14, 5: 217-220.

DOU, S.X., BRADSHAW, A.V. and BLAIRS, S., 1988. Reduction of hematite doped with vanadium oxide. *Ironmaking and Steelmaking*, 15, 2: 74-81.

DU, S., SRINIVASAN, N.S. and STAFFANSSON, L.-I., 1988. Kinetics of reduction of fluxed hematite pellets by hydrogen at elevated temperatures, *Scan. J. Metallurgy*, 17 : 226-231.

EDSTROM, J.O., 1953. The mechanism of reduction of iron oxides, *Journal of the Iron and Steel Inst.*, Nov.: 298-304.

EKETORP, S.,1971. Fundamental basis for iron and steelmaking processes. *Proc. of the meeting 'Alternative Routes to Steel' of the ISI*, 5-6 May, The Iron and Steel Institute, London.

EL-GEASSY, A.A. and RAJAKUMAR, V.,1985. Gaseous reduction of wustite with H_2, CO and H_2-CO mixtures, *Trans. ISIJ*, 25: 449-458.

EL-GEASSY, A.A., SHEHATA, K.A. and EZZ, S.Y., 1976. Effect of lime on the reduction of iron oxide with hydrogen/carbon monoxide mixtures, *Iron and Steel International*, Dec.: 427-431.

EL-GEASSY, A.A., SHEHATA, K.A. and EZZ, S.Y., 1977. Mechanism of iron oxide reduction with hydrogen/carbon monoxide mixtures, *Trans. ISIJ*, 17: 629-635.

EMSLEY, J., 1988. The chemist's quick cook-book, *New Scientist*, Nov., 12: 56-60.

ENGLAND, B.M. and TURNER, K.E., 1983. *Report on a morphological and mineralogical study of selected ores from the Middleback Ranges, South Australia*, CRL/R/27/83, BHP-Central Research Laboratory.

ENGLAND, B.M. and TURNER, K.E., 1984. *Report on a morphological and mineralogical study of selected ores from the Kooland Island, Yampi Sound, Western Australia*, CRL/R/19/84, BHP-Central Research Laboratory.

EVANS, J.W. and KOO, C.-H., 1979. The reduction of metal oxides, in *"Rate Processes of Extractive Metallurgy"* (eds. H.Y. Sohn and M.E. Wadsworth), Sect.4.2., Plenum Press, New York.

EVANS, J.W., 1979. Mass transfer with chemical reaction, *Minerals Sci. Engng.*, Oct., 11, 4: 207-223.

FAKHOURY, S.S. and ROSENQVIST, T., 1978. Gas equilibria for the reduction of magnetite and commercial iron ore pellets with carbon monoxide at 700° - 900° C. *Scand. J. Metallurgy*, 7: 3-4.

FANSLOW, G., HOU, C., BLUHM, D. and MARKUSZEWKI, R., 1988. Microwave heating of coal and coal/caustic mixtures. *Journal of Microwave Power and Electromagnetic Energy*, 23, 4: 211-217.

GARDIOL, F.E., 1985. Microwave heating, in *"Introduction to Microwave"*, Chapt. 8.3., Archtech House: 394-411.

GHOSH, D., ROY, A.K. and GHOSH, A., 1984. Reduction of ferric oxide pellets with methane, *Trans. ISIJ*, 26 : 186-193.

GROLL, H.P., 1987. Industrial applications of Microwaves, in "Microwave Application", *Proc. Microwave Congress at the 8th International Congress Laser 87* (ed. H.Groll and W. Waidelich), Berlin, Springer-Verlag:12-27.

GUTTIERREZ, E., LOUPY, A., BRAM, G. and RUIZ-HITZKY, E., 1989. Inorganic solids in 'dry media' an efficient way for developing microwave irradiation activated organic reactions, *Tetrahedron Lett.*, 30, 8: 945-948.

HAYES, P.C. and GRIEVESON, P., 1981a. The effect of nucleation and growth on the reduction of Fe_2O_3 to Fe_3O_4, *Metallurgical Trans. B*, Jun., 12B: 319-326.

HAYES, P.C.and GRIEVESON, P., 1981b. Microstructural changes on the reduction of hematite to magnetite, *Metallurgical Trans. B*, Sep., 12B: 479-587.

HONE, M. and WARD, R.G., 1969. Reduction tests on prereduced pellets under simulated blast furnace conditions, *Journal of the Iron and Steel Institute*, Feb.: 159-166.

ISHIDA, M. and WEN, C.Y., 1968. Comparison of kinetic and diffusional models for solid-gas reactions, *A.I.Ch.E.J.*, 14: 311-317.

JACOBS, I.S., ZAVITSANOS, P.D. and GOLDEN, J.A., 1982. Tracking pyritic sulfur in the microwave desulfurization of coal, *Journal of Applied Physics*, Mar., 53, 3: 2730-2732.

KHANGOANKAR, P.R. and MISRA, V.N., 1976. Recent progress in understanding the theory of iron oxide reduction, *Journal of Scientific & Industrial Research*, Apr., 35: 231-238.

KOKUBU, H., KODAMA, T., ITAYA, H. and OGUCHI, Y., 1986, Formation of pores in iron ore sinters, *Trans. ISIJ*, 26: 182-185.

KOO, C.-H. and EVANS, J.W., 1979. Structural and reduction characteristics of some Venezuelan iron ores, *Trans. ISIJ*, 19 : 95-101.

KOPP, W.U. and MULLER, G., 1985. The preparation of porous materials, *Praktischen Metallographie*, 22: 490-500.

KRUESI, P.R., 1984. Microwave energy promises to improve the efficiency of metal extraction. *Chemical Engineering*, Nov., 12: 18.

KRUESI, W.H. and KRUESI, P.R., 1986. Microwaves in laterite processing, *Proc. 25th Annual Conference of Metallurgist* (eds. E. Ozberk and S.W. Marcuson), Canadian Instn. of Mining and Metallurgy, Montreal,17-20 Aug. : 1-11.

LANIGAN, P.G., 1989. MW energy potential uses in mineral extraction industries, *Symp. Proc. The First Australia Symposium on Microwave Power Application*, Wollongong, NSW, 15-17 Feb. : 160-176.

LLOYD, H.K., 1988. Steelmaking and iron ore smelting in Indonesia, *Ironmaking and Steelmaking*, 15, 2: 53-55.

LU, W.K., 1987. A critical review of blast furnace reactions, *Trans. of the ISS*, I & SM, Oct.: 51-62.

McGILL, S.L. and WALKIEWICS, J.W., 1987. Applications of microwave energy in extractive metallurgy, *Journal of Microwave Power and Electromagnetic Energy*, 22: 175-176.

McGILL, S.L. and WALKIEWICZ, J.W., 1988. Rapid microwave heating in mineral processing, *23rd Microwave Power Symposium*, International Microwave Power Institute: 47-48.

McGILL, S.L.,WALKIEWICZ, J.W. and SMYRES, G.A., 1988. The effect of power level on the microwave heating of selected chemicals and minerals, Paper No. M4.6, *Symp. Proc. Microwave Processing of Materials*, Mater. Res. Soc. 1988 Spring Meeting, 5-8 Apr., Reno, NV.

McKEWAN, W.M., 1960. Kinetics of iron oxide reduction, *Trans. Metallurgical Society of AIME*, Feb., 218: 2-6.

MEDVEDEVA, L.I., ROSTOVTSEV, S.T., SIMONOV, V.K. and NIZHEGORODOVA, T.E.,1977. Influence of carbon monoxide pressure on the reduction and metallisation kinetics of iron ore materials, *Russian Metallurgy (Metally)* : 5-10.

MERAIKIB, M. and FRIEDRICHS, H.A., 1987. On the isothermal reduction of iron ore pellets with carbon monoxide, hydrogen and their mixtures, *Steel Research*, 58, 10: 439-445.

METAXAS, A.C. and MEREDITH, R.J., 1983. *"Industrial Microwave Heating"*, IEE Power Engineering Series No.4, Peter Peregrinus, London.

METAXAS, A.C., 1974. *Trans. of the International Microwave Power Institute*, 2: 19-47.

MITRA, A.N., MUKHERJEE, T. and IRANI, J.J., 1978. Laboratory investigation on the size degradation of hematite ores and sinter in the upper stack region of the blast furnace, *Proc. 3rd Int. Iron and Steel Congress*, 16-20 Apr., Chicago, Ill., American Society for Metals: 460-471.

OHMI, M. and USUI, T.,1982. Improved theory on the rate of reduction of single particles and fixed beds of iron oxide pellets with hydrogen, *Trans. ISIJ*, 22: 66-74.

OHMI, M., USUI, T., MINAMIDE, Y. and NAITO, M., 1978. Reduction of single particles and fixed beds of hematite pellets with hydrogen, *Proc. 3rd Int. Iron and Steel Congress*, 16-20 Apr., Chicago, Ill., American Society for Metals: 472-478.

OSTWALD, J., 1981. Mineralogy of Australian iron ores, *BHP Tech. Bull.*, 25, 1: 4-12.

PARK, J.Y. and LEVENSPIEL, O., 1975. The crackling core model for the reaction of solid particles, *Chemical Engineering Science*, 30: 1207-1214.

PARK, J.Y. and LEVENSPIEL, O., 1977. The crackling core model for the multistep reaction of solid particles, *Chemical Engineering Science*, 32: 233-234.

PICKLES, C.A. and TUMIDAJSKI, P.J., 1983. The influence of various parameters on the strength of iron oxide briquettes under reducing conditions, *ISS Trans.*, 2: 65-70.

RAMACHANDRAN, P.A. and DORAISWAMY, L.K., 1982. Journal Review: Modeling of non-catalytic gas-solid reactions, *AIChE Journal*, Nov., 26, 6: 881-900.

RAO, Y.K. and AL-KAHTANY, M.M., 1984a. Reduction of magnetite with hydrogen: Part 2 gas mixtures, *Ironmaking and Steelmaking*, 11, 1: 34-40.

RAO, Y.K. and AL-KAHTANY, M.M., 1984b. Reduction of magnetite with hydrogen: Part 3 nucleation and growth, *Ironmaking and Steelmaking*, 11, 2: 88-94.

RAU, M., RIECK, D. and EVANS, J.W.,1987. Iron oxide reduction by TEM; microstructure aspect: nucleation, growth and morphology of second solid phases, *Met. Trans. B*, Mar., 18B: 257-278.

ROSS, H., McADAMS, D. and MARSHAL, T., 1980. Physical Chemistry: Part I. Reaction Kinetics, in *"Direct Reduced Iron"*, (ed. R.L. Stephenson *et al*), Warrendale, The Iron and Steel Society of AIME: 26-34.

ROSS, H.U., 1972. A review of problems in iron ore reduction by solid state processes, *Canadian Metallurgical Quarterly*, 11, 4: 621-627.

ROSS, H.U., 1980. Physical Chemistry: Part I. Thermodynamics, in *"Direct Reduced Iron"*, (ed. R.L. Stephenson *et al.*). Warrendale, The Iron and Steel Society of AIME: 9-25.

RUSTIADI, 1985. Struktur mikro bijih besi Pematang Burhan. *Metallurgi*, Lembaga Metallurgi Nasional - LIPI, 5, 1, Oct.: 3-9.

SAKAMOTO, M., FUKOYO, H., IWATA, Y. and MIYASHITA, T., 1978. A mineralogical investigation on the reducibility and the reduction degradation based on sinter structure, *Burden design for the blast furnace*, McMaster Symp. No. 12 (ed. W.K. Iu), May: 137-151.

SCHIFFMANN, R.F., 1987. Microwave and dielectric drying, in *"Handbook of Industrial Drying"* (ed. A.S. Mujumdar), Marcel Dekker, New York and Basel: 327-356.

SETH, B.B.L. and ROSS, H.U., 1965. *Trans. TMS-AIME*, 233: 180-185.

SHEPPARD, L.M., 1988. Manufacturing ceramics with microwaves: The potential for economical production, *Ceramics Bull.*, 67, 10: 1656-1661.

SHIMOMURA, Y., OKAMOTO, A. and NAITO, M., 1984. Reduction, softening and melting behavior of sinter under simulated blast furnace conditions, *Burden design for the blast furnace*, McMaster Symp. No. 12 (ed. W.K. Iu), May: 114-136.

SHKOL'NIKOV, V.N., DEMENT'YEV, V.M., SAKHARNOVA, T.M., VANZHA, A.N. and MAKSIMENKO, A.S., 1977. Strengthening of magnetite pellets from superconcentrates during firing and reduction, *Russian Metallurgy (Metally)* : 46-47.

SLACK, W.W. and LI, K., "Nucleation, Growth and Impurities Effects in Crystallization Process Engng.", *AIChE Symposium Series*,78, 216: 97-103.

SOHN, H.Y. and SZEKELY, J., 1972. A structural model for gas-solid reaction with a moving boundary-III: A general dimensionless representation of the irreversible reaction between a porous solid and a reactant gas, *Chemical Engineering Science*, 27: 763.

SOHN, H.Y.,1985. Development in physical chemistry and basic principles of extractive and process metallurgy in1984, *Journal of Metals*, Apr.: 51-57.

SPITZER, R.H., MANNING, F.S., and PHILBROOK, W.O., 1966. Mixed-control reaction kinetics in the gaseous reduction of hematite, *Trans.Metallurgical Society of AIME*, May, 236: 726 - 742.

SPJUT, E.R., BOLSAITIS, P. and ELLIOTT, J.F., 1986. High temperature gas solid reaction: Introductory of thermoelectrodynamic balance (TEB), *Proc. the 6th Process Technology Conference*, Washington Meeting, Apr., 6: 3-17.

SRAKU-LARTEY, K., PARKER, R.H. and HAWKINS, J.,1984. Oxidation of sponge iron particles and pellets produced by reduction of hematite in hydrogen, *Ironmaking and Steelmaking*, , 11, 1: 23-33.

SRINIVASAN, N.V. and SHEABY, J.S.,1981. Study of the reduction of hematite to magnetite using a stabilized zirconia cell, *Metallurgical Trans. B*, 12B, Mar. : 177-185.

ST.JOHN, D.H., MATTHEW, S.P. and HAYES, P.C., 1985. Microstructural changes during the reduction of wustite, *Bull. Proc. Australas. Inst. Min. Metall.*, Sep., 290 , 6: 61-65.

STANDISH, N., 1988. Fundamental of Ironmaking in the Charcoal Blast Furnace, *Paper presented in 32nd Conference of SEASI*, 1-3 Jun., Bali.

STEINMETZ, E., STEFFEN, R. and THIELMAN, R.,1986. Present state and development potential of the processes for the direct reduction and smelting reduction of iron ores, *Stahl u. Eisen*, May , 106, 9: 421-428.

STRUMILLO, C. and KUDRA, T., 1986. *"Drying: Principles, Applications and Design"*, Chapter 9, Gordon and Breach, New York etc.

SUGIYAMA, T., YAGI, J. and OMORI, Y., *Proc. 3rd Int. Iron and Steel Congress*, 16-20 Apr. 1978, Chicago, Ill., American Society for Metals, 479-488.

SZEKELY, J. and THEMELIS, N.J., 1971. *"Rate Phenomena in Applied Metallurgy"*, Wiley, New York: 630.

SZEKELY, J., EVANS, J.W. and SOHN, H.Y., 1976. *"Gas - Solid Reactions"*, New York, Academic Press: 205-247.

TANJUNG, A.F.A., 1987. *Gassification kinetics of single charcoal particle in carbon dioxide atmosphere*, M. Met. Thesis, Dept. of Metallurgy and Materials Engineering, University of Wollongong.

The 54th (Ironmaking) Committee, Japan Society for the Promotion of Science.1967. Standard methods for identifying the microstructure of iron ore sinters and pellets, *Trans. ISIJ*, 7: 126-133.

THEMELIS, N.J. and GAUVIN, W.H.,1963. A generalized rate equation for the reduction of iron oxides, *Trans. of Metallurgical Society of AIME*, Apr. , 227: 290-300.

TIEN, R.H. and TURKDOGAN, E.T.,1972. Gaseous reduction of iron oxides: Part IV. Mathematical analysis of partial internal reduction diffusion control. *Metallurgical Trans.*, Aug., 3: 2039-2048.

TOWHIDI, N. and SZEKELY, J.,1981. Reduction kinetics of commercial low silica hematite pellets with CO-H_2 mixtures over temperature range 600° - 1234° C, *Ironmaking and Steelmaking*, . 6: 237-249.

TURKDOGAN, E.T. and VINTERS, J.V., 1971. Gaseous reduction of iron oxides: Part I. Reduction hematite in hydrogen, *Metallurgical Trans.*, Nov., 2: 3175-3188.

TURKDOGAN, E.T. and VINTERS, J.V., 1972. Gaseous reduction of iron oxides: Part III. Reduction-oxidation of porous and dense iron oxide and iron. *Metallurgical Transaction*, Jun.: 1561-1574.

TURKDOGAN, E.T. and VINTERS, J.V.,1973. Reducibility of iron ore pellets and effect of additions, *Canadian Metallurgical Quarterly*, 12, 1: 9-21.

TURKDOGAN, E.T., OLSSON, R.G. and VINTERS, J.V., 1971. Gaseous reduction of iron oxides: Part II. Pore charactristics of iron reduced from hematite in hydrogen, *Metallurgical Transactions*, Nov., 2: 3179-3196.

TYLER, R.J. and WRIGHT, J.K., 1979. The effect of reduction temperature on pore structure of iron ores and pellets reduced in a fluid bed, *Trans. Section C Inst. Min. Met.*, 88: C25-C30.

UWADIALE, G.G.O.O. and WHEWELL, R.J., 1988. Effect of temperature on magnetizing reduction of Agbaja iron ore, *Metallurgical Trans. B*, Oct., 19B: 731-735.

VAN DE PIJPEKAMP, B.,1971. Discussion on preparation and polishing of specimens, *Mineralogy & Materials News Bulletin for Quantitative Microscopic Methods* (ed. N.F.M. Henry), 2-3-4, Cambridge, England.

WALKIEWICZ, J.W., KAZONICH, G. and McGILL, S.L., 1988. Microwave heating characteristics of selected minerals and compounds, *Minerals and Metallurgical Processing*, Feb., 5: 39-42.

WALKIEWICZ, J.W., McGILL, S.L. and MOYER, L.A., 1988. Improved grindability of iron ores using microwave energy, Paper No. M.4.7, *Symp. Proc. Microwave Processing of Materials*, Mater. Res. Soc. 1988 Spring Meeting,5-8 Apr., Reno, NV.

WARNER, N.A.,1964. Kinetics of the gaseous reduction of hematite, *Aust. Inst. of Mining and Metallurgy*, 210: 163-176.

WARNER, N.A.,1964. Reduction kinetics of hematite and the influence of gaseous diffusion, *Trans. of the Metallurgical Society of AIME*, Feb. , 230: 163-176.

WATANABE, S. and YOSHINAGA, M., 1968. The abnormal behaviour of some ore constituents and their effect on blast furnace operation, *Trans. Society of Mining Engineers*, Mar.: 1-15.

WATTS, A., YOUNG,C.C. and BOWLING,K.McG.,1988. Batch reduction of iron ore with hydrogen in a fluidized bed, *Trans.Instn. Min.Metall. (Sect. C: Mineral Process. Extr. Metall.)*, Jun., 97: C61-C71.

WOODCOCK, J.T., SPARROW, G.J. and BRADHURST, D.H., 1989. Possibilities for using microwave energy in the extraction of gold, *Symp. Proc. The First Australia Symposium on Microwave Power Application*, Wollongong, NSW, 15-17 Feb. : 139-159.

WORNER, H.K. and STANDISH, N., 1988. Effect of microwave drying on the results of subsequent analytical tests, *Analyst*, Jan.: 114.

WORNER, H.K., REILLY, L. and JONES, J., 1989. Microwaves in pyrometallurgy, *Symp. Proc. The First Australia Symposium on Microwave Power Application*, Wollongong, NSW, 15-17 Feb. : 179-188.

WRIGHT, J.K. and MORRISON, A.L., 1982. Changes in diffusivity due to sintering in metallized iron oxide pellets, *Metallurgical Trans. B*, Sep., 13B: 518-520.

WRIGHT, J.K. and MORRISON, A.L.,1985. Test method for the laboratory evaluation of iron burdens for gaseous direct reduction processes: Current practice and recommendation for future standards, *SEAISI Quarterly*, Jan.: 51-67.

WRIGHT, J.K. and TYLER, R.J., 1979. Pore structure of sintered and metallized iron oxide compacts, *Powder Tech.*, 24: 49-55.

WRIGHT, J.K., 1976. The effect of firing conditions on the strength of hematite compacts, *Powder Technology*, 14: 103-113.

WRIGHT, J.K., 1977. Volume changes of high-grade iron ore pellets reduced in a fixed bed under isothermal and non-isothermal conditions, *Trans. ISIJ*, 17: 726-731.

WRIGHT, J.K., 1981. The effect of calcium oxide on the sintering of ferric oxide compacts, *Powder Technology*, 30: 185-194.

YAGI, S. and KUNII, D., 1955. Combustion of carbon particles in flames and fluidized beds, *Procc. 5th Symp. on Combustion*, Pittsburgh: 231-244.

YAGI, T. and ONO, Y., 1968. A method of analysis for reduction of iron oxide in mixed-control kinetics, *Trans. ISIJ*, 8: 377-381.

YANAGIYA, T., YAGI, J. and OMORI, Y., 1978. Theoretical and experimental study on the reduction of iron oxide pellets in moving bed, *Proc. 3rd Int. Iron and Steel Congress*, 16-20 Apr., Chicago, Ill., American Society for Metals: 449-459.

APPENDIX A-1

DATA LOGGING AND RECOVERY PROGRAM

```
 10 ON ERROR GOTO 1000
 20 CLS
 30 MODE7
 40 PRINT ''"BBC CHYO BALANCE LOGGING PROGRAM"
 50 REM VERSION B.CHYO2 - MOD.
 52 INPUT''"IRON ORE INITIAL WEIGHT  ";CHARCOAL
 54 INPUT''"FURNACE TEMPERATURE  ";TEMP
 56 INPUT''"GAS FLOW RATE  ";GAS
 60 INPUT ''"   SAMPLE INTERVAL IN SECONDS  ";SEC
 70 ST=SEC*100
 80 INPUT'' "   FILE NO. FOR DATA  ";FILE$
 90 Y%=OPENOUT(FILE$)
100 *FX2,2
110 *FX7,4
120 *FX8,4
140 DIM A(500)
150 M=0
160 *FX21,1
170 OSBYTE=&FFF4
180 T=TIME
190 REPEAT
200 A%=138:X%=2
210 IF ADVAL(-1)>0 AND ADVAL(-3)>0 THEN Y%=GET:CALL OSBYTE
220 *FX2,1
230 IF ADVAL(-2)>0 THEN INPUT A
240 *FX2,2
250 IF INKEY$(1)="F" THEN 280
260 IF TIME>=T+30 THEN A(M)=A:PRINTTAB(20);M :M=M+1 :T=TIME+ST
270 UNTIL FALSE
280 PRINT "FILE NO.  ";FILE$
290 PRINT#Y%,FILE$
292 PRINT''"IRON ORE INITIAL WEIGHT  ";CHARCOAL
293 PRINT#Y%,CHARCOAL
294 PRINT''"FURNACE TEMPERATURE  ";TEMP
295 PRINT#Y%,TEMP
296 PRINT''"GAS FLOW RATE  ";GAS
297 PRINT#Y%,GAS
300 PRINT "SAMPLES TAKEN  ";M
310 PRINT#Y%,M
320 PRINT "TIME INTERVAL _ ";SEC;" SECS"
330 PRINT#Y%,SEC
340FOR J = 0 TO M
350 PRINT A(J);
360 PRINT#Y%,A(J)
370 NEXT
380 CLOSE#Y%
390 *FX2,0
400 END
1000 REPORT:PRINT " at line ";ERL:GOTO 280
```

(Continued on next page)

```
  5 ON ERROR GOTO 999
 10 REM B.CHYOREC1
 20 REM PRINTS WEIGHTS,PERCENTAGE REDUCTION & GRAPHS PERCENTAGES FOR PRAM
 30 MODE7
 35 à%=&20308
 40 PRINT''" UNIVERSITY OF WOLLONGONG"
 50 PRINT''"CHYO BALANCE DATA RECOVERY PROGRAM"
 60 INPUT'' "FILE TO READ   ";FILE$
 80 Y%=OPENIN(FILE$)
 90 INPUT#Y%,FILE$
100 INPUT#Y%,CHARCOAL
110 INPUT#Y%,TEMP
120 INPUT#Y%,GAS
130 INPUT#Y%,NUM :REM NUMBER OF SAMPLES TAKEN
140 INPUT#Y%,SEC :REM SAMPLING TIME INTERVAL IN SECS.
150 DIM A(500) :DIM B(500) :REM MAX.HERE IS ABOUT 1300
160 CLS
170 REM LINE FEED TO PRINTER
180 *FX6,255
190 INPUT''"DO YOU WANT TO PRINT RESULTS ";P$
195 IF P$="Y" THEN VDU2,1,27,1,15
196 IF P$="Y" THEN VDU2,1,27,1,108,1,20
200  IF P$="Y" THEN VDU2 :REM ENABLES PRINTER
220 à%=10
230 PRINT"BBC CHYO BALANCE DATA REPORT"
240 PRINT"DATA FILE No.          :  ";FILE$
250 PRINT"REMOVABLE OXYGEN WEIGHT:  ";CHARCOAL ;"  GRAM"
260 PRINT"FURNACE TEMPERATURE    :  ";TEMP   ;"  DEG. C"
270 PRINT"GAS FLOW RATE          :  ";GAS    ;"  L/MIN"
280 PRINT"NUMBER OF SAMPLES TAKEN:  ";NUM
290 PRINT"SAMPLING INTERVAL      :  ";SEC    ;"  SECONDS"
300 PRINT'''"       WEIGHT LOSS"
305 PRINT
310 à%=&2030A :REM FORMATING
320 FOR J = 0 TO NUM-1 :REM LOOP TO READ IN DATA FROM CHYO1
330 INPUT#Y%,A(J):NEXT
334 m=0:REPEAT
335 FOR K=1 TO 10
340 PRINTTAB(K*9);A(m);
350 A(0)=0
360 B(m)=(A(0)-A(m))/CHARCOAL*100 :REM TO CALC % REDUCTION
365 IF m=NUM-1 THEN 375
370 m=m+1:NEXT:PRINT
375 UNTIL m=NUM-1
380 IF P$<>"Y" THEN PRINT''"  PRESS ANY KEY TO CONTINUE"
390 IF P$<>"Y" THEN X=INKEY(10000)
400 PRINT'''"       PERCENTAGE REDUCTION"
410 PRINT
420 à%=&2020A
430 n=0:REPEAT
435 FOR L=1 TO 10
438 IF n=NUM-1 THEN 455
440 PRINTTAB(L*9);B(n);
445 n=n+1
450 NEXT:PRINT
455 UNTIL n=NUM-1
460 CLOSE#Y%
470 PRINT'''"        GRAPH"
475 VDU2,1,18
```

(Continued on next page)

```
477 PRINT
480 VDU3 :REM TURNS PRINTER OFF
490 IF P$<>"Y" THEN PRINT''"  PRESS ANY KEY TO CONTINUE"
495 PRINT"        GRAPH"
497 PRINT
500 IF P$<>"Y" THEN X=INKEY(10000)
505 PRINT"        GRAPH"
507 PRINT
510 à%=10
520MODE4
530MOVE 160,150:DRAW 1160,150: REM DRAW X AXIS
540MOVE 160,950:DRAW 1160,950: REM DRAW UPPER-SIDE X AXIS
550FOR I=360 TO 1160 STEP 200
560MOVE I,150 :DRAW I,170
570MOVE I,950 :DRAW I,930
571FOR K=210 TO 1160 STEP 50
572MOVE K,150 :DRAW K,160
573MOVE K,950 :DRAW K,940
574NEXT K
580NEXT I
590PRINT TAB(5,28);0;TAB(10,28);40;TAB(16,28);80;TAB(22,28);120;TAB(28,28);160;
595PRINT TAB(34,28);200 ;TAB(17,30);"TIME, minutes"
600MOVE 160,150 :DRAW 160,950 :REM DRAW Y AXIS
610MOVE 1160,150 :DRAW 1160,950 :REM DRAW R-H SIDE Y AXIS
620FOR I=310 TO 950 STEP 160
630MOVE 160,I :DRAW 180,I
640MOVE 1160,I :DRAW 1140,I
641FOR K=190 TO 950 STEP 40
642MOVE 160,K :DRAW 170,K
643MOVE 1160,K :DRAW 1150,K
644NEXT K
650NEXT I
660 PRINT TAB(2,2);100;TAB(3,7);80;TAB(3,12);60;TAB(3,17);40;TAB(3,22);20;TAB(4,27);0
670 REM LABEL Y AXIS
680PRINT TAB(1,6);"R";TAB(1,7);"E";TAB(1,8);"D";TAB(1,9);"U";TAB(1,10);"C";
685PRINTTAB(1,11);"T";TAB(1,12);"I";TAB(1,13);"O";TAB(1,14);"N";TAB(1,15);","
690 PRINT TAB(1,18);"p";TAB(1,19);"e";TAB(1,20);"r";TAB(1,21);"c";
695PRINT TAB(1,22);"e";TAB(1,23);"n";TAB(1,24);"t"
700 DIM X(500),Y(500)
710FOR I=0 TO NUM-1 :REM LOOP TO PLOT GRAPH
720Y(I)=(B(I)*8)+150
730X(I)=(I*5*SEC/60)+160
740PLOT 69,X(I),Y(I)
750NEXT
760 FOR I=1 TO 3 :REM PAPER FEED
770  PRINTCHR$(10)
780 NEXT
790 IF P$="Y" THEN *EPSON4
795 VDU2,1,27,1,108,1,0
796 VDU3
800 VDU5 :MOVE 0,1050 :END
999 REPORT: PRINT"  at  line  ";ERL:CLOSE#0:VDU2,1,18:VDU2,1,27,1,108,1,0:VDU3:END
)
```

APPENDIX A-2

FURNACE TEMPERATURE PROFILES

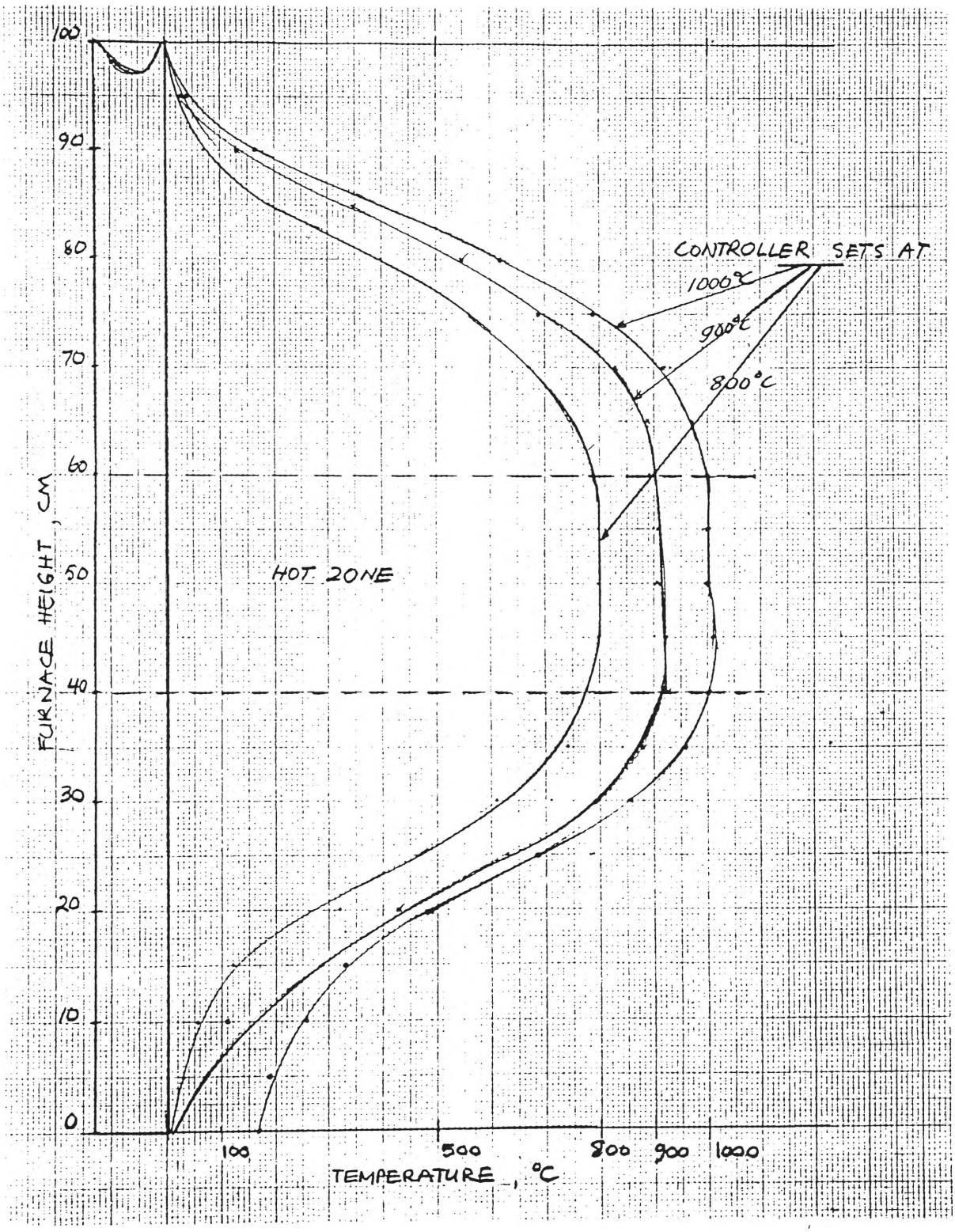

APPENDIX A-3

GAS FLOWRATE CHART

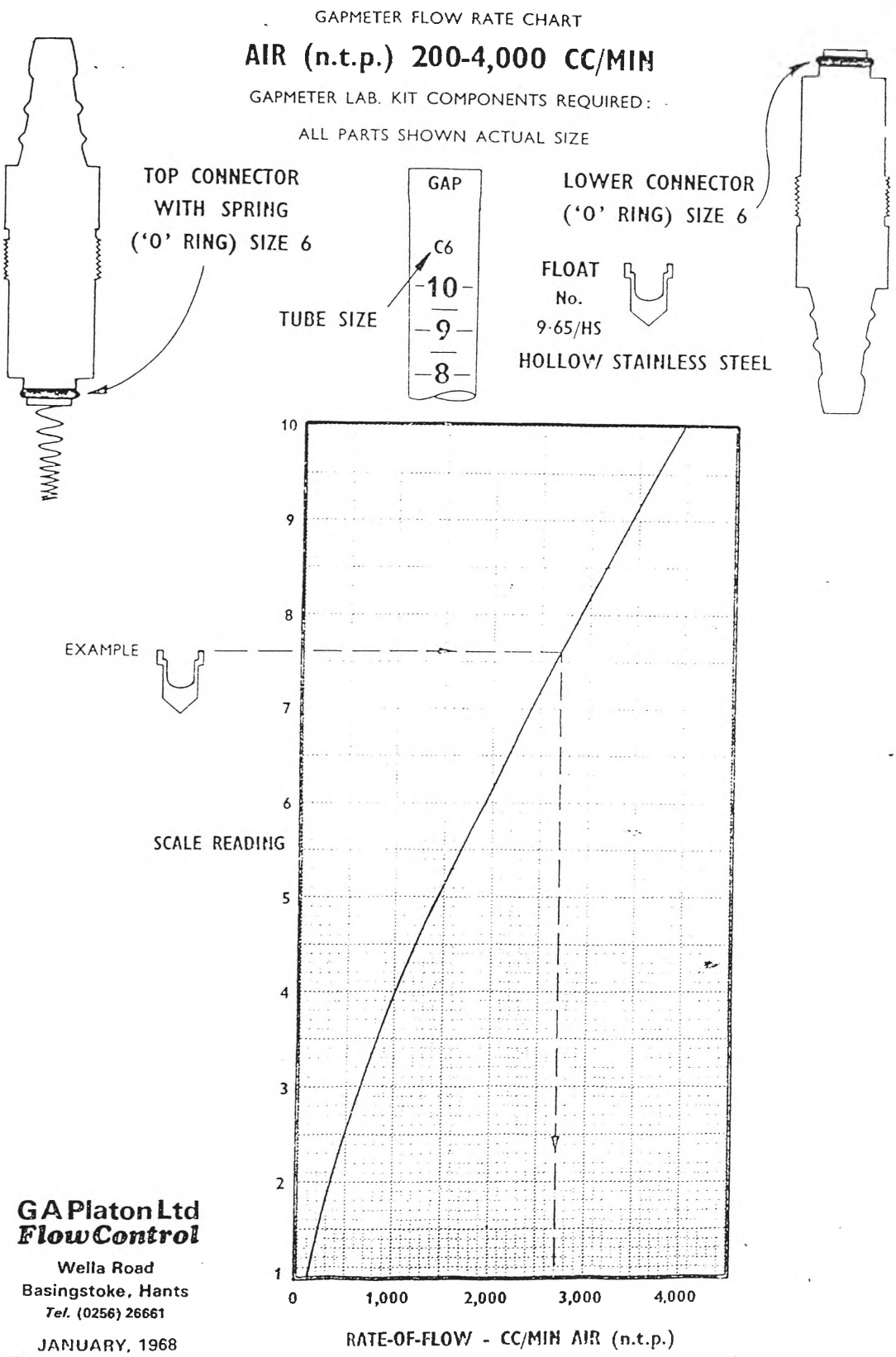

GA Platon Ltd
Flow Control
Wella Road
Basingstoke, Hants
Tel. (0256) 26661

JANUARY, 1968

APPENDIX A-4

SEM & EDX ANALYSIS OF SAMPLE No.2

(a)

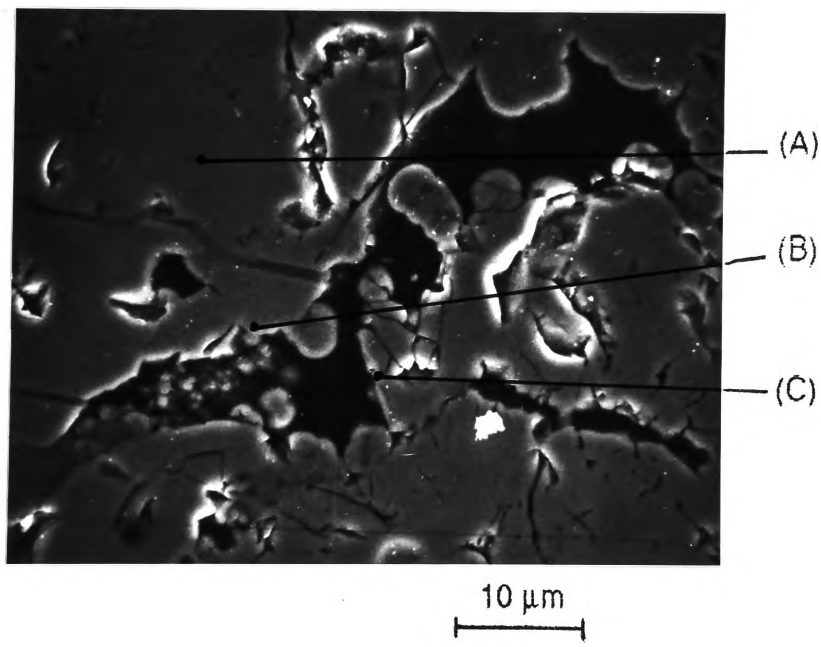

Figure A-4. (a) SEM photomicrograph analysis of sample No.2, showing cavities in the grains boundary, together with the corresponding EDX microanalysis from (b) Area A (c) Area B and (d) Area C.

(continued on next page)

(b)

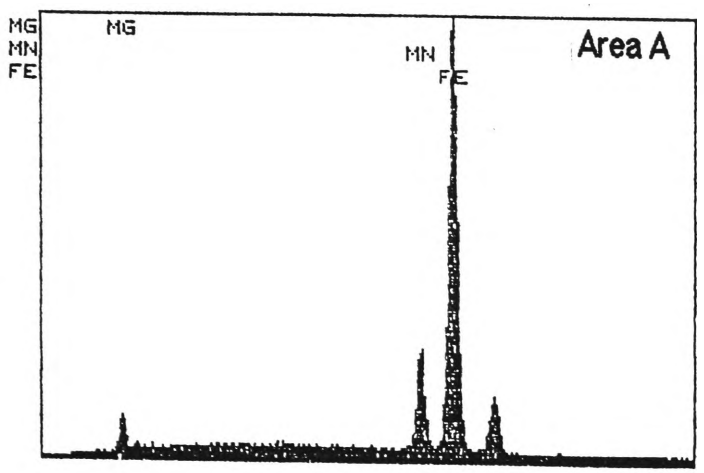

(c)

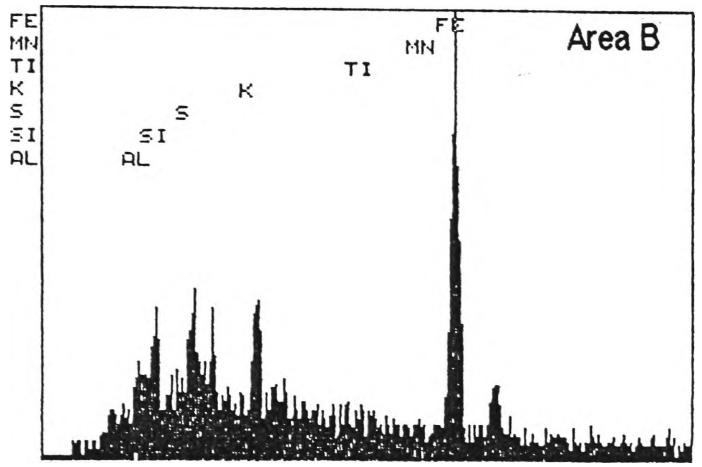

(d)

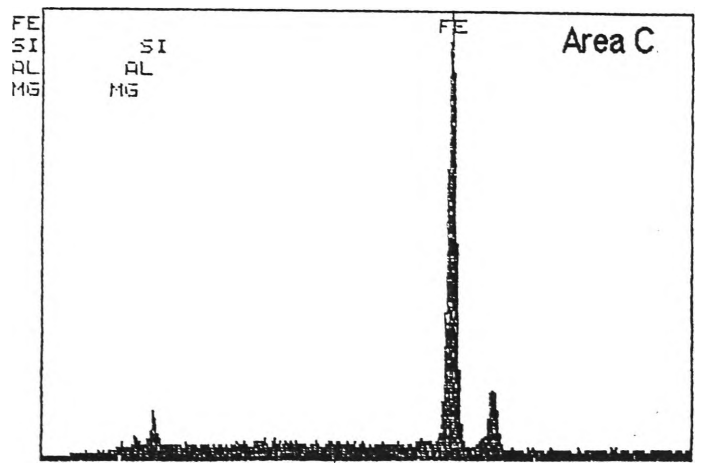

Figure A-4. (Continued)

APPENDIX A-5

SEM & EDX ANALYSIS OF WHYALLA ORE

(a)

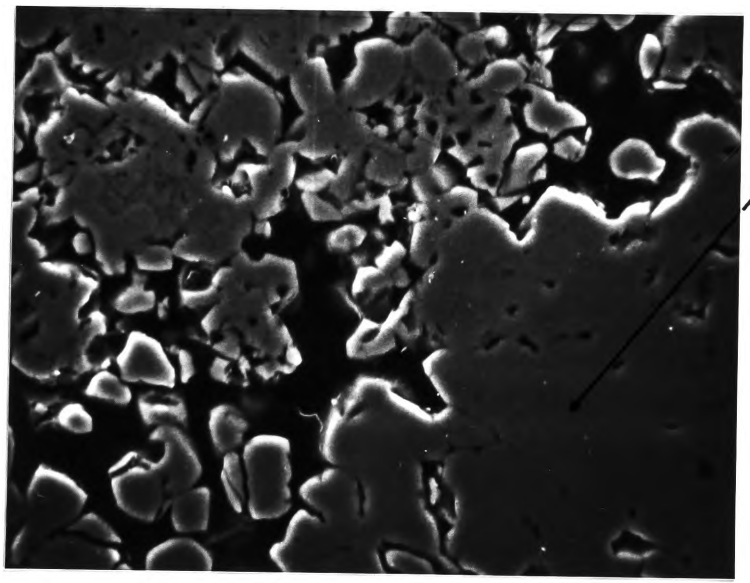

(b)

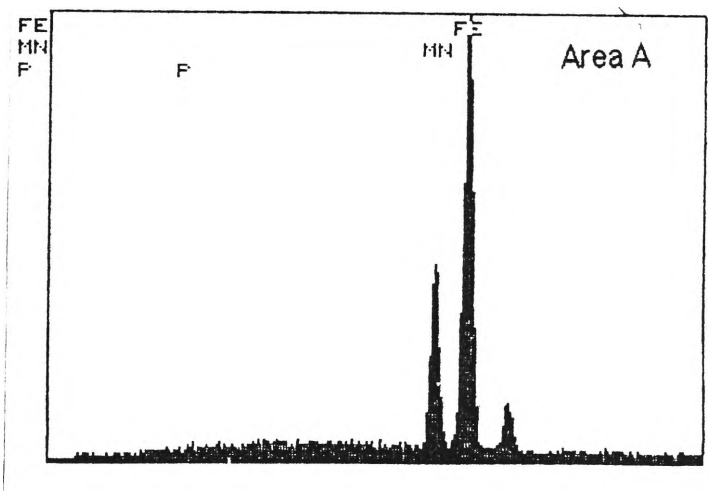

Figure A-5. (a) SEM photomicrograph analysis of Whyalla Ore, showing cavities in the grains boundary, together with the corresponding EDX microanalysis from (b) Area A.

APPENDIX A-6

DENSITY & POROSITY OF RAW ORE

Sample No.	Density, g cm^{-3}	Porosity, percent
1	6.59	4.47
	7.26	4.49
	11.98	4.15
	14.18	4.25
Average value	10.00	4.34
2	8.93	4.27
	12.09	4.56
	14.09	3.95
Average value	12.39	4.23
3	3.94	4.58
	4.47	4.45
	5.82	4.46
	6.10	4.40
	8.76	4.34
	9.52	4.47
Average value	6.44	4.45
4	10.52	4.38
	13.02	4.10
	22.11	3.94
Average value	15.22	4.14
5	12.64	4.20
	13.43	3.92
	18.06	3.89
	20.82	3.73
Average value	16.24	3.94

APPENDIX A-7

POROSITY, DENSITY & VOLUME CHANGES DURING REDUCTION

Reduction, percent	Porosity, percent Sample No.			Density, g cm^{-3} Sample No			Volume change, percent Sample No.		
	1	2	3	1	2	3	1	2	3
0	10.00	12.39	6.44	4.34	4.23	4.45	0	0	0
20	21.01	19.44	23.82	3.77	3.80	3.94	5.37	6.70	6.33
40	33.25	39.51	37.32	3.50	3.26	3.54	6.20	17.57	33.33
60	38.89	46.57	44.00	3.33	2.89	3.04	5.30	25.05	20.52
80	49.50	48.77	47.80	2.90	2.95	3.19	2.70	17.82	23.20
90	51.34	49.82	47.31	3.04	3.17	3.29	2.00	7.20	16.19
100	53.10	51.05	49.57	2.93	3.07	3.19	6.75	6.26	1.41

APPENDIX A-8

ANALYTICAL CALCULATION OF RAW ORE

Sample No.1 contains 66.9 percent total iron and 9.34 percent ferrous iron. It is assumed that the iron materials are magnetite and hematite (Ross, 1980).

Therefore :

magnetic iron assay	= 3* x 9.34	= 28.02	percent
non-magnetic iron assay	= 66.9 - 28.02	= 38.88	percent
hematite assay	= 1.4297# x 38.88	= 55.59	percent
magnetite assay	= 1.3826# x 28.02	= 38.72	percent
total iron oxide	= 55.59 + 38.72	= 94.31	percent
total oxygen	= 94.31 - 66.9	= 27.41	percent

Note :

* The iron in magnetite : one-third ferrous and two-thirds ferric iron

\# From the iron-oxygen system (after Darken and Gurry, 1946)

in hematite : O/Fe = 30.06 / 69.94 = 0.4297

or hematite assay = 1.4297 x non-magnetic iron assay

in magnetite: O/Fe = 27.64 / 72.46 = 0.3826

or magnetite assay = 1.3826 x magnetic iron assay

(Continued on next page)

APPENDIX A-8 (Continued)

SAMPLE ANALYTICAL CALCULATION OF RAW ORE

Similar for sample No.1, the iron assay is calculated based on the assumption that the iron materials are magnetite and hematite.

Analysis	Sample No.				
	1	2	3	4	5
Total iron	66.9	66.9	63.8	67.0	66.8
Fe^{2+}	9.34	7.23	6.02	9.06	5.80
Magnetic iron (3 x Fe^{2+})	28.02	21.69	18.06	27.18	17.4
Non-magnetic iron (Fe_{total} - magnetic iron)	38.88	45.21	45.74	39.82	49.4
Hematite (1.4297 x non-magnetic Fe)	55.59	64.64	65.39	56.93	70.63
Magnetite (1.3826 x magnetic iron)	38.72	29.97	24.96	37.56	24.05
Total iron oxide	94.31	94.61	90.35	94.49	94.68
Total oxygen	27.41	27.71	26.55	27.49	27.88

APPENDIX A-9

REDUCTION DATA

Example of Data File No. : y.C.PRAMx

y	:	disk number
x	:	run number
C	:	effect of flowrate (Sample No.2)
D	:	effect of temperature (Sample No.2)
E	:	partly reduced samples for microscopical identifications (Sample No.2)
F	:	effect of flowrate fo small particles (Sample No.2)
H	:	effect of particle size & partly reduced samples for chemical analysis (Sample No.2)
I	:	effect of particle size (Whyalla Ore)
N	:	effect of temperature (Sample No.5)
O	:	effect of microwave treatment on single particle
Q	:	effect of microwave treatment on ores A and B

BBC CHYO BALANCE DATA REPORT
DATA FILE No. : :1.C.PRAM1
REMOVABLE OXYGEN WEIGHT: 1.44 GRAM
FURNACE TEMPERATURE : 1000 DEG. C
GAS FLOW RATE : 4 L/MIN
NUMBER OF SAMPLES TAKEN: 62
SAMPLING INTERVAL : 60 SECONDS

WEIGHT LOSS

0.000	-0.040	-0.078	-0.117	-0.154	-0.190	-0.225	-0.255	-0.283	-0.309
-0.334	-0.355	-0.378	-0.399	-0.417	-0.435	-0.454	-0.472	-0.490	-0.508
-0.527	-0.546	-0.563	-0.582	-0.601	-0.618	-0.639	-0.656	-0.675	-0.692
-0.712	-0.734	-0.752	-0.778	-0.798	-0.816	-0.832	-0.846	-0.812	-0.878
-0.892	-0.912	-0.924	-0.935	-0.946	-0.957	-0.965	-0.977	-0.988	-0.997
-1.007	-1.019	-1.029	-1.037	-1.047	-1.056	-1.064	-1.073	-1.081	-1.091
-1.098	-1.101								

PERCENTAGE REDUCTION

0.00	2.78	5.42	8.12	10.69	13.19	15.62	17.71	19.65	21.46
23.19	24.65	26.25	27.71	28.96	30.21	31.53	32.78	34.03	35.28
36.60	37.92	39.10	40.42	41.74	42.92	44.37	45.56	46.87	48.06
49.44	50.97	52.22	54.03	55.42	56.67	57.78	58.75	56.39	60.97
61.94	63.33	64.17	64.93	65.69	66.46	67.01	67.85	68.61	69.24
69.93	70.76	71.46	72.01	72.71	73.33	73.89	74.51	75.07	75.76
76.25									

BBC CHYO BALANCE DATA REPORT
DATA FILE No. : :1.C.PRAM2
REMOVABLE OXYGEN WEIGHT: 2.54 GRAM
FURNACE TEMPERATURE : 1000 DEG. C
GAS FLOW RATE : 2 L/MIN
NUMBER OF SAMPLES TAKEN: 123
SAMPLING INTERVAL : 60 SECONDS

WEIGHT LOSS

0.000	-0.009	-0.055	-0.101	-0.148	-0.195	-0.240	-0.285	-0.328	-0.368
-0.405	-0.441	-0.473	-0.503	-0.531	-0.558	-0.582	-0.606	-0.630	-0.651
-0.673	-0.694	-0.715	-0.737	-0.756	-0.778	-0.798	-0.819	-0.839	-0.861
-0.882	-0.903	-0.925	-0.947	-0.968	-0.990	-1.012	-1.034	-1.056	-1.078
-1.101	-1.122	-1.144	-1.166	-1.188	-1.209	-1.231	-1.253	-1.274	-1.295
-1.317	-1.338	-1.357	-1.378	-1.399	-1.418	-1.438	-1.457	-1.476	-1.494
-1.512	-1.530	-1.547	-1.565	-1.581	-1.598	-1.613	-1.628	-1.644	-1.659
-1.674	-1.688	-1.702	-1.715	-1.728	-1.741	-1.754	-1.767	-1.779	-1.791
-1.803	-1.814	-1.826	-1.837	-1.848	-1.859	-1.870	-1.880	-1.890	-1.901
-1.911	-1.921	-1.931	-1.941	-1.949	-1.959	-1.968	-1.976	-1.985	-1.994
-2.002	-2.010	-2.019	-2.027	-2.035	-2.043	-2.051	-2.058	-2.066	-2.074
-2.080	-2.088	-2.095	-2.102	-2.109	-2.116	-2.122	-2.128	-2.135	-2.141
-2.148	-2.155	-2.160							

PERCENTAGE REDUCTION

0.00	0.35	2.17	3.98	5.83	7.68	9.45	11.22	12.91	14.49
15.94	17.36	18.62	19.80	20.91	21.97	22.91	23.86	24.80	25.63
26.50	27.32	28.15	29.02	29.76	30.63	31.42	32.24	33.03	33.90
34.72	35.55	36.42	37.28	38.11	38.98	39.84	40.71	41.57	42.44
43.35	44.17	45.04	45.91	46.77	47.60	48.46	49.33	50.16	50.98
51.85	52.68	53.43	54.25	55.08	55.83	56.61	57.36	58.11	58.82
59.53	60.24	60.91	61.61	62.24	62.91	63.50	64.09	64.72	65.31
65.91	66.46	67.01	67.52	68.03	68.54	69.06	69.57	70.04	70.51
70.98	71.42	71.89	72.32	72.76	73.19	73.62	74.02	74.41	74.84
75.24	75.63	76.02	76.42	76.73	77.13	77.48	77.80	78.15	78.50
78.82	79.13	79.49	79.80	80.12	80.43	80.75	81.02	81.34	81.65
81.89	82.20	82.48	82.76	83.03	83.31	83.54	83.78	84.06	84.29
84.57	84.84								

BBC CHYO BALANCE DATA REPORT
DATA FILE No. : :1.C.PRAM3
REMOVABLE OXYGEN WEIGHT: 1.568 GRAM
FURNACE TEMPERATURE : 1000 DEG. C
GAS FLOW RATE : 2 L/MIN
NUMBER OF SAMPLES TAKEN: 91
SAMPLING INTERVAL : 60 SECONDS

WEIGHT LOSS

0.000	0.000	-0.043	-0.119	-0.194	-0.257	-0.310	-0.354	-0.395	-0.432
-0.467	-0.502	-0.533	-0.564	-0.597	-0.627	-0.657	-0.687	-0.715	-0.744
-0.771	-0.797	-0.824	-0.849	-0.874	-0.897	-0.921	-0.942	-0.937	-0.955
-0.973	-0.991	-1.009	-1.027	-1.044	-1.059	-1.074	-1.089	-1.103	-1.144
-1.152	-1.165	-1.175	-1.185	-1.195	-1.207	-1.219	-1.227	-1.239	-1.247
-1.254	-1.265	-1.275	-1.285	-1.294	-1.310	-1.316	-1.326	-1.340	-1.350
-1.361	-1.374	-1.392	-1.402	-1.413	-1.421	-1.431	-1.445	-1.456	-1.460
-1.473	-1.483	-1.493	-1.497	-1.507	-1.515	-1.519	-1.528	-1.529	-1.539
-1.544	-1.547	-1.551	-1.555	-1.557	-1.559	-1.561	-1.565	-1.563	-1.567

PERCENTAGE REDUCTION

0.00	0.00	2.74	7.59	12.37	16.39	19.77	22.58	25.19	27.55
29.78	32.02	33.99	35.97	38.07	39.99	41.90	43.81	45.60	47.45
49.17	50.83	52.55	54.15	55.74	57.21	58.74	60.08	59.76	60.91
62.05	63.20	64.35	65.50	66.58	67.54	68.49	69.45	70.34	72.96
73.47	74.30	74.94	75.57	76.21	76.98	77.74	78.25	79.02	79.53
79.97	80.68	81.31	81.95	82.53	83.55	83.93	84.57	85.46	86.10
86.80	87.63	88.78	89.41	90.11	90.62	91.26	92.16	92.86	93.11
93.94	94.58	95.22	95.47	96.11	96.62	96.87	97.45	97.51	98.15
98.47	98.66	98.92	99.17	99.30	99.43	99.55	99.81	99.68	99.94

BBC CHYO BALANCE DATA REPORT
DATA FILE No. : :1.C.PRAM4
REMOVABLE OXYGEN WEIGHT: 2.086 GRAM
FURNACE TEMPERATURE : 1000 DEG. C
GAS FLOW RATE : 2 L/MIN
NUMBER OF SAMPLES TAKEN: 321
SAMPLING INTERVAL : 60 SECONDS

WEIGHT LOSS

0.000	-0.003	-0.038	-0.085	-0.134	-0.182	-0.230	-0.275	-0.316	-0.356
-0.393	-0.424	-0.455	-0.483	-0.509	-0.534	-0.558	-0.580	-0.600	-0.620
-0.640	-0.660	-0.680	-0.701	-0.720	-0.741	-0.761	-0.782	-0.802	-0.822
-0.843	-0.866	-0.883	-0.903	-0.924	-0.945	-0.967	-0.988	-1.008	-1.013
-1.019	-1.027	-1.033	-1.040	-1.045	-1.054	-1.062	-1.071	-1.075	-1.081
-1.089	-1.096	-1.104	-1.111	-1.119	-1.124	-1.131	-1.140	-1.145	-1.153
-1.159	-1.166	-1.175	-1.181	-1.188	-1.194	-1.202	-1.207	-1.215	-1.220
-1.227	-1.233	-1.240	-1.246	-1.252	-1.260	-1.265	-1.275	-1.279	-1.286
-1.292	-1.298	-1.306	-1.311	-1.318	-1.324	-1.331	-1.338	-1.344	-1.351
-1.359	-1.366	-1.372	-1.378	-1.384	-1.392	-1.397	-1.406	-1.410	-1.418
-1.424	-1.429	-1.435	-1.442	-1.449	-1.455	-1.462	-1.469	-1.476	-1.481
-1.487	-1.492	-1.499	-1.507	-1.511	-1.517	-1.523	-1.530	-1.536	-1.541
-1.547	-1.553	-1.559	-1.565	-1.572	-1.577	-1.582	-1.586	-1.595	-1.599
-1.604	-1.609	-1.617	-1.620	-1.625	-1.630	-1.635	-1.641	-1.645	-1.650
-1.654	-1.660	-1.664	-1.669	-1.673	-1.678	-1.683	-1.686	-1.689	-1.693
-1.698	-1.701	-1.706	-1.709	-1.712	-1.716	-1.719	-1.723	-1.726	-1.729
-1.733	-1.737	-1.740	-1.743	-1.746	-1.751	-1.754	-1.757	-1.761	-1.765
-1.769	-1.774	-1.776	-1.779	-1.783	-1.785	-1.788	-1.791	-1.795	-1.797
-1.801	-1.804	-1.807	-1.810	-1.813	-1.817	-1.819	-1.823	-1.825	-1.828
-1.831	-1.835	-1.837	-1.839	-1.842	-1.845	-1.847	-1.849	-1.851	-1.854
-1.857	-1.859	-1.862	-1.864	-1.866	-1.868	-1.871	-1.873	-1.875	-1.876
-1.878	-1.880	-1.882	-1.884	-1.885	-1.888	-1.891	-1.892	-1.895	-1.896
-1.898	-1.899	-1.900	-1.902	-1.905	-1.906	-1.908	-1.908	-1.911	-1.913
-1.913	-1.914	-1.917	-1.918	-1.920	-1.921	-1.924	-1.926	-1.926	-1.928
-1.929	-1.931	-1.931	-1.933	-1.934	-1.936	-1.936	-1.938	-1.940	-1.941
-1.941	-1.943	-1.943	-1.945	-1.947	-1.947	-1.947	-1.947	-1.948	-1.949
-1.950	-1.950	-1.951	-1.954	-1.954	-1.955	-1.957	-1.957	-1.959	-1.960
-1.961	-1.961	-1.961	-1.963	-1.965	-1.964	-1.967	-1.967	-1.966	-1.970
-1.970	-1.969	-1.969	-1.970	-1.972	-1.972	-1.973	-1.974	-1.976	-1.975
-1.976	-1.977	-1.978	-1.978	-1.978	-1.980	-1.980	-1.981	-1.981	-1.983
-1.983	-1.984	-1.985	-1.984	-1.986	-1.987	-1.987	-1.989	-1.990	-1.990
-1.991	-1.991	-1.991	-1.993	-1.993	-1.993	-1.993	-1.995	-1.995	-1.995

PERCENTAGE REDUCTION

0.00	0.14	1.82	4.07	6.42	8.72	11.03	13.18	15.15	17.07
18.84	20.33	21.81	23.15	24.40	25.60	26.75	27.80	28.76	29.72
30.68	31.64	32.60	33.60	34.52	35.52	36.48	37.49	38.45	39.41
40.41	41.51	42.33	43.29	44.30	45.30	46.36	47.36	48.32	48.56
48.85	49.23	49.52	49.86	50.10	50.53	50.91	51.34	51.53	51.82
52.21	52.54	52.92	53.26	53.64	53.88	54.22	54.65	54.89	55.27
55.56	55.90	56.33	56.62	56.95	57.24	57.62	57.86	58.25	58.49
58.82	59.11	59.44	59.73	60.02	60.40	60.64	61.12	61.31	61.65
61.94	62.22	62.61	62.85	63.18	63.47	63.81	64.14	64.43	64.77
65.15	65.48	65.77	66.06	66.35	66.73	66.97	67.40	67.59	67.98
68.26	68.50	68.79	69.13	69.46	69.75	70.09	70.42	70.76	71.00
71.28	71.52	71.86	72.24	72.44	72.72	73.01	73.35	73.63	73.87
74.16	74.45	74.74	75.02	75.36	75.60	75.84	76.03	76.46	76.65
76.89	77.13	77.52	77.66	77.90	78.14	78.38	78.67	78.86	79.10
79.29	79.58	79.77	80.01	80.20	80.44	80.68	80.82	80.97	81.16
81.40	81.54	81.78	81.93	82.07	82.26	82.41	82.60	82.74	82.89
83.08	83.27	83.41	83.56	83.70	83.94	84.08	84.23	84.42	84.61
84.80	85.04	85.14	85.28	85.47	85.57	85.71	85.86	86.05	86.15
86.34	86.48	86.63	86.77	86.91	87.10	87.20	87.39	87.49	87.63
87.78	87.97	88.06	88.16	88.30	88.45	88.54	88.64	88.73	88.88
89.02	89.12	89.26	89.36	89.45	89.55	89.69	89.79	89.88	89.93
90.03	90.12	90.22	90.32	90.36	90.51	90.65	90.70	90.84	90.89
90.99	91.04	91.08	91.18	91.32	91.37	91.47	91.47	91.61	91.71
91.71	91.75	91.90	91.95	92.04	92.09	92.23	92.33	92.33	92.43
92.47	92.57	92.57	92.67	92.71	92.81	92.81	92.91	93.00	93.05
93.05	93.14	93.14	93.24	93.34	93.34	93.34	93.34	93.38	93.43

(Continued on next page)

93.48	93.48	93.53	93.67	93.67	93.72	93.82	93.82	93.91	93.96
94.01	94.01	94.01	94.10	94.20	94.15	94.30	94.30	94.25	94.44
94.44	94.39	94.39	94.44	94.53	94.53	94.58	94.63	94.73	94.68
94.73	94.77	94.82	94.82	94.82	94.92	94.92	94.97	94.97	95.06
95.06	95.11	95.16	95.11	95.21	95.25	95.25	95.35	95.40	95.40
95.45	95.45	95.45	95.54	95.54	95.54	95.54	95.64	95.64	95.64

BBC CHYO BALANCE DATA REPORT
DATA FILE No. : :1.D.PRAM1
REMOVABLE OXYGEN WEIGHT: 1.4 GRAM
FURNACE TEMPERATURE : 900 DEG. C
GAS FLOW RATE : 2 L/MIN
NUMBER OF SAMPLES TAKEN: 283
SAMPLING INTERVAL : 60 SECONDS

WEIGHT LOSS

-0.001	-0.011	-0.043	-0.078	-0.112	-0.137	-0.161	-0.183	-0.206	-0.221
-0.235	-0.257	-0.281	-0.277	-0.293	-0.308	-0.321	-0.332	-0.346	-0.351
-0.365	-0.373	-0.385	-0.397	-0.404	-0.410	-0.417	-0.420	-0.438	-0.439
-0.448	-0.453	-0.459	-0.467	-0.485	-0.484	-0.485	-0.494	-0.499	-0.505
-0.510	-0.512	-0.518	-0.523	-0.528	-0.536	-0.541	-0.550	-0.551	-0.555
-0.557	-0.565	-0.569	-0.573	-0.581	-0.584	-0.590	-0.598	-0.599	-0.603
-0.608	-0.615	-0.620	-0.624	-0.628	-0.635	-0.632	-0.644	-0.643	-0.650
-0.656	-0.661	-0.664	-0.667	-0.671	-0.675	-0.682	-0.685	-0.693	-0.696
-0.701	-0.706	-0.709	-0.716	-0.721	-0.724	-0.733	-0.733	-0.740	-0.745
-0.751	-0.759	-0.761	-0.769	-0.775	-0.783	-0.785	-0.790	-0.795	-0.802
-0.807	-0.815	-0.818	-0.828	-0.831	-0.837	-0.844	-0.848	-0.855	-0.864
-0.866	-0.873	-0.878	-0.883	-0.890	-0.895	-0.900	-0.906	-0.913	-0.918
-0.926	-0.928	-0.931	-0.934	-0.946	-0.949	-0.949	-0.956	-0.960	-0.966
-0.971	-0.975	-0.981	-0.986	-0.992	-0.997	-1.002	-1.006	-1.009	-1.012
-1.024	-1.023	-1.028	-1.034	-1.037	-1.040	-1.044	-1.048	-1.054	-1.057
-1.062	-1.066	-1.068	-1.072	-1.075	-1.081	-1.083	-1.086	-1.089	-1.094
-1.095	-1.099	-1.100	-1.103	-1.105	-1.116	-1.113	-1.115	-1.120	-1.120
-1.125	-1.126	-1.129	-1.133	-1.136	-1.138	-1.142	-1.143	-1.145	-1.150
-1.148	-1.150	-1.153	-1.156	-1.161	-1.162	-1.163	-1.165	-1.167	-1.169
-1.175	-1.175	-1.174	-1.181	-1.183	-1.182	-1.184	-1.191	-1.186	-1.190
-1.191	-1.191	-1.193	-1.195	-1.194	-1.195	-1.196	-1.198	-1.202	-1.204
-1.206	-1.206	-1.209	-1.208	-1.212	-1.213	-1.212	-1.213	-1.213	-1.214
-1.214	-1.218	-1.218	-1.220	-1.221	-1.223	-1.222	-1.224	-1.225	-1.226
-1.225	-1.229	-1.229	-1.230	-1.229	-1.234	-1.231	-1.237	-1.234	-1.236
-1.236	-1.236	-1.240	-1.237	-1.239	-1.240	-1.243	-1.240	-1.242	-1.245
-1.246	-1.246	-1.246	-1.248	-1.250	-1.250	-1.251	-1.253	-1.253	-1.255
-1.255	-1.253	-1.255	-1.255	-1.255	-1.257	-1.258	-1.259	-1.260	-1.260
-1.261	-1.263	-1.261	-1.264	-1.264	-1.264	-1.266	-1.267	-1.269	-1.268
-1.269	-1.269	-1.270							

PERCENTAGE REDUCTION

0.00	0.79	3.07	5.57	8.00	9.79	11.50	13.07	14.71	15.79
16.79	18.36	20.07	19.79	20.93	22.00	22.93	23.71	24.71	25.07
26.07	26.64	27.50	28.36	28.86	29.29	29.79	30.00	31.29	31.36
32.00	32.36	32.79	33.36	34.64	34.57	34.64	35.29	35.64	36.07
36.43	36.57	37.00	37.36	37.71	38.29	38.64	39.29	39.36	39.64
39.79	40.36	40.64	40.93	41.50	41.71	42.14	42.71	42.79	43.07
43.43	43.93	44.29	44.57	44.86	45.36	45.14	46.00	45.93	46.43
46.86	47.21	47.43	47.64	47.93	48.21	48.71	48.93	49.50	49.71
50.07	50.43	50.64	51.14	51.50	51.71	52.36	52.36	52.86	53.21
53.64	54.21	54.36	54.93	55.36	55.93	56.07	56.43	56.79	57.29
57.64	58.21	58.43	59.14	59.36	59.79	60.29	60.57	61.07	61.71
61.86	62.36	62.71	63.07	63.57	63.93	64.29	64.71	65.21	65.57
66.14	66.29	66.50	66.71	67.57	67.79	67.79	68.29	68.57	69.00
69.36	69.64	70.07	70.43	70.86	71.21	71.57	71.86	72.07	72.29
73.14	73.07	73.43	73.86	74.07	74.29	74.57	74.86	75.29	75.50
75.86	76.14	76.29	76.57	76.79	77.21	77.36	77.57	77.79	78.14
78.21	78.50	78.57	78.79	78.93	79.71	79.50	79.64	80.00	80.00
80.36	80.43	80.64	80.93	81.14	81.29	81.57	81.64	81.79	82.14
82.00	82.14	82.36	82.57	82.93	83.00	83.07	83.21	83.36	83.50
83.93	83.93	83.86	84.36	84.50	84.43	84.57	85.07	84.71	85.00
85.07	85.07	85.21	85.36	85.29	85.36	85.43	85.57	85.86	86.00
86.14	86.14	86.36	86.29	86.57	86.64	86.57	86.64	86.64	86.71
86.71	87.00	87.00	87.14	87.21	87.36	87.29	87.43	87.50	87.57
87.50	87.79	87.79	87.86	87.79	88.14	87.93	88.36	88.14	88.29
88.29	88.29	88.57	88.36	88.50	88.57	88.79	88.57	88.71	88.93
89.00	89.00	89.00	89.14	89.29	89.29	89.36	89.50	89.50	89.64
89.64	89.50	89.64	89.64	89.64	89.79	89.86	89.93	90.00	90.00
90.07	90.21	90.07	90.29	90.29	90.29	90.43	90.50	90.64	90.57
90.64	90.64								

BBC CHYO BALANCE DATA REPORT
DATA FILE No. : :1.D.PRAM2
REMOVABLE OXYGEN WEIGHT: 1.4 GRAM
FURNACE TEMPERATURE : 1000 DEG. C
GAS FLOW RATE : 2 L/MIN
NUMBER OF SAMPLES TAKEN: 240
SAMPLING INTERVAL : 60 SECONDS

WEIGHT LOSS

0.006	-0.003	-0.048	-0.099	-0.133	-0.164	-0.197	-0.221	-0.234	-0.260
-0.277	-0.294	-0.306	-0.322	-0.336	-0.348	-0.356	-0.370	-0.380	-0.390
-0.399	-0.410	-0.418	-0.424	-0.433	-0.444	-0.449	-0.456	-0.462	-0.469
-0.473	-0.483	-0.489	-0.496	-0.504	-0.511	-0.518	-0.523	-0.534	-0.543
-0.550	-0.558	-0.564	-0.573	-0.581	-0.587	-0.592	-0.600	-0.608	-0.618
-0.622	-0.625	-0.638	-0.644	-0.655	-0.662	-0.670	-0.679	-0.685	-0.689
-0.700	-0.709	-0.718	-0.727	-0.737	-0.744	-0.755	-0.759	-0.771	-0.779
-0.787	-0.794	-0.801	-0.810	-0.823	-0.828	-0.837	-0.844	-0.853	-0.863
-0.868	-0.878	-0.882	-0.892	-0.901	-0.910	-0.917	-0.925	-0.934	-0.939
-0.942	-0.951	-0.959	-0.965	-0.975	-0.981	-0.986	-0.995	-0.997	-1.003
-1.011	-1.019	-1.026	-1.029	-1.034	-1.041	-1.045	-1.051	-1.058	-1.063
-1.069	-1.073	-1.078	-1.079	-1.089	-1.090	-1.092	-1.099	-1.107	-1.108
-1.118	-1.120	-1.124	-1.125	-1.130	-1.133	-1.138	-1.141	-1.151	-1.153
-1.162	-1.162	-1.167	-1.172	-1.173	-1.177	-1.187	-1.182	-1.188	-1.188
-1.193	-1.195	-1.196	-1.205	-1.207	-1.210	-1.213	-1.216	-1.219	-1.224
-1.227	-1.226	-1.225	-1.232	-1.232	-1.240	-1.240	-1.239	-1.245	-1.247
-1.248	-1.253	-1.254	-1.255	-1.254	-1.257	-1.258	-1.259	-1.260	-1.266
-1.269	-1.271	-1.274	-1.275	-1.276	-1.277	-1.282	-1.283	-1.281	-1.277
-1.285	-1.282	-1.283	-1.284	-1.291	-1.293	-1.288	-1.291	-1.295	-1.296
-1.301	-1.296	-1.296	-1.302	-1.301	-1.302	-1.303	-1.303	-1.302	-1.308
-1.310	-1.307	-1.310	-1.312	-1.309	-1.308	-1.310	-1.311	-1.313	-1.316
-1.317	-1.318	-1.319	-1.318	-1.317	-1.319	-1.319	-1.318	-1.323	-1.318
-1.320	-1.323	-1.324	-1.322	-1.323	-1.324	-1.323	-1.328	-1.326	-1.325
-1.328	-1.326	-1.328	-1.329	-1.332	-1.336	-1.334	-1.338	-1.337	-1.336

PERCENTAGE REDUCTION

0.00	0.21	3.43	7.07	9.50	11.71	14.07	15.79	16.71	18.57
19.79	21.00	21.86	23.00	24.00	24.86	25.43	26.43	27.14	27.86
28.50	29.29	29.86	30.29	30.93	31.71	32.07	32.57	33.00	33.50
33.79	34.50	34.93	35.43	36.00	36.50	37.00	37.36	38.14	38.79
39.29	39.86	40.29	40.93	41.50	41.93	42.29	42.86	43.43	44.14
44.43	44.64	45.57	46.00	46.79	47.29	47.86	48.50	48.93	49.21
50.00	50.64	51.29	51.93	52.64	53.14	53.93	54.21	55.07	55.64
56.21	56.71	57.21	57.86	58.79	59.14	59.79	60.29	60.93	61.64
62.00	62.71	63.00	63.71	64.36	65.00	65.50	66.07	66.71	67.07
67.29	67.93	68.50	68.93	69.64	70.07	70.43	71.07	71.21	71.64
72.21	72.79	73.29	73.50	73.86	74.36	74.64	75.07	75.57	75.93
76.36	76.64	77.00	77.07	77.79	77.86	78.00	78.50	79.07	79.14
79.86	80.00	80.29	80.36	80.71	80.93	81.29	81.50	82.21	82.36
83.00	83.00	83.36	83.71	83.79	84.07	84.79	84.43	84.86	84.86
85.21	85.36	85.43	86.07	86.21	86.43	86.64	86.86	87.07	87.43
87.64	87.57	87.50	88.00	88.00	88.57	88.57	88.50	88.93	89.07
89.14	89.50	89.57	89.64	89.57	89.79	89.86	89.93	90.00	90.43
90.64	90.79	91.00	91.07	91.14	91.21	91.57	91.64	91.50	91.21
91.79	91.57	91.64	91.71	92.21	92.36	92.00	92.21	92.50	92.57
92.93	92.57	92.57	93.00	92.93	93.00	93.07	93.07	93.00	93.43
93.57	93.36	93.57	93.71	93.50	93.43	93.57	93.64	93.79	94.00
94.07	94.14	94.21	94.14	94.07	94.21	94.21	94.14	94.50	94.14
94.29	94.50	94.57	94.43	94.50	94.57	94.50	94.86	94.71	94.64
94.86	94.71	94.86	94.93	95.14	95.43	95.29	95.57	95.50	

BBC CHYO BALANCE DATA REPORT
DATA FILE No. : :1.D.PRAM3
REMOVABLE OXYGEN WEIGHT: 1.4 GRAM
FURNACE TEMPERATURE : 1100 DEG. C
GAS FLOW RATE : 2 L/MIN
NUMBER OF SAMPLES TAKEN: 261
SAMPLING INTERVAL : 60 SECONDS

WEIGHT LOSS

-0.001	-0.027	-0.081	-0.129	-0.170	-0.207	-0.239	-0.262	-0.287	-0.307
-0.326	-0.345	-0.358	-0.371	-0.383	-0.394	-0.405	-0.412	-0.424	-0.435
-0.442	-0.451	-0.459	-0.470	-0.478	-0.487	-0.495	-0.504	-0.514	-0.521
-0.531	-0.538	-0.547	-0.556	-0.566	-0.575	-0.584	-0.593	-0.603	-0.611
-0.622	-0.629	-0.637	-0.648	-0.657	-0.662	-0.672	-0.680	-0.690	-0.700
-0.706	-0.718	-0.725	-0.730	-0.740	-0.747	-0.758	-0.764	-0.772	-0.779
-0.786	-0.791	-0.799	-0.803	-0.816	-0.825	-0.827	-0.835	-0.843	-0.848
-0.853	-0.863	-0.870	-0.877	-0.883	-0.888	-0.895	-0.899	-0.905	-0.912
-0.919	-0.925	-0.931	-0.938	-0.940	-0.950	-0.954	-0.960	-0.965	-0.972
-0.976	-0.982	-0.987	-0.992	-0.999	-1.002	-1.007	-1.011	-1.019	-1.018
-1.024	-1.029	-1.033	-1.038	-1.043	-1.046	-1.052	-1.057	-1.058	-1.064
-1.068	-1.077	-1.078	-1.084	-1.088	-1.089	-1.094	-1.103	-1.105	-1.106
-1.110	-1.117	-1.117	-1.122	-1.128	-1.130	-1.135	-1.138	-1.138	-1.147
-1.149	-1.153	-1.155	-1.160	-1.164	-1.166	-1.167	-1.174	-1.174	-1.177
-1.182	-1.184	-1.188	-1.189	-1.198	-1.198	-1.198	-1.203	-1.203	-1.207
-1.209	-1.211	-1.217	-1.218	-1.222	-1.223	-1.224	-1.231	-1.232	-1.234
-1.238	-1.243	-1.241	-1.246	-1.245	-1.248	-1.251	-1.252	-1.255	-1.262
-1.262	-1.264	-1.262	-1.265	-1.270	-1.270	-1.270	-1.274	-1.276	-1.278
-1.277	-1.280	-1.283	-1.282	-1.283	-1.287	-1.293	-1.293	-1.295	-1.291
-1.298	-1.300	-1.302	-1.304	-1.301	-1.304	-1.308	-1.307	-1.309	-1.308
-1.311	-1.314	-1.317	-1.315	-1.318	-1.319	-1.318	-1.318	-1.322	-1.320
-1.322	-1.322	-1.323	-1.324	-1.328	-1.326	-1.329	-1.326	-1.333	-1.331
-1.332	-1.334	-1.333	-1.334	-1.336	-1.338	-1.336	-1.340	-1.339	-1.341
-1.342	-1.340	-1.343	-1.344	-1.345	-1.343	-1.347	-1.349	-1.347	-1.347
-1.351	-1.350	-1.354	-1.352	-1.352	-1.354	-1.355	-1.356	-1.355	-1.351
-1.357	-1.358	-1.360	-1.358	-1.357	-1.359	-1.359	-1.363	-1.360	-1.361

PERCENTAGE REDUCTION

0.00	1.93	5.79	9.21	12.14	14.79	17.07	18.71	20.50	21.93
23.29	24.64	25.57	26.50	27.36	28.14	28.93	29.43	30.29	31.07
31.57	32.21	32.79	33.57	34.14	34.79	35.36	36.00	36.71	37.21
37.93	38.43	39.07	39.71	40.43	41.07	41.71	42.36	43.07	43.64
44.43	44.93	45.50	46.29	46.93	47.29	48.00	48.57	49.29	50.00
50.43	51.29	51.79	52.14	52.86	53.36	54.14	54.57	55.14	55.64
56.14	56.50	57.07	57.36	58.29	58.93	59.07	59.64	60.21	60.57
60.93	61.64	62.14	62.64	63.07	63.43	63.93	64.21	64.64	65.14
65.64	66.07	66.50	67.00	67.14	67.86	68.14	68.57	68.93	69.43
69.71	70.14	70.50	70.86	71.36	71.57	71.93	72.21	72.79	72.71
73.14	73.50	73.79	74.14	74.50	74.71	75.14	75.50	75.57	76.00
76.29	76.93	77.00	77.43	77.71	77.79	78.14	78.79	78.93	79.00
79.29	79.79	79.79	80.14	80.57	80.71	81.07	81.29	81.29	81.93
82.07	82.36	82.50	82.86	83.14	83.29	83.36	83.86	83.86	84.07
84.43	84.57	84.86	84.93	85.57	85.57	85.57	85.93	85.93	86.21
86.36	86.50	86.93	87.00	87.29	87.36	87.43	87.93	88.00	88.14
88.43	88.79	88.64	89.00	88.93	89.14	89.36	89.43	89.64	90.14
90.14	90.29	90.14	90.36	90.71	90.71	90.71	91.00	91.14	91.29
91.21	91.43	91.64	91.57	91.64	91.93	92.36	92.36	92.50	92.21
92.71	92.86	93.00	93.14	92.93	93.14	93.43	93.36	93.50	93.43
93.64	93.86	94.07	93.93	94.14	94.21	94.14	94.14	94.43	94.29
94.43	94.43	94.50	94.57	94.86	94.71	94.93	94.71	95.21	95.07
95.14	95.29	95.21	95.29	95.43	95.57	95.43	95.71	95.64	95.79
95.86	95.71	95.93	96.00	96.07	95.93	96.21	96.36	96.21	96.21
96.50	96.43	96.71	96.57	96.57	96.71	96.79	96.86	96.79	96.50
96.93	97.00	97.14	97.00	96.93	97.07	97.07	97.36	97.14	97.21

BBC CHYO BALANCE DATA REPORT
DATA FILE No. : :1.D.PRAM4
REMOVABLE OXYGEN WEIGHT: 1.4 GRAM
FURNACE TEMPERATURE : 1200 DEG. C
GAS FLOW RATE : 2 L/MIN
NUMBER OF SAMPLES TAKEN: 269
SAMPLING INTERVAL : 60 SECONDS

WEIGHT LOSS

0.002	-0.034	-0.104	-0.166	-0.215	-0.251	-0.283	-0.314	-0.336	-0.359
-0.374	-0.383	-0.390	-0.402	-0.414	-0.425	-0.431	-0.435	-0.444	-0.457
-0.456	-0.465	-0.478	-0.493	-0.499	-0.495	-0.500	-0.506	-0.511	-0.520
-0.518	-0.525	-0.530	-0.541	-0.547	-0.554	-0.562	-0.558	-0.571	-0.582
-0.581	-0.590	-0.593	-0.605	-0.591	-0.613	-0.618	-0.624	-0.627	-0.636
-0.640	-0.649	-0.652	-0.657	-0.663	-0.657	-0.672	-0.672	-0.688	-0.692
-0.685	-0.698	-0.695	-0.715	-0.719	-0.723	-0.726	-0.733	-0.740	-0.738
-0.747	-0.757	-0.759	-0.768	-0.765	-0.776	-0.782	-0.765	-0.791	-0.794
-0.797	-0.797	-0.801	-0.814	-0.817	-0.826	-0.822	-0.829	-0.838	-0.843
-0.847	-0.851	-0.856	-0.852	-0.859	-0.850	-0.847	-0.866	-0.880	-0.881
-0.885	-0.884	-0.897	-0.904	-0.904	-0.912	-0.914	-0.921	-0.914	-0.918
-0.928	-0.937	-0.943	-0.943	-0.945	-0.953	-0.957	-0.956	-0.970	-0.949
-0.967	-0.963	-0.981	-0.989	-0.984	-0.983	-0.991	-0.999	-1.001	-1.002
-1.010	-1.019	-1.020	-1.019	-1.027	-1.029	-1.033	-1.039	-1.040	-1.041
-1.041	-1.052	-1.055	-1.051	-1.055	-1.058	-1.066	-1.065	-1.077	-1.076
-1.084	-1.085	-1.087	-1.089	-1.092	-1.098	-1.094	-1.104	-1.112	-1.115
-1.115	-1.114	-1.110	-1.127	-1.126	-1.125	-1.134	-1.128	-1.137	-1.129
-1.140	-1.149	-1.145	-1.148	-1.156	-1.158	-1.160	-1.170	-1.165	-1.165
-1.174	-1.168	-1.172	-1.183	-1.170	-1.173	-1.182	-1.195	-1.195	-1.192
-1.197	-1.198	-1.196	-1.209	-1.208	-1.211	-1.214	-1.205	-1.220	-1.211
-1.208	-1.224	-1.221	-1.224	-1.231	-1.229	-1.231	-1.222	-1.236	-1.239
-1.239	-1.243	-1.245	-1.232	-1.249	-1.244	-1.243	-1.249	-1.245	-1.251
-1.253	-1.256	-1.252	-1.259	-1.250	-1.263	-1.263	-1.249	-1.267	-1.264
-1.257	-1.267	-1.260	-1.265	-1.270	-1.277	-1.277	-1.277	-1.271	-1.278
-1.323	-1.279	-1.283	-1.286	-1.277	-1.289	-1.284	-1.281	-1.282	-1.283
-1.285	-1.290	-1.292	-1.285	-1.284	-1.284	-1.285	-1.285	-1.288	-1.288
-1.287	-1.287	-1.287	-1.297	-1.297	-1.295	-1.292	-1.291	-1.294	

PERCENTAGE REDUCTION

0.00	2.43	7.43	11.86	15.36	17.93	20.21	22.43	24.00	25.64
26.71	27.36	27.86	28.71	29.57	30.36	30.79	31.07	31.71	32.64
32.57	33.21	34.14	35.21	35.64	35.36	35.71	36.14	36.50	37.14
37.00	37.50	37.86	38.64	39.07	39.57	40.14	39.86	40.79	41.57
41.50	42.14	42.36	43.21	42.21	43.79	44.14	44.57	44.79	45.43
45.71	46.36	46.57	46.93	47.36	46.93	48.00	48.00	49.14	49.43
48.93	49.86	49.64	51.07	51.36	51.64	51.86	52.36	52.86	52.71
53.36	54.07	54.21	54.86	54.64	55.43	55.86	54.64	56.50	56.71
56.93	56.93	57.21	58.14	58.36	59.00	58.71	59.21	59.86	60.21
60.50	60.79	61.14	60.86	61.36	60.71	60.50	61.86	62.86	62.93
63.21	63.14	64.07	64.57	64.57	65.14	65.29	65.79	65.29	65.57
66.29	66.93	67.36	67.36	67.50	68.07	68.36	68.29	69.29	67.79
69.07	68.79	70.07	70.64	70.29	70.21	70.79	71.36	71.50	71.57
72.14	72.79	72.86	72.79	73.36	73.50	73.79	74.21	74.29	74.36
74.36	75.14	75.36	75.07	75.36	75.57	76.14	76.07	76.93	76.86
77.43	77.50	77.64	77.79	78.00	78.43	78.14	78.86	79.43	79.64
79.64	79.57	79.29	80.50	80.43	80.36	81.00	80.57	81.21	80.64
81.43	82.07	81.79	82.00	82.57	82.71	82.86	83.57	83.21	83.21
83.86	83.43	83.71	84.50	83.57	83.79	84.43	85.36	85.36	85.14
85.50	85.57	85.43	86.36	86.29	86.50	86.71	86.07	87.14	86.50
86.29	87.43	87.21	87.43	87.93	87.79	87.93	87.29	88.29	88.50
88.50	88.79	88.93	88.00	89.21	88.86	88.79	89.21	88.93	89.36
89.50	89.71	89.43	89.93	89.29	90.21	90.21	89.21	90.50	90.29
89.79	90.50	90.00	90.36	90.71	91.21	91.21	91.21	90.79	91.29
94.50	91.36	91.64	91.86	91.21	92.07	91.71	91.50	91.57	91.64
91.79	92.14	92.29	91.79	91.71	91.71	91.79	91.79	92.00	92.00
91.93	91.93	91.93	92.64	92.64	92.50	92.29	92.21		

BBC CHYO BALANCE DATA REPORT
DATA FILE No. : :3.E.PRAM1
REMOVABLE OXYGEN WEIGHT: 1.438 GRAM
FURNACE TEMPERATURE : 1000 DEG. C
GAS FLOW RATE : 1 L/MIN
NUMBER OF SAMPLES TAKEN: 19
SAMPLING INTERVAL : 60 SECONDS

WEIGHT LOSS

0.000	-0.001	-0.005	-0.009	-0.012	-0.019	-0.045	-0.072	-0.099	-0.124
-0.147	-0.169	-0.189	-0.208	-0.226	-0.243	-0.260	-0.275	-0.290	

PERCENTAGE REDUCTION

0.00	0.07	0.35	0.63	0.83	1.32	3.13	5.01	6.88	8.62
10.22	11.75	13.14	14.46	15.72	16.90	18.08	19.12		

BBC CHYO BALANCE DATA REPORT
DATA FILE No. : :3.E.PRAM2
REMOVABLE OXYGEN WEIGHT: 1.563 GRAM
FURNACE TEMPERATURE : 1000 DEG. C
GAS FLOW RATE : 1 L/MIN
NUMBER OF SAMPLES TAKEN: 56
SAMPLING INTERVAL : 60 SECONDS

WEIGHT LOSS

0.000	-0.002	-0.005	-0.013	-0.035	-0.056	-0.074	-0.092	-0.112	-0.135
-0.148	-0.163	-0.185	-0.203	-0.224	-0.243	-0.258	-0.271	-0.289	-0.301
-0.314	-0.324	-0.336	-0.346	-0.356	-0.363	-0.372	-0.381	-0.389	-0.395
-0.401	-0.407	-0.411	-0.415	-0.422	-0.426	-0.432	-0.433	-0.435	-0.438
-0.442	-0.444	-0.449	-0.450	-0.453	-0.455	-0.460	-0.457	-0.459	-0.461
-0.459	-0.462	-0.466	-0.466	-0.467	-0.470				

PERCENTAGE REDUCTION

0.00	0.13	0.32	0.83	2.24	3.58	4.73	5.89	7.17	8.64
9.47	10.43	11.84	12.99	14.33	15.55	16.51	17.34	18.49	19.26
20.09	20.73	21.50	22.14	22.78	23.22	23.80	24.38	24.89	25.27
25.66	26.04	26.30	26.55	27.00	27.26	27.64	27.70	27.83	28.02
28.28	28.41	28.73	28.79	28.98	29.11	29.43	29.24	29.37	29.49
29.37	29.56	29.81	29.81	29.88					

BBC CHYO BALANCE DATA REPORT
DATA FILE No. : :3.E.PRAM3
REMOVABLE OXYGEN WEIGHT: 1.4 GRAM
FURNACE TEMPERATURE : 1000 DEG. C
GAS FLOW RATE : 1 L/MIN
NUMBER OF SAMPLES TAKEN: 106
SAMPLING INTERVAL : 60 SECONDS

WEIGHT LOSS

0.002	0.006	-0.009	-0.038	-0.062	-0.088	-0.110	-0.132	-0.150	-0.168
-0.184	-0.199	-0.212	-0.226	-0.238	-0.249	-0.260	-0.270	-0.279	-0.288
-0.295	-0.301	-0.310	-0.316	-0.320	-0.328	-0.333	-0.338	-0.342	-0.349
-0.352	-0.357	-0.361	-0.366	-0.368	-0.373	-0.376	-0.380	-0.381	-0.384
-0.385	-0.387	-0.390	-0.390	-0.393	-0.394	-0.396	-0.396	-0.397	-0.398
-0.397	-0.401	-0.399	-0.401	-0.401	-0.401	-0.402	-0.402	-0.401	-0.401
-0.402	-0.401	-0.401	-0.402	-0.400	-0.399	-0.399	-0.400	-0.400	-0.401
-0.401	-0.400	-0.401	-0.401	-0.401	-0.399	-0.401	-0.402	-0.403	-0.402
-0.403	-0.403	-0.402	-0.402	-0.400	-0.400	-0.401	-0.399	-0.399	-0.399
-0.401	-0.401	-0.400	-0.402	-0.401	-0.404	-0.402	-0.404	-0.404	-0.403
-0.403	-0.403	-0.403	-0.404	-0.403	-0.403				

PERCENTAGE REDUCTION

0.00	-0.43	0.64	2.71	4.43	6.29	7.86	9.43	10.71	12.00
13.14	14.21	15.14	16.14	17.00	17.79	18.57	19.29	19.93	20.57
21.07	21.50	22.14	22.57	22.86	23.43	23.79	24.14	24.43	24.93
25.14	25.50	25.79	26.14	26.29	26.64	26.86	27.14	27.21	27.43
27.50	27.64	27.86	27.86	28.07	28.14	28.29	28.29	28.36	28.43
28.36	28.64	28.50	28.64	28.64	28.64	28.71	28.71	28.64	28.64
28.71	28.64	28.64	28.71	28.57	28.50	28.50	28.57	28.57	28.64
28.64	28.57	28.64	28.64	28.64	28.50	28.64	28.71	28.79	28.71
28.79	28.79	28.71	28.71	28.57	28.57	28.64	28.50	28.50	28.50
28.64	28.64	28.57	28.71	28.64	28.86	28.71	28.86	28.86	28.79
28.79	28.79	28.79	28.86	28.79					

BBC CHYO BALANCE DATA REPORT
DATA FILE No. : :3.E.PRAM4
REMOVABLE OXYGEN WEIGHT: 1.5 GRAM
FURNACE TEMPERATURE : 1000 DEG. C
GAS FLOW RATE : 1 L/MIN
NUMBER OF SAMPLES TAKEN: 15
SAMPLING INTERVAL : 60 SECONDS

WEIGHT LOSS

-0.001	0.007	-0.006	-0.032	-0.059	-0.092	-0.115	-0.134	-0.164	-0.191
-0.204	-0.229	-0.214	-0.204	-0.200					

PERCENTAGE REDUCTION

0.00	-0.47	0.40	2.13	3.93	6.13	7.67	8.93	10.93	12.73
13.60	15.27	14.27	13.60						

BBC CHYO BALANCE DATA REPORT
DATA FILE No. : :3.F.PRAM1
REMOVABLE OXYGEN WEIGHT: 1.2 GRAM
FURNACE TEMPERATURE : 1000 DEG. C
GAS FLOW RATE : 1.5 L/MIN
NUMBER OF SAMPLES TAKEN: 64
SAMPLING INTERVAL : 60 SECONDS

WEIGHT LOSS

0.005	0.007	0.003	-0.018	-0.053	-0.091	-0.121	-0.151	-0.174	-0.199
-0.217	-0.236	-0.256	-0.267	-0.283	-0.296	-0.306	-0.317	-0.328	-0.336
-0.347	-0.354	-0.363	-0.371	-0.380	-0.387	-0.394	-0.401	-0.409	-0.415
-0.420	-0.428	-0.435	-0.442	-0.448	-0.454	-0.460	-0.465	-0.471	-0.479
-0.486	-0.487	-0.496	-0.501	-0.505	-0.511	-0.518	-0.522	-0.530	-0.536
-0.542	-0.545	-0.550	-0.555	-0.561	-0.568	-0.570	-0.578	-0.583	-0.588
-0.594	-0.598	-0.602	-0.609						

PERCENTAGE REDUCTION

0.00	-0.58	-0.25	1.50	4.42	7.58	10.08	12.58	14.50	16.58
18.08	19.67	21.33	22.25	23.58	24.67	25.50	26.42	27.33	28.00
28.92	29.50	30.25	30.92	31.67	32.25	32.83	33.42	34.08	34.58
35.00	35.67	36.25	36.83	37.33	37.83	38.33	38.75	39.25	39.92
40.50	40.58	41.33	41.75	42.08	42.58	43.17	43.50	44.17	44.67
45.17	45.42	45.83	46.25	46.75	47.33	47.50	48.17	48.58	49.00
49.50	49.83	50.17							

BBC CHYO BALANCE DATA REPORT
DATA FILE No. : :3.F.PRAM2
REMOVABLE OXYGEN WEIGHT: 1.3 GRAM
FURNACE TEMPERATURE : 1000 DEG. C
GAS FLOW RATE : 2 L/MIN
NUMBER OF SAMPLES TAKEN: 42
SAMPLING INTERVAL : 60 SECONDS

WEIGHT LOSS

0.002	-0.003	-0.052	-0.096	-0.136	-0.172	-0.202	-0.231	-0.253	-0.276
-0.295	-0.313	-0.333	-0.348	-0.363	-0.380	-0.395	-0.405	-0.422	-0.432
-0.446	-0.454	-0.469	-0.483	-0.491	-0.499	-0.509	-0.522	-0.533	-0.542
-0.551	-0.563	-0.573	-0.584	-0.593	-0.600	-0.611	-0.618	-0.628	-0.639
-0.645	-0.655								

PERCENTAGE REDUCTION

0.00	0.23	4.00	7.38	10.46	13.23	15.54	17.77	19.46	21.23
22.69	24.08	25.62	26.77	27.92	29.23	30.38	31.15	32.46	33.23
34.31	34.92	36.08	37.15	37.77	38.38	39.15	40.15	41.00	41.69
42.38	43.31	44.08	44.92	45.62	46.15	47.00	47.54	48.31	49.15
49.62									

BBC CHYO BALANCE DATA REPORT
DATA FILE No. : :3.F.PRAM3
REMOVABLE OXYGEN WEIGHT: 0.8500000001 GRAM
FURNACE TEMPERATURE : 1000 DEG. C
GAS FLOW RATE : 2.5 L/MIN
NUMBER OF SAMPLES TAKEN: 111
SAMPLING INTERVAL : 60 SECONDS

WEIGHT LOSS

0.002	0.000	-0.020	-0.051	-0.082	-0.109	-0.133	-0.156	-0.176	-0.191
-0.207	-0.219	-0.235	-0.244	-0.257	-0.267	-0.276	-0.282	-0.296	-0.304
-0.312	-0.319	-0.328	-0.336	-0.342	-0.351	-0.360	-0.369	-0.377	-0.386
-0.393	-0.401	-0.409	-0.416	-0.423	-0.431	-0.439	-0.445	-0.455	-0.463
-0.471	-0.477	-0.489	-0.497	-0.505	-0.513	-0.528	-0.536	-0.542	-0.553
-0.560	-0.568	-0.577	-0.589	-0.598	-0.605	-0.614	-0.624	-0.632	-0.636
-0.646	-0.655	-0.662	-0.668	-0.675	-0.682	-0.688	-0.691	-0.701	-0.705
-0.705	-0.714	-0.723	-0.726	-0.732	-0.735	-0.742	-0.747	-0.752	-0.752
-0.758	-0.758	-0.759	-0.764	-0.765	-0.774	-0.779	-0.774	-0.781	-0.781
-0.782	-0.785	-0.790	-0.792	-0.790	-0.795	-0.795	-0.800	-0.798	-0.800
-0.806	-0.801	-0.804	-0.809	-0.811	-0.810	-0.814	-0.810	-0.814	-0.812

PERCENTAGE REDUCTION

0.00	0.00	2.35	6.00	9.65	12.82	15.65	18.35	20.71	22.47
24.35	25.76	27.65	28.71	30.24	31.41	32.47	33.18	34.82	35.76
36.71	37.53	38.59	39.53	40.24	41.29	42.35	43.41	44.35	45.41
46.24	47.18	48.12	48.94	49.76	50.71	51.65	52.35	53.53	54.47
55.41	56.12	57.53	58.47	59.41	60.35	62.12	63.06	63.76	65.06
65.88	66.82	67.88	69.29	70.35	71.18	72.24	73.41	74.35	74.82
76.00	77.06	77.88	78.59	79.41	80.24	80.94	81.29	82.47	82.94
82.94	84.00	85.06	85.41	86.12	86.47	87.29	87.88	88.47	88.47
89.18	89.18	89.29	89.88	90.00	91.06	91.65	91.06	91.88	91.88
92.00	92.35	92.94	93.18	92.94	93.53	93.53	94.12	93.88	94.12
94.82	94.24	94.59	95.18	95.41	95.29	95.76	95.29	95.76	95.53

BBC CHYO BALANCE DATA REPORT
DATA FILE No. : :3.F.PRAM4
REMOVABLE OXYGEN WEIGHT: 0.9299999999 GRAM
FURNACE TEMPERATURE : 1000 DEG. C
GAS FLOW RATE : 2 L/MIN
NUMBER OF SAMPLES TAKEN: 128
SAMPLING INTERVAL : 60 SECONDS

WEIGHT LOSS

-0.001	-0.007	-0.051	-0.087	-0.121	-0.150	-0.171	-0.188	-0.208	-0.224
-0.240	-0.252	-0.267	-0.280	-0.291	-0.299	-0.309	-0.321	-0.328	-0.339
-0.346	-0.357	-0.359	-0.368	-0.378	-0.381	-0.388	-0.399	-0.403	-0.411
-0.417	-0.427	-0.428	-0.440	-0.443	-0.452	-0.459	-0.464	-0.471	-0.479
-0.483	-0.490	-0.496	-0.502	-0.506	-0.513	-0.520	-0.525	-0.531	-0.539
-0.542	-0.547	-0.553	-0.560	-0.563	-0.572	-0.576	-0.582	-0.586	-0.595
-0.598	-0.601	-0.608	-0.598	-0.615	-0.626	-0.629	-0.638	-0.641	-0.648
-0.650	-0.652	-0.664	-0.671	-0.678	-0.680	-0.689	-0.696	-0.702	-0.709
-0.716	-0.723	-0.727	-0.737	-0.736	-0.749	-0.755	-0.760	-0.766	-0.770
-0.777	-0.785	-0.786	-0.788	-0.796	-0.800	-0.808	-0.809	-0.816	-0.821
-0.824	-0.828	-0.834	-0.837	-0.843	-0.844	-0.848	-0.852	-0.855	-0.859
-0.862	-0.866	-0.868	-0.871	-0.874	-0.878	-0.880	-0.883	-0.884	-0.886
-0.888	-0.890	-0.894	-0.897	-0.900	-0.894	-0.900	-0.902		

PERCENTAGE REDUCTION

0.00	0.75	5.48	9.35	13.01	16.13	18.39	20.22	22.37	24.09
25.81	27.10	28.71	30.11	31.29	32.15	33.23	34.52	35.27	36.45
37.20	38.39	38.60	39.57	40.65	40.97	41.72	42.90	43.33	44.19
44.84	45.91	46.02	47.31	47.63	48.60	49.35	49.89	50.65	51.51
51.94	52.69	53.33	53.98	54.41	55.16	55.91	56.45	57.10	57.96
58.28	58.82	59.46	60.22	60.54	61.51	61.94	62.58	63.01	63.98
64.30	64.62	65.38	64.30	66.13	67.31	67.63	68.60	68.92	69.68
69.89	70.11	71.40	72.15	72.90	73.12	74.09	74.84	75.48	76.24
76.99	77.74	78.17	79.25	79.14	80.54	81.18	81.72	82.37	82.80
83.55	84.41	84.52	84.73	85.59	86.02	86.88	86.99	87.74	88.28
88.60	89.03	89.68	90.00	90.65	90.75	91.18	91.61	91.94	92.37
92.69	93.12	93.33	93.66	93.98	94.41	94.62	94.95	95.05	95.27
95.48	95.70	96.13	96.45	96.77	96.13	96.77			

BBC CHYO BALANCE DATA REPORT
DATA FILE No. : :3.F.PRAM5
REMOVABLE OXYGEN WEIGHT: 0.9299999999 GRAM
FURNACE TEMPERATURE : 1000 DEG. C
GAS FLOW RATE : 1.5 L/MIN
NUMBER OF SAMPLES TAKEN: 121
SAMPLING INTERVAL : 60 SECONDS

WEIGHT LOSS

0.002	0.000	-0.023	-0.052	-0.080	-0.105	-0.128	-0.144	-0.162	-0.179
-0.192	-0.206	-0.212	-0.226	-0.237	-0.246	-0.250	-0.263	-0.267	-0.279
-0.282	-0.291	-0.295	-0.305	-0.310	-0.317	-0.320	-0.324	-0.327	-0.334
-0.341	-0.345	-0.349	-0.355	-0.361	-0.367	-0.370	-0.377	-0.382	-0.386
-0.391	-0.397	-0.401	-0.407	-0.414	-0.416	-0.422	-0.423	-0.428	-0.432
-0.437	-0.440	-0.444	-0.448	-0.450	-0.447	-0.459	-0.461	-0.466	-0.469
-0.476	-0.477	-0.483	-0.487	-0.494	-0.496	-0.500	-0.504	-0.507	-0.510
-0.517	-0.521	-0.525	-0.530	-0.531	-0.537	-0.539	-0.545	-0.550	-0.551
-0.556	-0.562	-0.567	-0.570	-0.574	-0.577	-0.584	-0.589	-0.592	-0.592
-0.598	-0.602	-0.605	-0.611	-0.614	-0.618	-0.625	-0.629	-0.631	-0.635
-0.637	-0.642	-0.644	-0.649	-0.655	-0.658	-0.662	-0.666	-0.670	-0.675
-0.679	-0.684	-0.688	-0.692	-0.698	-0.701	-0.704	-0.711	-0.714	-0.719

PERCENTAGE REDUCTION

0.00	0.00	2.47	5.59	8.60	11.29	13.76	15.48	17.42	19.25
20.65	22.15	22.80	24.30	25.48	26.45	26.88	28.28	28.71	30.00
30.32	31.29	31.72	32.80	33.33	34.09	34.41	34.84	35.16	35.91
36.67	37.10	37.53	38.17	38.82	39.46	39.78	40.54	41.08	41.51
42.04	42.69	43.12	43.76	44.52	44.73	45.38	45.48	46.02	46.45
46.99	47.31	47.74	48.17	48.39	48.06	49.35	49.57	50.11	50.43
51.18	51.29	51.94	52.37	53.12	53.33	53.76	54.19	54.52	54.84
55.59	56.02	56.45	56.99	57.10	57.74	57.96	58.60	59.14	59.25
59.78	60.43	60.97	61.29	61.72	62.04	62.80	63.33	63.66	63.66
64.30	64.73	65.05	65.70	66.02	66.45	67.20	67.63	67.85	68.28
68.49	69.03	69.25	69.78	70.43	70.75	71.18	71.61	72.04	72.58
73.01	73.55	73.98	74.41	75.05	75.38	75.70	76.45	76.77	77.31

BBC CHYO BALANCE DATA REPORT
DATA FILE No. : :3.F.PRAM6
REMOVABLE OXYGEN WEIGHT: 2 GRAM
FURNACE TEMPERATURE : 1000 DEG. C
GAS FLOW RATE : 3 L/MIN
NUMBER OF SAMPLES TAKEN: 119
SAMPLING INTERVAL : 60 SECONDS

WEIGHT LOSS

12.036	-0.010	-0.059	-0.126	-0.186	-0.245	-0.298	-0.345	-0.388	-0.422
-0.455	-0.487	-0.513	-0.535	-0.562	-0.588	-0.613	-0.655	-0.649	-0.681
-0.677	-0.720	-0.720	-0.757	-0.749	-0.793	-0.789	-0.823	-0.843	-0.857
-0.876	-0.872	-0.905	-0.909	-0.931	-0.933	-0.956	-0.972	-0.997	-1.005
-1.024	-1.033	-1.046	-1.055	-1.067	-1.070	-1.100	-1.130	-1.131	-1.137
-1.150	-1.167	-1.182	-1.194	-1.204	-1.221	-1.242	-1.251	-1.275	-1.291
-1.299	-1.325	-1.335	-1.328	-1.356	-1.375	-1.387	-1.403	-1.413	-1.431
-1.454	-1.468	-1.478	-1.499	-1.518	-1.535	-1.547	-1.557	-1.574	-1.595
-1.600	-1.624	-1.626	-1.656	-1.678	-1.674	-1.695	-1.706	-1.715	-1.724
-1.751	-1.759	-1.785	-1.784	-1.793	-1.805	-1.818	-1.818	-1.838	-1.853
-1.860	-1.872	-1.877	-1.886	-1.895	-1.906	-1.906	-1.929	-1.928	-1.930
-1.952	-1.948	-1.954	-1.956	-1.965	-1.978	-1.988	-1.990	-1.997	

PERCENTAGE REDUCTION

0.00	0.50	2.95	6.30	9.30	12.25	14.90	17.25	19.40	21.10
22.75	24.35	25.65	26.75	28.10	29.40	30.65	32.75	32.45	34.05
33.85	36.00	36.00	37.85	37.45	39.65	39.45	41.15	42.15	42.85
43.80	43.60	45.25	45.45	46.55	46.65	47.80	48.60	49.85	50.25
51.20	51.65	52.30	52.75	53.35	53.50	55.00	56.50	56.55	56.85
57.50	58.35	59.10	59.70	60.20	61.05	62.10	62.55	63.75	64.55
64.95	66.25	66.75	66.40	67.80	68.75	69.35	70.15	70.65	71.55
72.70	73.40	73.90	74.95	75.90	76.75	77.35	77.85	78.70	79.75
80.00	81.20	81.30	82.80	83.90	83.70	84.75	85.30	85.75	86.20
87.55	87.95	89.25	89.20	89.65	90.25	90.90	90.90	91.90	92.65
93.00	93.60	93.85	94.30	94.75	95.30	95.30	96.45	96.40	96.50
97.60	97.40	97.70	97.80	98.25	98.90	99.40	99.50		

BBC CHYO BALANCE DATA REPORT
DATA FILE No. : :3.F.PRAM7
REMOVABLE OXYGEN WEIGHT: 1.98 GRAM
FURNACE TEMPERATURE : 1000 DEG. C
GAS FLOW RATE : 2.5 L/MIN
NUMBER OF SAMPLES TAKEN: 123
SAMPLING INTERVAL : 60 SECONDS

WEIGHT LOSS

-0.004	-0.014	-0.076	-0.137	-0.192	-0.236	-0.268	-0.307	-0.337	-0.367
-0.388	-0.415	-0.453	-0.479	-0.495	-0.510	-0.527	-0.559	-0.567	-0.587
-0.602	-0.613	-0.635	-0.645	-0.652	-0.680	-0.684	-0.721	-0.731	-0.723
-0.742	-0.765	-0.775	-0.789	-0.815	-0.810	-0.841	-0.850	-0.857	-0.868
-0.872	-0.890	-0.904	-0.910	-0.924	-0.954	-0.950	-0.951	-0.969	-0.984
-0.995	-1.013	-1.021	-1.038	-1.038	-1.059	-1.080	-1.083	-1.097	-1.102
-1.115	-1.125	-1.135	-1.156	-1.163	-1.175	-1.202	-1.209	-1.215	-1.220
-1.228	-1.254	-1.252	-1.264	-1.268	-1.284	-1.297	-1.307	-1.316	-1.329
-1.341	-1.343	-1.369	-1.374	-1.395	-1.398	-1.421	-1.418	-1.432	-1.452
-1.453	-1.459	-1.475	-1.481	-1.498	-1.504	-1.510	-1.534	-1.523	-1.541
-1.548	-1.567	-1.591	-1.590	-1.589	-1.609	-1.614	-1.640	-1.635	-1.637
-1.658	-1.657	-1.670	-1.681	-1.687	-1.713	-1.716	-1.712	-1.716	-1.728
-1.739	-1.749	-1.746							

PERCENTAGE REDUCTION

0.00	0.71	3.84	6.92	9.70	11.92	13.54	15.51	17.02	18.54
19.60	20.96	22.88	24.19	25.00	25.76	26.62	28.23	28.64	29.65
30.40	30.96	32.07	32.58	32.93	34.34	34.55	36.41	36.92	36.52
37.47	38.64	39.14	39.85	41.16	40.91	42.47	42.93	43.28	43.84
44.04	44.95	45.66	45.96	46.67	48.18	47.98	48.03	48.94	49.70
50.25	51.16	51.57	52.42	52.42	53.48	54.55	54.70	55.40	55.66
56.31	56.82	57.32	58.38	58.74	59.34	60.71	61.06	61.36	61.62
62.02	63.33	63.23	63.84	64.04	64.85	65.51	66.01	66.46	67.12
67.73	67.83	69.14	69.39	70.45	70.61	71.77	71.62	72.32	73.33
73.38	73.69	74.49	74.80	75.66	75.96	76.26	77.47	76.92	77.83
78.18	79.14	80.35	80.30	80.25	81.26	81.52	82.83	82.58	82.68
83.74	83.69	84.34	84.90	85.20	86.52	86.67	86.46	86.67	87.27
87.83	88.33								

BBC CHYO BALANCE DATA REPORT
DATA FILE No. : :3.F.PRAM8
REMOVABLE OXYGEN WEIGHT: 1.92 GRAM
FURNACE TEMPERATURE : 1000 DEG. C
GAS FLOW RATE : 2 L/MIN
NUMBER OF SAMPLES TAKEN: 124
SAMPLING INTERVAL : 60 SECONDS

WEIGHT LOSS

0.002	0.003	-0.035	-0.088	-0.132	-0.181	-0.224	-0.263	-0.301	-0.330
-0.357	-0.382	-0.414	-0.422	-0.444	-0.456	-0.478	-0.499	-0.515	-0.528
-0.546	-0.558	-0.574	-0.587	-0.606	-0.616	-0.627	-0.639	-0.651	-0.665
-0.674	-0.689	-0.698	-0.710	-0.720	-0.733	-0.741	-0.754	-0.764	-0.773
-0.786	-0.797	-0.805	-0.817	-0.825	-0.836	-0.848	-0.859	-0.868	-0.877
-0.888	-0.897	-0.909	-0.917	-0.929	-0.941	-0.945	-0.956	-0.968	-0.977
-0.986	-0.992	-1.001	-1.014	-1.021	-1.029	-1.039	-1.046	-1.057	-1.066
-1.077	-1.085	-1.095	-1.103	-1.115	-1.124	-1.132	-1.140	-1.150	-1.159
-1.167	-1.174	-1.186	-1.195	-1.205	-1.214	-1.223	-1.231	-1.242	-1.251
-1.259	-1.266	-1.275	-1.284	-1.295	-1.305	-1.312	-1.322	-1.332	-1.342
-1.354	-1.362	-1.370	-1.378	-1.388	-1.398	-1.405	-1.416	-1.426	-1.435
-1.444	-1.452	-1.464	-1.470	-1.480	-1.490	-1.498	-1.506	-1.515	-1.524
-1.530	-1.539	-1.548	-1.557						

PERCENTAGE REDUCTION

0.00	-0.16	1.82	4.58	6.87	9.43	11.67	13.70	15.68	17.19
18.59	19.90	21.56	21.98	23.12	23.75	24.90	25.99	26.82	27.50
28.44	29.06	29.90	30.57	31.56	32.08	32.66	33.28	33.91	34.64
35.10	35.89	36.35	36.98	37.50	38.18	38.59	39.27	39.79	40.26
40.94	41.51	41.93	42.55	42.97	43.54	44.17	44.74	45.21	45.68
46.25	46.72	47.34	47.76	48.39	49.01	49.22	49.79	50.42	50.89
51.35	51.67	52.14	52.81	53.18	53.59	54.11	54.48	55.05	55.52
56.09	56.51	57.03	57.45	58.07	58.54	58.96	59.37	59.90	60.36
60.78	61.15	61.77	62.24	62.76	63.23	63.70	64.11	64.69	65.16
65.57	65.94	66.41	66.87	67.45	67.97	68.33	68.85	69.37	69.90
70.52	70.94	71.35	71.77	72.29	72.81	73.18	73.75	74.27	74.74
75.21	75.62	76.25	76.56	77.08	77.60	78.02	78.44	78.91	79.38
79.69	80.16	80.62							

BBC CHYO BALANCE DATA REPORT
DATA FILE No. : :3.F.PRAM9
REMOVABLE OXYGEN WEIGHT: 1.89 GRAM
FURNACE TEMPERATURE : 1000 DEG. C
GAS FLOW RATE : 1.5 L/MIN
NUMBER OF SAMPLES TAKEN: 140
SAMPLING INTERVAL : 60 SECONDS

WEIGHT LOSS

0.001	0.003	-0.036	-0.078	-0.121	-0.161	-0.196	-0.230	-0.259	-0.286
-0.311	-0.332	-0.354	-0.375	-0.390	-0.409	-0.425	-0.439	-0.452	-0.467
-0.479	-0.495	-0.506	-0.517	-0.527	-0.538	-0.548	-0.556	-0.567	-0.578
-0.589	-0.595	-0.606	-0.613	-0.623	-0.630	-0.638	-0.649	-0.656	-0.664
-0.673	-0.681	-0.689	-0.696	-0.705	-0.714	-0.722	-0.726	-0.735	-0.742
-0.750	-0.758	-0.766	-0.773	-0.780	-0.788	-0.795	-0.801	-0.810	-0.821
-0.825	-0.834	-0.839	-0.847	-0.855	-0.864	-0.867	-0.874	-0.881	-0.890
-0.897	-0.903	-0.911	-0.917	-0.924	-0.933	-0.941	-0.947	-0.955	-0.963
-0.970	-0.978	-0.984	-0.989	-0.999	-1.007	-1.013	-1.020	-1.024	-1.034
-1.040	-1.048	-1.057	-1.063	-1.072	-1.077	-1.087	-1.093	-1.102	-1.108
-1.118	-1.124	-1.137	-1.141	-1.149	-1.159	-1.165	-1.169	-1.180	-1.187
-1.194	-1.200	-1.210	-1.216	-1.225	-1.232	-1.244	-1.251	-1.254	-1.261
-1.268	-1.277	-1.282	-1.290	-1.300	-1.306	-1.312	-1.320	-1.326	-1.336
-1.341	-1.352	-1.345	-1.332	-1.327	-1.322	-1.315	-1.310	-1.307	-1.302

PERCENTAGE REDUCTION

0.00	-0.16	1.90	4.13	6.40	8.52	10.37	12.17	13.70	15.13
16.46	17.57	18.73	19.84	20.63	21.64	22.49	23.23	23.92	24.71
25.34	26.19	26.77	27.35	27.88	28.47	28.99	29.42	30.00	30.58
31.16	31.48	32.06	32.43	32.96	33.33	33.76	34.34	34.71	35.13
35.61	36.03	36.46	36.83	37.30	37.78	38.20	38.41	38.89	39.26
39.68	40.11	40.53	40.90	41.27	41.69	42.06	42.38	42.86	43.44
43.65	44.13	44.39	44.81	45.24	45.71	45.87	46.24	46.61	47.09
47.46	47.78	48.20	48.52	48.89	49.37	49.79	50.11	50.53	50.95
51.32	51.75	52.06	52.33	52.86	53.28	53.60	53.97	54.18	54.71
55.03	55.45	55.93	56.24	56.72	56.98	57.51	57.83	58.31	58.62
59.15	59.47	60.16	60.37	60.79	61.32	61.64	61.85	62.43	62.80
63.17	63.49	64.02	64.34	64.81	65.19	65.82	66.19	66.35	66.72
67.09	67.57	67.83	68.25	68.78	69.10	69.42	69.84	70.16	70.69
70.95	71.53	71.16	70.48	70.21	69.95	69.58	69.31	69.15	

BBC CHYO BALANCE DATA REPORT
DATA FILE No. : :1.H.PRAM0
REMOVABLE OXYGEN WEIGHT: 1.232 GRAM
FURNACE TEMPERATURE : 1000 DEG. C
GAS FLOW RATE : 2 L/MIN
NUMBER OF SAMPLES TAKEN: 122
SAMPLING INTERVAL : 60 SECONDS

WEIGHT LOSS

-0.008	-0.029	-0.079	-0.125	-0.164	-0.196	-0.225	-0.250	-0.275	-0.294
-0.315	-0.333	-0.352	-0.368	-0.384	-0.399	-0.414	-0.428	-0.443	-0.456
-0.469	-0.482	-0.495	-0.509	-0.520	-0.534	-0.545	-0.556	-0.568	-0.581
-0.593	-0.604	-0.615	-0.627	-0.637	-0.649	-0.659	-0.670	-0.680	-0.691
-0.701	-0.710	-0.721	-0.731	-0.741	-0.750	-0.759	-0.768	-0.778	-0.787
-0.797	-0.805	-0.814	-0.822	-0.830	-0.839	-0.848	-0.857	-0.865	-0.872
-0.881	-0.889	-0.897	-0.905	-0.911	-0.920	-0.927	-0.934	-0.942	-0.949
-0.957	-0.964	-0.971	-0.981	-0.988	-0.995	-1.003	-1.010	-1.017	-1.024
-1.033	-1.040	-1.047	-1.056	-1.063	-1.070	-1.078	-1.086	-1.093	-1.100
-1.107	-1.115	-1.121	-1.126	-1.134	-1.138	-1.145	-1.150	-1.156	-1.161
-1.168	-1.171	-1.176	-1.181	-1.185	-1.190	-1.193	-1.196	-1.201	-1.204
-1.208	-1.211	-1.214	-1.216	-1.218	-1.221	-1.223	-1.224	-1.225	-1.228
-1.229	-1.231								

PERCENTAGE REDUCTION

0.00	2.35	6.41	10.15	13.31	15.91	18.26	20.29	22.32	23.86
25.57	27.03	28.57	29.87	31.17	32.39	33.60	34.74	35.96	37.01
38.07	39.12	40.18	41.31	42.21	43.34	44.24	45.13	46.10	47.16
48.13	49.03	49.92	50.89	51.70	52.68	53.49	54.38	55.19	56.09
56.90	57.63	58.52	59.33	60.15	60.88	61.61	62.34	63.15	63.88
64.69	65.34	66.07	66.72	67.37	68.10	68.83	69.56	70.21	70.78
71.51	72.16	72.81	73.46	73.94	74.68	75.24	75.81	76.46	77.03
77.68	78.25	78.81	79.63	80.19	80.76	81.41	81.98	82.55	83.12
83.85	84.42	84.98	85.71	86.28	86.85	87.50	88.15	88.72	89.29
89.85	90.50	90.99	91.40	92.05	92.37	92.94	93.34	93.83	94.24
94.81	95.05	95.45	95.86	96.19	96.59	96.83	97.08	97.48	97.73
98.05	98.30	98.54	98.70	98.86	99.11	99.27	99.35	99.43	99.68
99.76									

BBC CHYO BALANCE DATA REPORT
DATA FILE No. : :1.H.PRAM2
REMOVABLE OXYGEN WEIGHT: 1.232 GRAM
FURNACE TEMPERATURE : 1000 DEG. C
GAS FLOW RATE : 2 L/MIN
NUMBER OF SAMPLES TAKEN: 122
SAMPLING INTERVAL : 60 SECONDS

WEIGHT LOSS

-0.008	-0.029	-0.079	-0.125	-0.164	-0.196	-0.225	-0.250	-0.275	-0.294
-0.315	-0.333	-0.352	-0.368	-0.384	-0.399	-0.414	-0.428	-0.443	-0.456
-0.469	-0.482	-0.495	-0.509	-0.520	-0.534	-0.545	-0.556	-0.568	-0.581
-0.593	-0.604	-0.615	-0.627	-0.637	-0.649	-0.659	-0.670	-0.680	-0.691
-0.701	-0.710	-0.721	-0.731	-0.741	-0.750	-0.759	-0.768	-0.778	-0.787
-0.797	-0.805	-0.814	-0.822	-0.830	-0.839	-0.848	-0.857	-0.865	-0.872
-0.881	-0.889	-0.897	-0.905	-0.911	-0.920	-0.927	-0.934	-0.942	-0.949
-0.957	-0.964	-0.971	-0.981	-0.988	-0.995	-1.003	-1.010	-1.017	-1.024
-1.033	-1.040	-1.047	-1.056	-1.063	-1.070	-1.078	-1.086	-1.093	-1.100
-1.107	-1.115	-1.121	-1.126	-1.134	-1.138	-1.145	-1.150	-1.156	-1.161
-1.168	-1.171	-1.176	-1.181	-1.185	-1.190	-1.193	-1.196	-1.201	-1.204
-1.208	-1.211	-1.214	-1.216	-1.218	-1.221	-1.223	-1.224	-1.225	-1.228
-1.229	-1.231								

PERCENTAGE REDUCTION

0.00	2.35	6.41	10.15	13.31	15.91	18.26	20.29	22.32	23.86
25.57	27.03	28.57	29.87	31.17	32.39	33.60	34.74	35.96	37.01
38.07	39.12	40.18	41.31	42.21	43.34	44.24	45.13	46.10	47.16
48.13	49.03	49.92	50.89	51.70	52.68	53.49	54.38	55.19	56.09
56.90	57.63	58.52	59.33	60.15	60.88	61.61	62.34	63.15	63.88
64.69	65.34	66.07	66.72	67.37	68.10	68.83	69.56	70.21	70.78
71.51	72.16	72.81	73.46	73.94	74.68	75.24	75.81	76.46	77.03
77.68	78.25	78.81	79.63	80.19	80.76	81.41	81.98	82.55	83.12
83.85	84.42	84.98	85.71	86.28	86.85	87.50	88.15	88.72	89.29
89.85	90.50	90.99	91.40	92.05	92.37	92.94	93.34	93.83	94.24
94.81	95.05	95.45	95.86	96.19	96.59	96.83	97.08	97.48	97.73
98.05	98.30	98.54	98.70	98.86	99.11	99.27	99.35	99.43	99.68
99.76									

BBC CHYO BALANCE DATA REPORT
DATA FILE No. : :1.H.PRAM3
REMOVABLE OXYGEN WEIGHT: 0.6240000001 GRAM
FURNACE TEMPERATURE : 1000 DEG. C
GAS FLOW RATE : 2 L/MIN
NUMBER OF SAMPLES TAKEN: 115
SAMPLING INTERVAL : 60 SECONDS

WEIGHT LOSS

-0.003	-0.018	-0.045	-0.069	-0.092	-0.111	-0.124	-0.141	-0.155	-0.166
-0.178	-0.192	-0.203	-0.213	-0.222	-0.231	-0.240	-0.249	-0.258	-0.264
-0.274	-0.282	-0.289	-0.297	-0.304	-0.313	-0.319	-0.328	-0.333	-0.339
-0.349	-0.358	-0.365	-0.371	-0.380	-0.389	-0.397	-0.403	-0.410	-0.420
-0.428	-0.431	-0.438	-0.448	-0.457	-0.464	-0.470	-0.475	-0.482	-0.490
-0.496	-0.501	-0.506	-0.511	-0.517	-0.521	-0.522	-0.531	-0.535	-0.537
-0.544	-0.544	-0.549	-0.551	-0.557	-0.559	-0.561	-0.564	-0.568	-0.570
-0.573	-0.574	-0.577	-0.578	-0.579	-0.582	-0.585	-0.583	-0.587	-0.590
-0.592	-0.590	-0.592	-0.595	-0.597	-0.598	-0.601	-0.603	-0.603	-0.604
-0.605	-0.604	-0.608	-0.609	-0.608	-0.608	-0.611	-0.610	-0.614	-0.614
-0.613	-0.617	-0.616	-0.618	-0.618	-0.620	-0.619	-0.620	-0.619	-0.622
-0.621	-0.623	-0.624	-0.622	-0.624					

PERCENTAGE REDUCTION

0.00	2.88	7.21	11.06	14.74	17.79	19.87	22.60	24.84	26.60
28.53	30.77	32.53	34.13	35.58	37.02	38.46	39.90	41.35	42.31
43.91	45.19	46.31	47.60	48.72	50.16	51.12	52.56	53.37	54.33
55.93	57.37	58.49	59.46	60.90	62.34	63.62	64.58	65.71	67.31
68.59	69.07	70.19	71.79	73.24	74.36	75.32	76.12	77.24	78.53
79.49	80.29	81.09	81.89	82.85	83.49	83.65	85.10	85.74	86.06
87.18	87.18	87.98	88.30	89.26	89.58	89.90	90.38	91.03	91.35
91.83	91.99	92.47	92.63	92.79	93.27	93.75	93.43	94.07	94.55
94.87	94.55	94.87	95.35	95.67	95.83	96.31	96.63	96.63	96.79
96.96	96.79	97.44	97.60	97.44	97.44	97.92	97.76	98.40	98.40
98.24	98.88	98.72	99.04	99.04	99.36	99.20	99.36	99.20	99.68
99.52	99.84	100.00	99.68						

BBC CHYO BALANCE DATA REPORT
DATA FILE No. : :1.H.PRAM4
REMOVABLE OXYGEN WEIGHT: 0.33 GRAM
FURNACE TEMPERATURE : 1000 DEG. C
GAS FLOW RATE : 2 L/MIN
NUMBER OF SAMPLES TAKEN: 87
SAMPLING INTERVAL : 60 SECONDS

WEIGHT LOSS

0.000	-0.021	-0.040	-0.055	-0.068	-0.077	-0.086	-0.094	-0.102	-0.108
-0.115	-0.121	-0.126	-0.134	-0.139	-0.145	-0.150	-0.155	-0.160	-0.165
-0.171	-0.175	-0.180	-0.185	-0.190	-0.194	-0.199	-0.204	-0.209	-0.213
-0.218	-0.223	-0.228	-0.233	-0.236	-0.242	-0.247	-0.251	-0.255	-0.260
-0.263	-0.266	-0.270	-0.274	-0.277	-0.278	-0.282	-0.285	-0.287	-0.289
-0.291	-0.293	-0.295	-0.296	-0.297	-0.299	-0.299	-0.302	-0.302	-0.304
-0.305	-0.305	-0.306	-0.308	-0.308	-0.308	-0.309	-0.309	-0.310	-0.311
-0.312	-0.312	-0.312	-0.313	-0.313	-0.314	-0.314	-0.315	-0.315	-0.315
-0.315	-0.316	-0.316	-0.316	-0.316	-0.318	-0.316			

PERCENTAGE REDUCTION

0.00	6.36	12.12	16.67	20.61	23.33	26.06	28.48	30.91	32.73
34.85	36.67	38.18	40.61	42.12	43.94	45.45	46.97	48.48	50.00
51.82	53.03	54.55	56.06	57.58	58.79	60.30	61.82	63.33	64.55
66.06	67.58	69.09	70.61	71.52	73.33	74.85	76.06	77.27	78.79
79.70	80.61	81.82	83.03	83.94	84.24	85.45	86.36	86.97	87.58
88.18	88.79	89.39	89.70	90.00	90.61	90.61	91.52	91.52	92.12
92.42	92.42	92.73	93.33	93.33	93.33	93.64	93.64	93.94	94.24
94.55	94.55	94.55	94.85	94.85	95.15	95.15	95.45	95.45	95.45
95.45	95.76	95.76	95.76	95.76	96.36				

BBC CHYO BALANCE DATA REPORT
DATA FILE No. : :1.H.PRAM5
REMOVABLE OXYGEN WEIGHT: 0.441 GRAM
FURNACE TEMPERATURE : 1000 DEG. C
GAS FLOW RATE : 2 L/MIN
NUMBER OF SAMPLES TAKEN: 38
SAMPLING INTERVAL : 60 SECONDS

WEIGHT LOSS

0.000	-0.020	-0.055	-0.082	-0.108	-0.128	-0.149	-0.166	-0.181	-0.193
-0.207	-0.224	-0.233	-0.245	-0.254	-0.261	-0.274	-0.278	-0.287	-0.292
-0.300	-0.304	-0.310	-0.315	-0.321	-0.328	-0.333	-0.340	-0.346	-0.353
-0.360	-0.366	-0.373	-0.379	-0.386	-0.392	-0.397	-0.402		

PERCENTAGE REDUCTION

0.00	4.54	12.47	18.59	24.49	29.02	33.79	37.64	41.04	43.76
46.94	50.79	52.83	55.56	57.60	59.18	62.13	63.04	65.08	66.21
68.03	68.93	70.29	71.43	72.79	74.38	75.51	77.10	78.46	80.05
81.63	82.99	84.58	85.94	87.53	88.89	90.02			

BBC CHYO BALANCE DATA REPORT
DATA FILE No. : :1.H.PRAM6
REMOVABLE OXYGEN WEIGHT: 0.537 GRAM
FURNACE TEMPERATURE : 1000 DEG. C
GAS FLOW RATE : 2 L/MIN
NUMBER OF SAMPLES TAKEN: 27
SAMPLING INTERVAL : 60 SECONDS

WEIGHT LOSS

-0.001	-0.025	-0.068	-0.102	-0.130	-0.154	-0.176	-0.195	-0.214	-0.231
-0.245	-0.260	-0.273	-0.285	-0.296	-0.307	-0.317	-0.328	-0.339	-0.350
-0.361	-0.373	-0.384	-0.396	-0.407	-0.419	-0.429			

PERCENTAGE REDUCTION

0.00	4.66	12.66	18.99	24.21	28.68	32.77	36.31	39.85	43.02
45.62	48.42	50.84	53.07	55.12	57.17	59.03	61.08	63.13	65.19
67.23	69.46	71.51	73.74	75.79	76.03				

BBC CHYO BALANCE DATA REPORT
DATA FILE No. : :1.H.PRAM7
REMOVABLE OXYGEN WEIGHT: 0.353 GRAM
FURNACE TEMPERATURE : 1000 DEG. C
GAS FLOW RATE : 2 L/MIN
NUMBER OF SAMPLES TAKEN: 15
SAMPLING INTERVAL : 60 SECONDS

WEIGHT LOSS

0.000	-0.019	-0.045	-0.068	-0.089	-0.105	-0.122	-0.135	-0.149	-0.162
-0.173	-0.183	-0.193	-0.203	-0.211					

PERCENTAGE REDUCTION

0.00	5.39	12.75	19.26	25.21	29.75	34.56	38.24	42.21	45.89
49.01	51.84	54.67	57.51						

BBC CHYO BALANCE DATA REPORT
DATA FILE No. : :1.H.PRAM8
REMOVABLE OXYGEN WEIGHT: 0.534 GRAM
FURNACE TEMPERATURE : 1000 DEG. C
GAS FLOW RATE : 2 L/MIN
NUMBER OF SAMPLES TAKEN: 12
SAMPLING INTERVAL : 60 SECONDS

WEIGHT LOSS

-0.002	-0.024	-0.055	-0.083	-0.106	-0.124	-0.144	-0.159	-0.174	-0.190
-0.202	-0.218								

PERCENTAGE REDUCTION

0.00	4.49	10.30	15.54	19.85	23.22	26.97	29.78	32.58	35.58
37.83									

BBC CHYO BALANCE DATA REPORT
DATA FILE No. : :1.H.PRAM9
REMOVABLE OXYGEN WEIGHT: 0.55 GRAM
FURNACE TEMPERATURE : 1000 DEG. C
GAS FLOW RATE : 2 L/MIN
NUMBER OF SAMPLES TAKEN: 5
SAMPLING INTERVAL : 60 SECONDS

WEIGHT LOSS

0.000 -0.020 -0.056 -0.087 -0.114

PERCENTAGE REDUCTION

0.00 3.64 10.18 15.82

BBC CHYO BALANCE DATA REPORT
DATA FILE No. : :1.H.PRAM10
REMOVABLE OXYGEN WEIGHT: 0.318 GRAM
FURNACE TEMPERATURE : 1000 DEG. C
GAS FLOW RATE : 2 L/MIN
NUMBER OF SAMPLES TAKEN: 3
SAMPLING INTERVAL : 60 SECONDS

WEIGHT LOSS

0.002 -0.010 -0.029

PERCENTAGE REDUCTION

0.00 3.14

BBC CHYO BALANCE DATA REPORT
DATA FILE No. : :1.I.PRAM3
REMOVABLE OXYGEN WEIGHT: 0.7 GRAM
FURNACE TEMPERATURE : 1000 DEG. C
GAS FLOW RATE : 2 L/MIN
NUMBER OF SAMPLES TAKEN: 53
SAMPLING INTERVAL : 60 SECONDS

WEIGHT LOSS

0.002	-0.025	-0.063	-0.094	-0.120	-0.144	-0.165	-0.183	-0.200	-0.217
-0.229	-0.241	-0.255	-0.268	-0.280	-0.291	-0.301	-0.315	-0.323	-0.336
-0.345	-0.354	-0.366	-0.373	-0.382	-0.393	-0.403	-0.411	-0.422	-0.430
-0.438	-0.447	-0.455	-0.465	-0.472	-0.478	-0.486	-0.495	-0.502	-0.509
-0.514	-0.523	-0.527	-0.536	-0.538	-0.545	-0.553	-0.558	-0.564	-0.569
-0.573	-0.579	-0.584							

PERCENTAGE REDUCTION

0.00	3.57	9.00	13.43	17.14	20.57	23.57	26.14	28.57	31.00
32.71	34.43	36.43	38.29	40.00	41.57	43.00	45.00	46.14	48.00
49.29	50.57	52.29	53.29	54.57	56.14	57.57	58.71	60.29	61.43
62.57	63.86	65.00	66.43	67.43	68.29	69.43	70.71	71.71	72.71
73.43	74.71	75.29	76.57	76.86	77.86	79.00	79.71	80.57	81.29
81.86	82.71								

BBC CHYO BALANCE DATA REPORT
DATA FILE No. : :1.I.PRAM2
REMOVABLE OXYGEN WEIGHT: 0.98 GRAM
FURNACE TEMPERATURE : 1000 DEG. C
GAS FLOW RATE : 2 L/MIN
NUMBER OF SAMPLES TAKEN: 92
SAMPLING INTERVAL : 60 SECONDS

WEIGHT LOSS

0.002	-0.030	-0.080	-0.121	-0.155	-0.186	-0.213	-0.235	-0.255	-0.276
-0.294	-0.313	-0.328	-0.345	-0.360	-0.376	-0.389	-0.404	-0.417	-0.431
-0.445	-0.456	-0.467	-0.483	-0.495	-0.504	-0.518	-0.530	-0.540	-0.554
-0.565	-0.578	-0.588	-0.600	-0.610	-0.618	-0.629	-0.642	-0.652	-0.662
-0.671	-0.680	-0.689	-0.699	-0.704	-0.715	-0.724	-0.732	-0.739	-0.749
-0.756	-0.764	-0.770	-0.777	-0.782	-0.787	-0.796	-0.802	-0.811	-0.813
-0.820	-0.823	-0.830	-0.835	-0.842	-0.846	-0.853	-0.856	-0.860	-0.865
-0.870	-0.872	-0.876	-0.880	-0.881	-0.885	-0.886	-0.892	-0.896	-0.898
-0.900	-0.900	-0.902	-0.903	-0.907	-0.909	-0.909	-0.910	-0.910	-0.909
-0.914	-0.914								

PERCENTAGE REDUCTION

0.00	3.06	8.16	12.35	15.82	18.98	21.73	23.98	26.02	28.16
30.00	31.94	33.47	35.20	36.73	38.37	39.69	41.22	42.55	43.98
45.41	46.53	47.65	49.29	50.51	51.43	52.86	54.08	55.10	56.53
57.65	58.98	60.00	61.22	62.24	63.06	64.18	65.51	66.53	67.55
68.47	69.39	70.31	71.33	71.84	72.96	73.88	74.69	75.41	76.43
77.14	77.96	78.57	79.29	79.80	80.31	81.22	81.84	82.76	82.96
83.67	83.98	84.69	85.20	85.92	86.33	87.04	87.35	87.76	88.27
88.78	88.98	89.39	89.80	89.90	90.31	90.41	91.02	91.43	91.63
91.84	91.84	92.04	92.14	92.55	92.76	92.76	92.86	92.86	92.76
93.27									

BBC CHYO BALANCE DATA REPORT
DATA FILE No. : :1.I.PRAM1
REMOVABLE OXYGEN WEIGHT: 1.88 GRAM
FURNACE TEMPERATURE : 1000 DEG. C
GAS FLOW RATE : 2 L/MIN
NUMBER OF SAMPLES TAKEN: 105
SAMPLING INTERVAL : 60 SECONDS

WEIGHT LOSS

0.002	-0.047	-0.122	-0.189	-0.252	-0.308	-0.356	-0.400	-0.438	-0.470
-0.505	-0.527	-0.554	-0.578	-0.602	-0.623	-0.645	-0.667	-0.686	-0.707
-0.727	-0.748	-0.768	-0.789	-0.810	-0.829	-0.849	-0.868	-0.889	-0.911
-0.929	-0.948	-0.971	-0.990	-1.014	-1.032	-1.052	-1.073	-1.094	-1.113
-1.133	-1.152	-1.173	-1.189	-1.212	-1.230	-1.249	-1.267	-1.284	-1.304
-1.320	-1.340	-1.358	-1.374	-1.392	-1.411	-1.424	-1.442	-1.459	-1.474
-1.490	-1.506	-1.522	-1.535	-1.548	-1.563	-1.577	-1.592	-1.605	-1.617
-1.630	-1.642	-1.654	-1.664	-1.678	-1.687	-1.698	-1.708	-1.719	-1.729
-1.737	-1.747	-1.754	-1.759	-1.766	-1.780	-1.787	-1.795	-1.801	-1.809
-1.812	-1.820	-1.827	-1.831	-1.835	-1.839	-1.843	-1.848	-1.851	-1.852
-1.857	-1.858	-1.858	-1.861	-1.866					

PERCENTAGE REDUCTION

0.00	2.50	6.49	10.05	13.40	16.38	18.94	21.28	23.30	25.00
26.86	28.03	29.47	30.74	32.02	33.14	34.31	35.48	36.49	37.61
38.67	39.79	40.85	41.97	43.09	44.10	45.16	46.17	47.29	48.46
49.41	50.43	51.65	52.66	53.94	54.89	55.96	57.07	58.19	59.20
60.27	61.28	62.39	63.24	64.47	65.43	66.44	67.39	68.30	69.36
70.21	71.28	72.23	73.09	74.04	75.05	75.74	76.70	77.61	78.40
79.26	80.11	80.96	81.65	82.34	83.14	83.88	84.68	85.37	86.01
86.70	87.34	87.98	88.51	89.26	89.73	90.32	90.85	91.44	91.97
92.39	92.93	93.30	93.56	93.94	94.68	95.05	95.48	95.80	96.22
96.38	96.81	97.18	97.39	97.61	97.82	98.03	98.30	98.46	98.51
98.78	98.83	98.83	98.99						

BBC CHYO BALANCE DATA REPORT
DATA FILE No. : :3.0.PRAM10
REMOVABLE OXYGEN WEIGHT: 0.95 GRAM
FURNACE TEMPERATURE : 1000 DEG. C
GAS FLOW RATE : 2 L/MIN
NUMBER OF SAMPLES TAKEN: 141
SAMPLING INTERVAL : 60 SECONDS

WEIGHT LOSS

0.000	-0.011	-0.035	-0.059	-0.081	-0.102	-0.122
-0.140	-0.159	-0.176	-0.191	-0.206	-0.219	-0.232
-0.244	-0.255	-0.266	-0.276	-0.287	-0.297	-0.307
-0.316	-0.326	-0.336	-0.345	-0.354	-0.365	-0.374
-0.385	-0.395	-0.406	-0.416	-0.428	-0.440	-0.452
-0.466	-0.478	-0.491	-0.504	-0.516	-0.529	-0.541
-0.555	-0.566	-0.577	-0.588	-0.601	-0.611	-0.621
-0.631	-0.640	-0.651	-0.660	-0.669	-0.678	-0.686
-0.694	-0.702	-0.709	-0.717	-0.724	-0.730	-0.736
-0.743	-0.750	-0.756	-0.761	-0.766	-0.772	-0.778
-0.783	-0.789	-0.794	-0.799	-0.802	-0.808	-0.812
-0.815	-0.821	-0.824	-0.829	-0.833	-0.837	-0.839
-0.845	-0.848	-0.853	-0.855	-0.858	-0.863	-0.865
-0.868	-0.871	-0.873	-0.877	-0.879	-0.881	-0.883
-0.885	-0.889	-0.892	-0.894	-0.896	-0.898	-0.900
-0.902	-0.905	-0.905	-0.908	-0.910	-0.909	-0.913
-0.914	-0.916	-0.916	-0.918	-0.921	-0.921	-0.923
-0.925	-0.926	-0.928	-0.929	-0.930	-0.932	-0.931
-0.934	-0.935	-0.936	-0.937	-0.938	-0.939	-0.939
-0.939	-0.943	-0.942	-0.943	-0.944	-0.944	-0.945

PERCENTAGE REDUCTION

0.00	1.16	3.68	6.21	8.53	10.74	12.84
14.74	16.74	18.53	20.11	21.68	23.05	24.42
25.68	26.84	28.00	29.05	30.21	31.26	32.32
33.26	34.32	35.37	36.32	37.26	38.42	39.37
40.53	41.58	42.74	43.79	45.05	46.32	47.58
49.05	50.32	51.68	53.05	54.32	55.68	56.95
58.42	59.58	60.74	61.89	63.26	64.32	65.37
66.42	67.37	68.53	69.47	70.42	71.37	72.21
73.05	73.89	74.63	75.47	76.21	76.84	77.47
78.21	78.95	79.58	80.11	80.63	81.26	81.89
82.42	83.05	83.58	84.11	84.42	85.05	85.47
85.79	86.42	86.74	87.26	87.68	88.11	88.32
88.95	89.26	89.79	90.00	90.32	90.84	91.05
91.37	91.68	91.89	92.32	92.53	92.74	92.95
93.16	93.58	93.89	94.11	94.32	94.53	94.74
94.95	95.26	95.26	95.58	95.79	95.68	96.11
96.21	96.42	96.42	96.63	96.95	96.95	97.16
97.37	97.47	97.68	97.79	97.89	98.11	98.00
98.32	98.42	98.53	98.63	98.74	98.84	98.84
98.84	99.26	99.16	99.26	99.37	99.37	99.47

BBC CHYO BALANCE DATA REPORT

DATA FILE No.	:3.U.PRAM9
REMOVABLE OXYGEN WEIGHT:	0.9369999999 GI
FURNACE TEMPERATURE :	1000 DEG. C
GAS FLOW RATE :	2 L/MIN
NUMBER OF SAMPLES TAKEN:	111
SAMPLING INTERVAL :	60 SECONDS

WEIGHT LOSS

0.000	-0.011	-0.035	-0.060	-0.086	-0.110	-0.132
-0.155	-0.176	-0.194	-0.213	-0.229	-0.245	-0.259
-0.273	-0.285	-0.297	-0.309	-0.320	-0.331	-0.342
-0.354	-0.365	-0.378	-0.389	-0.401	-0.414	-0.427
-0.441	-0.454	-0.468	-0.482	-0.496	-0.511	-0.525
-0.539	-0.554	-0.568	-0.582	-0.594	-0.609	-0.622
-0.635	-0.647	-0.659	-0.671	-0.682	-0.693	-0.703
-0.714	-0.724	-0.733	-0.743	-0.751	-0.759	-0.768
-0.777	-0.783	-0.790	-0.796	-0.803	-0.809	-0.816
-0.821	-0.826	-0.832	-0.837	-0.841	-0.846	-0.851
-0.855	-0.859	-0.862	-0.866	-0.871	-0.874	-0.878
-0.879	-0.883	-0.886	-0.888	-0.890	-0.893	-0.896
-0.898	-0.900	-0.903	-0.904	-0.907	-0.908	-0.910
-0.911	-0.913	-0.914	-0.916	-0.917	-0.919	-0.920
-0.920	-0.921	-0.922	-0.924	-0.926	-0.927	-0.926
-0.927	-0.928	-0.930	-0.930	-0.931	-0.932	

PERCENTAGE REDUCTION

0.00	1.17	3.74	6.40	9.18	11.74	14.09
16.54	18.78	20.70	22.73	24.44	26.15	27.64
29.14	30.42	31.70	32.98	34.15	35.33	36.50
37.78	38.95	40.34	41.52	42.80	44.18	45.57
47.07	48.45	49.95	51.44	52.93	54.54	56.03
57.52	59.12	60.62	62.11	63.39	64.99	66.38
67.77	69.05	70.33	71.61	72.79	73.96	75.03
76.20	77.27	78.23	79.30	80.15	81.00	81.96
82.92	83.56	84.31	84.95	85.70	86.34	87.09
87.62	88.15	88.79	89.33	89.75	90.29	90.82
91.25	91.68	92.00	92.42	92.96	93.28	93.70
93.81	94.24	94.56	94.77	94.98	95.30	95.62
95.84	96.05	96.37	96.48	96.80	96.91	97.12
97.23	97.44	97.55	97.76	97.87	98.08	98.19
98.19	98.29	98.40	98.61	98.83	98.93	98.83
98.93	99.04	99.25	99.25	99.36		

BBC CHYO BALANCE DATA REPORT
DATA FILE No. : 13.0.PRAMO
REMOVABLE OXYGEN WEIGHT: 0.845 GRAM
FURNACE TEMPERATURE : 1000 DEG. C
GAS FLOW RATE : 2 L/MIN
NUMBER OF SAMPLES TAKEN: 146
SAMPLING INTERVAL : 60 SECONDS

WEIGHT LOSS

0.000	-0.009	-0.032	-0.054	-0.075	-0.096	-0.113
-0.129	-0.144	-0.158	-0.171	-0.183	-0.193	-0.204
-0.214	-0.223	-0.233	-0.242	-0.250	-0.259	-0.267
-0.276	-0.283	-0.292	-0.300	-0.308	-0.316	-0.323
-0.332	-0.340	-0.348	-0.356	-0.365	-0.373	-0.382
-0.391	-0.401	-0.413	-0.422	-0.431	-0.440	-0.451
-0.461	-0.471	-0.482	-0.492	-0.502	-0.513	-0.522
-0.533	-0.541	-0.551	-0.560	-0.568	-0.575	-0.583
-0.591	-0.599	-0.606	-0.613	-0.620	-0.627	-0.632
-0.640	-0.646	-0.651	-0.656	-0.663	-0.669	-0.675
-0.679	-0.683	-0.690	-0.692	-0.699	-0.703	-0.709
-0.712	-0.715	-0.720	-0.727	-0.726	-0.734	-0.736
-0.738	-0.741	-0.748	-0.748	-0.754	-0.756	-0.758
-0.758	-0.764	-0.768	-0.770	-0.775	-0.777	-0.779
-0.782	-0.787	-0.788	-0.790	-0.792	-0.795	-0.797
-0.799	-0.798	-0.798	-0.804	-0.802	-0.806	-0.809
-0.810	-0.811	-0.813	-0.816	-0.818	-0.814	-0.819
-0.818	-0.818	-0.821	-0.822	-0.823	-0.825	-0.827
-0.825	-0.830	-0.828	-0.830	-0.828	-0.829	-0.832
-0.832	-0.834	-0.833	-0.836	-0.835	-0.837	-0.838
-0.838	-0.845	-0.841	-0.841	-0.841	-0.842	

PERCENTAGE REDUCTION

0.00	1.07	3.79	6.39	8.88	11.36	13.37
15.27	17.04	18.70	20.24	21.66	22.84	24.14
25.33	26.39	27.57	28.64	29.59	30.65	31.60
32.66	33.49	34.56	35.50	36.45	37.40	38.22
39.29	40.24	41.18	42.13	43.20	44.14	45.21
46.27	47.46	48.88	49.94	51.01	52.07	53.37
54.56	55.74	57.04	58.22	59.41	60.71	61.78
63.08	64.02	65.21	66.27	67.22	68.05	68.99
69.94	70.89	71.72	72.54	73.37	74.20	74.79
75.74	76.45	77.04	77.63	78.46	79.17	79.88
80.36	80.83	81.66	81.89	82.72	83.20	83.91
84.26	84.62	85.21	86.04	85.92	86.86	87.10
87.34	87.69	88.52	88.52	89.23	89.47	89.70
89.70	90.41	90.89	91.12	91.72	91.95	92.19
92.54	93.14	93.25	93.49	93.73	94.08	94.32
94.56	94.44	94.44	95.15	94.91	95.38	95.74
95.86	95.98	96.21	96.57	96.80	96.33	96.92
96.80	96.80	97.16	97.28	97.40	97.63	97.87
97.63	98.22	97.99	98.22	97.99	98.11	98.46
98.46	98.70	98.58	98.93	98.82	99.05	99.17
99.17	100.00	99.53	99.53	99.53		

BBC CHYO BALANCE DATA REPORT
DATA FILE No. : :3.O.PRAM7
REMOVABLE OXYGEN WEIGHT: 0.7490000001 G
FURNACE TEMPERATURE : 1000 DEG. C
GAS FLOW RATE : 2 L/MIN
NUMBER OF SAMPLES TAKEN: 123
SAMPLING INTERVAL : 60 SECONDS

WEIGHT LOSS

-0.001	-0.008	-0.025	-0.042	-0.057	-0.072	-0.086
-0.099	-0.111	-0.122	-0.134	-0.144	-0.154	-0.164
-0.172	-0.181	-0.190	-0.198	-0.208	-0.216	-0.225
-0.233	-0.241	-0.249	-0.257	-0.264	-0.273	-0.280
-0.288	-0.296	-0.303	-0.311	-0.318	-0.326	-0.334
-0.340	-0.348	-0.354	-0.362	-0.370	-0.377	-0.385
-0.393	-0.400	-0.407	-0.415	-0.423	-0.430	-0.438
-0.446	-0.454	-0.462	-0.471	-0.479	-0.487	-0.496
-0.504	-0.511	-0.520	-0.528	-0.535	-0.544	-0.551
-0.560	-0.566	-0.573	-0.580	-0.588	-0.595	-0.601
-0.607	-0.614	-0.620	-0.626	-0.633	-0.638	-0.643
-0.649	-0.654	-0.660	-0.662	-0.669	-0.671	-0.675
-0.680	-0.683	-0.687	-0.689	-0.693	-0.695	-0.699
-0.701	-0.702	-0.705	-0.709	-0.709	-0.713	-0.714
-0.716	-0.718	-0.720	-0.720	-0.723	-0.724	-0.725
-0.727	-0.728	-0.730	-0.732	-0.733	-0.734	-0.735
-0.737	-0.737	-0.739	-0.741	-0.739	-0.743	-0.742
-0.744	-0.743	-0.744	-0.745			

PERCENTAGE REDUCTION

0.00	1.07	3.34	5.61	7.61	9.61	11.48
13.22	14.82	16.29	17.89	19.23	20.56	21.90
22.96	24.17	25.37	26.44	27.77	28.84	30.04
31.11	32.18	33.24	34.31	35.25	36.45	37.38
38.45	39.52	40.45	41.52	42.46	43.52	44.59
45.39	46.46	47.26	48.33	49.40	50.33	51.40
52.47	53.40	54.34	55.41	56.48	57.41	58.48
59.55	60.61	61.68	62.88	63.95	65.02	66.22
67.29	68.22	69.43	70.49	71.43	72.63	73.56
74.77	75.57	76.50	77.44	78.50	79.44	80.24
81.04	81.98	82.78	83.58	84.51	85.18	85.85
86.65	87.32	88.12	88.38	89.32	89.59	90.12
90.79	91.19	91.72	91.99	92.52	92.79	93.32
93.59	93.72	94.13	94.66	94.66	95.19	95.33
95.59	95.86	96.13	96.13	96.53	96.66	96.80
97.06	97.20	97.46	97.73	97.86	98.00	98.13
98.40	98.40	98.66	98.93	98.66	99.20	99.07
99.33	99.20	99.33				

BBC CHYO BALANCE DATA REPORT
DATA FILE No. : :3.0.PRAM6
REMOVABLE OXYGEN WEIGHT: 0.753 GRAM
FURNACE TEMPERATURE : 1000 DEG. C
GAS FLOW RATE : 2 L/MIN
NUMBER OF SAMPLES TAKEN: 145
SAMPLING INTERVAL : 60 SECONDS

WEIGHT LOSS

0.000	-0.011	-0.031	-0.051	-0.070	-0.088	-0.105
-0.122	-0.137	-0.151	-0.166	-0.178	-0.189	-0.200
-0.210	-0.221	-0.229	-0.237	-0.246	-0.253	-0.261
-0.269	-0.277	-0.284	-0.292	-0.299	-0.307	-0.316
-0.324	-0.333	-0.342	-0.353	-0.363	-0.374	-0.384
-0.395	-0.404	-0.416	-0.427	-0.437	-0.448	-0.457
-0.466	-0.476	-0.484	-0.492	-0.503	-0.510	-0.520
-0.529	-0.535	-0.543	-0.548	-0.556	-0.562	-0.567
-0.574	-0.578	-0.585	-0.592	-0.597	-0.600	-0.606
-0.611	-0.616	-0.619	-0.623	-0.629	-0.632	-0.636
-0.641	-0.644	-0.648	-0.651	-0.654	-0.658	-0.661
-0.663	-0.666	-0.671	-0.673	-0.676	-0.678	-0.679
-0.682	-0.684	-0.686	-0.689	-0.692	-0.692	-0.696
-0.696	-0.699	-0.699	-0.702	-0.703	-0.706	-0.709
-0.709	-0.708	-0.711	-0.712	-0.714	-0.716	-0.718
-0.718	-0.720	-0.720	-0.722	-0.724	-0.724	-0.725
-0.725	-0.726	-0.728	-0.729	-0.729	-0.731	-0.732
-0.732	-0.734	-0.734	-0.734	-0.737	-0.738	-0.740
-0.736	-0.739	-0.739	-0.742	-0.742	-0.743	-0.742
-0.744	-0.742	-0.743	-0.745	-0.745	-0.744	-0.744
-0.745	-0.747	-0.747	-0.747	-0.748		

PERCENTAGE REDUCTION

0.00	1.46	4.12	6.77	9.30	11.69	13.94
16.20	18.19	20.05	22.05	23.64	25.10	26.56
27.89	29.35	30.41	31.47	32.67	33.60	34.66
35.72	36.79	37.72	38.78	39.71	40.77	41.97
43.03	44.22	45.42	46.88	48.21	49.67	51.00
52.46	53.65	55.25	56.71	58.03	59.50	60.69
61.89	63.21	64.28	65.34	66.80	67.73	69.06
70.25	71.05	72.11	72.78	73.84	74.63	75.30
76.23	76.76	77.69	78.62	79.28	79.68	80.48
81.14	81.81	82.20	82.74	83.53	83.93	84.46
85.13	85.52	86.06	86.45	86.85	87.38	87.78
88.05	88.45	89.11	89.38	89.77	90.04	90.17
90.57	90.84	91.10	91.50	91.90	91.90	92.43
92.43	92.83	92.83	93.23	93.36	93.76	94.16
94.16	94.02	94.42	94.56	94.82	95.09	95.35
95.35	95.62	95.62	95.88	96.15	96.15	96.28
96.28	96.41	96.68	96.81	96.81	97.08	97.21
97.21	97.48	97.48	97.48	97.88	98.01	98.27
97.74	98.14	98.14	98.54	98.54	98.67	98.54
98.80	98.54	98.67	98.94	98.94	98.80	98.80
98.94	99.20	99.20	99.20			

BBC CHYO BALANCE DATA REPORT
DATA FILE No. : 3.0.PRAMS
REMOVABLE OXYGEN WEIGHT: 1.371 GRAM
FURNACE TEMPERATURE : 1000 DEG. C
GAS FLOW RATE : 2 L/MIN
NUMBER OF SAMPLES TAKEN: 181
SAMPLING INTERVAL : 60 SECONDS

WEIGHT LOSS

-0.001	-0.013	-0.037	-0.063	-0.088	-0.112	-0.136
-0.159	-0.181	-0.201	-0.221	-0.240	-0.256	-0.273
-0.288	-0.304	-0.318	-0.332	-0.345	-0.358	-0.370
-0.383	-0.395	-0.406	-0.417	-0.429	-0.440	-0.451
-0.462	-0.472	-0.483	-0.495	-0.505	-0.515	-0.527
-0.538	-0.548	-0.560	-0.571	-0.583	-0.594	-0.605
-0.619	-0.630	-0.642	-0.654	-0.667	-0.679	-0.692
-0.703	-0.716	-0.729	-0.742	-0.754	-0.767	-0.778
-0.791	-0.804	-0.816	-0.829	-0.839	-0.851	-0.863
-0.875	-0.886	-0.898	-0.909	-0.920	-0.931	-0.941
-0.952	-0.963	-0.974	-0.983	-0.991	-1.001	-1.010
-1.020	-1.028	-1.036	-1.045	-1.053	-1.060	-1.068
-1.075	-1.082	-1.089	-1.096	-1.102	-1.109	-1.116
-1.121	-1.127	-1.133	-1.138	-1.144	-1.149	-1.156
-1.160	-1.165	-1.170	-1.175	-1.179	-1.184	-1.188
-1.192	-1.197	-1.201	-1.205	-1.210	-1.213	-1.216
-1.220	-1.224	-1.227	-1.230	-1.234	-1.236	-1.241
-1.244	-1.247	-1.249	-1.253	-1.255	-1.258	-1.260
-1.263	-1.266	-1.269	-1.271	-1.273	-1.275	-1.278
-1.280	-1.282	-1.284	-1.287	-1.289	-1.291	-1.292
-1.295	-1.297	-1.299	-1.301	-1.302	-1.303	-1.306
-1.307	-1.309	-1.310	-1.312	-1.314	-1.315	-1.317
-1.318	-1.320	-1.321	-1.322	-1.324	-1.325	-1.325
-1.327	-1.328	-1.329	-1.331	-1.332	-1.333	-1.333
-1.335	-1.336	-1.337	-1.338	-1.339	-1.340	-1.341
-1.342	-1.343	-1.344	-1.345	-1.346	-1.347	

PERCENTAGE REDUCTION

0.00	0.95	2.70	4.60	6.42	8.17	9.92
11.60	13.20	14.66	16.12	17.51	18.67	19.91
21.01	22.17	23.19	24.22	25.16	26.11	26.99
27.94	28.81	29.61	30.42	31.29	32.09	32.90
33.70	34.43	35.23	36.11	36.83	37.56	38.44
39.24	39.97	40.85	41.65	42.52	43.33	44.13
45.15	45.95	46.83	47.70	48.65	49.53	50.47
51.28	52.22	53.17	54.12	55.00	55.94	56.75
57.70	58.64	59.52	60.47	61.20	62.07	62.95
63.82	64.62	65.50	66.30	67.10	67.91	68.64
69.44	70.24	71.04	71.70	72.28	73.01	73.67
74.40	74.98	75.57	76.22	76.81	77.32	77.90
78.41	78.92	79.43	79.94	80.38	80.89	81.40
81.77	82.20	82.64	83.01	83.44	83.81	84.32
84.61	84.97	85.34	85.70	86.00	86.36	86.65
86.94	87.31	87.60	87.89	88.26	88.48	88.69
88.99	89.28	89.50	89.72	90.01	90.15	90.52
90.74	90.96	91.10	91.39	91.54	91.76	91.90
92.12	92.34	92.56	92.71	92.85	93.00	93.22
93.36	93.51	93.65	93.87	94.02	94.16	94.24
94.46	94.60	94.75	94.89	94.97	95.04	95.26
95.33	95.48	95.55	95.70	95.84	95.92	96.06
96.13	96.28	96.35	96.43	96.57	96.64	96.64
96.79	96.86	96.94	97.08	97.16	97.23	97.23
97.37	97.45	97.52	97.59	97.67	97.74	97.81
97.88	97.96	98.03	98.10	98.18		

BBC CHYO BALANCE DATA REPORT
DATA FILE No. : :3.0.PRAM3
REMOVABLE OXYGEN WEIGHT: 1.332 GRAM
FURNACE TEMPERATURE : 1000 DEG. C
GAS FLOW RATE : 2 L/MIN
NUMBER OF SAMPLES TAKEN: 143
SAMPLING INTERVAL : 60 SECONDS

WEIGHT LOSS

0.000	-0.019	-0.051	-0.082	-0.112	-0.139	-0.165
-0.189	-0.210	-0.231	-0.250	-0.268	-0.285	-0.301
-0.318	-0.332	-0.348	-0.363	-0.376	-0.390	-0.404
-0.418	-0.430	-0.442	-0.457	-0.468	-0.480	-0.491
-0.503	-0.514	-0.525	-0.536	-0.547	-0.557	-0.568
-0.579	-0.591	-0.601	-0.612	-0.624	-0.636	-0.646
-0.658	-0.670	-0.680	-0.692	-0.705	-0.717	-0.730
-0.742	-0.754	-0.766	-0.779	-0.791	-0.802	-0.815
-0.827	-0.838	-0.850	-0.861	-0.873	-0.883	-0.895
-0.906	-0.918	-0.929	-0.941	-0.951	-0.963	-0.974
-0.985	-0.994	-1.005	-1.016	-1.024	-1.033	-1.042
-1.052	-1.061	-1.069	-1.079	-1.087	-1.096	-1.103
-1.111	-1.118	-1.128	-1.134	-1.142	-1.150	-1.157
-1.163	-1.170	-1.176	-1.182	-1.188	-1.193	-1.200
-1.204	-1.210	-1.215	-1.219	-1.224	-1.228	-1.233
-1.239	-1.242	-1.246	-1.251	-1.253	-1.257	-1.261
-1.264	-1.267	-1.269	-1.273	-1.276	-1.278	-1.281
-1.283	-1.288	-1.289	-1.292	-1.294	-1.296	-1.298
-1.300	-1.302	-1.305	-1.306	-1.309	-1.312	-1.313
-1.315	-1.317	-1.319	-1.321	-1.323	-1.323	-1.326
-1.327	-1.329	-1.331				

PERCENTAGE REDUCTION

0.00	1.43	3.83	6.16	8.41	10.44	12.39
14.19	15.77	17.34	18.77	20.12	21.40	22.60
23.87	24.92	26.13	27.25	28.23	29.28	30.33
31.38	32.28	33.18	34.31	35.14	36.04	36.86
37.76	38.59	39.41	40.24	41.07	41.82	42.64
43.47	44.37	45.12	45.95	46.85	47.75	48.50
49.40	50.30	51.05	51.95	52.93	53.83	54.80
55.71	56.61	57.51	58.48	59.38	60.21	61.19
62.09	62.91	63.81	64.64	65.54	66.29	67.19
68.02	68.92	69.74	70.65	71.40	72.30	73.12
73.95	74.62	75.45	76.28	76.88	77.55	78.23
78.98	79.65	80.26	81.01	81.61	82.28	82.81
83.41	83.93	84.68	85.14	85.74	86.34	86.86
87.31	87.84	88.29	88.74	89.19	89.56	90.09
90.39	90.84	91.22	91.52	91.89	92.19	92.57
93.02	93.24	93.54	93.92	94.07	94.37	94.67
94.89	95.12	95.27	95.57	95.80	95.95	96.17
96.32	96.70	96.77	97.00	97.15	97.30	97.45
97.60	97.75	97.97	98.05	98.27	98.50	98.57
98.72	98.87	99.02	99.17	99.32	99.32	99.55
99.62	99.77					

BBC CHYO BALANCE DATA REPORT
DATA FILE No. : :3.0.PRAM2
REMOVABLE OXYGEN WEIGHT: 0.6229999999 GI
FURNACE TEMPERATURE : 1000 DEG. C
GAS FLOW RATE : 2 L/MIN
NUMBER OF SAMPLES TAKEN: 127
SAMPLING INTERVAL : 60 SECONDS

WEIGHT LOSS

0.000	-0.012	-0.029	-0.048	-0.069	-0.085	-0.099
-0.115	-0.125	-0.137	-0.148	-0.160	-0.169	-0.177
-0.185	-0.192	-0.200	-0.207	-0.213	-0.221	-0.227
-0.234	-0.240	-0.246	-0.252	-0.259	-0.265	-0.271
-0.278	-0.285	-0.293	-0.300	-0.309	-0.317	-0.323
-0.330	-0.337	-0.345	-0.354	-0.361	-0.369	-0.376
-0.384	-0.391	-0.398	-0.405	-0.413	-0.419	-0.427
-0.434	-0.439	-0.446	-0.451	-0.457	-0.464	-0.470
-0.474	-0.480	-0.485	-0.491	-0.496	-0.499	-0.505
-0.508	-0.511	-0.516	-0.520	-0.524	-0.527	-0.530
-0.533	-0.537	-0.540	-0.544	-0.543	-0.549	-0.550
-0.556	-0.559	-0.560	-0.562	-0.563	-0.567	-0.569
-0.569	-0.571	-0.573	-0.576	-0.578	-0.580	-0.580
-0.580	-0.582	-0.589	-0.586	-0.587	-0.590	-0.591
-0.593	-0.593	-0.597	-0.596	-0.599	-0.597	-0.601
-0.599	-0.601	-0.602	-0.603	-0.605	-0.604	-0.605
-0.607	-0.609	-0.610	-0.610	-0.611	-0.612	-0.614
-0.614	-0.614	-0.615	-0.616	-0.616	-0.617	-0.618

PERCENTAGE REDUCTION

0.00	1.93	4.65	7.70	11.08	13.64	15.89
18.46	20.06	21.99	23.76	25.68	27.13	28.41
29.70	30.82	32.10	33.23	34.19	35.47	36.44
37.56	38.52	39.49	40.45	41.57	42.54	43.50
44.62	45.75	47.03	48.15	49.60	50.88	51.85
52.97	54.09	55.38	56.82	57.95	59.23	60.35
61.64	62.76	63.88	65.01	66.29	67.26	68.54
69.66	70.47	71.59	72.39	73.35	74.48	75.44
76.08	77.05	77.85	78.81	79.61	80.10	81.06
81.54	82.02	82.83	83.47	84.11	84.59	85.07
85.55	86.20	86.68	87.32	87.16	88.12	88.28
89.25	89.73	89.89	90.21	90.37	91.01	91.33
91.33	91.65	91.97	92.46	92.78	93.10	93.10
93.10	93.42	94.54	94.06	94.22	94.70	94.86
95.18	95.18	95.83	95.67	96.15	95.83	96.47
96.15	96.47	96.63	96.79	97.11	96.95	97.11
97.43	97.75	97.91	97.91	98.07	98.23	98.56
98.56	98.56	98.72	98.88	98.88	99.04	99.20

BBC CHYO BALANCE DATA REPORT
DATA FILE No. : :3.O.PRAM1
REMOVABLE OXYGEN WEIGHT: 1.226 GRAM
FURNACE TEMPERATURE : 1000 DEG. C
GAS FLOW RATE : 2 L/MIN
NUMBER OF SAMPLES TAKEN: 137
SAMPLING INTERVAL : 60 SECONDS

WEIGHT LOSS

0.001	-0.013	-0.044	-0.073	-0.102	-0.131	-0.157
-0.182	-0.205	-0.227	-0.246	-0.265	-0.282	-0.299
-0.313	-0.327	-0.340	-0.351	-0.363	-0.374	-0.383
-0.393	-0.401	-0.410	-0.420	-0.425	-0.436	-0.445
-0.453	-0.462	-0.469	-0.480	-0.489	-0.498	-0.511
-0.517	-0.526	-0.534	-0.551	-0.560	-0.571	-0.578
-0.589	-0.596	-0.608	-0.617	-0.631	-0.640	-0.649
-0.660	-0.671	-0.683	-0.694	-0.707	-0.717	-0.721
-0.730	-0.742	-0.748	-0.759	-0.768	-0.771	-0.786
-0.794	-0.806	-0.811	-0.822	-0.829	-0.842	-0.843
-0.848	-0.861	-0.869	-0.873	-0.878	-0.886	-0.895
-0.901	-0.907	-0.913	-0.926	-0.927	-0.935	-0.940
-0.943	-0.950	-0.959	-0.960	-0.968	-0.977	-0.975
-0.981	-0.990	-0.991	-0.995	-0.998	-1.004	-1.007
-1.012	-1.018	-1.021	-1.023	-1.028	-1.032	-1.032
-1.038	-1.039	-1.043	-1.047	-1.050	-1.051	-1.055
-1.057	-1.061	-1.065	-1.067	-1.070	-1.070	-1.071
-1.075	-1.078	-1.079	-1.081	-1.084	-1.086	-1.096
-1.093	-1.093	-1.096	-1.093	-1.098	-1.099	-1.100
-1.104	-1.105	-1.108	-1.103			

PERCENTAGE REDUCTION

0.00	1.06	3.59	5.95	8.32	10.69	12.81
14.85	16.72	18.52	20.07	21.62	23.00	24.39
25.53	26.67	27.73	28.63	29.61	30.51	31.24
32.06	32.71	33.44	34.26	34.67	35.56	36.30
36.95	37.68	38.25	39.15	39.89	40.62	41.68
42.17	42.90	43.56	44.94	45.68	46.57	47.15
48.04	48.61	49.59	50.33	51.47	52.20	53.94
53.83	54.73	55.71	56.61	57.67	58.48	58.81
59.54	60.52	61.01	61.91	62.64	62.89	64.11
64.76	65.74	66.15	67.05	67.62	68.68	68.76
69.17	70.23	70.88	71.21	71.62	72.27	73.00
73.49	73.98	74.47	75.53	75.61	76.26	76.67
76.92	77.49	78.22	78.30	78.96	79.69	79.53
80.02	80.75	80.83	81.16	81.40	81.89	82.14
82.54	83.03	83.28	83.44	83.85	84.18	84.18
84.67	84.75	85.07	85.40	85.64	85.73	86.05
86.22	86.54	86.87	87.03	87.28	87.28	87.36
87.68	87.93	88.01	88.17	88.42	88.58	89.40
89.15	89.15	89.40	89.15	89.56	89.64	89.72
90.05	90.13	90.38				

BBC CHYO BALANCE DATA REPORT
DATA FILE No. : :3.N.PRAM1
REMOVABLE OXYGEN WEIGHT: 0.368 GRAM
FURNACE TEMPERATURE : 900 DEG. C
GAS FLOW RATE : 2 L/MIN
NUMBER OF SAMPLES TAKEN: 91
SAMPLING INTERVAL : 60 SECONDS

WEIGHT LOSS

0.000	-0.016	-0.029	-0.040	-0.052	-0.061	-0.070
-0.079	-0.087	-0.096	-0.106	-0.116	-0.127	-0.135
-0.144	-0.152	-0.160	-0.167	-0.175	-0.182	-0.188
-0.195	-0.201	-0.207	-0.214	-0.219	-0.224	-0.229
-0.234	-0.239	-0.243	-0.248	-0.251	-0.255	-0.259
-0.263	-0.266	-0.270	-0.272	-0.276	-0.279	-0.282
-0.284	-0.286	-0.289	-0.292	-0.293	-0.296	-0.298
-0.300	-0.302	-0.305	-0.306	-0.308	-0.310	-0.312
-0.314	-0.316	-0.316	-0.319	-0.320	-0.321	-0.323
-0.324	-0.326	-0.327	-0.328	-0.329	-0.330	-0.331
-0.332	-0.334	-0.335	-0.337	-0.335	-0.339	-0.338
-0.340	-0.341	-0.342	-0.342	-0.343	-0.343	-0.344
-0.344	-0.345	-0.346	-0.346	-0.347	-0.347	-0.348

PERCENTAGE REDUCTION

0.00	4.35	7.88	10.87	14.13	16.58	19.02
21.47	23.64	26.09	28.80	31.52	34.51	36.68
39.13	41.30	43.48	45.38	47.55	49.46	51.09
52.99	54.62	56.25	58.15	59.51	60.87	62.23
63.59	64.95	66.03	67.39	68.21	69.29	70.38
71.47	72.28	73.37	73.91	75.00	75.82	76.63
77.17	77.72	78.53	79.35	79.62	80.43	80.98
81.52	82.07	82.88	83.15	83.70	84.24	84.78
85.33	85.87	85.87	86.68	86.96	87.23	87.77
88.04	88.59	88.86	89.13	89.40	89.67	89.95
90.22	90.76	91.03	91.58	91.03	92.12	91.85
92.39	92.66	92.93	92.93	93.21	93.21	93.48
93.48	93.75	94.02	94.02	94.29	94.29	

BBC CHYO BALANCE DATA REPORT
DATA FILE No. : :3.N.PRAM2
REMOVABLE OXYGEN WEIGHT: 0.423 GRAM
FURNACE TEMPERATURE : 1000 DEG. C
GAS FLOW RATE : 2 L/MIN
NUMBER OF SAMPLES TAKEN: 146
SAMPLING INTERVAL : 60 SECONDS

WEIGHT LOSS

0.000	-0.010	-0.026	-0.042	-0.055	-0.069	-0.083
-0.096	-0.112	-0.127	-0.143	-0.157	-0.170	-0.183
-0.195	-0.208	-0.219	-0.230	-0.240	-0.250	-0.260
-0.270	-0.279	-0.288	-0.295	-0.304	-0.312	-0.318
-0.325	-0.332	-0.338	-0.344	-0.350	-0.355	-0.360
-0.365	-0.369	-0.373	-0.377	-0.381	-0.383	-0.387
-0.390	-0.393	-0.395	-0.397	-0.399	-0.401	-0.402
-0.404	-0.405	-0.407	-0.407	-0.408	-0.408	-0.408
-0.409	-0.409	-0.409	-0.409	-0.409	-0.408	-0.408
-0.408	-0.407	-0.408	-0.407	-0.407	-0.406	-0.406
-0.406	-0.405	-0.405	-0.404	-0.404	-0.404	-0.403
-0.403	-0.402	-0.402	-0.399	-0.401	-0.400	-0.400
-0.400	-0.399	-0.399	-0.398	-0.398	-0.397	-0.397
-0.397	-0.396	-0.395	-0.395	-0.395	-0.395	-0.394
-0.393	-0.393	-0.392	-0.391	-0.391	-0.390	-0.390
-0.389	-0.390	-0.389	-0.388	-0.388	-0.388	-0.387
-0.387	-0.386	-0.386	-0.385	-0.385	-0.385	-0.384
-0.384	-0.383	-0.382	-0.382	-0.381	-0.381	-0.380
-0.379	-0.380	-0.379	-0.379	-0.379	-0.379	-0.378
-0.377	-0.377	-0.376	-0.375	-0.375	-0.375	-0.374
-0.374	-0.373	-0.372	-0.373	-0.371	-0.370	

PERCENTAGE REDUCTION

0.00	2.36	6.15	9.93	13.00	16.31	19.62
22.70	26.48	30.02	33.81	37.12	40.19	43.26
46.10	49.17	51.77	54.37	56.74	59.10	61.47
63.83	65.96	68.09	69.74	71.87	73.76	75.18
76.83	78.49	79.91	81.32	82.74	83.92	85.11
86.29	87.23	88.18	89.13	90.07	90.54	91.49
92.20	92.91	93.38	93.85	94.33	94.80	95.04
95.51	95.74	96.22	96.22	96.45	96.45	96.45
96.69	96.69	96.69	96.69	96.69	96.45	96.45
96.45	96.22	96.45	96.22	96.22	95.98	95.98
95.98	95.74	95.74	95.51	95.51	95.51	95.27
95.27	95.04	95.04	94.33	94.80	94.56	94.56
94.56	94.33	94.33	94.09	94.09	93.85	93.85
93.85	93.62	93.38	93.38	93.38	93.38	93.14
92.91	92.91	92.67	92.43	92.43	92.20	92.20
91.96	92.20	91.96	91.73	91.73	91.73	91.49
91.49	91.25	91.25	91.02	91.02	91.02	90.78
90.78	90.54	90.31	90.31	90.07	90.07	89.83
89.60	89.83	89.60	89.60	89.60	89.60	89.36
89.13	89.13	88.89	88.65	88.65	88.65	88.42
88.42	88.18	87.94	88.18	87.71		

BBC CHYO BALANCE DATA REPORT
DATA FILE No. : :3.N.PRAM3
REMOVABLE OXYGEN WEIGHT: 0.433 GRAM
FURNACE TEMPERATURE : 1100 DEG. C
GAS FLOW RATE : 2 L/MIN
NUMBER OF SAMPLES TAKEN: 89
SAMPLING INTERVAL : 60 SECONDS

WEIGHT LOSS

0.000	-0.010	-0.027	-0.045	-0.061	-0.076	-0.090
-0.104	-0.119	-0.133	-0.146	-0.159	-0.172	-0.183
-0.194	-0.204	-0.214	-0.223	-0.232	-0.240	-0.248
-0.256	-0.263	-0.271	-0.278	-0.283	-0.291	-0.297
-0.302	-0.308	-0.313	-0.318	-0.322	-0.328	-0.331
-0.336	-0.340	-0.344	-0.347	-0.350	-0.355	-0.357
-0.361	-0.363	-0.365	-0.368	-0.371	-0.373	-0.375
-0.377	-0.379	-0.381	-0.383	-0.384	-0.385	-0.386
-0.387	-0.387	-0.390	-0.390	-0.390	-0.391	-0.392
-0.392	-0.392	-0.393	-0.393	-0.393	-0.394	-0.393
-0.393	-0.393	-0.393	-0.393	-0.392	-0.393	-0.393
-0.392	-0.393	-0.393	-0.393	-0.392	-0.392	-0.392
-0.391	-0.391	-0.392	-0.391	-0.390		

PERCENTAGE REDUCTION

0.00	2.31	6.24	10.39	14.09	17.55	20.79
24.02	27.48	30.72	33.72	36.72	39.72	42.26
44.80	47.11	49.42	51.50	53.58	55.43	57.27
59.12	60.74	62.59	64.20	65.36	67.21	68.59
69.75	71.13	72.29	73.44	74.36	75.75	76.44
77.60	78.52	79.45	80.14	80.83	81.99	82.45
83.37	83.83	84.30	84.99	85.68	86.14	86.61
87.07	87.53	87.99	88.45	88.68	88.91	89.15
89.38	89.38	90.07	90.07	90.07	90.30	90.53
90.53	90.53	90.76	90.76	90.76	90.99	90.76
90.76	90.76	90.76	90.76	90.53	90.76	90.76
90.53	90.76	90.76	90.76	90.53	90.53	90.53
90.30	90.30	90.53	90.30			

BBC CHYO BALANCE DATA REPORT
DATA FILE No. : :3.N.PRAM4
REMOVABLE OXYGEN WEIGHT: 0.464 GRAM
FURNACE TEMPERATURE : 1200 DEG. C
GAS FLOW RATE : 2 L/MIN
NUMBER OF SAMPLES TAKEN: 64
SAMPLING INTERVAL : 60 SECONDS

WEIGHT LOSS

-0.001	-0.012	-0.028	-0.044	-0.057	-0.069	-0.082
-0.093	-0.105	-0.117	-0.128	-0.138	-0.148	-0.158
-0.168	-0.179	-0.187	-0.197	-0.205	-0.214	-0.222
-0.232	-0.240	-0.249	-0.256	-0.264	-0.271	-0.279
-0.287	-0.294	-0.301	-0.309	-0.315	-0.322	-0.330
-0.337	-0.344	-0.351	-0.357	-0.364	-0.370	-0.376
-0.381	-0.385	-0.390	-0.394	-0.398	-0.400	-0.403
-0.405	-0.406	-0.408	-0.409	-0.410	-0.410	-0.411
-0.411	-0.410	-0.411	-0.411	-0.410	-0.413	-0.412

PERCENTAGE REDUCTION

0.00	2.59	6.03	9.48	12.28	14.87	17.67
20.04	22.63	25.22	27.59	29.74	31.90	34.05
36.21	38.58	40.30	42.46	44.18	46.12	47.84
50.00	51.72	53.66	55.17	56.90	58.41	60.13
61.65	63.36	64.87	66.59	67.89	69.40	71.12
72.63	74.14	75.65	76.94	78.45	79.74	81.03
82.11	82.97	84.05	84.91	85.78	86.21	86.85
87.28	87.50	87.93	88.15	88.36	88.36	88.58
88.58	88.36	88.58	88.58	88.36	89.01	88.79

BBC CHYO BALANCE DATA REPORT
DATA FILE No. : :3.Q.PRAM1
REMOVABLE OXYGEN WEIGHT: 29.16 GRAM
FURNACE TEMPERATURE : 1000 DEG. C
GAS FLOW RATE : 4 L/MIN
NUMBER OF SAMPLES TAKEN: 24
SAMPLING INTERVAL : 60 SECONDS

WEIGHT LOSS

0.010	-0.260	-0.800	-0.960	-1.440	-2.250	-1.980	-2.300	-2.510	-3.110
-2.990	-3.370	-3.920	-3.870	-4.210	-4.560	-4.500	-4.800	-5.130	-5.750
-5.660	-5.200	-6.030	-6.290						

PERCENTAGE REDUCTION

0.00	0.89	2.74	3.29	4.94	7.72	6.79	7.89	8.61	10.67
10.25	11.56	13.44	13.27	14.44	15.64	15.43	16.46	17.59	19.72
19.41	17.83	20.68							

BBC CHYO BALANCE DATA REPORT
DATA FILE No. : :3.Q.PRAM2
REMOVABLE OXYGEN WEIGHT: 27.89 GRAM
FURNACE TEMPERATURE : 1000 DEG. C
GAS FLOW RATE : 4 L/MIN
NUMBER OF SAMPLES TAKEN: 22
SAMPLING INTERVAL : 60 SECONDS

WEIGHT LOSS

0.000	-0.430	-0.870	-1.270	-1.660	-2.020	-2.360	-2.690	-3.000	-3.300
-3.590	-3.860	-4.130	-4.390	-4.640	-4.880	-5.120	-5.350	-5.580	-5.800
-6.010	-6.220								

PERCENTAGE REDUCTION

0.00	1.54	3.12	4.55	5.95	7.24	8.46	9.65	10.76	11.83
12.87	13.84	14.81	15.74	16.64	17.50	18.36	19.18	20.01	20.80
21.55									

BBC CHYO BALANCE DATA REPORT
DATA FILE No. : :3.Q.PRAM3
REMOVABLE OXYGEN WEIGHT: 27.89 GRAM
FURNACE TEMPERATURE : 1000 DEG. C
GAS FLOW RATE : 4 L/MIN
NUMBER OF SAMPLES TAKEN: 23
SAMPLING INTERVAL : 60 SECONDS

WEIGHT LOSS

0.000	-0.400	-0.780	-1.140	-1.500	-1.830	-2.160	-2.480	-2.800	-3.090
-3.380	-3.670	-3.940	-4.200	-4.470	-4.720	-4.960	-5.190	-5.420	-5.640
-5.860	-6.080	-6.270							

PERCENTAGE REDUCTION

0.00	1.43	2.80	4.09	5.38	6.56	7.74	8.89	10.04	11.08
12.12	13.16	14.13	15.06	16.03	16.92	17.78	18.61	19.43	20.22
21.01	21.80								

BBC CHYO BALANCE DATA REPORT
DATA FILE No. : :3.Q.PRAM4
REMOVABLE OXYGEN WEIGHT: 28.84 GRAM
FURNACE TEMPERATURE : 1000 DEG. C
GAS FLOW RATE : 4 L/MIN
NUMBER OF SAMPLES TAKEN: 24
SAMPLING INTERVAL : 60 SECONDS

WEIGHT LOSS

-0.060	-0.390	-0.710	-1.020	-1.330	-1.630	-1.920	-2.210	-2.490	-2.770
-3.050	-3.330	-3.590	-3.860	-4.120	-4.380	-4.640	-4.890	-5.140	-5.390
-5.630	-5.870	-6.110	-6.350						

PERCENTAGE REDUCTION

0.00	1.35	2.46	3.54	4.61	5.65	6.66	7.66	8.63	9.60
10.58	11.55	12.45	13.38	14.29	15.19	16.09	16.96	17.82	18.69
19.52	20.35	21.19							

BBC CHYO BALANCE DATA REPORT
DATA FILE No. : :3.Q.PRAM5
REMOVABLE OXYGEN WEIGHT: 29.11 GRAM
FURNACE TEMPERATURE : 1000 DEG. C
GAS FLOW RATE : 4 L/MIN
NUMBER OF SAMPLES TAKEN: 21
SAMPLING INTERVAL : 60 SECONDS

WEIGHT LOSS

-0.020	-0.460	-0.870	-1.270	-1.640	-1.990	-2.330	-2.670	-3.000	-3.320
-3.630	-3.930	-4.230	-4.520	-4.800	-5.080	-5.350	-5.620	-5.880	-6.130

PERCENTAGE REDUCTION

0.00	1.58	2.99	4.36	5.63	6.84	8.00	9.17	10.31	11.41
12.47	13.50	14.53	15.53	16.49	17.45	18.38	19.31	20.20	21.06

BBC CHYO BALANCE DATA REPORT
DATA FILE No. : :3.Q.PRAM6
REMOVABLE OXYGEN WEIGHT: 29.83 GRAM
FURNACE TEMPERATURE : 1000 DEG. C
GAS FLOW RATE : 4 L/MIN
NUMBER OF SAMPLES TAKEN: 183
SAMPLING INTERVAL : 6 SECONDS

WEIGHT LOSS

0.000	-0.020	-0.060	-0.100	-0.160	-0.210	-0.260	-0.300	-0.350	-0.400
-0.440	-0.480	-0.530	-0.570	-0.610	-0.670	-0.700	-0.750	-0.810	-0.840
-0.980	-0.950	-1.040	-1.010	-1.130	-1.160	-1.260	-1.250	-1.330	-1.340
-1.280	-1.400	-1.430	-1.520	-1.740	-1.570	-1.590	-1.600	-1.780	-1.890
-2.020	-2.030	-1.860	-1.900	-1.930	-1.970	-1.960	-2.030	-2.090	-2.080
-2.170	-2.170	-2.140	-2.220	-2.330	-2.360	-2.380	-2.420	-2.450	-2.550
-2.570	-2.620	-2.620	-2.710	-2.730	-2.710	-2.800	-2.800	-2.790	-2.860
-2.930	-3.000	-3.010	-3.080	-3.160	-3.180	-3.140	-3.120	-3.150	-3.220
-3.290	-3.380	-3.330	-3.440	-3.460	-3.430	-3.480	-3.670	-3.460	-3.470
-3.510	-3.590	-3.680	-3.720	-3.820	-3.760	-3.780	-3.770	-3.850	-3.910
-3.930	-3.960	-3.980	-4.070	-4.150	-4.030	-4.190	-4.180	-4.300	-4.250
-4.280	-4.230	-4.340	-4.530	-4.580	-4.650	-4.630	-4.410	-4.520	-4.600
-4.740	-4.500	-4.660	-4.570	-4.750	-4.740	-4.870	-4.800	-4.890	-4.940
-5.000	-5.090	-5.210	-4.900	-4.870	-4.970	-5.120	-5.050	-5.050	-5.100
-5.200	-5.220	-5.320	-5.310	-5.340	-5.330	-5.370	-5.490	-5.390	-5.520
-5.450	-5.450	-5.640	-5.580	-5.690	-5.590	-5.600	-5.760	-5.750	-5.850
-5.770	-5.670	-5.770	-5.810	-5.820	-6.010	-6.030	-5.940	-5.990	-6.020
-5.990	-6.050	-6.100	-6.080	-6.090	-6.150	-6.260	-6.350	-6.450	-6.150
-6.160	-6.330	-6.430							

PERCENTAGE REDUCTION

0.00	0.07	0.20	0.34	0.54	0.70	0.87	1.01	1.17	1.34
1.48	1.61	1.78	1.91	2.04	2.25	2.35	2.51	2.72	2.82
3.29	3.18	3.49	3.39	3.79	3.89	4.22	4.19	4.46	4.49
4.29	4.69	4.79	5.10	5.83	5.26	5.33	5.36	5.97	6.34
6.77	6.81	6.24	6.37	6.47	6.60	6.57	6.81	7.01	6.97
7.27	7.27	7.17	7.44	7.81	7.91	7.98	8.11	8.21	8.55
8.62	8.78	8.78	9.08	9.15	9.08	9.39	9.39	9.35	9.59
9.82	10.06	10.09	10.33	10.59	10.66	10.53	10.46	10.56	10.79
11.03	11.33	11.16	11.53	11.60	11.50	11.67	12.30	11.60	11.63
11.77	12.03	12.34	12.47	12.81	12.60	12.67	12.64	12.91	13.11
13.17	13.28	13.34	13.64	13.91	13.51	14.05	14.01	14.42	14.25
14.35	14.18	14.55	15.19	15.35	15.59	15.52	14.78	15.15	15.42
15.89	15.09	15.62	15.32	15.92	15.89	16.33	16.09	16.39	16.56
16.76	17.06	17.47	16.43	16.33	16.66	17.16	16.93	16.93	17.10
17.43	17.50	17.83	17.80	17.90	17.87	18.00	18.40	18.07	18.50
18.27	18.27	18.91	18.71	19.07	18.74	18.77	19.31	19.28	19.61
19.34	19.01	19.34	19.48	19.51	20.15	20.21	19.91	20.08	20.18
20.08	20.28	20.45	20.38	20.42	20.62	20.99	21.29	21.62	20.62
20.65	21.22								

BBC CHYO BALANCE DATA REPORT
DATA FILE No. : :3.Q.PRAM7
REMOVABLE OXYGEN WEIGHT: 29.28 GRAM
FURNACE TEMPERATURE : 1000 DEG. C
GAS FLOW RATE : 4 L/MIN
NUMBER OF SAMPLES TAKEN: 26
SAMPLING INTERVAL : 60 SECONDS

WEIGHT LOSS

0.020	-0.270	-0.670	-1.020	-1.340	-1.650	-1.870	-1.980	-2.050	-2.210
-2.480	-2.750	-3.010	-3.260	-3.510	-3.750	-3.990	-4.230	-4.460	-4.680
-4.900	-5.120	-5.330	-5.540	-5.750	-5.950				

PERCENTAGE REDUCTION

0.00	0.92	2.29	3.48	4.58	5.64	6.39	6.76	7.00	7.55
8.47	9.39	10.28	11.13	11.99	12.81	13.63	14.45	15.23	15.98
16.73	17.49	18.20	18.92	19.64					

BBC CHYO BALANCE DATA REPORT
DATA FILE No. : :3.Q.PRAM8
REMOVABLE OXYGEN WEIGHT: 29.17 GRAM
FURNACE TEMPERATURE : 1000 DEG. C
GAS FLOW RATE : 4 L/MIN
NUMBER OF SAMPLES TAKEN: 20
SAMPLING INTERVAL : 60 SECONDS

WEIGHT LOSS

-0.010	-0.410	-0.820	-1.200	-1.560	-1.910	-2.250	-2.580	-2.900	-3.210
-3.520	-3.820	-4.110	-4.400	-4.690	-4.970	-5.250	-5.530	-5.800	-6.060

PERCENTAGE REDUCTION

0.00	1.41	2.81	4.11	5.35	6.55	7.71	8.84	9.94	11.00
12.07	13.10	14.09	15.08	16.08	17.04	18.00	18.96	19.88	

BBC CHYO BALANCE DATA REPORT
DATA FILE No. : :3.Q.PRAM9
REMOVABLE OXYGEN WEIGHT: 23.4 GRAM
FURNACE TEMPERATURE : 1000 DEG. C
GAS FLOW RATE : 4 L/MIN
NUMBER OF SAMPLES TAKEN: 19
SAMPLING INTERVAL : 60 SECONDS

WEIGHT LOSS

0.000	-0.420	-0.800	-0.970	-1.090	-1.160	-1.500	-1.870	-2.230	-2.570
-2.900	-3.210	-3.510	-3.800	-4.080	-4.350	-4.600	-4.850	-5.090	

PERCENTAGE REDUCTION

0.00	1.79	3.42	4.15	4.66	4.96	6.41	7.99	9.53	10.98
12.39	13.72	15.00	16.24	17.44	18.59	19.66	20.73		

APPENDIX A-10

DATA OF ORE B

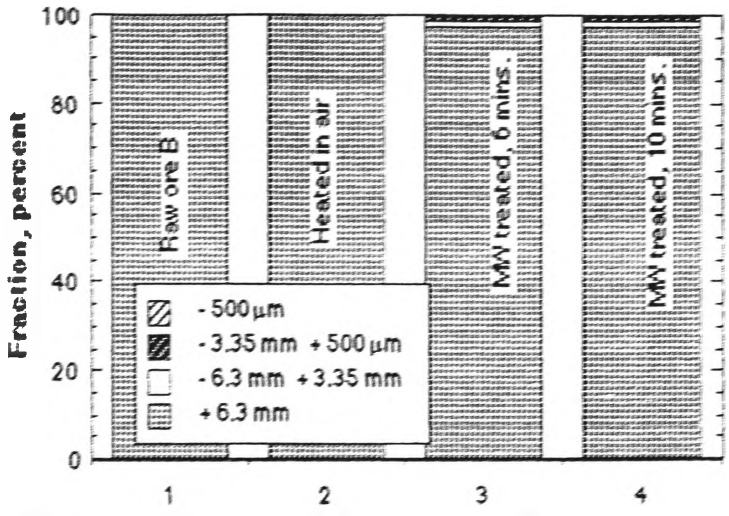

Figure A-9a. Size distribution diagram for Ore B before reduction.

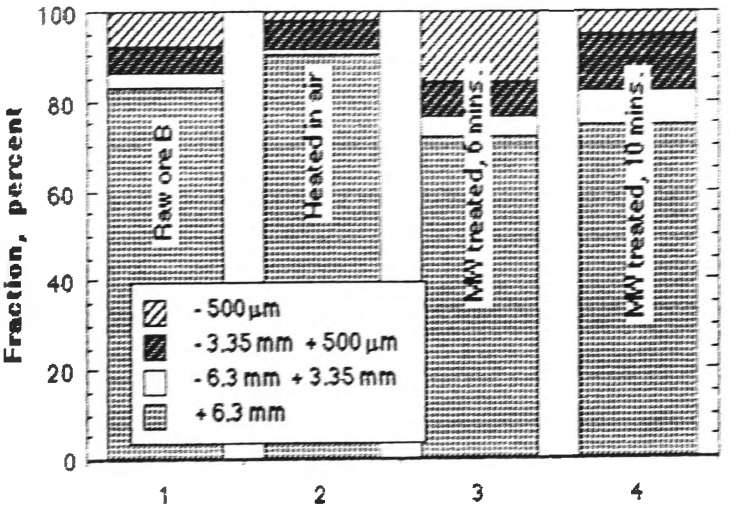

Figure A-9b. Size distribution diagram for ore B after reduction.

(continued on next page)

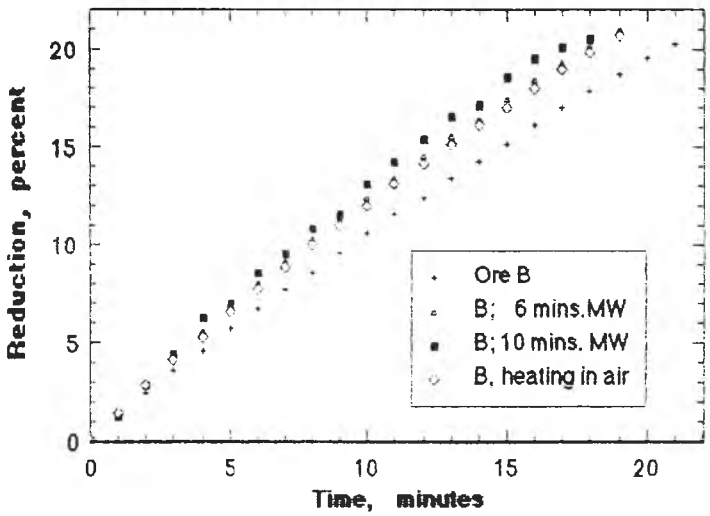

Figure A-9c. Reduction curves of ore B.

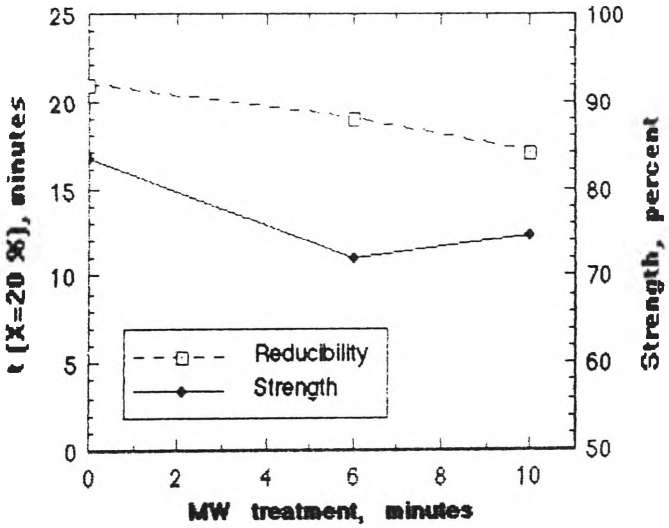

Figure A-9d. Effect of MW treatment on reduction time and strength of ore B.

(Continued on next page)

(Continued)

Appendix A-10

Table A-10 Results of modified drop test on magneto-hematite ore B

	Weight, percent			
	+ 6.3 mm	- 6.3 mm + 3.35 mm	- 3.35 mm + 500 μm	- 500 μm
Ore B	99.8	-	0.1	0.1
Ore B heating in air (700°C, 1hr)	99.8	-	0.1	0.1
Ore B MW treatment (1300W, 6 mins)	97.5	1.2	1.1	1.8
Ore B MW treatment (1300W, 10 mins)	93.2	3.2	2.5	0.2
Ore B reduced*	83.4	2.7	5.8	8.1
Ore B reduced (heating in air, 700°C)	90.0	1.8	6.0	2.2
Ore B reduced (6 mins MW treatment)	72.1	4.2	8.1	15.6
Ore B reduced (10 mins MW treatment)	74.6	7.9	12.6	4.9

*Reducing atmosphere 100% CO, 1000°C

Reduction degree : constant (20%)